

PDF hosted at the Radboud Repository of the Radboud University Nijmegen

The following full text is a publisher's version.

For additional information about this publication click this link.

<http://hdl.handle.net/2066/82951>

Please be advised that this information was generated on 2017-12-06 and may be subject to change.

Physiology of the distal convoluted tubule: convergence of electrolyte transport pathways

Henrik Dimke

Department of Physiology, Radboud University Nijmegen Medical Centre, the Netherlands.

The research presented in this thesis was performed at the department of Physiology, Radboud University Nijmegen Medical Centre, The Netherlands and financially supported by the Dutch Kidney Foundation, grant C05.2134.

Financial support by the Dutch Kidney Foundation for the publication of this thesis is gratefully acknowledged.

ISBN: 978-90-9025714-3

Print: Ipskamp Drukken, Nijmegen

Cover design: Kidney



Physiology of the distal convolution: convergence of electrolyte transport pathways

Een wetenschappelijke proeve
op het gebied van de Medische Wetenschappen

Proefschrift

ter verkrijging van de graad van doctor
aan de Radboud Universiteit Nijmegen
op gezag van de rector magnificus prof. mr. S.C.J.J. Kortmann,
volgens besluit van het college van decanen
in het openbaar te verdedigen op donderdag 4 november 2010
om 10:30 uur precies
door
Henrik Dimke
geboren op 8 november 1980
te Colombo, Sri Lanka

Promotores:

Prof. dr. R.J.M. Bindels

Prof. dr. J.G.J. Hoenderop

Copromotor:

Dr. J. Deinum

Manuscriptcommissie:

Prof. dr. J. Schalkwijk

Prof. dr. F.P.M. Cremers

Prof. dr. S. Florquin (UvA)



Physiology of the distal convolution: convergence of electrolyte transport pathways

An academic essay in Medical Sciences

Doctoral thesis

to obtain the degree of doctor

from Radboud University Nijmegen

on the authority of the Rector Magnificus, prof. dr. S.C.J.J. Kortmann,

according to the decision of the Council of Deans

to be defended in public on Thursday, 4th November 2010

at 10.30 hours

by

Henrik Dimke

born in Colombo, Sri Lanka.

on November 8th 1980

Supervisors:

Prof. Dr. R.J.M. Bindels

Prof. Dr. J.G.J. Hoenderop

Co-supervisor:

Dr. J. Deinum

Doctoral Thesis Committee:

Prof. Dr. J. Schalkwijk

Prof. Dr. F.P.M. Cremers

Prof. Dr. S. Florquin (University of Amsterdam)

Table of Contents

Chapter 1

General Introduction p. 9

Chapter 2

γ -Adducin functions as a novel regulator of the thiazide-sensitive NaCl-cotransporter p. 39

Chapter 3

Effects of the Epidermal Growth Factor Receptor (EGFR) kinase inhibitor Erlotinib on renal and systemic Mg^{2+} handling p. 71

Chapter 4

Testosterone increases urinary Ca^{2+} excretion and inhibits expression of renal calcium transport proteins p. 93

Chapter 5

Calcitonin-stimulated renal Ca^{2+} reabsorption occurs independently of TRPV5 p. 119

Chapter 6

Tissue transglutaminase inhibits TRPV5-dependent Ca^{2+} transport in a N-glycosylation-dependent manner p. 139

Chapter 7

A mouse model for autosomal dominant hypercalciuria due to a mutation in the epithelial Ca^{2+} channel TRPV5 p. 163

Chapter 8

General discussion and summary p. 195

Chapter 9

Samenvatting/Sammendrag p. 223

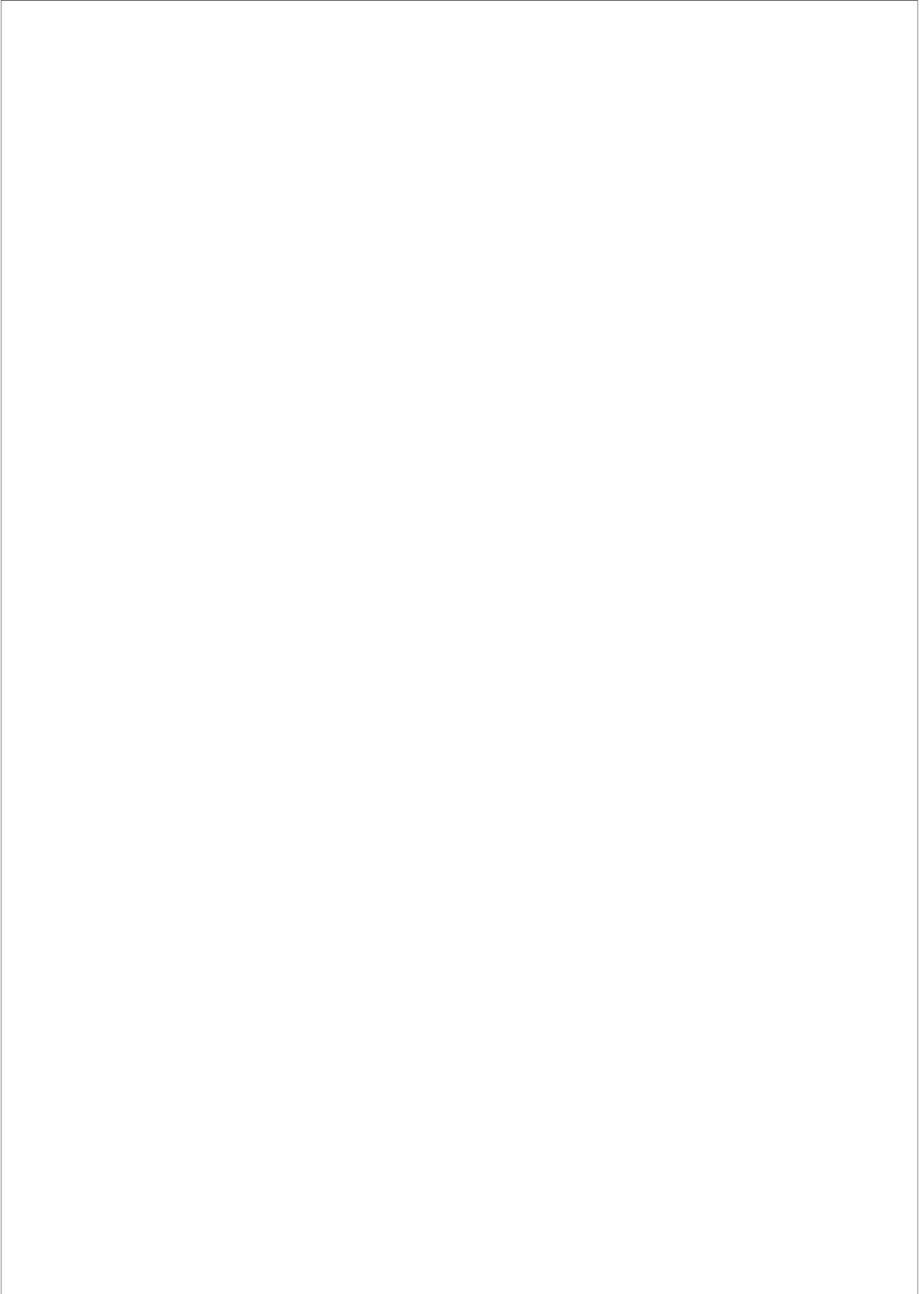
Chapter 10

Curriculum Vitae p. 239

List of abbreviations

List of publications

Acknowledgements



CHAPTER 1

General introduction

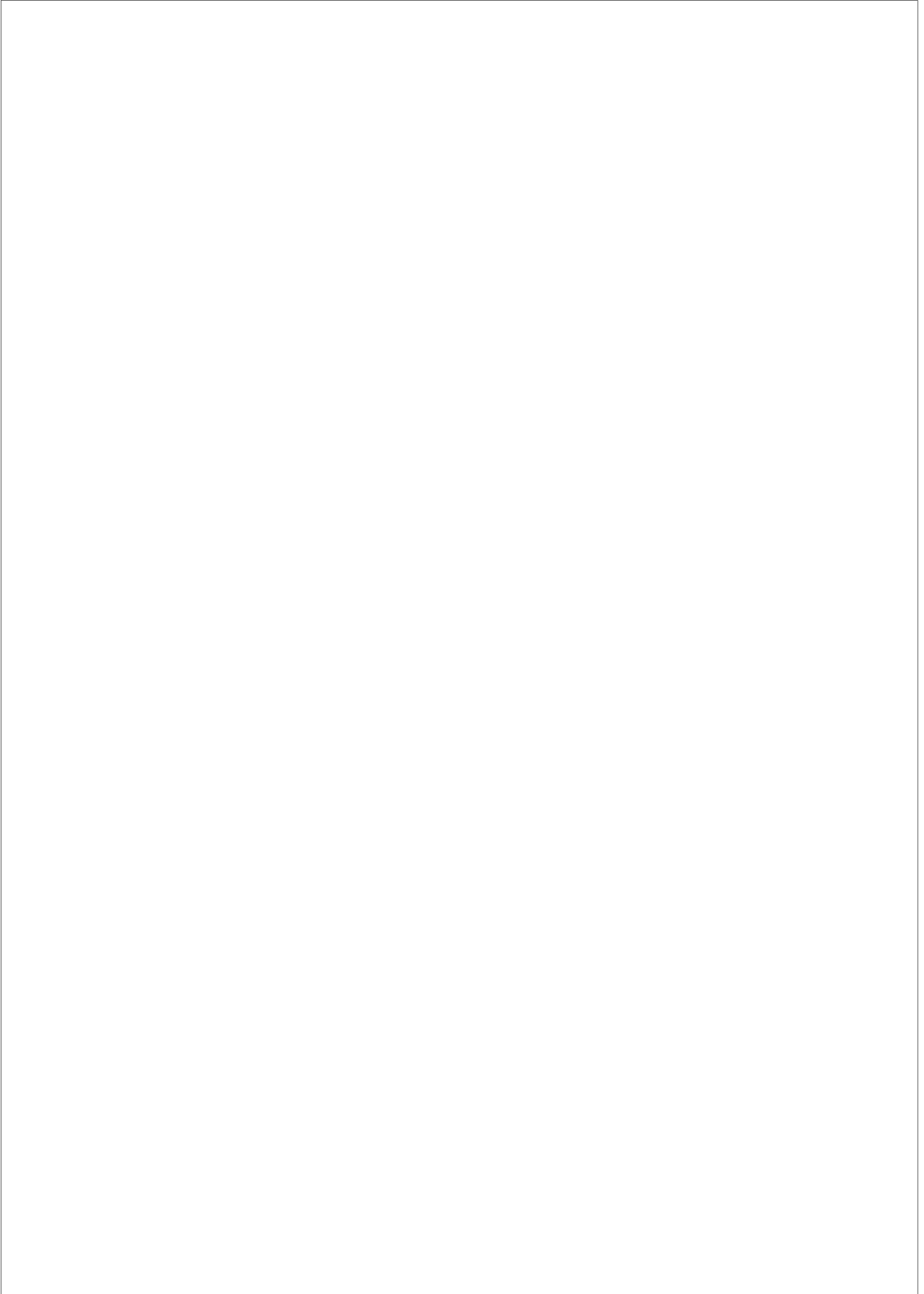
In part adapted after:

Hereditary tubular transport disorders: implications for renal handling of Ca²⁺ and Mg²⁺

By Henrik Dimke¹, Joost G. Hoenderop¹, René J. Bindels¹.

¹Department of Physiology, Radboud University Nijmegen Medical Centre, the Netherlands.

Clin Sci (Lond). 118:1-18, 2010.



General Introduction

Maintenance of serum electrolytes (such as Na^+ , Cl^- , Ca^{2+} , and Mg^{2+}) is essential for many physiological processes, such as blood pressure control, intracellular signaling, neural excitability, and bone formation. The kidney plays a central role in controlling the excretion of electrolytes in response to conditions of deprivation or excess of these ions (1-5). Transepithelial (i.e. net result of paracellular and transcellular) transport of divalents across the epithelia differs in the various nephron segments. Transport of Na^+ or Cl^- is often transcellular, but these ions are in some nephron segments partially transported via the paracellular route. Secondary active transport of Na^+ occurs in the proximal tubule (PT), thick ascending limb (TAL), distal convoluted tubule (DCT), connecting tubule (CNT) and associated collecting ducts (CD). Likewise, transcellular Cl^- transport is found predominantly in the TAL, DCT, CNT, and CDs. In addition, the PT and TAL reabsorb Mg^{2+} and Ca^{2+} in a paracellular manner, while active transcellular transport occurs in the DCT and CNT, respectively (Figure 1).

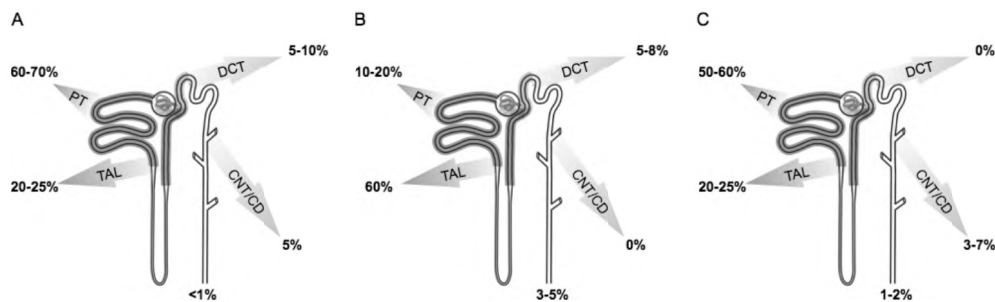


Figure 1. Schematic model of the renal electrolyte reabsorptive capacity. (A) Renal Na^+ reabsorption in individual nephron segments within the kidney. (B) Renal Mg^{2+} reabsorption in individual nephron segments. (C) Renal Ca^{2+} reabsorption in individual nephron. PT, proximal tubules; TAL, thick ascending limb of the loop of Henle; DCT, distal convoluted tubule; CNT, connecting tubule; CD, collecting duct.

General introduction to the distal convolution

The distal convolution is an anatomical structure comprising the DCT, CNT, and the initial CD (6).

The structure is a main site in the active reabsorption of Na^+ , Cl^- , Ca^{2+} , and Mg^{2+} from the filtrate.

Chapter 1

As these segments represent one of the final structures in the kidney where electrolyte reabsorption occurs, it plays a key role in fine-tuning the final urinary excretion of these ions. As such, the structure serves as an important determinant of the systemic concentration of electrolytes, by amending the urinary excretion. Several species differences can be noted in the composition and borders of the individual nephron segments of the distal convolution, particularly between rabbit in comparison to man, mice, and rat (6-8). While the transition between the different nephron segments ends abruptly in the rabbit, the borders between these segments are more intermingled in the other species (6-8). The cellular composition in rabbit has well-defined DCT cells, with the subsequent appearance of CNT principal-like cells blended with acid or base secreting intercalated cells (6-8). The CNT cells are then substituted with CD principal cells towards the end of the distal convolutions. An important difference between CNT and CD cells is the higher transport capacity of the CNT (9). In species other than rabbit, an additional nephron segment exists, the so-called DCT2 segment where the thiazide-sensitive NaCl cotransporter (NCC) and the amiloride-sensitive epithelial Na⁺ channel (ENaC) are coexpressed (will be discussed below) (7, 10). Lumen negative transepithelial voltage increases from approximately -5 mV in the early convolution till values approximating -40 mV or more towards the end of the late convolution (11-15). However, some variability in the measured voltages have been reported (11).

Electrolyte transport pathways in the DCT

NaCl transport in the DCT

The DCT reclaims some 5-10% of Na⁺ from the renal ultrafiltrate (11). It is, therefore not surprising that disorders, which disturb transport processes in this segment, affect the renal reabsorptive capacity for NaCl and thereby influence systemic blood pressure. The tubular fluid to plasma ratio of Na⁺ declines progressively along the length of the DCT, emphasizing the role of this segment in dilution of the luminal fluid (16). Detailed physiological measurements using

General introduction

micropuncture have shown that vectorial Na^+ transport in the DCT is load dependent, thus an increased Na^+ delivery increases Na^+ reabsorption in this nephron segment (3, 4). The mechanism that amends the reabsorptive capacity of the DCT to changes in Na^+ load is entirely sensitive to thiazide diuretics (17). The majority of NaCl reclaimed by the DCT, is taken up via the thiazide-sensitive cotransporter, NCC (18) (Figure 2). NCC was originally cloned from the urinary bladder of the winter flounder, *Pseudopleuronectes americanus* (19). The cotransporter takes up Na^+ and Cl^- in the stoichiometric relationship 1:1. In the mammalian kidney, the cotransporter localizes to apical membrane domains of the DCT cell (20-22). The driving force for NaCl transport across the apical membrane, is provided by the basolaterally located Na^+ , K^+ -ATPase (23). Inwardly transported Cl^- exits the cell via the Cl^- channel located in the basolateral membrane of the DCT (24) (Figure 2).

Mg²⁺ transport in the DCT

Detailed physiological measurements suggest that the distal convolutions are responsible for reabsorbing 5-6% of the filtered Mg^{2+} (25, 26). These values were determined by subtracting the delivery of ions to the distal sites and the final urine. Similar experiments reported that between early and late distal collections, approximately 8% of the filtered load is reabsorbed (27). Based on their early and late distal micropuncture data, Brunette and colleagues suggested that reabsorption of Mg^{2+} is localized in the early portion, rather than along the whole distal convolution, thus predominantly in the DCT. The early distal convolution constitutes a high resistance epithelium with a lumen negative voltage of approximately -5 mV (12, 13, 28). Moreover, the transepithelial movement of Mg^{2+} appears to be unidirectional. These observations support the presence of active transcellular Mg^{2+} transport in this segment (29). This is further corroborated by the observation that the cellular Mg^{2+} concentration in the DCT ranges between 0.2-1.0 mM (30, 31), while the concentration of the lumen is maintained around 0.2-0.7 mM (1). Under these conditions, uptake of Mg^{2+} across the apical membrane would be

Chapter 1

dictated largely by the negative intracellular membrane potential found in the DCT cell (32, 33). In addition, distal reabsorption of Mg^{2+} appears to be load dependent, as increasing delivery augments reabsorption (29, 34). Cellular influx of Mg^{2+} likely occurs through the Transient Receptor Potential Melastin 6 channel (TRPM6), a channel selective for divalent cations (35) (Figure 2). TRPM6 is structurally similar to other TRP channels with 6 transmembrane segments. Only shared with TRPM7 is the unique α -kinase domain fused to the C-termini (36). It is worth noting that current debate questions whether TRPM6 functions as a homo-tetramer or as a heteromer with TRPM7 (35, 37-42). Thus the exact molecular composition of the Mg^{2+} influx pathway in transporting epithelia remains to be determined. TRPM6 mRNA expression is restricted to the kidney, lung, and intestine (43, 44). Immunohistochemical localization of the channel has been reported, where TRPM6 is restricted to the apical membrane domains of the DCT cell (35). Intracellular carrier proteins and basolateral excursion mechanisms are yet to be identified (Figure 2).

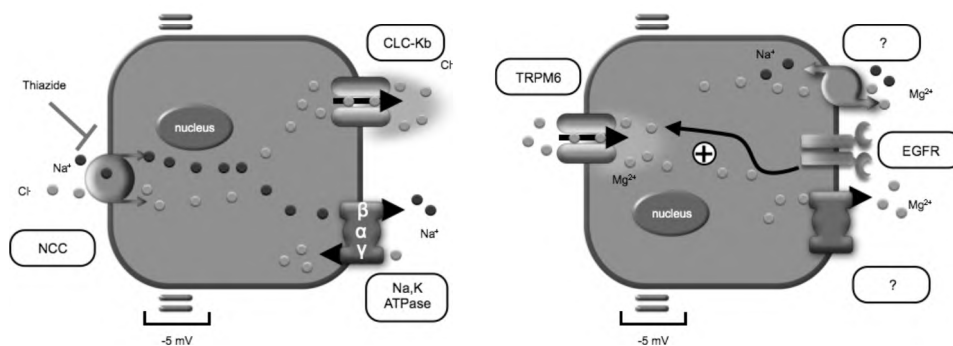


Figure 2. Schematic model of the cellular composition of renal ion transport proteins within the distal convoluted tubule (DCT). NCC, thiazide-sensitive NaCl cotransporter; CLC-Kb, Cl⁻ channel Kb; TRPM6, transient receptor potential melastatin 6 Mg^{2+} channel; EGFR, epidermal growth factor receptor. Na⁺, K⁺-ATPase consisting of α , β , and γ subunits.

Electrolyte transport pathways in the DCT2/CNT

NaCl transport in the CNT

The CNT segment is composed of several cell types, the Na⁺ transporting CNT cell (similar to the

General introduction

CD principal cells), as well as acid/base secreting intercalated cells (3). Vectorial Na^+ transport in the CNT and CD is mediated via the epithelial Na^+ channel, ENaC. ENaC is located in the apical plasma membrane of the CNT and CCD cells (45, 46) (Figure 3). The channel is composed of three subunits termed α , β , and γ (47). As in the DCT, transepithelial Na^+ transport is driven by the basolateral Na^+ , K^+ -ATPase (23, 48). In addition, these segments play an important role in K^+ homeostasis, and Na^+ reabsorption is here functionally coupled with K^+ secretion. The apically located renal outer medulla K^+ channel (ROMK1) is responsible for the secretion of K^+ (49-51) (Figure 3). The CNT and CD cells also possess the aquaporin 2 water channel (AQP2), which plays a key role in vasopressin-mediated water reabsorption (52) (Figure 3).

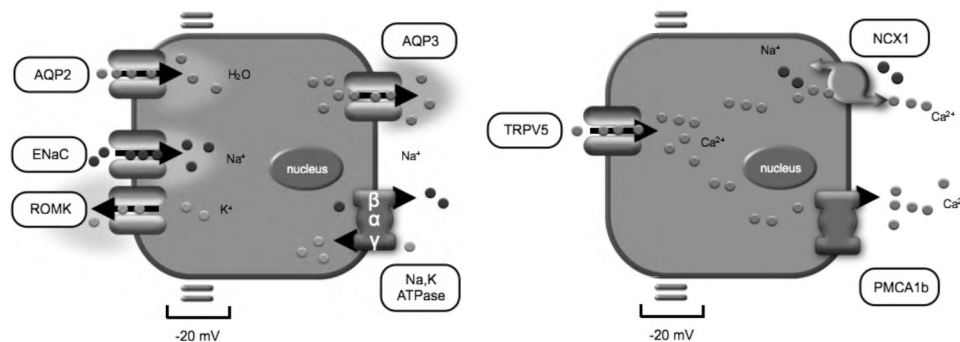


Figure 3. Schematic model of the cellular composition of renal ion and water transport proteins within the connecting tubule (CNT)/collecting duct (CD) cell. AQP2-3, Aquaporin 2-3; ENaC, epithelial Na^+ channel; ROMK, renal outer medullary K^+ channel; TRPV5, transient receptor potential vanilloid 5 Ca^{2+} channel. Na^+ , K^+ -ATPase consisting of α , β , and γ subunits.

Ca²⁺ transport in the DCT2/CNT

Detailed micropuncture studies have estimated that approximately 3-7% of the filtered Ca^{2+} is reclaimed between the early or late sites in the distal convolution and the final urine in the rat (26, 53, 54). However, the absence of direct determinations of delivery in juxtamedullary nephrons may only provide rough estimates. It is unclear whether these punctures represent the whole

Chapter 1

Ca²⁺-transporting segment in the distal convolutions. Approximately 2% of the filtered load is reabsorbed between early and late distal collections in the same nephron, while the amount doubles in the presence of parathyroid hormone (PTH) (27). Ca²⁺ reabsorption is essentially thought to be active, as it occurs in the presence of lower intraluminal Ca²⁺ concentrations and lumen negative transepithelial voltages (54). The transient receptor potential vanilloid 5 channel (TRPV5) provides the main apical entry step for Ca²⁺ in the distal convolutions. TRPV5 was originally cloned from primary cultures of rabbit renal CNT/CCD tubules (55). The channel localizes primarily to the CNT in the rabbit (7, 56). In other rodents, expression of TRPV5 is also found in the DCT2 segment, in addition to the CNT and the initial CD (7, 8, 57, 58) (Figure 3). In mouse, TRPV5 is highly expressed in apical membrane domains of particularly the late distal convoluted tubule (DCT2), with a gradual decrease along CNT and initial CD (2, 8), suggesting that TRPV5-mediated Ca²⁺ uptake predominates in the DCT2 segment. The channel co-localizes with the Ca²⁺-binding protein calbindin-D_{28K} and the basolateral extrusion proteins, the plasma membrane ATPase 1b (PMCA1b) and the Na⁺/Ca²⁺ exchanger type 1 (NCX1) (Figure 3). Transgenic mice lacking TRPV5 show augmented renal Ca²⁺ loss and micropuncture studies effectively demonstrate that Ca²⁺ reabsorption in the distal convolutions is disturbed (59). Several studies have shown TRPV5 as an essential constituent in transcellular Ca²⁺ reabsorption and it is, therefore, surprising that no monogenic disorders or polymorphisms have been identified thus far (60).

Hormonal regulation of electrolyte transport in the distal convoluted tubule

Aldosterone

Aldosterone is an important hormone involved in blood pressure maintenance and K⁺ secretion. The distal convoluted tubule is sensitive to the hormone, which augments transport in these segments, resulting in many of the systemic changes observed contributed to aldosterone excess. Thus, when mineralocorticoids or glucocorticoids are infused in the rat, the amount of tritium-labeled

General introduction

metolazone binding sites (indirect measurement of NCC transporters) increases (61, 62). Later studies revealed that an increase in NCC protein abundance occurs after application of aldosterone (21). Aldosterone is also the key regulator of ENaC. Administration of the hormone increases the expression of α -ENaC as well as targets the heteromeric complex to the membrane (45, 63-65). This increase in vectorial Na^+ transport in the CNT/CD segments allows the secretion of K^+ . In addition, aldosterone has been shown to stimulate the expression of ROMK mRNA (66).

Angiotensin II

Upon intravascular volume depletion, the juxtaglomerular apparatus secretes renin. The release of renin from the juxtaglomerular cells ultimately results in increased Angiotensin II production. Angiotensin II has multiple functions, acting *i*) as a powerful vasoconstrictor, *ii*) causing Na^+ retention via direct effects on the renal epithelial cells, and *iii*) increases aldosterone release from the adrenal cortex. These processes serve to restore extracellular volume and arterial pressure. Angiotensin II has been shown to act within the distal convoluted tubule both acutely and chronically. As such, Candesartan, an angiotensin receptor type 1 antagonist, has been shown to reduce the expression of NCC (67). Chronic administration of angiotensin II also increases the abundance of ENaC (68). Angiotensin II acutely provokes trafficking of NCC to the apical membrane of the DCT (69). Furthermore, Angiotensin II has been shown to increase the activity of NCC via a With-No-Lysine (WNK) 4 dependent mechanism, augmenting phosphorylation of the N-terminal domain in the transporter (70). In addition, acute application of Angiotensin II stimulates amiloride-sensitive Na^+ transport in the distal convoluted tubule, suggesting activation of ENaC channels (71). The effects of Angiotensin II within the distal convoluted tubule all serve to restore extracellular volume loss and hence arterial pressure.

Chapter 1

Vasopressin

Vasopressin (antidiuretic hormone) is secreted from the posterior lobe of the pituitary in response to changes in serum osmolality and extracellular fluid volume. The hormone acts by constricting blood vessels, and stimulating water reabsorption in the kidney. Increased renal water reabsorption is achieved by modulating CNT/CD water permeability, increasing medullary urea transport, and stimulating the furosemide-sensitive Na^+ , K^+ , Cl^- cotransporter (NKCC2) in the TAL. In addition to these effects, vasopressin also acts within the distal convoluted tubule to increase Na^+ transport. In the DCT, vasopressin acutely activates NCC via phosphorylation of its N-terminal domain (72). The underlying physiological explanation for this observation remains obscure, but may be related to vasopressin's role in extracellular fluid balance. Chronic stimulation of the vasopressin receptor type 2 reduces Na^+ excretion in healthy humans (73). This can be explained by an increased expression of the β - and γ - subunits of ENaC in the CNT and CD (74). In addition, vasopressin also acutely stimulates the insertion of ENaC channels into the apical membrane of the cell (75, 76).

Parathyroid hormone (PTH)

PTH is released from the parathyroid glands in response to changes in the systemic Ca^{2+} concentration. The organ detects very small changes in the serum Ca^{2+} via the Ca^{2+} -sensing receptor (CaSR), and responds by releasing PTH when serum Ca^{2+} is low and *vice versa*. PTH acts on several organs, including the kidney, intestine, and bone to increase Ca^{2+} (re-) absorption and release. The distal convoluted tubule is also a target of PTH (77), here the hormone stimulates Ca^{2+} transport on multiple levels. Parathyroidectomy causes hypocalcemia due to a reduction in circulating PTH concentrations. In rats, this procedure decreases the renal abundance of the Ca^{2+} -transport proteins TRPV5, calbindin- $\text{D}_{28\text{K}}$, and NCX1 (78). Using primary isolated rabbit CNT/cortical CD (CCD) cultures, it has been shown that PTH application stimulates transepithelial Ca^{2+} transport (79). It was subsequently delineated that PTH stimulates

General introduction

TRPV5 activity via a protein kinase A signaling cascade, which phosphorylates the channel, increasing open probability and hence Ca^{2+} reabsorption (80).

1,25-dihydroxyvitamin D₃

1,25-dihydroxyvitamin D₃ is a key regulator of Ca^{2+} handling. The hormone undergoes several conversion steps, including the final 1α -hydroxylation in the kidney, which leads to biologically active 1,25-dihydroxyvitamin D₃ (81). Dietary Ca^{2+} and PTH both regulate 1α -hydroxylase activity in the kidney. The main effect of 1,25-dihydroxyvitamin D₃ is in the intestine, but the hormone also modulates Ca^{2+} transport in the distal convoluted tubule. 1,25-dihydroxyvitamin D₃ stimulates transepithelial Ca^{2+} transport in rabbit primary CNT/CCD cultures (79). In line with this observation, is the increased expression of TRPV5 in the presence of 1,25-dihydroxyvitamin D₃ (57). Calbindin D_{28k} expression is also regulated by 1,25-dihydroxyvitamin D₃.

Estrogen and gender

Gender-associated differences can be noted in the urinary excretion of Na^+ and can be related to the actions of sex hormones on the kidney. As such, estrogen is known to reduce the urinary Na^+ excretion (82). In line with this, is the apparent higher abundance of NCC in the distal convoluted tubule of female rats, compared to that of males (83). The effects of estrogen on renal Na^+ excretion, may be related to its actions on the renin-angiotensin-aldosterone system (84). Removal of testosterone from males also increases the expression of NCC, suggesting an opposing relationship between the two hormones.

Several studies have reported gender differences in the urinary Ca^{2+} excretion, with greater urinary Ca^{2+} losses occurring in males (85, 86). Estrogens have been shown to increase the renal reabsorption of Ca^{2+} , which would explain the observed gender differences (87). This augmentation in Ca^{2+} reabsorption has subsequently shown to coincide with an increase in the abundance of TRPV5 (87). Whether testosterone plays opposing roles to that of estrogen

Chapter 1

remains unclear.

Estrogens also affect renal Mg^{2+} handling, as urinary Mg^{2+} losses in postmenopausal women is significantly decreased after estrogen replacement (88, 89). Lack of estrogens also reduce the abundance of TRPM6 in rats, while re-supplementation normalizes the expression, in line with the renal effects of estrogen (43).

Calcitonin (CT)

CT is synthesized by the C cells of the thyroid gland and is secreted in response to increases in the systemic Ca^{2+} concentration (90). This is largely achieved by inhibiting osteoclast-mediated bone resorption. In the kidney, CT stimulates the reabsorption of Ca^{2+} (91-94). This is in part achieved by increasing the reabsorption of Ca^{2+} in the thick ascending limb (91-93). However, additional actions of CT on the distal convoluted tubule have also been reported, where the hormone stimulates the vectorial movement of Ca^{2+} (94).

Transport defects affecting electrolyte handling in the distal convoluted tubule

Gitelman's syndrome

Gitelman's syndrome is a salt-losing disorder characterized by hypokalemic metabolic alkalosis, hypomagnesemia, and hypocalciuria (95). Renin activity and aldosterone concentrations are elevated, but only marginally in comparison to Bartter's patients. The disorder is autosomal recessive and is caused by mutations in the gene encoding the thiazide-sensitive NaCl transporter NCC (*Slc12a3*) (96). The Gitelman phenotype is mimicked by chronic thiazide treatment, a potent blocker of NCC (97, 98). The loss of NaCl from the DCT leads to a compensatory increase in Na^+ reabsorption segments distal to the DCT. This compensation is largely responsible for the hypokalemia observed in Gitelman patients. Mice with a targeted deletion of NCC show no mean arterial pressure variation when maintained on a normal diet.

General introduction

However, when reducing dietary NaCl content, NCC deficient mice develop hypotension (99).

The hypocalciuric effect of NCC gene deletion or chronic thiazide administration is likely due to hypovolemia, although some reports have suggested an additional direct effect on Ca^{2+} reabsorption in the distal convolutions (100, 101). Volume contraction causes secondary increases in proximal tubular Na^+ transport, and thus facilitates paracellular hyperabsorption of Ca^{2+} . This is supported by several observations. Micropuncture studies in mice with genetic ablation of the NCC gene, showed a reduced delivery of Na^+ and Ca^{2+} to the late PT, consistent with increased Na^+ and Ca^{2+} reabsorption in the PT. In addition, these micropuncture experiments indicate that Ca^{2+} reabsorptive rates were similar in the distal convolutions in the wild-type and NCC deficient mice, further confirming that the effect is proximal (102). In wild-type mice administered thiazide diuretics, similar observations were made using micropuncture studies, suggesting that the hypocalciuric effect localizes to the PT (103). Furthermore, thiazide-induced hypocalciuria can still be observed in TRPV5 deficient mice, which effectively lack Ca^{2+} transport in the distal convolutions (103). This nicely confirms that the mechanism by which hypocalciuria develops after thiazide usage and likely also in Gitelman's syndrome is independent of distal Ca^{2+} reabsorption.

Hypomagnesemia is a consistent feature of Gitelman's syndrome. The phenotypic characteristic is likely the result of a decreased abundance of TRPM6, leading to renal Mg^{2+} wasting. However, the mechanism that decreases renal TRPM6 expression in Gitelman's syndrome remains incompletely understood. Mice deficient in NCC as well as rats given thiazides show severe atrophy of the DCT (i.e. the fractional volume of the early DCT is drastically reduced) (102, 104). In addition, NCC-deficient mice show a decreased expression of TRPM6, which localizes intrarenally solely within the DCT (103). Interestingly, in contrast to previous results, administration of lower doses of thiazides, produce no changes in the morphology of the DCT, while expression of TRPM6 remains decreased (103). Aldosteronism, a recurring feature of Gitelman's syndrome, has been implicated in renal Mg^{2+} wasting (105-107).

Chapter 1

Similarly, lack of aldosterone can be associated with hypermagnesemia (105, 106). Spironolactone, a mineralocorticoid receptor antagonist has been shown to consistently reduce urinary Mg^{2+} excretion in a number of patient groups (105, 106, 108). In patients with Gitelman's syndrome, spironolactone treatment increases serum Mg^{2+} concentration and reduces the fractional tubular excretion of Mg^{2+} (108). Thus, these studies suggest that the apparent aldosterone excess observed in Gitelman's syndrome might be an underlying cause. Conversely, chronic infusion of aldosterone does not change the renal mRNA abundance of TRPM6 in mice (107). Moreover, marked hyperaldosteronism is observed in antenatal Bartter's patients, while less than 20% of these individuals display hypomagnesemia. The positive effect of spironolactone on Mg^{2+} balance deserves further research. Currently, the absence of NCC in DCT has been shown to induce hypocalciuria via changes in PT reabsorption and hypomagnesemia by reducing TRPM6 expression.

Pseudohypoaldosteronism type II (PHAII)

The WNK kinase family consists of serine-threonine kinases with a characteristic displacement of a catalytic lysine residue, necessary for ATP binding (109, 110). The recent identification of the WNK family members as multifunctional proteins required for ambient blood pressure maintenance and renal electrolyte handling has progressively broadened the knowledge of how these processes are regulated (111, 112). PHAII, also known as Gordon syndrome, is an autosomal dominant disorder associated with hypertension, an augmented renal reabsorption of NaCl, and impaired secretion of K^+ and H^+ (112, 113). The genetic defects in PHAII are due to loss-of-function mutations in WNK4 as well as activating mutations in WNK1 caused by intronic deletions in the gene (112). Several studies have now shown that WNK1 and WNK4 play important roles in modulating electrolyte transport pathways in the distal convolutions (114-117). WNK4 functions primarily by inhibiting thiazide-sensitive transport, by removing NCC from the membrane into lysosomal compartments (114, 118, 119). In addition, the inhibitory actions of

General introduction

WNK1 and WNK4 influence membrane abundance and hence activity of the transporter (114, 117). WNK4 also inhibits ENaC (120), while both WNKs impair K^+ secretion via ROMK (115, 116, 121).

In addition to the often hypertensive phenotype, hypercalciuria and nephrolithiasis have been reported in PHAI patients (122, 123). Accordingly, individuals carrying a WNK4 Q565E PHAI mutation, present with hypercalciuria and a decreased bone mineral density. Conversely, affected members with activating WNK1 mutations, present with normocalciuria (124). It is interesting to note that no apparent change is observed in serum Mg^{2+} concentrations or renal Mg^{2+} handling of PHAI patients (124-126). The mechanism by which dysfunctional WNK4 stimulates calciuria in PHAI is unclear, but may occur via several mechanisms: *i*) Secondary to volume expansion, a condition that is predicted to reduce proximal tubule Na^+ reabsorption, resulting in decreased electrochemical driving force for Ca^{2+} uptake across the PT epithelia (103, 127, 128). As the majority of Ca^{2+} reabsorption occurs in the proximal tubule, volume expansion might be the largest contributor to the hypercalciuria in PHAI. Even so, individuals carrying the WNK1 deletion have normocalciuria, in the presence of elevated blood pressure (and likely an expanded ECV); *ii*) Alternatively, the hypercalciuric phenotype in PHAI may be due to impaired interactions between WNK4 and renal Ca^{2+} transport proteins (129). In line with this, it has been reported that WNK4 directly activates Ca^{2+} transport by increasing surface expression TRPV5 in the *Xenopus* oocyte expression system (129). However, the WNK4 PHAI mutants showed a similar activating effect on TRPV5. Using lentivirus-induced gene delivery to primary rabbit CNT/CD cells, we found that cells infected with WNK4 and the WNK4 Q565E mutant, both decreased transepithelial Ca^{2+} transport (Dimke, Hoenderop, and Bindels, unpublished observations). Consequently, the exact etiology behind the hypercalcemia in PHAI needs further clarification. It is interesting to note, that while PHAI is considered as a mirror image of Gitelman's syndrome, no changes in serum Mg^{2+} have been observed in these individuals.

Chapter 1

Hypomagnesemia with secondary hypocalcemia (HSH)

TRPM6 was originally identified as the causative gene of the autosomal recessive disorder known as HSH (44, 130). Individuals suffering from HSH present in early infancy with symptoms related to neuromuscular excitability, such as muscle spasms, tetany, and generalized convulsions (131). These symptoms likely occur as a consequence of a severe fall in plasma Mg^{2+} and Ca^{2+} concentrations. Symptoms can be reduced by high dose Mg^{2+} administration. Interestingly, this Mg^{2+} supplementation normalizes the plasma Ca^{2+} concentration, while plasma Mg^{2+} remains subnormal (132). A patient with HSH displayed failure to effectively absorb Mg^{2+} from low intraluminal intestinal Mg^{2+} concentrations (133). However, the HSH patient had a positive Ca^{2+} balance, excluding a common defect in Mg^{2+} and Ca^{2+} transport mechanisms. These data support a role for TRPM6 in saturable active Mg^{2+} transport, serving as an apical entry mechanism for Mg^{2+} in the enterocyte. Although the hypomagnesemia in HSH appears to be primarily the result of mal-absorption of Mg^{2+} in the intestine, there is also a serious, although not well studied renal Mg^{2+} leak. HSH patients have been reported to display either normal renal Mg^{2+} conservation (132-134), or show an additional renal Mg^{2+} leak (44, 130, 135). However, when patients with HSH were administered an intravenous Mg^{2+} load, renal wasting was clearly noticeable (130). Thus, these individuals waste urinary Mg^{2+} at a lower plasma concentration, than normal individuals do. Agus previously described that maintaining a fractional Mg^{2+} excretion above 2% in the presence of hypomagnesemia should be considered a renal leak in itself (136). This is corroborated by a report showing an inappropriately high fractional excretion given severe hypomagnesemia in HSH patients (44).

Isolated autosomal recessive hypomagnesemia (IRH)

This rare form of hypomagnesemia was initially described in two siblings who presented with low serum Mg^{2+} concentrations and an inappropriately high fractional excretion of Mg^{2+} . In addition, these individuals suffered from psychomotor retardation during their youth and are presently

General introduction

suffering from moderate mental retardation and epileptic seizures (137, 138). Thus, these observations indicated a potential defect largely related to the renal Mg^{2+} transport, similar to that observed for Mg^{2+} loaded patients with HSH. Interestingly, there were no observable secondary changes in the handling of Ca^{2+} (137), which may to some extent explain why these patients are devoid of tetany. Detailed homozygosity mapping approaches and direct sequencing revealed that these sisters had a mutation in the pro-epidermal growth factor (EGF) gene, causing a defect in the routing of the EGF precursor to the basolateral plasma membrane (138). This mutation resulted in impaired autocrine/paracrine secretion of EGF to the interstitium, thereby inhibiting the activation of basolateral EGF receptors (EGFR) in the DCT. Subsequent patch clamp analysis and classical biochemical experiments showed that application of EGF activates TRPM6 and shuttles it from endomembrane compartments to the membrane (138, 139). Interestingly, inhibition of the EGFR by monoclonal antibodies targeting the EGFR (Cetuximab) causes pronounced hypomagnesemia in colorectal cancer patients (138, 140). Unlike patients with impaired sorting of the EGF protein, cetuximab treatment produces secondary hypocalcemia in patients with moderate to severe hypomagnesemia (grade 2 or higher), likely resulting from impaired PTH secretion (140). Similarly, patients with severe hypomagnesemia did show signs of fatigue and cramps. The syndrome of IRH and related inhibition of the EGFR by cetuximab diverges from HSH in several of the phenotypic characteristics, suggesting additional effects of EGF on Mg^{2+} handling. Incubation of TRPM6 expressing cells with cetuximab completely abolishes the EGF-induced increases in channel currents. Unlike TRPM6, current literature suggests that TRPM7 is not activated by EGF and thus appears an unlikely target (139). Whether other transporters are involved in conferring hypomagnesemia in IRH remains to be defined. Taken together, these results indicate that EGF is a novel magnesiotropic factor acting primarily to increase renal Mg^{2+} reabsorption.

Chapter 1

Aims of the thesis

This thesis aims to understand the physiological implications of regulating transport within the distal convolution of the kidney. Dissecting the molecular mechanisms responsible for transepithelial electrolyte transport in these nephron segments, allows us to extrapolate how these processes may impact overall electrolyte homeostasis.

NCC plays a key role in renal salt reabsorption and thereby the maintenance of systemic blood pressure. A better understanding of the regulation of NaCl transport by NCC may ultimately increase our understanding of how blood pressure is maintained and the etiology underlying primary hypertension. In an effort to understand how NCC is regulated, we performed pull-down experiments using the N-terminal domain as bait and subsequently screened binding partners from mouse kidney by mass spectrometry. In **chapter 2** we describe the identification of γ -adducin, a novel regulator of NCC that functions by interacting with the phosphorylatable N-terminal domain of the cotransporter.

Monoclonal antibodies such as Cetuximab targeting the extracellular EGFR domain have been implicated in the regulation of epithelial Mg^{2+} transport. While mostly patients with colorectal cancer are treated with Cetuximab, numerous patient groups suffering from cancer receive the EGFR tyrosine kinase inhibitor, Erlotinib. To better understand the role of EGFR blockade in cancer patients and its relevance for managing hypomagnesemia, **chapter 3** details the effects of the EGFR inhibitor Erlotinib on renal and systemic Mg^{2+} handling.

Regulation of systemic Ca^{2+} balance is of major importance for the maintenance of many physiological processes such as neuromuscular stability, bone formation etc. Thus, understanding how hormones and molecular factors regulate TRPV5 may help elucidate how serum Ca^{2+} is maintained and how it is perturbed in pathophysiological conditions. As such, the overall contribution of androgens to gender differences in renal handling of Ca^{2+} and hence overall Ca^{2+} balance remains unclear. Therefore, **chapter 4** investigates the effect of testosterone on the expression of renal Ca^{2+} transport proteins and the urinary Ca^{2+} excretion.

General introduction

Similarly, **chapter 5** delineates the potential role of TRPV5 in the calcitonin-stimulated Ca^{2+} reabsorption. Tissue transglutaminase is a Ca^{2+} dependent enzyme involved in covalent crosslinking of proteins and is regulated by TRPV channels, however it remains unclear whether TRPV5 could be regulated as well. **Chapter 6** shows that tissue transglutaminase functions as a novel molecular inhibitor of TRPV5.

Hypercalciuria is the most common abnormality found in individuals with Ca^{2+} stone formation. As Ca^{2+} transport is an integral part of the distal convoluted tubule, dysregulation thereof may cause kidney stone disease (nephrolithiasis). Nephrolithiasis is a global health problem that affects approximately 10% of the population by the seventh decade of life. Utilizing a *N*-ethyl-*N*-nitrosourea mouse mutagenesis resource to identify new genetic models of hypercalciuria, **chapter 7** characterized a novel mouse model with an autosomal dominant serine 682 proline missense mutation in TRPV5 resulting in hypercalciuria and tubulointerstitial nephritis.

Chapter 8 summarizes the findings made within the frame of this thesis and provides a detailed discussion pertaining to these observations, by placing them in the context of the current knowledge regarding the distal convoluted tubule and renal electrolyte handling.

Chapter 1

References

1. Dai LJ, Ritchie G, Kerstan D, Kang HS, Cole DE, Quamme GA. Mg^{2+} transport in the renal distal convoluted tubule. *Physiol Rev.* 2001;81(1):51-84.
2. Hoenderop JG, Nilius B, Bindels RJ. Ca^{2+} absorption across epithelia. *Physiol Rev.* 2005;85(1):373-422.
3. Khuri RN, Strieder N, Wiederholt M, Giebisch G. Effects of graded solute diuresis on renal tubular Na^+ transport in the rat. *Am J Physiol.* 1975;228(4):1262-1268.
4. Kunau RT, Jr., Webb HL, Borman SC. Characteristics of Na^+ reabsorption in the loop of Henle and distal tubule. *Am J Physiol.* 1974;227(5):1181-1191.
5. Stein JH, Osgood RW, Boonjarern S, Cox JW, Ferris TF. Segmental Na^+ reabsorption in rats with mild and severe volume depletion. *Am J Physiol.* 1974;227(2):351-359.
6. Kriz W, Bankir L. A standard nomenclature for structures of the kidney. The Renal Commission of the International Union of Physiological Sciences (IUPS). *Kidney Int.* 1988;33(1):1-7.
7. Loffing J, Kaissling B. Na^+ and Ca^{2+} transport pathways along the mammalian distal nephron: from rabbit to human. *Am J Physiol Renal Physiol.* 2003;284(4):F628-643.
8. Loffing J, Loffing-Cueni D, Valderrabano V, Klausli L, Hebert SC, Rossier BC, Hoenderop JG, Bindels RJ, Kaissling B. Distribution of transcellular Ca^{2+} and Na^+ transport pathways along mouse distal nephron. *Am J Physiol Renal Physiol.* 2001;281(6):F1021-1027.
9. Almeida AJ, Burg MB. Na^+ transport in the rabbit connecting tubule. *Am J Physiol.* 1982;243(4):F330-334.
10. Obermuller N, Bernstein P, Velazquez H, Reilly R, Moser D, Ellison DH, Bachmann S. Expression of the thiazide-sensitive NaCl cotransporter in rat and human kidney. *Am J Physiol.* 1995;269(6 Pt 2):F900-910.
11. Reilly RF, Ellison DH. Mammalian Distal Tubule: Physiology, Pathophysiology, and Molecular Anatomy. *Physiol. Rev.* 2000;80(1):277-313.
12. Malnic G, Giebisch G. Some electrical properties of distal tubular epithelium in the rat. *Am J Physiol.* 1972;223(4):797-808.
13. Wright FS. Increasing magnitude of electrical potential along the renal distal tubule. *Am J Physiol.* 1971;220(3):624-638.
14. Giebisch G, Malnic G, Klose RM, Windhager EE. Effect of ionic substitutions on distal potential differences in rat kidney. *Am J Physiol.* 1966;211(3):560-568.
15. Solomon S. Transtubular potential differences of rat kidney. *J Cell Physiol.* 1957;49(2):351-365.
16. Malnic G, Klose RM, Giebisch G. Micropuncture study of distal tubular K^+ and Na^+ transport in rat nephron. *Am J Physiol.* 1966;211(3):529-547.
17. Ellison DH, Velazquez H, Wright FS. Adaptation of the distal convoluted tubule of the rat. Structural and functional effects of dietary salt intake and chronic diuretic infusion. *J Clin*

General introduction

- Invest.* 1989;83(1):113-126.
18. Ellison DH, Velazquez H, Wright FS. Thiazide-sensitive NaCl cotransport in early distal tubule. *Am J Physiol.* 1987;253(3 Pt 2):F546-554.
 19. Gamba G, Saltzberg SN, Lombardi M, Miyanoshita A, Lytton J, Hediger MA, Brenner BM, Hebert SC. Primary structure and functional expression of a cDNA encoding the thiazide-sensitive, electroneutral NaCl cotransporter. *Proc Natl Acad Sci U S A.* 1993;90(7):2749-2753.
 20. Bostanjoglo M, Reeves WB, Reilly RF, Velazquez H, Robertson N, Litwack G, Morsing P, Dorup J, Bachmann S, Ellison DH. 11Beta-hydroxysteroid dehydrogenase, mineralocorticoid receptor, and thiazide-sensitive NaCl cotransporter expression by distal tubules. *J Am Soc Nephrol.* 1998;9(8):1347-1358.
 21. Kim GH, Masilamani S, Turner R, Mitchell C, Wade JB, Knepper MA. The thiazide-sensitive NaCl cotransporter is an aldosterone-induced protein. *Proc Natl Acad Sci U S A.* 1998;95(24):14552-14557.
 22. Plotkin MD, Kaplan MR, Verlander JW, Lee WS, Brown D, Poch E, Gullans SR, Hebert SC. Localization of the thiazide sensitive NaCl cotransporter, rTSC1 in the rat kidney. *Kidney Int.* 1996;50(1):174-183.
 23. Kashgarian M, Biemesderfer D, Caplan M, Forbush B, 3rd. Monoclonal antibody to Na⁺,K⁺-ATPase: immunocytochemical localization along nephron segments. *Kidney Int.* 1985;28(6):899-913.
 24. Yoshikawa M, Uchida S, Yamauchi A, Miyai A, Tanaka Y, Sasaki S, Marumo F. Localization of rat CLC-K2 Cl⁻ channel mRNA in the kidney. *Am J Physiol.* 1999;276(4 Pt 2):F552-558.
 25. Brunette MG, Vigneault N, Carriere S. Micropuncture study of Mg²⁺ transport along the nephron in the young rat. *Am J Physiol.* 1974;227(4):891-896.
 26. Le Grimellec C, Roinel N, Morel F. Simultaneous Mg²⁺, Ca²⁺, PO₃⁴⁻,K⁺, Na⁺ and Cl⁻ analysis in rat tubular fluid. I. During perfusion of either inulin or ferrocyanide. *Pflugers Arch.* 1973;340(3):181-196.
 27. Bailly C, Roinel N, Amiel C. Stimulation by glucagon and PTH of Ca²⁺ and Mg²⁺ reabsorption in the superficial distal tubule of the rat kidney. *Pflugers Arch.* 1985;403(1):28-34.
 28. Greger R, Velazquez H. The cortical thick ascending limb and early distal convoluted tubule in the urinary concentrating mechanism. *Kidney Int.* 1987;31(2):590-596.
 29. Quamme GA, Dirks JH. Intraluminal and contraluminal Mg²⁺ on Mg²⁺ and Ca²⁺ transfer in the rat nephron. *Am J Physiol.* 1980;238(3):F187-198.
 30. Grubbs RD. Intracellular Mg²⁺ and Mg²⁺ buffering. *Biometals.* 2002;15(3):251-259.
 31. Quamme GA, Dai LJ. Presence of a novel influx pathway for Mg²⁺ in MDCK cells. *Am J Physiol.* 1990;259(3 Pt 1):C521-525.

Chapter 1

32. Cohen B, Giebisch G, Hansen LL, Teuscher U, Wiederholt M. Relationship between peritubular membrane potential and net fluid reabsorption in the distal renal tubule of *Amphiuma*. *J Physiol*. 1984;348(115-134).
33. Hansen LL, Schilling AR, Wiederholt M. Effect of Ca^{2+} , furosemide and chlorothiazide on net volume reabsorption and basolateral membrane potential of the distal tubule. *Pflugers Arch*. 1981;389(2):121-126.
34. Quamme GA. Effect of furosemide on Ca^{2+} and Mg^{2+} transport in the rat nephron. *Am J Physiol*. 1981;241(4):F340-347.
35. Voets T, Nilius B, Hoefs S, van der Kemp AW, Droogmans G, Bindels RJ, Hoenderop JG. TRPM6 forms the Mg^{2+} influx channel involved in intestinal and renal Mg^{2+} absorption. *J Biol Chem*. 2004;279(1):19-25.
36. Montell C. Mg^{2+} homeostasis: the Mg^{2+} -sensitive TRPM channel kinases. *Curr Biol*. 2003;13(20):R799-801.
37. Li M, Du J, Jiang J, Ratzan W, Su LT, Runnels LW, Yue L. Molecular determinants of Mg^{2+} and Ca^{2+} permeability and pH sensitivity in TRPM6 and TRPM7. *J Biol Chem*. 2007;282(35):25817-25830.
38. Li M, Jiang J, Yue L. Functional characterization of homo- and heteromeric channel kinases TRPM6 and TRPM7. *J Gen Physiol*. 2006;127(5):525-537.
39. Chubanov V, Schlingmann KP, Waring J, Heinzinger J, Kaske S, Waldegger S, Schnitzler MM, Gudermann T. Hypomagnesemia with secondary hypocalcemia due to a missense mutation in the putative pore-forming region of TRPM6. *J Biol Chem*. 2007;282(10):7656-7667.
40. Chubanov V, Waldegger S, Mederos y Schnitzler M, Vitzthum H, Sassen MC, Seyberth HW, Konrad M, Gudermann T. Disruption of TRPM6/TRPM7 complex formation by a mutation in the TRPM6 gene causes hypomagnesemia with secondary hypocalcemia. *Proc Natl Acad Sci U S A*. 2004;101(9):2894-2899.
41. Schlingmann KP, Gudermann T. A critical role of TRPM channel-kinase for human Mg^{2+} transport. *J Physiol*. 2005;566(Pt 2):301-308.
42. Schmitz C, Dorovkov MV, Zhao X, Davenport BJ, Ryazanov AG, Perraud AL. The channel kinases TRPM6 and TRPM7 are functionally nonredundant. *J Biol Chem*. 2005;280(45):37763-37771.
43. Groenestege WM, Hoenderop JG, van den Heuvel L, Knoers N, Bindels RJ. The epithelial Mg^{2+} channel transient receptor potential melastatin 6 is regulated by dietary Mg^{2+} content and estrogens. *J Am Soc Nephrol*. 2006;17(4):1035-1043.
44. Schlingmann KP, Weber S, Peters M, Niemann Nejsum L, Vitzthum H, Klingel K, Kratz M, Haddad E, Ristoff E, Dinour D, et al. Hypomagnesemia with secondary hypocalcemia is caused by mutations in TRPM6, a new member of the TRPM gene family. *Nat Genet*. 2002;31(2):166-170.

General introduction

45. Loffing J, Pietri L, Aregger F, Bloch-Faure M, Ziegler U, Meneton P, Rossier BC, Kaissling B. Differential subcellular localization of ENaC subunits in mouse kidney in response to high- and low-Na⁺ diets. *Am J Physiol Renal Physiol.* 2000;279(2):F252-258.
46. Sauter D, Fernandes S, Goncalves-Mendes N, Boulkroun S, Bankir L, Loffing J, Bouby N. Long-term effects of vasopressin on the subcellular localization of ENaC in the renal collecting system. *Kidney Int.* 2006;69(6):1024-1032.
47. Canessa CM, Schild L, Buell G, Thorens B, Gautschi I, Horisberger JD, Rossier BC. Amiloride-sensitive epithelial Na⁺ channel is made of three homologous subunits. *Nature.* 1994;367(6462):463-467.
48. Feraille E, Mordasini D, Gonin S, Deschenes G, Vinciguerra M, Doucet A, Vandewalle A, Summa V, Verrey F, Martin PY. Mechanism of control of Na⁺,K⁺-ATPase in principal cells of the mammalian collecting duct. *Ann N Y Acad Sci.* 2003;986(570-578).
49. Kohda Y, Ding W, Phan E, Housini I, Wang J, Star RA, Huang CL. Localization of the ROMK K⁺ channel to the apical membrane of distal nephron in rat kidney. *Kidney Int.* 1998;54(4):1214-1223.
50. Mennitt PA, Wade JB, Ecelbarger CA, Palmer LG, Frindt G. Localization of ROMK channels in the rat kidney. *J Am Soc Nephrol.* 1997;8(12):1823-1830.
51. Xu JZ, Hall AE, Peterson LN, Bienkowski MJ, Eessalu TE, Hebert SC. Localization of the ROMK protein on apical membranes of rat kidney nephron segments. *Am J Physiol.* 1997;273(5 Pt 2):F739-748.
52. Nielsen S, DiGiovanni SR, Christensen EI, Knepper MA, Harris HW. Cellular and subcellular immunolocalization of vasopressin-regulated water channel in rat kidney. *Proc Natl Acad Sci U S A.* 1993;90(24):11663-11667.
53. Agus ZS, Chiu PJ, Goldberg M. Regulation of urinary Ca²⁺ excretion in the rat. *Am J Physiol.* 1977;232(6):F545-549.
54. Lassiter WE, Gottschalk CW, Mylle M. Micropuncture study of renal tubular reabsorption of Ca²⁺ in normal rodents. *Am J Physiol.* 1963;204(5):771-775.
55. Hoenderop JG, van der Kemp AW, Hartog A, van de Graaf SF, van Os CH, Willems PH, Bindels RJ. Molecular identification of the apical Ca²⁺ channel in 1, 25-dihydroxyvitamin D₃-responsive epithelia. *J Biol Chem.* 1999;274(13):8375-8378.
56. Hoenderop JG, Hartog A, Stuijver M, Doucet A, Willems PH, Bindels RJ. Localization of the epithelial Ca²⁺ channel in rabbit kidney and intestine. *J Am Soc Nephrol.* 2000;11(7):1171-1178.
57. Hoenderop JG, Muller D, Van Der Kemp AW, Hartog A, Suzuki M, Ishibashi K, Imai M, Sweep F, Willems PH, Van Os CH, et al. Calcitriol controls the epithelial Ca²⁺ channel in kidney. *J Am Soc Nephrol.* 2001;12(7):1342-1349.
58. Hofmeister MV, Fenton RA, Praetorius J. Fluorescence-isolation of mouse late distal convoluted tubules and connecting tubules: effects of vasopressin and vitamin D₃ on Ca²⁺

Chapter 1

- signaling. *Am J Physiol Renal Physiol*. 2008.
59. Hoenderop JG, van Leeuwen JP, van der Eerden BC, Kersten FF, van der Kemp AW, Merillat AM, Waarsing JH, Rossier BC, Vallon V, Hummler E, et al. Renal Ca²⁺ wasting, hyperabsorption, and reduced bone thickness in mice lacking TRPV5. *J Clin Invest*. 2003;112(12):1906-1914.
 60. Renkema KY, Lee K, Topala CN, Goossens M, Houillier P, Bindels RJ, Hoenderop JG. TRPV5 gene polymorphisms in renal hypercalciuria. *Nephrol Dial Transplant*. 2009.
 61. Chen Z, Vaughn DA, Blakely P, Fanestil DD. Adrenocortical steroids increase renal thiazide diuretic receptor density and response. *J Am Soc Nephrol*. 1994;5(6):1361-1368.
 62. Velazquez H, Bartiss A, Bernstein P, Ellison DH. Adrenal steroids stimulate thiazide-sensitive NaCl transport by rat renal distal tubules. *Am J Physiol*. 1996;270(1 Pt 2):F211-219.
 63. Garty H, Palmer LG. Epithelial Na⁺ channels: function, structure, and regulation. *Physiol Rev*. 1997;77(2):359-396.
 64. Loffing J, Zecevic M, Feraille E, Kaissling B, Asher C, Rossier BC, Firestone GL, Pearce D, Verrey F. Aldosterone induces rapid apical translocation of ENaC in early portion of renal collecting system: possible role of SGK. *Am J Physiol Renal Physiol*. 2001;280(4):F675-682.
 65. Masilamani S, Kim GH, Mitchell C, Wade JB, Knepper MA. Aldosterone-mediated regulation of ENaC alpha, beta, and gamma subunit proteins in rat kidney. *J Clin Invest*. 1999;104(7):R19-23.
 66. Beesley AH, Hornby D, White SJ. Regulation of distal nephron K⁺ channels (ROMK) mRNA expression by aldosterone in rat kidney. *J Physiol*. 1998;509 (Pt 3):629-634.
 67. Madala Halagappa VK, Tiwari S, Riaz S, Hu X, Ecelbarger CM. Chronic candesartan alters expression and activity of NKCC2, NCC, and ENaC in the obese Zucker rat. *Am J Physiol Renal Physiol*. 2008;294(5):F1222-1231.
 68. Beutler KT, Masilamani S, Turban S, Nielsen J, Brooks HL, Ageloff S, Fenton RA, Packer RK, Knepper MA. Long-term regulation of ENaC expression in kidney by angiotensin II. *Hypertension*. 2003;41(5):1143-1150.
 69. Sandberg MB, Riquier AD, Pihakaski-Maunsbach K, McDonough AA, Maunsbach AB. ANG II provokes acute trafficking of distal tubule NaCl cotransporter to apical membrane. *Am J Physiol Renal Physiol*. 2007;293(3):F662-669.
 70. San-Cristobal P, Pacheco-Alvarez D, Richardson C, Ring AM, Vazquez N, Rafiqi FH, Chari D, Kahle KT, Leng Q, Bobadilla NA, et al. Angiotensin II signaling increases activity of the renal NaCl cotransporter through a WNK4-SPAK-dependent pathway. *Proc Natl Acad Sci U S A*. 2009;106(11):4384-4389.
 71. Wang T, Giebisch G. Effects of angiotensin II on electrolyte transport in the early and late distal tubule in rat kidney. *Am J Physiol*. 1996;271(1 Pt 2):F143-149.

General introduction

72. Pedersen NB, Hofmeister MV, Rosenbaek LL, Nielsen J, Fenton RA. Vasopressin induces phosphorylation of the thiazide-sensitive NaCl cotransporter in the distal convoluted tubule. *Kidney Int.*
73. Bankir L, Fernandes S, Bardoux P, Bouby N, Bichet DG. Vasopressin-V2 receptor stimulation reduces Na⁺ excretion in healthy humans. *J Am Soc Nephrol.* 2005;16(7):1920-1928.
74. Ecelbarger CA, Kim GH, Terris J, Masilamani S, Mitchell C, Reyes I, Verbalis JG, Knepper MA. Vasopressin-mediated regulation of epithelial Na⁺ channel abundance in rat kidney. *Am J Physiol Renal Physiol.* 2000;279(1):F46-53.
75. Butterworth MB, Edinger RS, Johnson JP, Frizzell RA. Acute ENaC stimulation by cAMP in a kidney cell line is mediated by exocytic insertion from a recycling channel pool. *J Gen Physiol.* 2005;125(1):81-101.
76. Morris RG, Schafer JA. cAMP increases density of ENaC subunits in the apical membrane of MDCK cells in direct proportion to amiloride-sensitive Na⁺ transport. *J Gen Physiol.* 2002;120(1):71-85.
77. Greger R, Lang F, Oberleithner H. Distal site of Ca²⁺ reabsorption in the rat nephron. *Pflugers Arch.* 1978;374(2):153-157.
78. van Abel M, Hoenderop JG, van der Kemp AW, Friedlaender MM, van Leeuwen JP, Bindels RJ. Coordinated control of renal Ca²⁺ transport proteins by parathyroid hormone. *Kidney Int.* 2005;68(4):1708-1721.
79. Bindels RJ, Hartog A, Timmermans J, Van Os CH. Active Ca²⁺ transport in primary cultures of rabbit kidney CCD: stimulation by 1,25-dihydroxyvitamin D₃ and PTH. *Am J Physiol.* 1991;261(5 Pt 2):F799-807.
80. de Groot T, Lee K, Langeslag M, Xi Q, Jalink K, Bindels RJ, Hoenderop JG. Parathyroid hormone activates TRPV5 via PKA-dependent phosphorylation. *J Am Soc Nephrol.* 2009;20(8):1693-1704.
81. Fraser DR, Kodicek E. Unique biosynthesis by kidney of a biological active vitamin D metabolite. *Nature.* 1970;228(5273):764-766.
82. Christy NP, Shaver JC. Estrogens and the kidney. *Kidney Int.* 1974;6(5):366-376.
83. Chen Z, Vaughn DA, Fanestil DD. Influence of gender on renal thiazide diuretic receptor density and response. *J Am Soc Nephrol.* 1994;5(4):1112-1119.
84. Oelkers WK. Effects of estrogens and progestogens on the renin-aldosterone system and blood pressure. *Steroids.* 1996;61(4):166-171.
85. Morgan B, Robertson WG. The urinary excretion of Ca²⁺. An analysis of the distribution of values in relation to sex, age and Ca²⁺ deprivation. *Clin Orthop Relat Res.* 1974;101):254-267.
86. Davis RH, Morgan DB, Rivlin RS. The excretion of Ca²⁺ in the urine and its relation to Ca²⁺ intake, sex and age. *Clin Sci.* 1970;39(1):1-12.

Chapter 1

87. Van Abel M, Hoenderop JG, Dardenne O, St Arnaud R, Van Os CH, Van Leeuwen HJ, Bindels RJ. 1,25-dihydroxyvitamin D(3)-independent stimulatory effect of estrogen on the expression of ECaC1 in the kidney. *J Am Soc Nephrol*. 2002;13(8):2102-2109.
88. McNair P, Christiansen C, Transbol I. Effect of menopause and estrogen substitutional therapy on Mg²⁺ metabolism. *Miner Electrolyte Metab*. 1984;10(2):84-87.
89. Schlemmer A, Podenphant J, Riis BJ, Christiansen C. Urinary mg²⁺ in early postmenopausal women. Influence of hormone therapy on Ca²⁺. *Magnes Trace Elem*. 1991;10(1):34-39.
90. Pondel M. Calcitonin and calcitonin receptors: bone and beyond. *Int J Exp Pathol*. 2000;81(6):405-422.
91. Vuillemin T, Teulon J, Geniteau-Legendre M, Baudouin B, Estrade S, Cassingena R, Ronco P, Vandewalle A. Regulation by calcitonin of Na⁺-K⁺-Cl⁻ cotransport in a rabbit thick ascending limb cell line. *Am J Physiol*. 1992;263(3 Pt 1):C563-572.
92. Di Stefano A, Wittner M, Nitschke R, Braitsch R, Greger R, Bailly C, Amiel C, Roinel N, de Rouffignac C. Effects of parathyroid hormone and calcitonin on Na⁺, Cl⁻, K⁺, Mg²⁺ and Ca²⁺ transport in cortical and medullary thick ascending limbs of mouse kidney. *Pflugers Arch*. 1990;417(2):161-167.
93. Elalouf JM, Roinel N, de Rouffignac C. ADH-like effects of calcitonin on electrolyte transport by Henle's loop of rat kidney. *Am J Physiol*. 1984;246(2 Pt 2):F213-220.
94. Elalouf JM, Roinel N, de Rouffignac C. Stimulation by human calcitonin of electrolyte transport in distal tubules of rat kidney. *Pflugers Arch*. 1983;399(2):111-118.
95. Gitelman HJ, Graham JB, Welt LG. A new familial disorder characterized by hypokalemia and hypomagnesemia. *Trans Assoc Am Physicians*. 1966;79(221-235).
96. Simon DB, Nelson-Williams C, Bia MJ, Ellison D, Karet FE, Molina AM, Vaara I, Iwata F, Cushner HM, Koolen M, et al. Gitelman's variant of Bartter's syndrome, inherited hypokalaemic alkalosis, is caused by mutations in the thiazide-sensitive NaCl cotransporter. *Nat Genet*. 1996;12(1):24-30.
97. Costanzo LS, Windhager EE, Ellison DH. Ca²⁺ and Na⁺ transport by the distal convoluted tubule of the rat. *J Am Soc Nephrol*. 1978;11(8):1562-1580.
98. Moore MJ. Thiazide-induced hypomagnesemia. *Jama*. 1978;240(12):1241.
99. Schultheis PJ, Lorenz JN, Meneton P, Nieman ML, Riddle TM, Flagella M, Duffy JJ, Doetschman T, Miller ML, Shull GE. Phenotype resembling Gitelman's syndrome in mice lacking the apical NaCl cotransporter of the distal convoluted tubule. *J Biol Chem*. 1998;273(44):29150-29155.
100. Friedman PA. Codependence of renal Ca²⁺ and Na⁺ transport. *Annu Rev Physiol*. 1998;60(179-197).
101. Nijenhuis T, Hoenderop JG, Loffing J, van der Kemp AW, van Os CH, Bindels RJ. Thiazide-induced hypocalciuria is accompanied by a decreased expression of Ca²⁺

General introduction

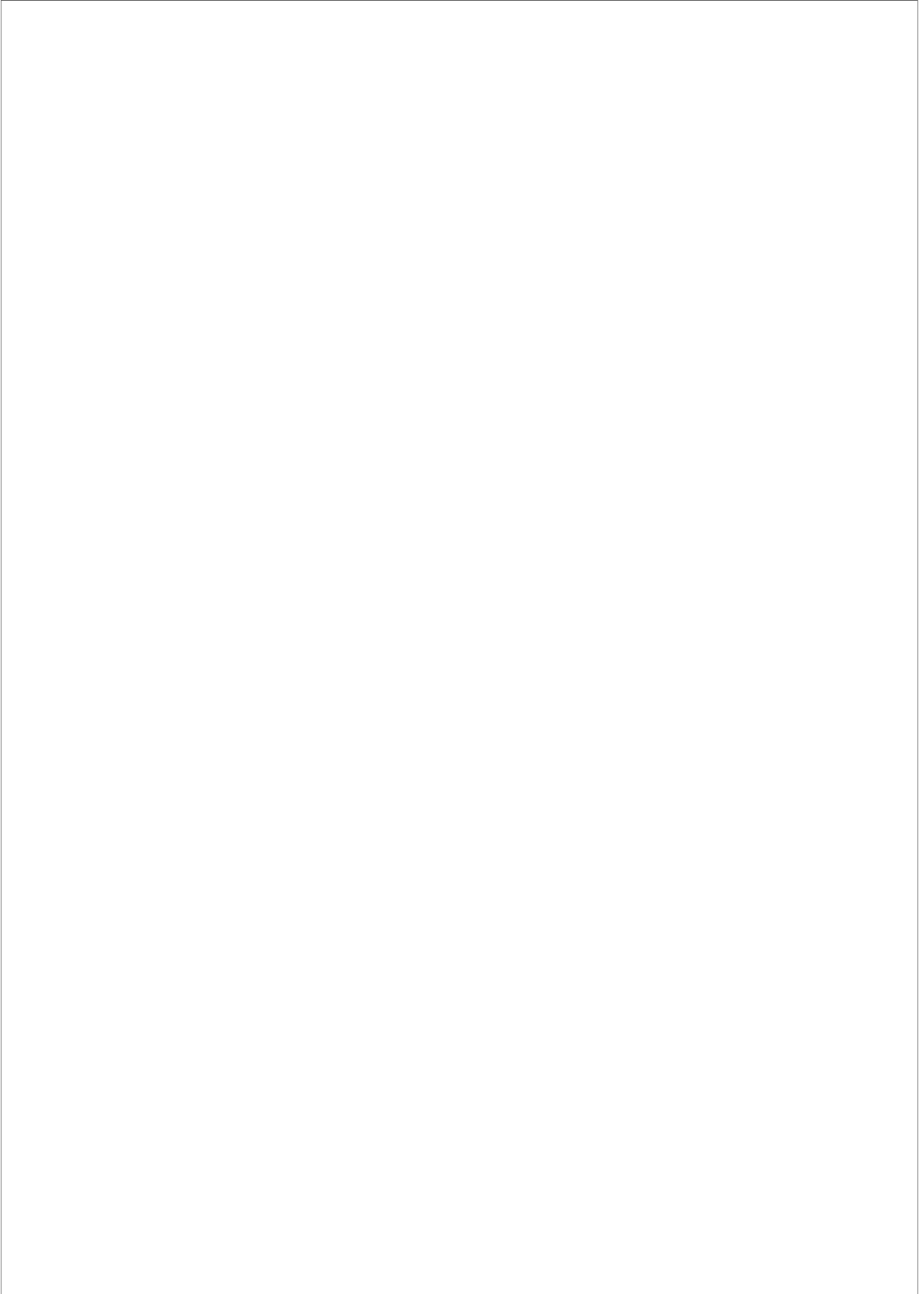
- transport proteins in kidney. *Kidney Int.* 2003;64(2):555-564.
102. Loffing J, Vallon V, Loffing-Cueni D, Aregger F, Richter K, Pietri L, Bloch-Faure M, Hoenderop JG, Shull GE, Meneton P, et al. Altered renal distal tubule structure and renal Na⁺ and Ca²⁺ handling in a mouse model for Gitelman's syndrome. *J Am Soc Nephrol.* 2004;15(9):2276-2288.
 103. Nijenhuis T, Vallon V, van der Kemp AW, Loffing J, Hoenderop JG, Bindels RJ. Enhanced passive Ca²⁺ reabsorption and reduced Mg²⁺ channel abundance explains thiazide-induced hypocalciuria and hypomagnesemia. *J Clin Invest.* 2005;115(6):1651-1658.
 104. Loffing J, Loffing-Cueni D, Hegyi I, Kaplan MR, Hebert SC, Le Hir M, Kaissling B. Thiazide treatment of rats provokes apoptosis in distal tubule cells. *Kidney Int.* 1996;50(4):1180-1190.
 105. Horton R, Biglieri EG. Effect of aldosterone on the metabolism of Mg²⁺. *J Clin Endocrinol Metab.* 1962;22(1187-1192).
 106. Ellison DH. Divalent cation transport by the distal nephron: insights from Bartter's and Gitelman's syndromes. *Am J Physiol Renal Physiol.* 2000;279(4):F616-625.
 107. Sontia B, Montezano AC, Paravicini T, Tabet F, Touyz RM. Downregulation of renal TRPM7 and increased inflammation and fibrosis in aldosterone-infused mice: effects of Mg²⁺. *Hypertension.* 2008;51(4):915-921.
 108. Colussi G, Rombola G, De Ferrari ME, Macaluso M, Minetti L. Correction of hypokalemia with antialdosterone therapy in Gitelman's syndrome. *Am J Nephrol.* 1994;14(2):127-135.
 109. Xu B, English JM, Wilsbacher JL, Stippec S, Goldsmith EJ, Cobb MH. WNK1, a novel mammalian serine/threonine protein kinase lacking the catalytic lysine in subdomain II. *J Biol Chem.* 2000;275(22):16795-16801.
 110. Verissimo F, Jordan P. WNK kinases, a novel protein kinase subfamily in multi-cellular organisms. *Oncogene.* 2001;20(39):5562-5569.
 111. Zambrowicz BP, Abuin A, Ramirez-Solis R, Richter LJ, Piggott J, BeltrandelRio H, Buxton EC, Edwards J, Finch RA, Friddle CJ, et al. Wnk1 kinase deficiency lowers blood pressure in mice: a gene-trap screen to identify potential targets for therapeutic intervention. *Proc Natl Acad Sci U S A.* 2003;100(24):14109-14114.
 112. Wilson FH, Disse-Nicodeme S, Choate KA, Ishikawa K, Nelson-Williams C, Desitter I, Gunel M, Milford DV, Lipkin GW, Achard JM, et al. Human hypertension caused by mutations in WNK kinases. *Science.* 2001;293(5532):1107-1112.
 113. Gordon RD. The syndrome of hypertension and hyperkalemia with normal glomerular filtration rate: Gordon's syndrome. *Aust N Z J Med.* 1986;16(2):183-184.
 114. Yang CL, Angell J, Mitchell R, Ellison DH. WNK kinases regulate thiazide-sensitive NaCl cotransport. *J Clin Invest.* 2003;111(7):1039-1045.
 115. Kahle KT, Wilson FH, Leng Q, Lalioti MD, O'Connell AD, Dong K, Rapson AK,

Chapter 1

- MacGregor GG, Giebisch G, Hebert SC, et al. WNK4 regulates the balance between renal NaCl reabsorption and K⁺ secretion. *Nat Genet.* 2003;35(4):372-376.
116. Lazrak A, Liu Z, Huang CL. Antagonistic regulation of ROMK by long and kidney-specific WNK1 isoforms. *Proc Natl Acad Sci U S A.* 2006;103(5):1615-1620.
117. Yang CL, Zhu X, Ellison DH. The thiazide-sensitive Na-Cl cotransporter is regulated by a WNK kinase signaling complex. *J Clin Invest.* 2007;117(11):3403-3411.
118. Wilson FH, Kahle KT, Sabath E, Lalioti MD, Rapson AK, Hoover RS, Hebert SC, Gamba G, Lifton RP. Molecular pathogenesis of inherited hypertension with hyperkalemia: the NaCl cotransporter is inhibited by wild-type but not mutant WNK4. *Proc Natl Acad Sci U S A.* 2003;100(2):680-684.
119. Zhou B, Zhuang J, Gu D, Wang H, Cebotaru L, Guggino WB, Cai H. WNK4 Enhances the Degradation of NCC through a Sortilin-Mediated Lysosomal Pathway. *J Am Soc Nephrol.* 2009.
120. Ring AM, Cheng SX, Leng Q, Kahle KT, Rinehart J, Lalioti MD, Volkman HM, Wilson FH, Hebert SC, Lifton RP. WNK4 regulates activity of the epithelial Na⁺ channel in vitro and in vivo. *Proc Natl Acad Sci U S A.* 2007;104(10):4020-4024.
121. Cope G, Murthy M, Golbang AP, Hamad A, Liu CH, Cuthbert AW, O'Shaughnessy KM. WNK1 affects surface expression of the ROMK K⁺ channel independent of WNK4. *J Am Soc Nephrol.* 2006;17(7):1867-1874.
122. Rodriguez-Soriano J, Vallo A, Dominguez MJ. "Cl⁻-shunt" syndrome: an overlooked cause of renal hypercalciuria. *Pediatr Nephrol.* 1989;3(2):113-121.
123. Stratton JD, McNicholas TA, Farrington K. Recurrent Ca²⁺ stones in Gordon's syndrome. *Br J Urol.* 1998;82(6):925.
124. Achard JM, Warnock DG, Disse-Nicodeme S, Fiquet-Kempf B, Corvol P, Fournier A, Jeunemaitre X. Familial hyperkalemic hypertension: phenotypic analysis in a large family with the WNK1 deletion mutation. *Am J Med.* 2003;114(6):495-498.
125. Mayan H, Vered I, Mouallem M, Tzadok-Witkon M, Puzner R, Farfel Z. Pseudohypoaldosteronism type II: marked sensitivity to thiazides, hypercalciuria, normomagnesemia, and low bone mineral density. *J Clin Endocrinol Metab.* 2002;87(7):3248-3254.
126. Mayan H, Munter G, Shaharabany M, Mouallem M, Puzner R, Holtzman EJ, Farfel Z. Hypercalciuria in familial hyperkalemia and hypertension accompanies hyperkalemia and precedes hypertension: description of a large family with the Q565E WNK4 mutation. *J Clin Endocrinol Metab.* 2004;89(8):4025-4030.
127. Suki WN, Schwetmann RS, Rector FC, Jr., Seldin DW. Effect of chronic mineralocorticoid administration on Ca²⁺ excretion in the rat. *Am J Physiol.* 1968;215(1):71-74.
128. Lau K, Eby BK. Tubular mechanism for the spontaneous hypercalciuria in laboratory rat.

General introduction

- J Clin Invest.* 1982;70(4):835-844.
129. Jiang Y, Ferguson WB, Peng JB. WNK4 enhances TRPV5-mediated Ca^{2+} transport: potential role in hypercalciuria of familial hyperkalemic hypertension caused by gene mutation of WNK4. *Am J Physiol Renal Physiol.* 2006.
 130. Walder RY, Landau D, Meyer P, Shalev H, Tsoia M, Borochowitz Z, Boettger MB, Beck GE, Englehardt RK, Carmi R, et al. Mutation of TRPM6 causes familial hypomagnesemia with secondary hypocalcemia. *Nat Genet.* 2002;31(2):171-174.
 131. Paunier L, Radde IC, Kooh SW, Conen PE, Fraser D. Primary hypomagnesemia with secondary hypocalcemia in an infant. *Pediatrics.* 1968;41(2):385-402.
 132. Shalev H, Phillip M, Galil A, Carmi R, Landau D. Clinical presentation and outcome in primary familial hypomagnesaemia. *Arch Dis Child.* 1998;78(2):127-130.
 133. Milla PJ, Aggett PJ, Wolff OH, Harries JT. Studies in primary hypomagnesaemia: evidence for defective carrier-mediated small intestinal transport of Mg^{2+} . *Gut.* 1979;20(11):1028-1033.
 134. Stromme JH, Steen-Johnsen J, Harnaes K, Hofstad F, Brandtzaeg P. Familial hypomagnesemia--a follow-up examination of three patients after 9 to 12 years of treatment. *Pediatr Res.* 1981;15(8):1134-1139.
 135. Matzkin H, Lotan D, Boichis H. Primary hypomagnesemia with a probable double mg^{2+} transport defect. *Nephron.* 1989;52(1):83-86.
 136. Agus ZS. Hypomagnesemia. *J Am Soc Nephrol.* 1999;10(7):1616-1622.
 137. Geven WB, Monnens LA, Willems JL, Buijs W, Hamel CJ. Isolated autosomal recessive renal mg^{2+} loss in two sisters. *Clin Genet.* 1987;32(6):398-402.
 138. Groenestege WM, Thebault S, van der Wijst J, van den Berg D, Janssen R, Tejpar S, van den Heuvel LP, van Cutsem E, Hoenderop JG, Knoers NV, et al. Impaired basolateral sorting of pro-EGF causes isolated recessive renal hypomagnesemia. *J Clin Invest.* 2007;117(8):2260-2267.
 139. Thebault S, Alexander RT, Tiel Groenestege WM, Hoenderop JG, Bindels RJ. EGF Increases TRPM6 Activity and Surface Expression. *J Am Soc Nephrol.* 2009;20(1):78-85.
 140. Tejpar S, Piessevaux H, Claes K, Piront P, Hoenderop JG, Verslype C, Van Cutsem E. Mg^{2+} wasting associated with epidermal-growth-factor receptor-targeting antibodies in colorectal cancer: a prospective study. *Lancet Oncol.* 2007;8(5):387-394.



CHAPTER 2

γ -Adducin functions as a novel regulator of the thiazide-sensitive NaCl-cotransporter

Henrik Dimke^{1*}, Pedro San-Cristobal^{1*}, Mark de Graaf¹, Jacques W. Lenders^{2,3},

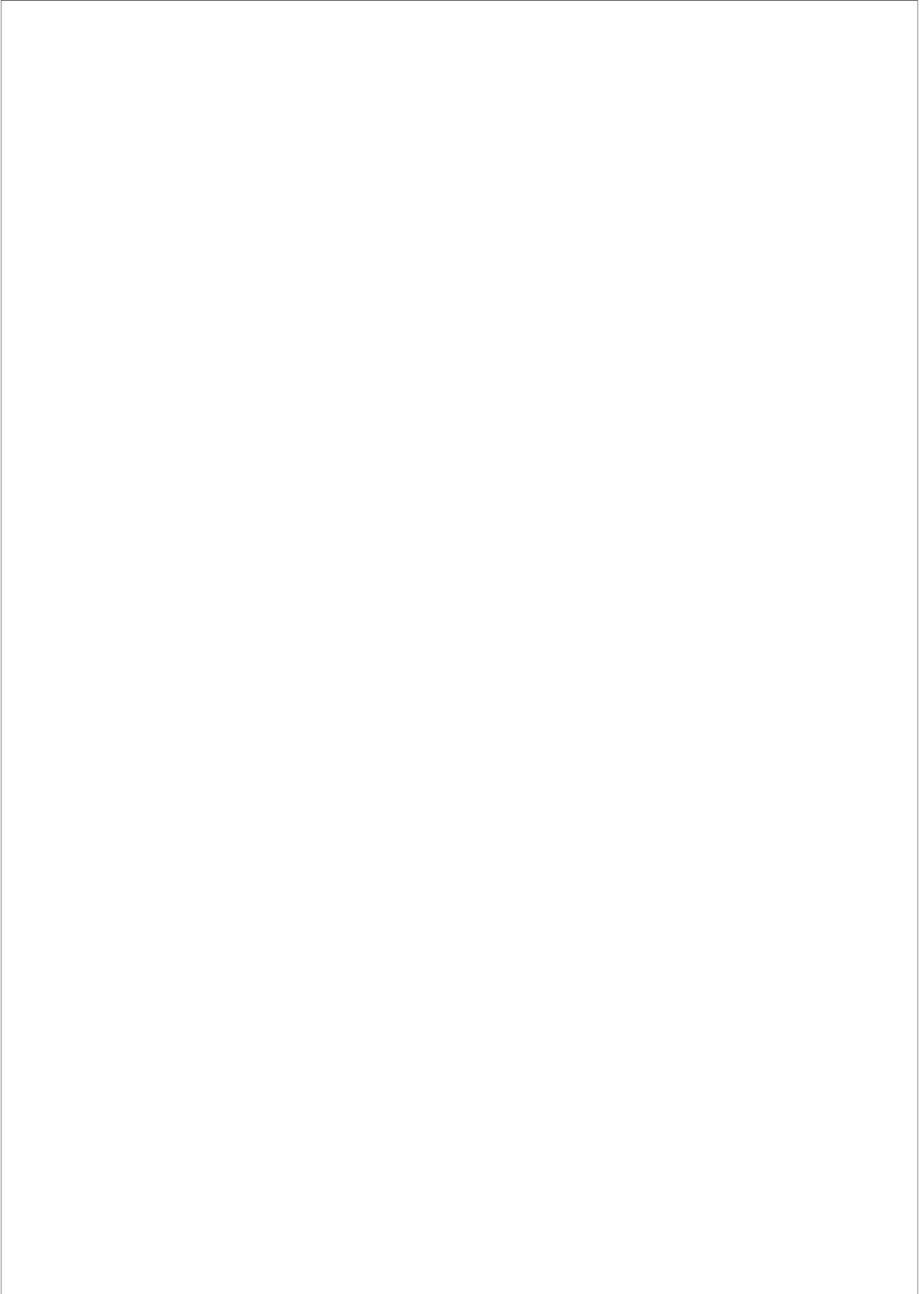
Jaap Deinum², Joost G. Hoenderop¹, René J. Bindels¹.

¹Department of Physiology, Radboud University Nijmegen Medical Centre, the Netherlands.

²Department of Internal Medicine, Section of Vascular Medicine, Radboud University Nijmegen Medical Centre, The Netherlands,

³Department of Medicine III, Carl Gustav Carus University Medical Centre, Dresden, Germany

*Authors contributed equally



γ -Adducin and thiazide-sensitive NaCl transport

Abstract

Hypertension is projected to affect more than 1 billion individuals worldwide. Primary hypertension remains a major risk factor for the development of cardiovascular and chronic kidney diseases. The thiazide-sensitive NaCl cotransporter (NCC) plays a key role in renal salt reabsorption and thereby the maintenance of systemic blood pressure. This study was designed to further elucidate the molecular mechanisms governing the regulation of NCC. Pull down experiments coupled to mass spectrometry identified γ -adducin as a novel interactor of the transporter. γ -Adducin co-localized with NCC to the distal convoluted tubule and stimulated NCC activity in a dose-dependent manner. The stimulatory effect of γ -adducin occurs upstream from the With-No-Lysine Kinase 4. The binding site of γ -adducin mapped to the amino (N)-terminus of NCC encompassing three previously reported phosphorylation sites. Furthermore, competition with the N-terminal domain of NCC abolished the stimulatory effect of γ -adducin on the transporter. γ -Adducin was unable to increase NCC activity when these phosphorylation sites were made constitutively inactive or active. In addition, γ -adducin bound only to the dephosphorylated N-terminal of NCC. Taken together, our observations suggest that γ -adducin functions as a novel dynamic regulator of NCC, likely by amending the phosphorylation state of the transporter and consequently its activity.

Introduction

Hypertension is a highly prevalent clinical condition and has been estimated to affect as many as 1.56 billion individuals in the year 2025 (1). Primary hypertension is a key contributor to cardiovascular complications. As such, hypertension has been estimated to account for a large fraction of strokes and ischaemic heart disease on a global scale (2). The National Vital Statistics Report lists heart disease as the primary cause of death, affecting more than 20 million people in the U.S. alone (3). In addition, elevated blood pressure is a leading cause in the development of

Chapter 2

chronic renal failure (4). Kidney disease remains both a cause and a consequence of hypertension (3, 4). According to the Guytonian model, the kidney plays an essential role in chronic blood pressure maintenance by adjusting blood volume in response to changes in systemic pressure (5). Such modifications are achieved in part by amending the urinary excretion of NaCl. Consequently, defects in genes encoding renal salt transporters often lead to hypo- or hypertensive phenotypes (6).

The Joint National Committee for the detection, evaluation, and treatment of high blood pressure recommends thiazides as the first line treatment of uncomplicated stage I hypertension, or combined with other antihypertensive agents for patients with stage II hypertension (7). Thiazides act by blocking NaCl reabsorption in the distal convoluted tubule (DCT), which reclaims 5-10% of Na⁺ from the renal ultrafiltrate (8). It is, therefore, not surprising that disorders disturbing transport processes in this segment, affect the renal reabsorptive capacity for NaCl and, thereby, influence systemic blood pressure. The thiazide-sensitive NaCl transporter (NCC) is responsible for the majority of inward Na⁺ transport in the DCT. In line with this, renal NaCl wasting and secondary hypokalemic metabolic alkalosis can be observed in Gitelman patients (OMIM 263800) that carry a defect in the *SLC12A3* gene encoding NCC (9, 10). In addition, blockage of NCC with thiazide diuretics leads to a Gitelman-like phenotype (8). Conversely, pseudohypoaldosteronism type II (PHAII, Gordon syndrome, OMIM 145260) augments renal reabsorption of NaCl and can, thereby, increase systemic blood pressure (11, 12). PHAII results from mutations in the With-No-Lysine (WNK) kinases 1 and 4, which play an instrumental role in regulating electrolyte transport pathways in the distal part of the nephron, for instance, by modifying the activity of NCC (12-15).

A better understanding of the regulation of NaCl transport by NCC may ultimately increase our understanding of how blood pressure is maintained and the etiology underlying primary hypertension. During the last decade, research within this field has greatly expanded our knowledge about how NaCl transport via NCC is controlled. The cotransporter contains several

γ -Adducin and thiazide-sensitive NaCl transport

phosphorylation sites in its amino (N)-terminal domain, a feature that is well conserved among several members of the SLC12 family (16-19). Phosphorylation of these residues are critically important for the activation of NCC in response to chloride (Cl⁻)-depletion (16). Serine/threonine kinases of the STE20 family (such as the Ste20-related proline-alanine-rich kinase (SPAK) and oxidative stress response 1 (OSR1)) have been shown to play an important role in modulating the phosphorylation state of NCC (20). In addition, kinases in the WNK family as well as the serum- and glucocorticoid-inducible kinase 1 (SGK1) have been shown to interact within this network, thereby changing the activity of SPAK and OSR1, and potentially altering the phosphorylation state of the transporter (21-24). As shown in detail by Yang, Ellison and co-workers, trafficking of the NCC transporter is particularly affected by the concerted action of the WNK kinases (WNK1, WNK3, and WNK4) (14, 25). Genetically modified mice strains largely support these observations and solidify the important role of NCC regulation in blood pressure maintenance (13, 26-30). However, the molecular mechanisms governing NCC phosphorylation and trafficking have yet to be fully elucidated.

The aim of the present study was to identify novel interactors of NCC, which could be involved in modulating its function. As the N-terminal domain has been shown to play an important role in activation of the transporter, pull down experiments were performed with this domain of NCC in mouse kidney lysates and subsequently coupled with mass spectrometry. This study describes the identification of γ -adducin, as a novel auxiliary factor interacting with NCC. Adducins were originally identified as heteromeric membrane skeletal proteins implicated in the binding of spectrin to actin (31). γ -Adducin was selected as an interesting candidate gene based on the previous involvement of this protein family in primary hypertension in both humans and rats (32-34). Here, we delineated the molecular basis by which γ -adducin stimulates the activity of NCC.

Chapter 2

Results

γ-Adducin stimulates the activity of the thiazide-sensitive cotransporter NCC

Mass spectrometry identified γ -adducin as a potential binding partner to the N-terminal cytoplasmic terminal domain of NCC. The interaction was confirmed by pull down experiments in Human Embryonic Kidney (HEK) 293 cells transiently transfected with glutathione S-transferase (GST)-conjugated terminal domains of NCC and hemagglutinin (HA)-tagged γ -adducin. The resulting cell lysates were incubated with glutathione-coupled Sepharose beads to precipitate GST-bound complexes. Strong binding was seen by γ -adducin towards the N-terminal domain of NCC (Figure 1A). Immunohistochemical stainings showed that γ -adducin co-localizes to DCT tubules that also express NCC (Figure 1B). Here, γ -adducin localized to cytoplasmic and (baso)-lateral domains of the cell. γ -Adducin was not restricted to the DCT, as expression was also found in the proximal tubule and thick ascending limb as reported previously (35). DCT fragments were isolated from mice expressing enhanced green fluorescent protein (eGFP) after the parvalbumin promoter (36). The restricted renal expression of this protein to the DCT allowed fluorescence-based sorting of the segment using a Complex Object Parametric Analyzer and Sorter (COPAS) (37). Thus, this method permits evaluation of whether the abundance of γ -adducin is enriched in the DCT in comparison to other tubules in the renal cortex. In line with the more ubiquitous expression of the protein, the relative enrichment of γ -adducin mRNA in the DCT remained, while that for NCC was markedly enriched (Figure 1C). To estimate the functional effect of γ -adducin on the transport capacity of NCC, $^{22}\text{Na}^+$ uptake studies were performed using the *Xenopus laevis* oocyte system. Oocytes injected with cRNA encoding NCC showed a significant thiazide-sensitive $^{22}\text{Na}^+$ uptake compared to water-injected oocytes. Co-injection with increasing amounts of γ -adducin cRNA stimulated NCC activity in a dose-dependent manner (Figure 1D). In addition, no difference in the expression level of HA-NCC could be detected between oocytes injected without or with increasing concentrations of HA-tagged γ -adducin in the presence of HA-NCC. A dose-dependent increase was observed

γ -Adducin and thiazide-sensitive NaCl transport

in the abundance of the HA-tagged γ -adducin. Injection of small interference (si) RNA against endogenous *Xenopus laevis* γ -adducin, in oocytes pre-injected with NCC, resulted in a significant decrease in thiazide-sensitive $^{22}\text{Na}^+$ uptake (Figure 2).

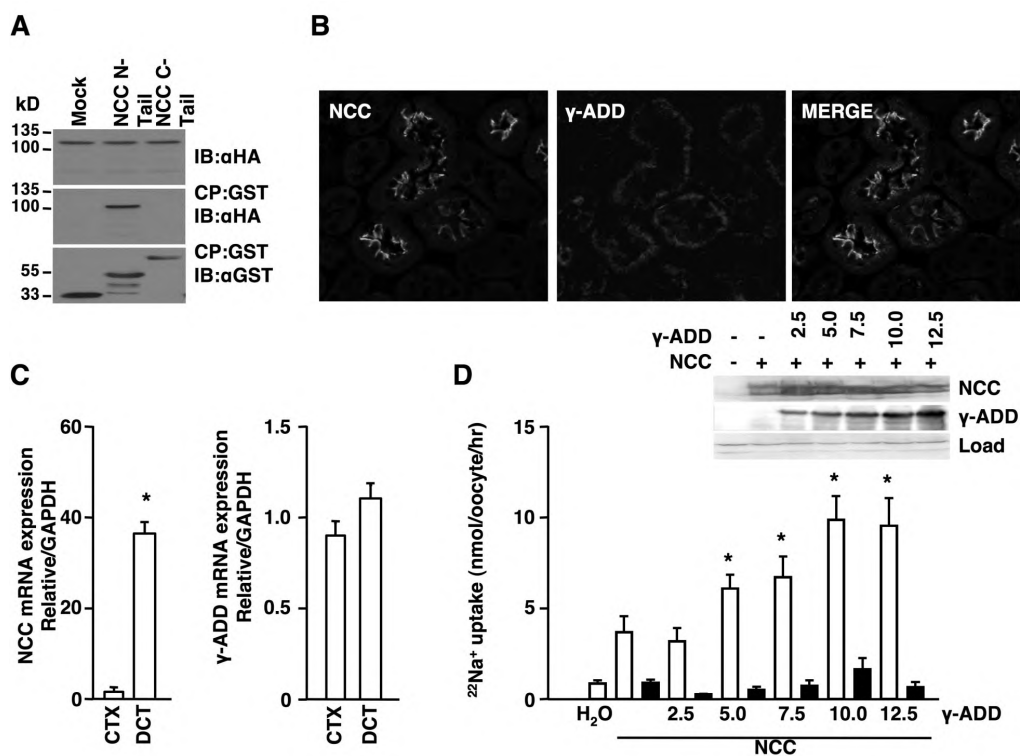


Figure 1. γ -Adducin binds strongly to the N-terminus of NCC and stimulates the activity of the cotransporter. (A) GST-pull down assay in HEK293 cells transiently transfected with either the GST-tagged N- or C-terminal of NCC or GST alone, all in combination with γ -adducin, was used to evaluate binding of γ -adducin to NCC. CP denotes co-precipitate and IB represents the protein immunoblotted against. (B) γ -Adducin co-localizes with NCC to the DCT. Representative immunohistochemical images are shown as obtained by confocal laser-microscopy. Sections were incubated with specific antibodies against NCC and γ -adducin and stained using Alexa-conjugated secondary antibodies. (C) γ -Adducin mRNA is expressed in the DCT as well as in other nephron segments. Semi-quantitative real-time PCR was used to determine the abundance of NCC and γ -adducin mRNA extracted from fluorescently sorted DCT tubules and the kidney cortex (CTX). (D) Effect of γ -adducin upon NCC function. γ -Adducin stimulated NCC activity in a dose-dependent manner. $^{22}\text{Na}^+$ uptakes in *Xenopus laevis* oocytes microinjected with water, 5 ng of HA-tagged human NCC cRNA alone, or in combination with increasing amounts of HA-tagged γ -adducin cRNA. The experiment was performed in the absence (open bars) or presence (closed bars) of 0.1 mM thiazide. Data is presented as means \pm SEM. * $p < 0.05$ is statistically significant as compared to NCC injected oocytes. Western blots were used to quantify the expression of NCC and γ -adducin in groups of oocytes injected as described above. Data is presented as means \pm SEM.

Chapter 2

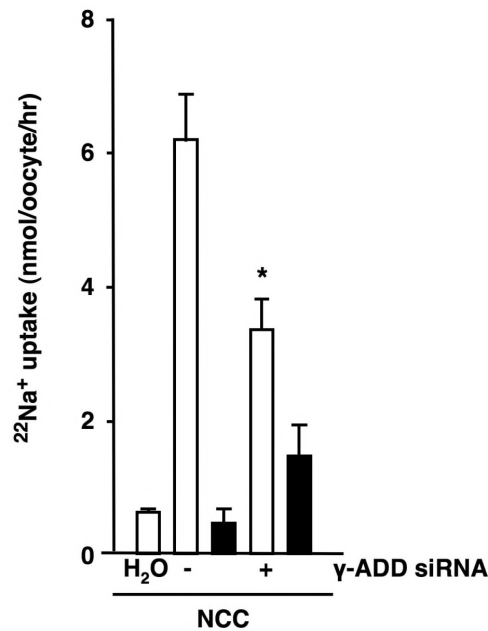


Figure 2. Effect of siRNA against endogenous *Xenopus laevis* γ -adducin on $^{22}\text{Na}^+$ uptakes in oocytes injected with NCC. Oocytes were injected with 5 ng of NCC cRNA in the presence or absence of 10 ng of γ -adducin cRNA. 1 ng of double-stranded siRNA was injected 24 hrs prior to the $^{22}\text{Na}^+$ uptake. Closed bars denote the presence of 0.1 mM thiazide. * $p < 0.05$ is considered statistically significant from the group injected with NCC.

γ -Adducin abrogates the inhibitory effect of WNK4.

To investigate whether γ -adducin affects NCC activity via the same signaling cascade as WNK4, the effect of WNK4 on γ -adducin-stimulated Na^+ transport was evaluated. WNK4 has been shown to reduce NCC activity by directing the protein to the lysosomal compartment (14, 38). In line with this, WNK4 was able to inhibit NCC-dependent $^{22}\text{Na}^+$ uptake (Figure 3A). Importantly, the stimulatory effect of γ -adducin was also observed in the presence of WNK4 (Figure 3A). Moreover, injections of increasing concentrations of γ -adducin completely reverted the inhibitory effect of WNK4 on NCC-mediated $^{22}\text{Na}^+$ uptake (Figure 3B). Furthermore, the effect of γ -adducin abrogated the WNK4-dependent reduction in NCC activity, as the stimulatory effect of γ -adducin was still present when increasing amounts of WNK4 cRNA were injected (Figure 3C).

γ -Adducin and thiazide-sensitive NaCl transport

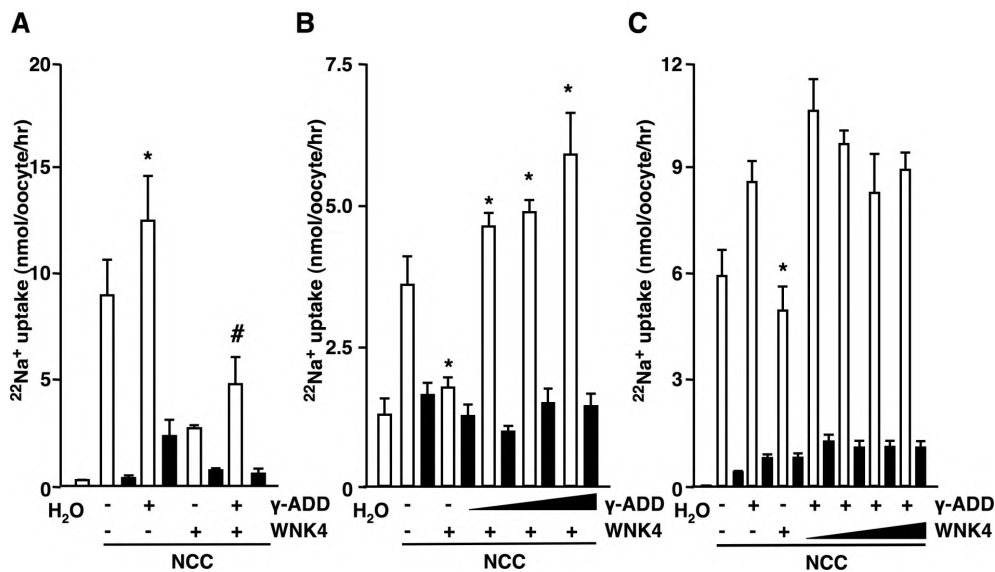


Figure 3. γ -Adducin reverts the inhibitory effect of WNK4. (A) WNK4 did not inhibit γ -adducin-stimulated NCC activity. *Xenopus laevis* oocytes were injected with 5 ng of NCC cRNA, in the presence or absence of 10 ng γ -adducin as well as 10 ng of WNK4. cRNA. (B) WNK4 did not revert the stimulatory effect of γ -adducin. ²²Na⁺ uptakes in oocytes co-injected with 5 ng of NCC cRNA, 10 ng of γ -adducin cRNA, and with increasing amounts of WNK4 cRNA (from 20 ng to 60 ng). (C) Increasing amounts of γ -adducin reverted the inhibitory effect of WNK4 on NCC. ²²Na⁺ uptakes in oocytes co-injected with 5 ng of NCC cRNA, 10 ng of WNK4 cRNA, and with increasing amounts of γ -adducin cRNA (from 20 ng to 40 ng). Closed bars denote the presence of 0.1 mM thiazide. *p < 0.05 is statistically significant from NCC injected oocytes. #p < 0.05 is statistically significant from the group co-injected with WNK4 and NCC.

γ -adducin stimulates NCC activity independent of membrane trafficking

The stimulatory effect of γ -adducin on NCC may be explained by increased trafficking of the transporter to the plasma membrane or by changes in the intrinsic activity of the transporter. To evaluate whether the membrane abundance of NCC increases in the presence of γ -adducin, cell surface expression of eGFP-NCC was determined by confocal laser scanning microscopy. The intensity of the eGFP signal at the plasma membrane as well as the ²²Na⁺ uptake rates correlated dose-dependently with the amount of injected eGFP-NCC cRNA (Figure 4, A and B). Thus, this method was used to determine semi-quantitatively the presence of NCC at the plasma membrane. Co-injection of γ -adducin significantly increased eGFP-NCC-dependent ²²Na⁺ uptake, while the auxiliary protein γ -adducin did not significantly affect the plasma membrane expression of eGFP-NCC (Figure 4, C and D).

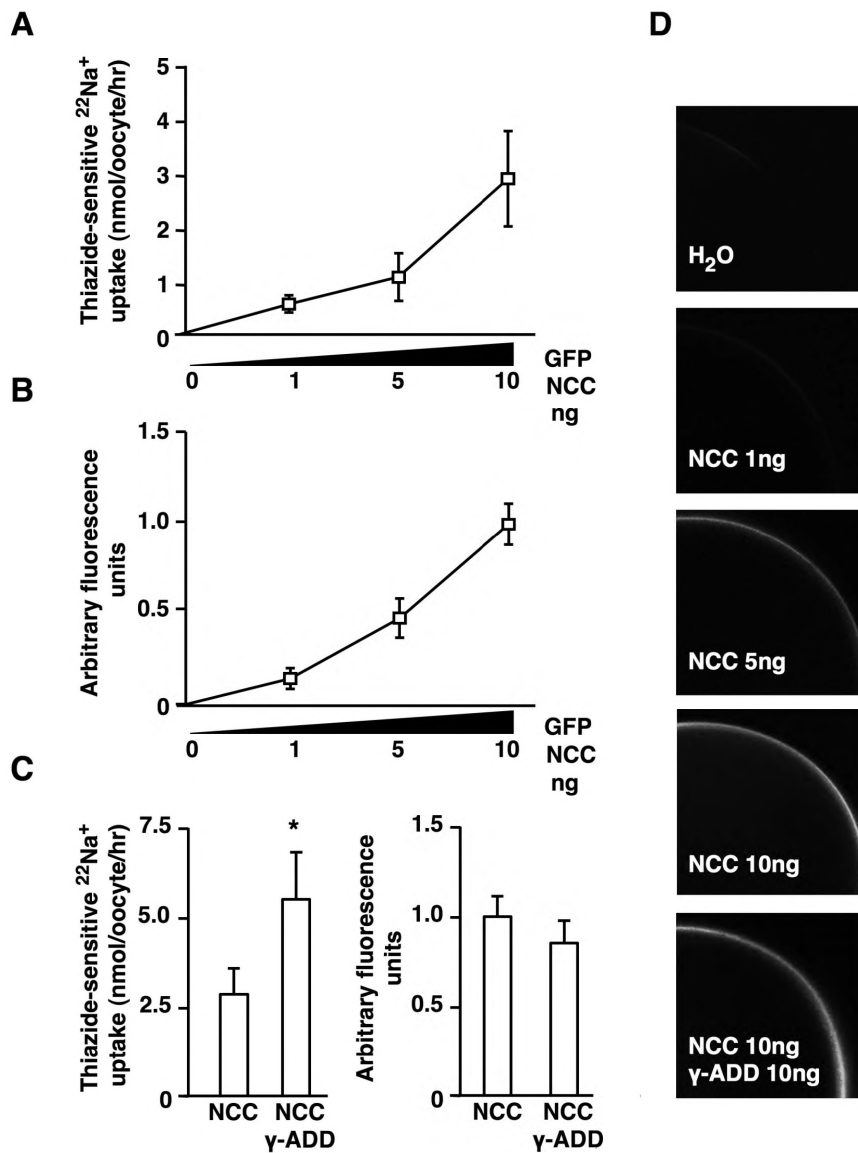


Figure 4. The effect of γ -adducin occurs independent of NCC trafficking to the oocyte membrane. (A) $^{22}\text{Na}^+$ uptakes in *Xenopus laevis* oocytes injected with 1-10 ng of GFP-NCC cRNA. (B) Corresponding GFP fluorescence at the membrane of oocytes injected with 1-10 ng of GFP-NCC cRNA. (C) Effect of thiazide-sensitive $^{22}\text{Na}^+$ uptake (left) and quantification of the GFP fluorescence in the membrane (right) of *Xenopus laevis* oocytes injected with 10 ng of GFP-NCC cRNA, in the presence or absence of 10 ng of γ -adducin cRNA. (D) Representative images of GFP fluorescence at the oocyte membrane after injected with increasing amounts of GFP-NCC cRNA as well as the group co-injected with 10 ng of γ -adducin cRNA using confocal laser scanning microscopy. *p < 0.05 is statistically significant.

γ -Adducin and thiazide-sensitive NaCl transport

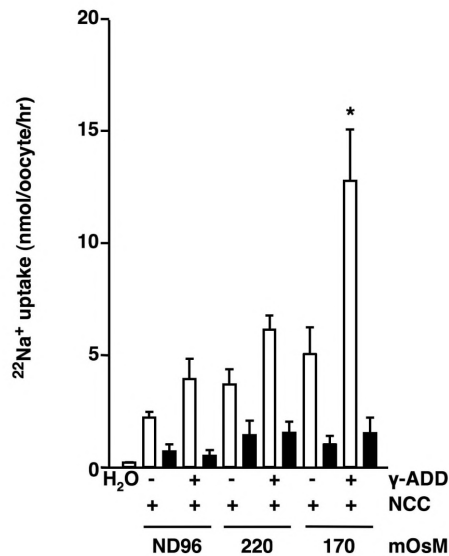


Figure 5. Role of hypo-osmotic Cl⁻ depletion on γ -adducin stimulated NCC activity. Oocytes were injected with 5 ng of NCC cRNA, in the presence or absence of 10 ng of γ -adducin cRNA and incubated for 16 hrs in iso- (200 mOsM) and hypo-osmotic (170 mOsM) Cl⁻ free solutions. Closed bars represent the addition of 0.1 mM thiazide. *p < 0.05 is statistically significant from the NCC injected group kept in hypo-osmotic media.

γ -adducin stimulates NCC activity in hypo-osmotic Cl⁻ depleted conditions

Hypotonicity has previously been shown to increase the activity of NCC. The effect of hypotonicity could be replicated in our experiments, resulting in an increase in NCC activity. In addition, during hypotonic conditions γ -adducin was still able to increase transporter activity (Figure 5).

The stimulatory effect of γ -adducin depends on the N-terminal phosphorylation sites in NCC

To delineate whether γ -adducin affects NCC function by its interaction with the N-terminus of NCC, competition assays were performed in which NCC and γ -adducin were co-injected together with increasing amounts of the N-terminus of NCC. During these conditions, injection of the NCC N-terminus abolished the stimulatory effect of γ -adducin on NCC activity (Figure 6A). The binding site of γ -adducin in the N-terminus of NCC was subsequently mapped by pull down analysis. For

Chapter 2

determination of the binding site, a series of fragments from the N-terminal domain of NCC were generated as depicted in figure 6B, with the 1-135 representing the full-length N-tail. All N-terminal fragments were fused to GST to allow precipitation using glutathione-coupled Sepharose beads. N-terminal deletion fragments of NCC were expressed transiently in HEK293 cells together with γ -adducin. GST-pull down experiments revealed that γ -adducin only binds the N-terminus when the 1-80 fragment is present, albeit at a lower affinity than to the full length N-tail (Figure 6, C and D). As this region encompasses the three phosphorylation-sites of NCC (Thr⁵⁵, Thr⁶⁰, Ser⁷³ in human NCC), which previously have been shown necessary for activation of the protein in response to Cl⁻-depletion (16), the role of γ -adducin on the phosphorylation of NCC was evaluated. γ -Adducin was co-injected with triple phosphorylation-site NCC mutants (converted to alanines (A) or aspartates (D) to mimic either the constitutively inactive or active sites, respectively) and ²²Na⁺ uptakes were performed. The stimulatory effect of γ -adducin on NCC-mediated Na⁺ transport was lost when the three phosphorylation sites were converted into constitutively active sites (D) (Figure 6E), suggesting an important role of γ -adducin in modulating the phosphorylation of NCC. Similarly, when the N-terminal phosphorylation sites were converted to inactive phosphorylation sites (A), NCC-dependent ²²Na⁺ transport dropped markedly in line with previously published data (Figure 6E) (16). Also in this experimental setting, when the phosphorylation sites were made constitutively inactive, γ -adducin had no effect on NCC-mediated ²²Na⁺ transport.

These data suggest that the stimulatory effect of γ -adducin is critically dependent on the phosphorylation sites in the N-terminal domain of NCC. To further elucidate the relationship between γ -adducin and NCC, pull down experiments were performed to determine whether binding of γ -adducin to the N-tail of NCC was dependent on the phosphorylation status of this domain. Thus, GST-pull downs were performed using the N-terminus of NCC as well as the N-terminal constitutively inactive or active phosphorylation forms (Figure 6F). Binding of γ -adducin was found to the N-terminus of wild-type NCC and the constitutively inactive form,

γ -Adducin and thiazide-sensitive NaCl transport

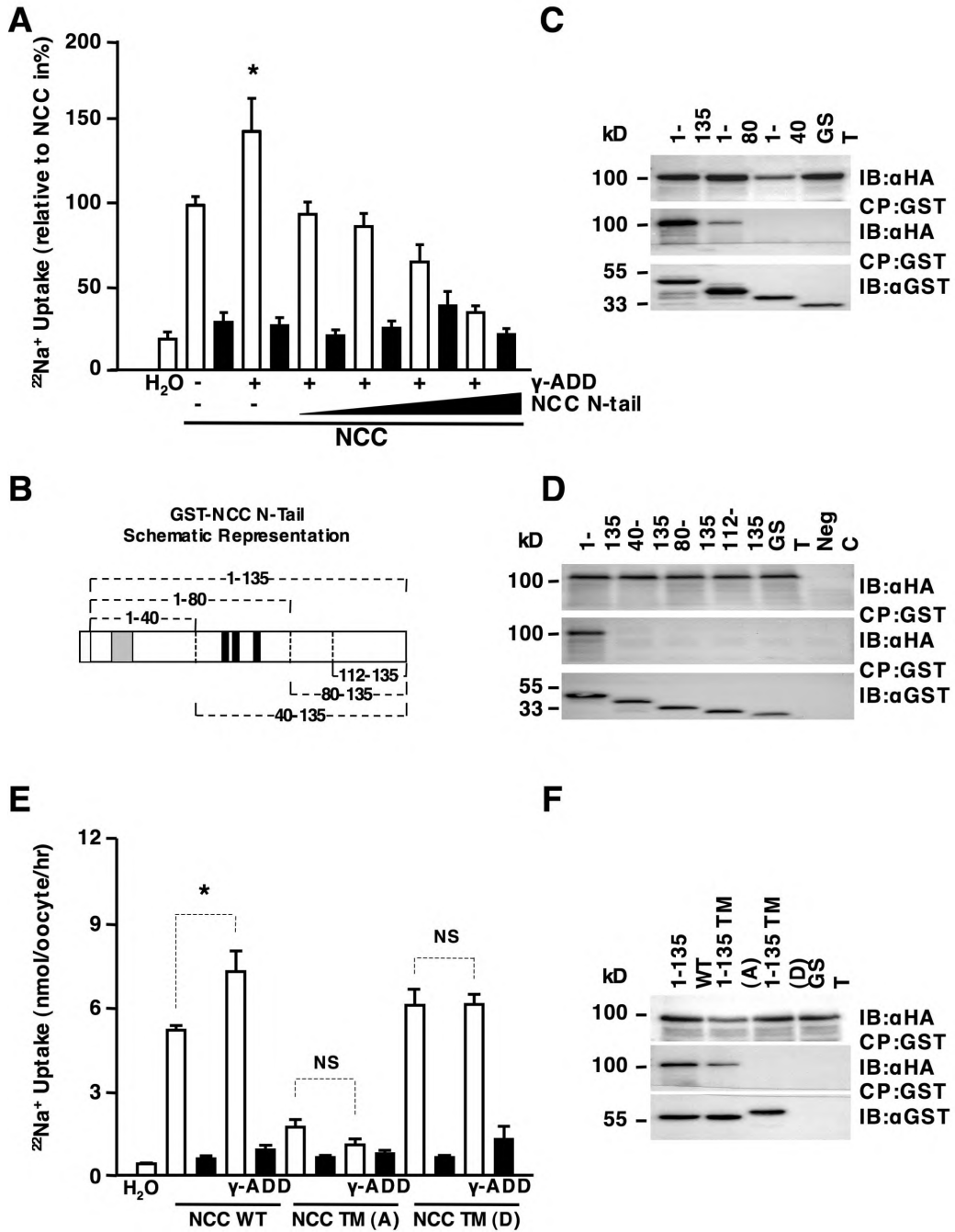
while no binding was observed to the constitutive active phosphorylation form of NCC.

Discussion

NCC is of crucial importance for the reabsorption of NaCl by the kidney, thus influencing arterial pressure. Here, we report the identification of γ -adducin, a novel auxiliary protein interacting with the N-terminal domain of NCC. Our study is the first to delineate the stimulatory action of γ -adducin on the thiazide-sensitive NaCl cotransporter and highlights that the effect of γ -adducin is critically dependent on the phosphorylation status of NCC. These observations are based on the following data: *i*) the identified protein γ -adducin binds strongly to the N-terminal domain of NCC and markedly stimulates the activity of the transporter; *ii*) the stimulatory actions of γ -adducin occur in the regulatory cascade prior to the WNK4-dependent lysosomal shuttling of NCC; *iii*) competition with increasing amounts of the N-terminal part of NCC completely reverts the stimulatory action of γ -adducin on thiazide-sensitive $^{22}\text{Na}^+$ transport; *iv*) the γ -adducin binding site is mapped to the exact region encompassing three phosphorylation sites that previously have been shown to affect the activity of the cotransporter; *v*) NCC forms lacking phosphorylatable sites in the N-terminus do not exhibit increased $^{22}\text{Na}^+$ transport rates when co-injected with γ -adducin; *vi*) γ -adducin dissociates from NCC when the phospho-residues are converted to aspartates, mimicking a constitutively active phosphorylated state.

γ -Adducin was originally cloned from rat kidney (39). The protein exhibits homology with the previously identified α - and β -adducin family members. Adducins are heteromeric membrane skeletal proteins originally implicated in spectrin-actin binding (31). γ -Adducin contains a N-terminal globular head domain, a so-called neck domain, and a protease sensitive C-terminal domain. The protein shows a wide tissue distribution, but with a robust expression in kidney (39). In addition, γ -adducin contains several sites that are necessary for its regulation by calmodulin, protein kinase A, and protein kinase C (40). The adducins form heteromeric proteins composed

Chapter 2



γ -Adducin and thiazide-sensitive NaCl transport

Figure 6. Phosphorylation of the N-terminal domain of NCC is essential for the stimulatory effect of γ -adducin on NCC activity. (A) The ability of the NCC N-terminal domain to inhibit γ -adducin-stimulated transport of the cotransporter as evaluated by $^{22}\text{Na}^+$ uptakes. Oocytes were co-injected with 5 ng of NCC cRNA, 10 ng of γ -adducin cRNA, and increasing amounts of the N-terminal domain of NCC (from 2.5 ng to 10 ng). * $p < 0.05$ is statistically significant from all other groups. (B) Schematic drawing representing the GST fusion proteins containing different portions of the N-terminal tail of NCC. These were generated to map the binding site of γ -adducin to NCC. Black domains represent the N-terminal phosphorylation sites, while gray denotes the SPAK binding site. (C) GST-pull down assay in HEK293 cells. Deletion fragments of the NCC N-terminal domain (aa 1-135; 1-80; 1-40) coupled to GST were generated to determine the HA- γ -adducin binding site within the cotransporter. (D) GST-pull down assay repeated, but the N-terminus was truncated from the opposite end (aa 1-135; 40-135; 80-135; 112-135). Note γ -adducin binds only in the presence of the full-length terminus or the 1-80 fragment. (E) The effect of γ -adducin requires phosphorylatable NCC sites. $^{22}\text{Na}^+$ uptakes were performed in oocytes injected with 5 ng of NCC cRNA, 5 ng of constitutively inactive (NCC TM(A); T55A, T60A, S73A), or 5 ng of the constitutively active (NCC TM(D); T55D, T60D, S73D) NCC phospho-mutants, in the presence or absence of 10 ng of γ -adducin cRNA. (F) GST-pull down assay in HEK293 cells. Co-precipitation of HA-tagged γ -adducin with the native GST-N-terminus, and the GST-N-terminus containing constitutively inactive and active phosphorylation sites. CP denotes co-precipitate and IB indicates the protein which was immunoblotted against. The $^{22}\text{Na}^+$ uptake experiments were performed in the presence (closed bars) or absence (open bars) of 0.1 mM thiazide. * $p < 0.05$ is statistically significant from NCC injected oocytes. NS, not statistically significant.

of either α - and β -subunits or α - and γ -subunits. As the β -subunit has a restricted expression and is primarily found in brain and hemopoietic tissues, it has been suggested that the α - and γ -subunit functions as heteromers in tissues where the β -subunit is absent (39). It is interesting to note that while γ -adducin localizes to the DCT with NCC, α -adducin which is also expressed in the kidney seems absent from the distal part of the nephron (35). This may suggest that γ -adducin has a unique function in DCT where it could function as a homomer. Mutations in rat α - and β -adducin identified in the Milan hypertensive rat strain (MHS) have been shown to alter the activity of the Na^+ , K^+ -ATPase *in vitro* (41). In contrast, little is known about the function of γ -adducin in terms of renal NaCl transport processes. Our data suggest that γ -adducin plays an important role in regulating epithelial electrolyte transport in the DCT.

γ -Adducin is able to completely revert the inhibitory effect of WNK4 on NCC. Consequently, our observation infers that γ -adducin protects against the inhibitory actions of WNK4, either by affecting processes occurring before lysosomal removal of the protein or by directly blocking the WNK4-dependent inhibitory action on NCC. As no changes in the membrane localization of NCC were observed after co-injection of γ -adducin, one may conclude

Chapter 2

that γ -adducin controls processes preceding lysosomal shuttling of NCC. The functional effect of phosphorylation of the thiazide-sensitive NCC transporter has not been fully delineated. Previous studies have reported that when the N-terminal phosphorylation sites in NCC are converted to alanines mimicking inactive phosphorylation sites, the activity of the transporter is markedly decreased. This occurs even though the membrane abundance remains unaffected, suggesting that the intrinsic activity is inhibited (16). Similarly, when the transporter is incubated at hypotonic low Cl⁻ conditions, which noticeably increases its phosphorylation level, NCC increases its activity, again independent of trafficking to the oocyte membrane (16). In line with this finding is the observation that the Thr⁹⁶ and Thr¹⁰¹-phosphorylated form of the related family member, the rat furosemide-sensitive Na⁺, K⁺, 2Cl⁻-cotransporter (NKCC2) (corresponding to Thr⁵⁵, Thr⁶⁰ phospho-form of human NCC), is found exclusively at the membrane as evaluated by electron microscopy (42). Similarly to NCC in oocytes, when the phosphorylation level of NKCC2 is increased by growth hormone, no change in trafficking of the transporter can be observed (16, 42). Consequently, the γ -adducin-stimulated NCC activity needs to be explained by an intrinsic change in transporter activity, as the amount of transporters in the membrane remains unchanged. Such changes could ensue, for instance, if affinity constants for Na⁺ or Cl⁻ will shift, to such a degree that the maximal velocity is altered. Thus, the data obtained in our study as well as the previous literature strongly imply a link between the phosphorylation state and the intrinsic activity of the transporter.

We found that the effect of γ -adducin is entirely dependent on the phosphorylation sites of NCC. The sequence of γ -adducin does not suggest that the protein is a kinase. Furthermore, there is no experimental evidence showing that γ -adducin or other members of the family possesses kinase activity. The most likely explanation is that γ -adducin associates with kinases involved in the phosphorylation of the transporter, thereby anchoring them to the dephosphorylated N-terminal of the transporter. The STE20 family of kinases, comprising members such as SPAK and OSR1, has been shown to increase the phosphorylation state of

γ -Adducin and thiazide-sensitive NaCl transport

NCC *in vitro* and *in vivo* (20, 29). In addition, WNK1, via SPAK and OSR1, has previously been shown to be responsible for increasing the transport activity and phosphorylation level of NCC during hypotonic Cl⁻-depleted conditions (20). Moreover, WNK4 plays an important role in stimulating the NCC phosphorylation via SPAK and OSR1 in response to angiotensin II-mediated receptor activation (43). The phosphorylation state of NCC is also markedly enhanced by dietary NaCl restriction, an effect that appears aldosterone-dependent and is lost in transgenic animals with a PHA1 mutation in WNK4 (44). Consequently, phosphorylation of the N-terminal domain in NCC seems to be a common final pathway by which several stimuli converge to regulate the activity of the transporter. Here, we report that γ -adducin may function as an important component in the phosphorylation cascade of NCC.

Based on the data generated in our study, a schematic model predicting the functional role of γ -adducin was generated. As depicted in Figure 7, γ -adducin may stimulate NCC activity by anchoring a kinase, likely SPAK or OSR1 to the dephosphorylated transporter (step 1). Subsequently, the kinase increases the phosphorylation level of NCC, thereby stimulating the activity of the transporter (step 2). After the kinase-mediated phosphorylation event, γ -adducin dissociates from NCC and may also facilitate the release of the associated kinase (step 3). Dephosphorylation of the transporter reduces the activity of NCC to its basal state. However, this event also allows for the binding of γ -adducin to the N-terminal again, and the cycle can be repeated (step 4). Thus, these speculations infer a dynamic model in which γ -adducin binding and dissociation to NCC is directly correlated with the dephosphorylation and phosphorylation of the transporter, respectively.

The adducin gene family has previously been implicated in arterial hypertension. A G460W polymorphism in the α -adducin gene showed linkage to primary hypertension in certain patient groups (32). One intronic single nucleotide polymorphism (SNP) has currently been described in the γ -adducin gene (A/G; rs3731566), which correlates with peripheral and central pulse pressures (due to increases in systolic pressure), changes in the urinary Na⁺/K⁺ ratio, and

Chapter 2

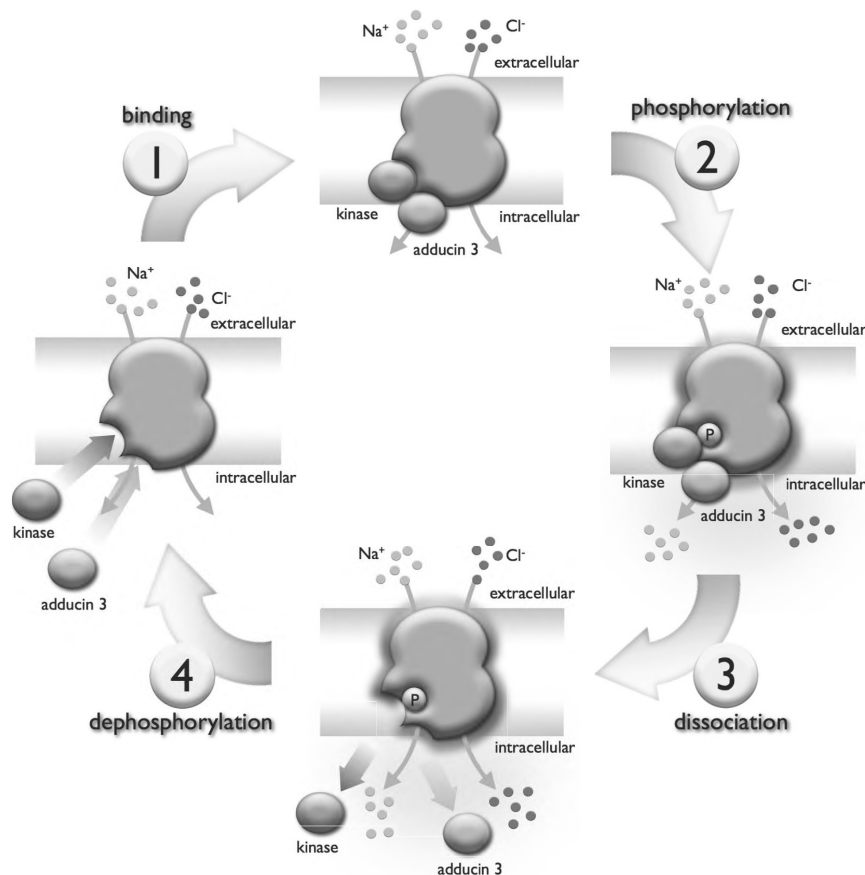


Figure 7. Proposed model for the regulation of NCC activity via phosphorylation by γ -adducin. *Step 1*) γ -Adducin binds to the dephosphorylated N-tail of NCC and may thereby facilitate the binding of a kinase to the transporter. *Step 2*) Upon binding, the kinase can phosphorylate NCC, which leads to an increase in the activity of the transporter. *Step 3*) The phosphorylation of the N-terminal domain in NCC causes γ -adducin to dissociate from the transporter and may also promote the release of the associated kinase. *Step 4*) After dephosphorylation of the N-tail of NCC, γ -adducin can again bind and the cycle can be repeated.

urinary aldosterone excretion, but only in individuals that also harbor the G460W polymorphism in α -adducin (45). These observations suggest that γ -adducin can affect blood pressure, however in order to be visible clinically, arterial pressure needs to be perturbed by the G460W polymorphism in α -adducin. Moreover, mutations in the rat α -adducin gene (F316Y) accounts for some of the blood pressure difference in crossings between the MHS strain and normotensive

γ -Adducin and thiazide-sensitive NaCl transport

controls (33). Conversely, rat β -adducin (Q526R) and rat γ -adducin (Q572K) have not been directly associated with the hypertensive phenotype, while they were shown to interact epistatically with the α -adducin gene (34). Blood pressure changes remain to be determined in mice with a targeted deletion of the α -adducin gene, however, these mice show severe growth retardation and many develop hydrocephaly (46). In addition, mice lacking β -adducin which is highly expressed in brain and hematopoietic tissues develop hypertension (47). Systolic blood pressure and pulse rate remain stable in mice lacking γ -adducin, which can be expected since also mice with a targeted deletion of NCC show no mean arterial pressure variation when maintained on a diet with normal dietary NaCl. However, when NCC-deficient mice were given a reduced dietary NaCl content, they developed hypotension (48). Whether similar dietary restrictions are needed in order to provoke hypotension in the γ -adducin-deficient mice remains to be established.

In conclusion, we identified γ -adducin as a novel regulator of NCC and showed that the stimulatory action of γ -adducin is intimately linked with the N-terminal phosphorylation sites in the cotransporter. Based on our data, γ -adducin may contribute importantly to the regulation of NCC and hence blood pressure maintenance. Our findings will aid in the understanding of the complex cascade regulating NCC activity. Importantly, the observations made in our study may help elucidate the molecular events underlying the formation of primary hypertension.

Materials and Methods

Constructs

HA-tagged human NCC in pT7Ts has been previously described (49). The human γ -adducin clone was obtained from Imclone systems (New York, USA), subcloned into a pCI-NEO-IRES-GFP vector and further subcloned into pT7Ts. GST-conjugated N- and C-terminal fragments of NCC were subcloned by PCR to pGEX-6p-2 for *E. Coli* protein production

Chapter 2

and further subcloned into pEBG vectors for expression of GST-fused proteins in HEK293 cells. GST-fused proteins containing different portions of the N-terminal domain of NCC were constructed according to the schematic drawing in figure 6B. These constructs inserted in pEBG vectors were generated either by PCR subcloning or truncated by stop codons using the QuikChange site-directed mutagenesis kit (Stratagene, La Jolla, CA, US). In addition, the N-terminal domain of NCC (amino acids 1-135) for the competition assay was generated by insertion of a stop codon by site directed mutagenesis in the full length NCC in pT7Ts. The triple phospho sites (Thr⁵⁵, Thr⁶⁰, Ser⁷³) in NCC mimicking constitutively inactive (converted to alanines) or active (converted to aspartates) phospho-proteins were generated by site directed mutagenesis in pT7Ts vectors. Similarly, the N-termini with modified phosphorylation sites were further subcloned by PCR into pEBG for GST-pull down analysis. A Myc-tag was inserted in front of WNK4 by subcloning and the complete insert was placed into a pT7Ts vector using the gateway system (Invitrogen, Breda, the Netherlands). For generation of eGFP-NCC in pT7Ts, hNCC was subcloned by PCR from hNCC pT7Ts and constructed behind eGFP in a pCB7 vector. The complete insert was thereafter subcloned into pT7Ts. All inserts were verified by direct sequencing.

GST-pull down and Mass-spectrometry

The intracellular N- and C-terminal domains of NCC coupled to GST were produced in *E. Coli* BL21 cells. The bacteria were lysed and the GST-NCC terminal fusion domains were purified on glutathione–Sepharose 4B beads (Amersham Pharmacia Biotech). C57BL/6 mice were killed under 1.5% v/v isoflurane anesthesia (Nicholas Piramal Limited, London, United Kingdom) and the kidneys were homogenized in lysis buffer (20 mM Tris/HCl, 140 mM NaCl, 1 mM CaCl₂, 0.2% (v/v) Triton-X-100, 0.2% (v/v) NP-40, pH 7.4) containing protease inhibitors (0.10 mg/ml leupeptin, 0.05 mg/ml pepstatin-A, 1 mM phenylmethylsulfonyl fluoride, and 5 mg/ml aprotinin). The precipitated GST-terminal proteins were incubated overnight at 4°C with mouse kidney

γ -Adducin and thiazide-sensitive NaCl transport

lysates. After extensive washing, the precipitates were placed on a SDS-PAGE gel and analyzed by the Nijmegen Proteomics Facility (Radboud University Nijmegen Medical Centre, The Netherlands, <http://www.proteomicsnijmegen.nl/>). Proteins were in-gel digested with trypsin. After extraction from the gel, peptides were analyzed using nano-flow liquid chromatography coupled to a linear ion trap fourier-transform mass spectrometer (LTQ FT, Thermo Fisher Scientific). Peptide and protein identifications were extracted from the data by means of the search program Mascot using the NCBI database 20080103 containing *Mus musculus* taxonomy with addition of known contaminant proteins such as trypsin and human keratins.

Precipitation of GST-coupled fusion domains of NCC with HA-tagged γ -adducin in HEK293 cells was done as described in detail previously (50).

COPAS sorting and semi-quantitative Real-Time PCR Analysis

Transgene mice expressing eGFP after the parvalbumin promoter have been described previously (36). The animals were anesthetized by an intraperitoneal injection of Hellabrunn mixture (ketamine 0.05 mg/g bodyweight and xylazine 0.02 mg/g bodyweight), and perfused transcardially with digestion solution (1 mg/ml collagenase A (#1088793, Roche Diagnostics, Mannheim, Germany) and 1 mg/ml hyaluronidase (#H3884, Sigma Aldrich, Zwijndrecht, the Netherlands) in KREBS (145 mM NaCl, 10 mM HEPES, 5 mM KCl, 1 mM NaH₂PO₄, 2.5 mM CaCl₂, 1.8 mM MgSO₄, 5 mM glucose, pH 7.3). The animal ethics board of Radboud University Nijmegen approved all experimental procedures. The kidney cortex was finely minced and incubated in digestion solution for 22 min at 37°C, subsequently sieved through a series of meshes and finally collected on a 40 μ m filter. Fluorescently labeled DCT tubules were isolated from transgenic animals, using a COPAS sorter as described in detail previously (37). The GFP-positive fraction consists of DCT fragments. The remainder was saved and denoted whole kidney tubules. Tubule RNA was extracted using TriZol Total RNA Isolation Reagent (Life Technologies BRL, Breda, The Netherlands), and processed into cDNA. The cDNA was mixed

Chapter 2

with Power SYBR® green PCR mastermix (Applied Biosystems, Foster City, CA, USA) and exon overlapping primers against γ -adducin (5'-CACATCCACACCCTTGCCAC-3'; 5'-CCTGGTAGTCATAGTAGGCGAC-3'), NCC (5'-CTTCGGCCACTGGCATTCTG-3'; 5'-GATGGCAAGGTAGGAGATGG-3'), and the housekeeping gene glyceraldehyde-3-phosphate dehydrogenase (GAPDH; 5'- AACATCAAATGGGGTGA-3'; 5'-GGTTCACACCCATCACAA-3').

In vitro cRNA translation

pT7Ts plasmid vectors were linearized by restriction digestion at the 3'-end of the insert. The plasmids were transcribed *in vitro* using the mMMESSAGE mMACHINE® T7 Kit (Ambion, Austin, TX, USA) to generate cRNA. The integrity of the product was confirmed on 1% (w/v) agarose, 37% (v/v) formaldehyde gels. RNA concentrations were determined spectrophotometrically at 260 nm. The cRNA aliquots were stored at -80°C .

Evaluation of NCC function

All animal experiments described below received the approval from the animal ethics board of Radboud University Nijmegen. Isolation and $^{22}\text{Na}^{+}$ uptakes in oocytes were done as described previously (51, 52), with minor modifications. Briefly, *Xenopus laevis* oocytes were surgically collected after decapitation, manually separated, and incubated in collagenase A (1 mg/ml). Incubations were done in Ca^{2+} -free ND96 solution (96 mM NaCl, 2 mM KCl, 1 mM MgCl_2 , and 5 mM HEPES/NaOH, pH 7.4, 50 mg/l gentamicin). The following day, stage V and VI oocytes were selected and injected with the appropriate cRNAs in a final volume of 50 nl/oocyte. The oocytes were subsequently incubated in Ca^{2+} -containing ND96 including 1.8 mM CaCl_2 for 2-3 days at 16°C . 16 hrs prior to the uptake, oocytes were placed in Cl^{-} -depleted media (96 mM Na-isethionate, 2 mM K-gluconate, 1.8 mM Ca-gluconate, 1 mM $\text{Mg}(\text{NO}_3)_2$, 5 mM HEPES/NaOH, pH 7.4, 50 mg/dl gentamicin, ~ 200 mOsm) or hypotonic Cl^{-} -depleted media (same as above but

γ -Adducin and thiazide-sensitive NaCl transport

with 79.7 mM Na-isethionate, ~170 mOsm). Before the uptake, oocytes were preincubated in 1 mM ouabain, 0.1 mM amiloride, and 0.1 mM bumetanide in the presence or absence of 0.1 mM thiazide in Cl⁻-depleted media. ²²Na⁺ uptake (1 μ Ci ²²Na⁺/ml, Perkin Elmer) was done in K⁺-free isotonic uptake buffer (40 mM NaCl, 56 mM NMDG-Cl, 1.8 mM CaCl₂, 1 mM MgCl₂, 5 mM HEPES/NaOH, pH 7.4) for 1 hr. Oocytes were washed 5 times at the end of the ²²Na⁺ incubation with ice-cold uptake medium, transferred to scintillation vials, and lysed in 10% (w/v) Na⁺-dodecyl sulfate. Radioactivity was counted in a liquid scintillation counter.

Evaluation of total expression of NCC and γ -adducin in the oocyte

HA-NCC was detected in total membrane isolates, while HA- γ -adducin was detected in the remaining cytosolic fraction. As described in detail previously (49), membrane preparations and total lysates were prepared, blotted onto membranes, and detected using an enhanced chemiluminescence system (Pierce, Rockford, IL).

Quantification of eGFP-NCC in the oocyte membrane

Oocytes were injected with 1, 5, or 10 ng of eGFP-NCC cRNA as well as 10 ng eGFP-NCC cRNA in the presence of 10 ng of γ -adducin. cRNA. Images were acquired on an Olympus FV1000 laser-scanning microscope (Center Valley, PA, USA) using a 20X objective. Background subtraction and semi-quantitative determination of eGFP-NCC abundance at the plasma membrane was done using Image J (image processing program, NIH, USA)

*SiRNA against *Xenopus laevis* γ -adducin*

To confirm endogenous expression of γ -adducin in *Xenopus laevis* oocytes, primers designed against γ -adducin in *Xenopus Tropicalis* were used to amplify a fragment by RT-PCR (TaKaRa Taq™, Shiga, Japan) from oocyte cDNA. The fragment was extracted from the gel and sequenced. Sequence similarity was identical to the previously published mRNA of hypothetical

Chapter 2

protein LOC432146 from *Xenopus laevis*. siRNA was designed using double stranded oligo-probes against the following sequence of endogenous *Xenopus laevis* γ -adducin, 5'-AATGACCCCGGCTACATCCGC.-3'. Oocytes were injected with 5 ng of HA-NCC siRNA as described above. siRNAs were injected 24 hrs prior to the uptake.

Immunohistochemistry

Kidneys from C57BL/6 mice were immersion fixated in 1% (w/v) periodate-lysine-paraformaldehyde fixative. 10 μ m cryosections were prepared and co-stained with anti- γ -adducin antibodies (1:25, rabbit, H-60, Santa Cruz Biotechnology, Santa Cruz, CA, USA) and NCC (1:100, guinea pig; generously provided by Jan Loffing, Switzerland). Images were acquired on an Olympus FV1000 laser-scanning microscope (Center Valley, PA, USA).

Statistical analysis.

All results obtained in oocytes were the average of at least 3 independent experiments, each containing a minimum of 10 oocytes per group. Overall statistical between groups was determined by one-way ANOVA. In case of significance, multiple comparisons between groups were performed by Bonferroni post hoc tests. Values are presented as means \pm SEM. $p < 0.05$ is considered statistically significant.

Acknowledgments

The authors are grateful to our colleagues Jan Janssen, Henk Arnts, Femke van Zeeland, Jolein Gloerich, AnneMiete van der Kemp, Huib Croes, and Ron Engels for technical assistance and helpful suggestions. We greatly appreciate the support of Dr. Hannah Monyer, Universitätsklinikum Heidelberg, Germany for kindly donating the transgenic mouse line B-Pv-E. This study was supported financially by the Dutch Kidney foundation (C05.4106), the

γ -Adducin and thiazide-sensitive NaCl transport

Netherlands Organization for Scientific Research (ZonMw 9120.6110; ALW 700.55.302), and EURYI award from the European Science Foundation to JH.

Chapter 2

References

1. Kearney PM, Whelton M, Reynolds K, Muntner P, Whelton PK, He J. Global burden of hypertension: analysis of worldwide data. *Lancet*. 2005;365(9455):217-223.
2. Lawes CM, Vander Hoorn S, Law MR, Elliott P, MacMahon S, Rodgers A. Blood pressure and the global burden of disease 2000. Part II: estimates of attributable burden. *J Hypertens*. 2006;24(3):423-430.
3. Minino AM, Arias E, Kochanek KD, Murphy SL, Smith BL. Deaths: final data for 2000. *Natl Vital Stat Rep*. 2002;50(15):1-119.
4. Bakris GL, Ritz E. The message for World Kidney Day 2009: hypertension and kidney disease--a marriage that should be prevented. *J Hypertens*. 2009;27(3):666-669.
5. Guyton AC. Blood pressure control-special role of the kidneys and body fluids. *Science*. 1991;252(5014):1813-1816.
6. Lifton RP, Gharavi AG, Geller DS. Molecular mechanisms of human hypertension. *Cell*. 2001;104(4):545-556.
7. Chobanian AV, Bakris GL, Black HR, Cushman WC, Green LA, Izzo JL, Jr., Jones DW, Materson BJ, Oparil S, Wright JT, Jr., et al. The Seventh Report of the Joint National Committee on Prevention, Detection, Evaluation, and Treatment of High Blood Pressure: the JNC 7 report. *Jama*. 2003;289(19):2560-2572.
8. Reilly RF, Ellison DH. Mammalian Distal Tubule: Physiology, Pathophysiology, and Molecular Anatomy. *Physiol. Rev*. 2000;80(1):277-313.
9. Gitelman HJ, Graham JB, Welt LG. A new familial disorder characterized by hypokalemia and hypomagnesemia. *Trans Assoc Am Physicians*. 1966;79(221-235).
10. Simon DB, Nelson-Williams C, Bia MJ, Ellison D, Karet FE, Molina AM, Vaara I, Iwata F, Cushner HM, Koolen M, et al. Gitelman's variant of Bartter's syndrome, inherited hypokalaemic alkalosis, is caused by mutations in the thiazide-sensitive Na-Cl cotransporter. *Nat Genet*. 1996;12(1):24-30.
11. Gordon RD. The syndrome of hypertension and hyperkalemia with normal glomerular filtration rate: Gordon's syndrome. *Aust N Z J Med*. 1986;16(2):183-184.
12. Wilson FH, Disse-Nicodeme S, Choate KA, Ishikawa K, Nelson-Williams C, Desitter I, Gunel M, Milford DV, Lipkin GW, Achard JM, et al. Human hypertension caused by mutations in WNK kinases. *Science*. 2001;293(5532):1107-1112.
13. Kahle KT, Wilson FH, Leng Q, Lalioti MD, O'Connell AD, Dong K, Rapson AK, MacGregor GG, Giebisch G, Hebert SC, et al. WNK4 regulates the balance between renal NaCl reabsorption and K⁺ secretion. *Nat Genet*. 2003;35(4):372-376.
14. Yang CL, Angell J, Mitchell R, Ellison DH. WNK kinases regulate thiazide-sensitive NaCl cotransport. *J Clin Invest*. 2003;111(7):1039-1045.
15. Wilson FH, Kahle KT, Sabath E, Lalioti MD, Rapson AK, Hoover RS, Hebert SC, Gamba G, Lifton RP. Molecular pathogenesis of inherited hypertension with hyperkalemia: the

γ -Adducin and thiazide-sensitive NaCl transport

- NaCl cotransporter is inhibited by wild-type but not mutant WNK4. *Proc Natl Acad Sci U S A*. 2003;100(2):680-684.
16. Pacheco-Alvarez D, Cristobal PS, Meade P, Moreno E, Vazquez N, Munoz E, Diaz A, Juarez ME, Gimenez I, Gamba G. The Na⁺:Cl⁻ cotransporter is activated and phosphorylated at the amino-terminal domain upon intracellular Cl⁻ depletion. *J Biol Chem*. 2006;281(39):28755-28763.
 17. Darman RB, Forbush B. A regulatory locus of phosphorylation in the N-terminus of the Na⁺-K⁺-Cl⁻ cotransporter, NKCC1. *J Biol Chem*. 2002;277(40):37542-37550.
 18. Gimenez I, Forbush B. Short-term stimulation of the renal Na⁺-K⁺-Cl⁻ cotransporter (NKCC2) by vasopressin involves phosphorylation and membrane translocation of the protein. *J Biol Chem*. 2003;278(29):26946-26951.
 19. Gimenez I, Forbush B. Regulatory phosphorylation sites in the N-terminus of the renal Na⁺-K⁺-Cl⁻ cotransporter (NKCC2). *Am J Physiol Renal Physiol*. 2005;289(6):F1341-1345.
 20. Richardson C, Rafiqi FH, Karlsson HK, Moleleki N, Vandewalle A, Campbell DG, Morrice NA, Alessi DR. Activation of the thiazide-sensitive NaCl cotransporter by the WNK-regulated kinases SPAK and OSR1. *J Cell Sci*. 2008;121(Pt 5):675-684.
 21. Vitari AC, Deak M, Morrice NA, Alessi DR. The WNK1 and WNK4 protein kinases that are mutated in Gordon's hypertension syndrome phosphorylate and activate SPAK and OSR1 protein kinases. *Biochem J*. 2005;391(Pt 1):17-24.
 22. Gagnon KB, England R, Delpire E. Volume sensitivity of cation-Cl⁻ cotransporters is modulated by the interaction of two kinases: Ste20-related proline-alanine-rich kinase and WNK4. *Am J Physiol Cell Physiol*. 2006;290(1):C134-142.
 23. Ring AM, Leng Q, Rinehart J, Wilson FH, Kahle KT, Hebert SC, Lifton RP. An SGK1 site in WNK4 regulates Na⁺ channel and K⁺ channel activity and has implications for aldosterone signaling and K⁺ homeostasis. *Proc Natl Acad Sci U S A*. 2007;104(10):4025-4029.
 24. Rozansky DJ, Cornwall T, Subramanya AR, Rogers S, Yang YF, David LL, Zhu X, Yang CL, Ellison DH. Aldosterone mediates activation of the thiazide-sensitive NaCl cotransporter through an SGK1 and WNK4 signaling pathway. *J Clin Invest*. 2009;119(9):2601-2612.
 25. Yang CL, Zhu X, Ellison DH. The thiazide-sensitive NaCl cotransporter is regulated by a WNK kinase signaling complex. *J Clin Invest*. 2007;117(11):3403-3411.
 26. Ohta A, Rai T, Yui N, Chiga M, Yang SS, Lin SH, Sohara E, Sasaki S, Uchida S. Targeted disruption of the Wnk4 gene decreases phosphorylation of Na-Cl cotransporter, increases Na⁺ excretion and lowers blood pressure. *Hum Mol Genet*. 2009;18(20):3978-3986.
 27. Yang SS, Morimoto T, Rai T, Chiga M, Sohara E, Ohno M, Uchida K, Lin SH, Moriguchi T,

Chapter 2

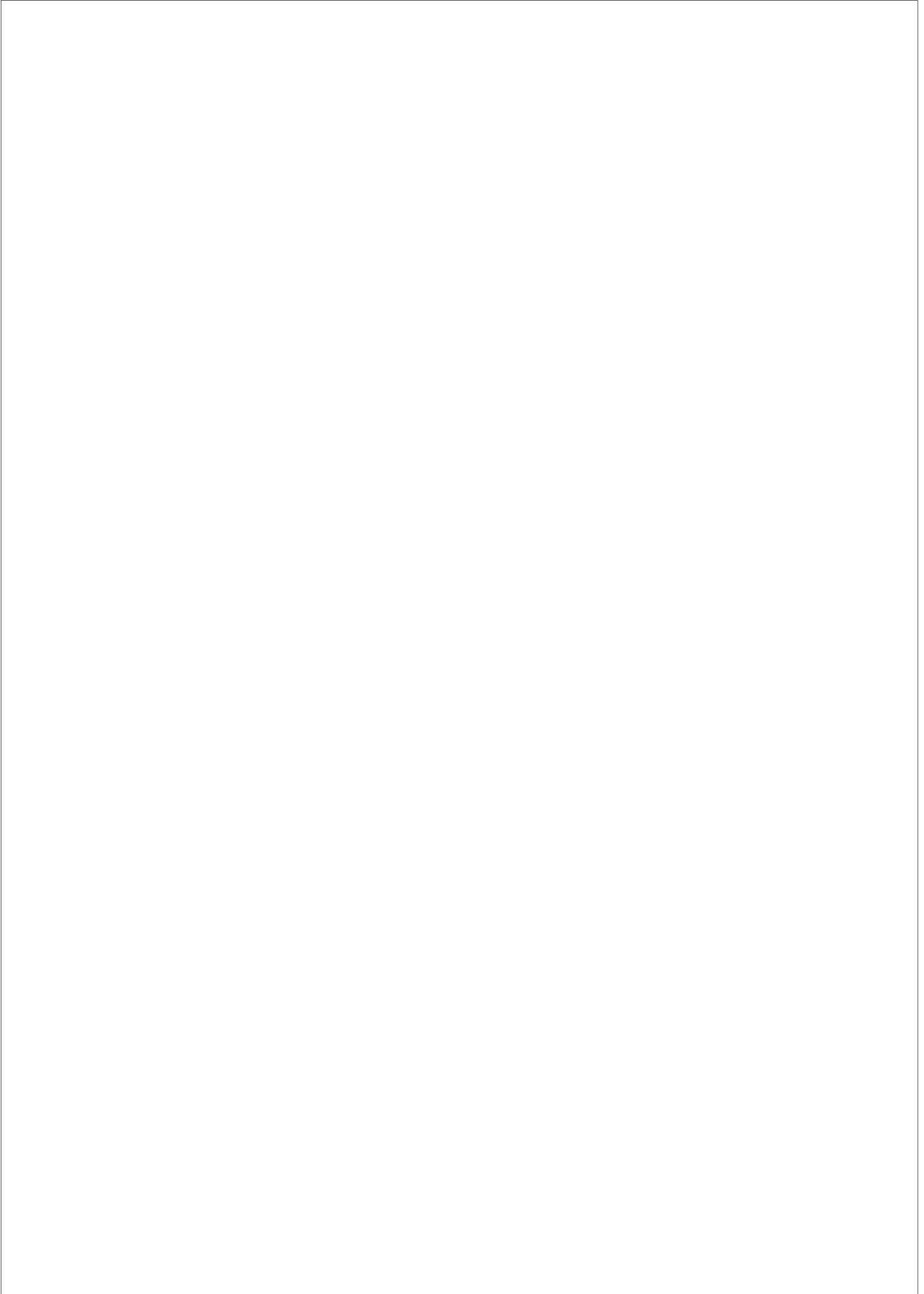
- Shibuya H, et al. Molecular pathogenesis of pseudohypoaldosteronism type II: generation and analysis of a *Wnk4*^{D561A/+} knockin mouse model. *Cell Metab.* 2007;5(5):331-344.
28. Zambrowicz BP, Abuin A, Ramirez-Solis R, Richter LJ, Piggott J, BeltrandelRio H, Buxton EC, Edwards J, Finch RA, Friddle CJ, et al. *Wnk1* kinase deficiency lowers blood pressure in mice: a gene-trap screen to identify potential targets for therapeutic intervention. *Proc Natl Acad Sci U S A.* 2003;100(24):14109-14114.
 29. Rafiqi FH, Zuber AM, Glover M, Richardson C, Fleming S, Jovanovic S, Jovanovic A, O'Shaughnessy KM, Alessi DR. Role of the WNK-activated SPAK kinase in regulating blood pressure. *EMBO Mol Med.* 2010;2(2):63-75.
 30. Vallon V, Schroth J, Lang F, Kuhl D, Uchida S. Expression and phosphorylation of the Na⁺-Cl⁻ cotransporter NCC in vivo is regulated by dietary NaCl, K⁺, and SGK1. *Am J Physiol Renal Physiol.* 2009;297(3):F704-712.
 31. Gardner K, Bennett V. Modulation of spectrin-actin assembly by erythrocyte adducin. *Nature.* 1987;328(6128):359-362.
 32. Cusi D, Barlassina C, Azzani T, Casari G, Citterio L, Devoto M, Glorioso N, Lanzani C, Manunta P, Righetti M, et al. Polymorphisms of alpha-adducin and salt sensitivity in patients with essential hypertension. *Lancet.* 1997;349(9062):1353-1357.
 33. Bianchi G, Tripodi G, Casari G, Salardi S, Barber BR, Garcia R, Leoni P, Torielli L, Cusi D, Ferrandi M, et al. Two point mutations within the adducin genes are involved in blood pressure variation. *Proc Natl Acad Sci U S A.* 1994;91(9):3999-4003.
 34. Zagato L, Modica R, Florio M, Torielli L, Bihoreau MT, Bianchi G, Tripodi G. Genetic mapping of blood pressure quantitative trait loci in Milan hypertensive rats. *Hypertension.* 2000;36(5):734-739.
 35. Fowler L, Everitt J, Stevens JL, Jaken S. Redistribution and enhanced protein kinase C-mediated phosphorylation of alpha- and gamma-adducin during renal tumor progression. *Cell Growth Differ.* 1998;9(5):405-413.
 36. Meyer AH, Katona I, Blatow M, Rozov A, Monyer H. In vivo labeling of parvalbumin-positive interneurons and analysis of electrical coupling in identified neurons. *J Neurosci.* 2002;22(16):7055-7064.
 37. Miller RL, Zhang P, Chen T, Rohrwasser A, Nelson RD. Automated method for the isolation of collecting ducts. *Am J Physiol Renal Physiol.* 2006;291(1):F236-245.
 38. Zhou B, Zhuang J, Gu D, Wang H, Cebotaru L, Guggino WB, Cai H. WNK4 Enhances the Degradation of NCC through a Sortilin-Mediated Lysosomal Pathway. *J Am Soc Nephrol.* 2009; 21(1):82-92.
 39. Dong L, Chapline C, Mousseau B, Fowler L, Ramsay K, Stevens JL, Jaken S. 35H, a sequence isolated as a protein kinase C binding protein, is a novel member of the adducin family. *J Biol Chem.* 1995;270(43):25534-25540.
 40. Matsuoka Y, Hughes CA, Bennett V. Adducin regulation. Definition of the

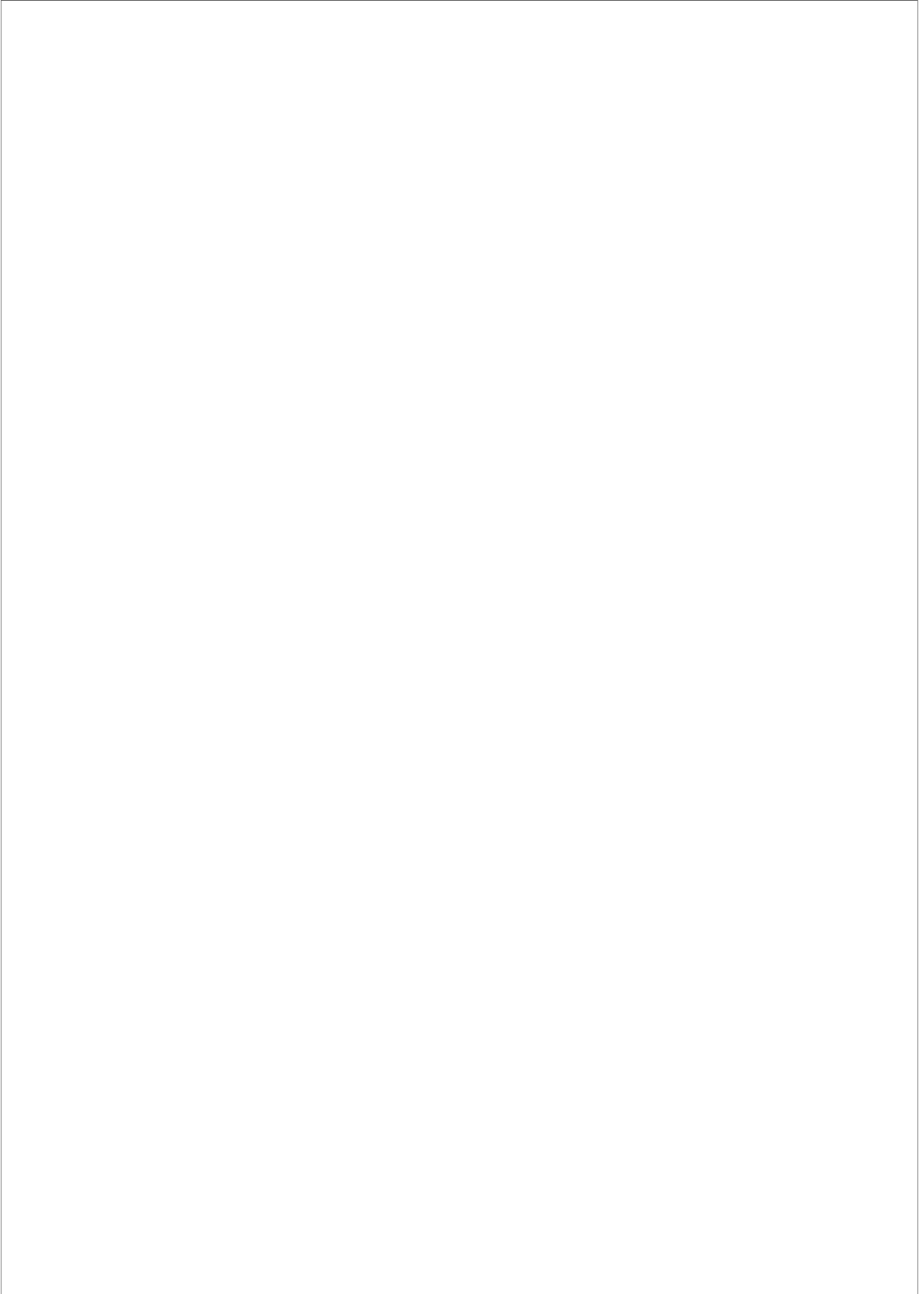
γ -Adducin and thiazide-sensitive NaCl transport

- calmodulin-binding domain and sites of phosphorylation by protein kinases A and C. *J Biol Chem.* 1996;271(41):25157-25166.
41. Tripodi G, Valtorta F, Torielli L, Chieregatti E, Salardi S, Trusolino L, Menegon A, Ferrari P, Marchisio PC, Bianchi G. Hypertension-associated point mutations in the adducin alpha and beta subunits affect actin cytoskeleton and ion transport. *J Clin Invest.* 1996;97(12):2815-2822.
 42. Dimke H, Flyvbjerg A, Bourgeois S, Thomsen K, Frokiaer J, Houillier P, Nielsen S, Frische S. Acute growth hormone administration induces antidiuretic and antinatriuretic effects and increases phosphorylation of NKCC2. *Am J Physiol Renal Physiol.* 2007;292(2):F723-735.
 43. San-Cristobal P, Pacheco-Alvarez D, Richardson C, Ring AM, Vazquez N, Rafiqi FH, Chari D, Kahle KT, Leng Q, Bobadilla NA, et al. Angiotensin II signaling increases activity of the renal NaCl cotransporter through a WNK4-SPAK-dependent pathway. *Proc Natl Acad Sci U S A.* 2009;106(11):4384-4389.
 44. Chiga M, Rai T, Yang SS, Ohta A, Takizawa T, Sasaki S, Uchida S. Dietary salt regulates the phosphorylation of OSR1/SPAK kinases and the NaCl cotransporter through aldosterone. *Kidney Int.* 2008;74(11):1403-1409.
 45. Cwynar M, Staessen JA, Ticha M, Nawrot T, Citterio L, Kuznetsova T, Wojciechowska W, Stolarz K, Filipovsky J, Kawecka-Jaszcz K, et al. Epistatic interaction between alpha- and gamma-adducin influences peripheral and central pulse pressures in white Europeans. *J Hypertens.* 2005;23(5):961-969.
 46. Robledo RF, Ciciotte SL, Gwynn B, Sahr KE, Gilligan DM, Mohandas N, Peters LL. Targeted deletion of alpha-adducin results in absent beta- and gamma-adducin, compensated hemolytic anemia, and lethal hydrocephalus in mice. *Blood.* 2008;112(10):4298-4307.
 47. Marro ML, Scremin OU, Jordan MC, Huynh L, Porro F, Roos KP, Gajovic S, Baralle FE, Muro AF. Hypertension in beta-adducin-deficient mice. *Hypertension.* 2000;36(3):449-453.
 48. Schultheis PJ, Lorenz JN, Meneton P, Nieman ML, Riddle TM, Flagella M, Duffy JJ, Doetschman T, Miller ML, Shull GE. Phenotype resembling Gitelman's syndrome in mice lacking the apical NaCl cotransporter of the distal convoluted tubule. *J Biol Chem.* 1998;273(44):29150-29155.
 49. de Jong JC, Willems PH, Mooren FJ, van den Heuvel LP, Knoers NV, Bindels RJ. The structural unit of the thiazide-sensitive NaCl cotransporter is a homodimer. *J Biol Chem.* 2003;278(27):24302-24307.
 50. Schoeber JP, Topala CN, Lee KP, Lambers TT, Ricard G, van der Kemp AW, Huynen MA, Hoenderop JG, Bindels RJ. Identification of Nipsnap1 as a novel auxiliary protein inhibiting TRPV6 activity. *Pflugers Arch.* 2008;457(1):91-101.

Chapter 2

51. De Jong JC, Van Der Vliet WA, Van Den Heuvel LP, Willems PH, Knoers NV, Bindels RJ. Functional expression of mutations in the human NaCl cotransporter: evidence for impaired routing mechanisms in Gitelman's syndrome. *J Am Soc Nephrol.* 2002;13(6):1442-1448.
52. Gamba G, Saltzberg SN, Lombardi M, Miyanoshita A, Lytton J, Hediger MA, Brenner BM, Hebert SC. Primary structure and functional expression of a cDNA encoding the thiazide-sensitive, electroneutral NaCl cotransporter. *Proc Natl Acad Sci U S A.* 1993;90(7):2749-2753.





CHAPTER 3

Effects of the Epidermal Growth Factor Receptor (EGFR) kinase inhibitor Erlotinib on renal and systemic Mg²⁺ handling

Henrik Dimke¹, Jenny van der Wijst¹, Todd R. Alexander¹, Inez M. J. Meijer², Gemma M. Mulder³, Harry van Goor³, Sabine Tejpar³, Joost G. Hoenderop¹, René J. Bindels¹.

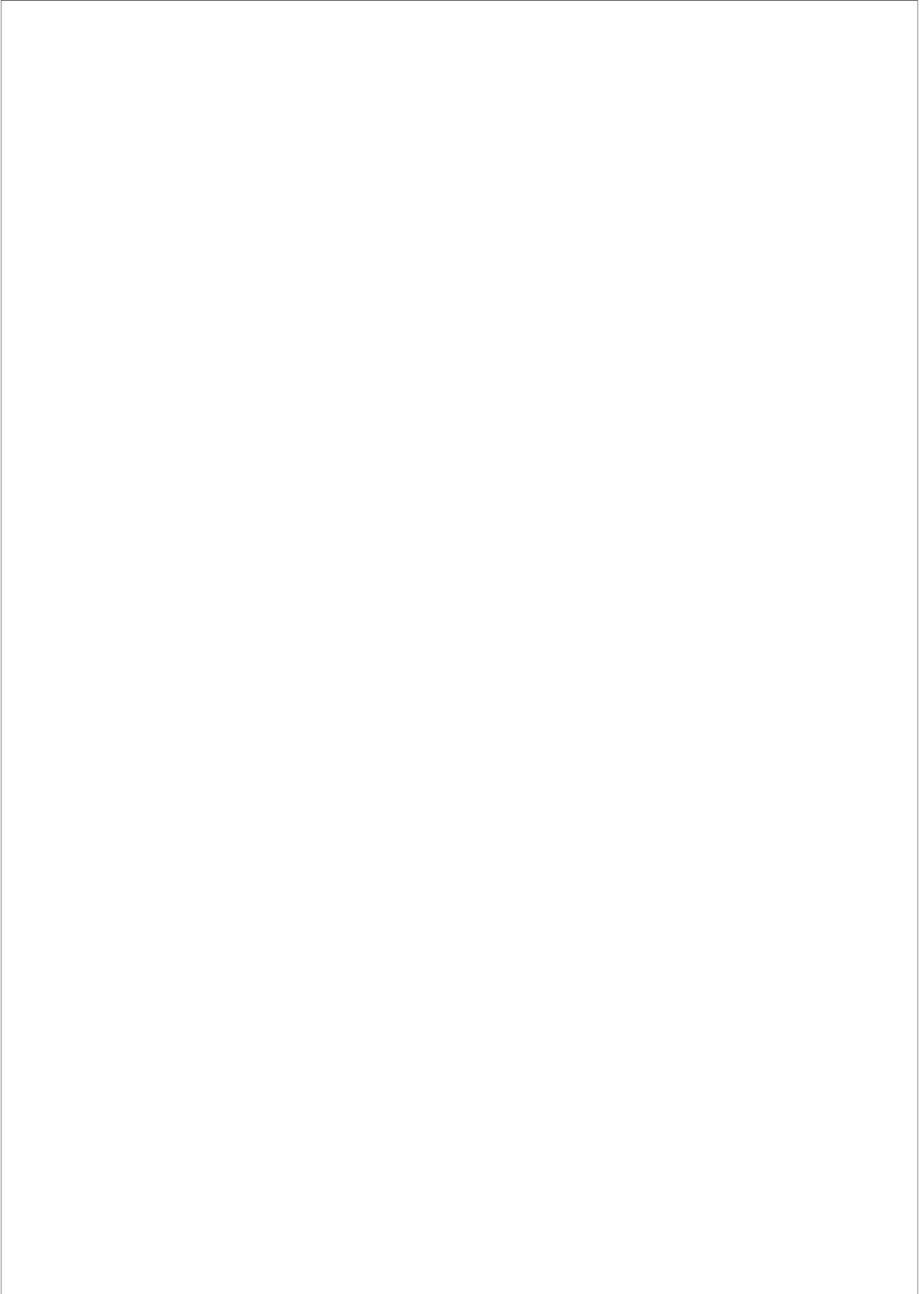
¹Department of Physiology, Radboud University Nijmegen Medical Centre, the Netherlands.

²Department of Cell Biology, Faculty of Science, Nijmegen Centre for Molecular Life Sciences, Radboud University Nijmegen, Nijmegen, The Netherlands.

³Department of Pathology and Medical Biology, University Medical Centre Groningen, the Netherlands.

⁴Digestive Oncology Unit, Department of Internal Medicine, University Hospital Gasthuisberg and Catholic University Leuven, Leuven, Belgium.

Journal of the American Society of Nephrology, 2010



Abstract

A mutation in pro-EGF causes isolated hypomagnesemia. Further, monoclonal antibodies targeting the extracellular EGFR domain have been implicated in the regulation of epithelial Mg^{2+} transport. However, the effect of the widely used EGFR tyrosine kinase inhibitor, Erlotinib, on Mg^{2+} homeostasis remains unknown. To investigate the potential role of Erlotinib on Mg^{2+} handling, C57BL/6 mice were given intraperitoneal injections for 23 days. In Erlotinib-injected mice, a small but significant decrease in serum Mg^{2+} concentrations was observed at day 16 and 23, while the fractional excretion of Mg^{2+} remained unchanged after 23 days. Semi-quantitative immunohistochemical evaluation did not reveal detectable changes in renal Transient Receptor Potential Melastatin 6 (TRPM6) protein expression. The effect of Erlotinib on TRPM6 was investigated in human embryonic kidney (HEK) 293 cells. Patch clamp analysis in TRPM6 expressing cells demonstrated that Erlotinib inhibited EGF-induced changes in TRPM6 current density at a concentration of 30 μ M. At lower concentrations (0.3 μ M), Erlotinib failed to inhibit EGF-mediated TRPM6 stimulation. Likewise, EGF-induced tyrosine phosphorylation of its receptor was only blocked by 30 μ M of Erlotinib. In addition, 30 μ M Erlotinib inhibited EGF-stimulated increases in the mobile fraction of endomembrane TRPM6 channels. In this mouse model, Erlotinib does influence Mg^{2+} handling. However, the effect on the systemic Mg^{2+} concentration seems less potent than that observed with antibody-based EGFR inhibitors *in vivo*. Currently, clinical data detailing the effect of Erlotinib on Mg^{2+} handling is lacking. Based on the doses given to cancer patients it is unlikely that Erlotinib severely affects serum Mg^{2+} concentrations in these individuals.

Introduction

Overall maintenance of serum Mg^{2+} concentration is essential for many cellular processes, including adequate function of neurological and cardiovascular systems. The Transient Receptor

Chapter 3

Potential Melastatin subtype 6 (TRPM6) was originally identified as the causative gene for the rare autosomal recessive disorder; hypomagnesemia with secondary hypocalcemia (1, 2). TRPM6, which is expressed in kidney and colon (1, 3, 4), constitutes the gatekeeper and postulated rate-limiting entry step for active Mg^{2+} (re-) absorption.

The effect of EGF on TRPM6 has been firmly established. Application of EGF readily increases TRPM6 current density (5, 6). Additional evidence suggests that EGF provokes trafficking of the channel to the plasma membrane, via activation of the Rho GTPase, Rac1 (5). These discoveries were prompted by the observations that anti-cancer treatments with monoclonal antibodies (Cetuximab), targeting an extracellular epitope on the epidermal growth factor receptor (EGFR), causes hypomagnesemia in patients with colorectal cancer. In addition, genetic linkage and sequence analysis implicated the pro-EGF gene in isolated recessive renal hypomagnesemia (6-8). The observed decline in serum Mg^{2+} is accompanied by renal Mg^{2+} wasting, as these patients maintain an inappropriately high fractional Mg^{2+} excretion (6).

While mostly patients with colorectal cancer are treated with monoclonal EGFR inhibitors, numerous patient groups suffering from cancer receive tyrosine kinase inhibitors, such as Erlotinib or Gefitinib. These include individuals being treated for non-small cell lung cancer as well as pancreatic cancer (9). Erlotinib has been grouped with platinum compounds in most trials, a combination that may potentiate the effects on serum Mg^{2+} concentrations (10). At present, there are no published clinical reports detailing the potential effect of tyrosine kinase inhibitors on systemic and renal Mg^{2+} handling. Given the pronounced effect of Cetuximab on Mg^{2+} homeostasis, we sought to ascertain whether Erlotinib alters Mg^{2+} handling. Thus Mg^{2+} homeostasis and TRPM6 expression levels were investigated in wild-type mice receiving Erlotinib for 23 days, and the effect of Erlotinib on current density and mobility of TRPM6 was studied in human embryonic kidney (HEK) 293 cells transiently overexpressing the channel.

Results

Erlotinib reduces serum Mg²⁺ concentration in C57Bl/6 mice

C57BL/6 mice were injected intraperitoneally with a high dose of Erlotinib or vehicle for 23 day (2 mg/mouse/day) (n=9 per group). Blood samples were obtained at day 16, by puncturing a vascular bundle in the sub-mandibular area. Serum Mg²⁺ concentration showed a significant decline in the Erlotinib-injected group (p<0.05) (Figure 1A), while no difference was detected in serum Ca²⁺ concentration between groups (Figure 1B).

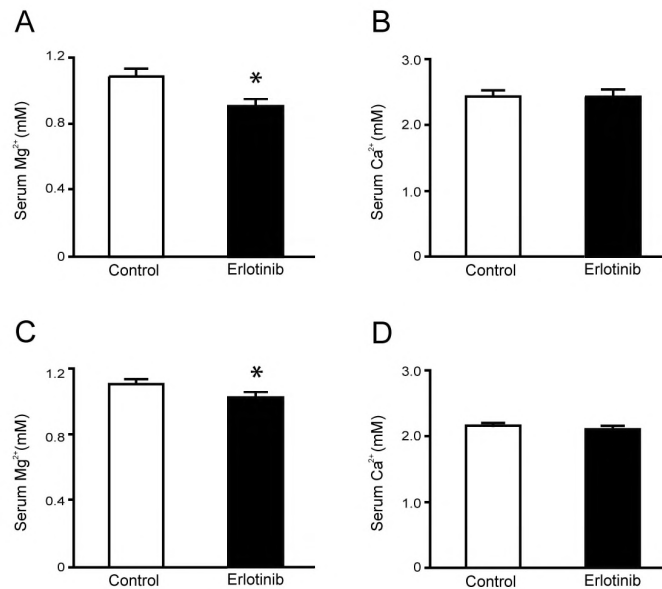


Figure 1. Effect of Erlotinib on serum Mg²⁺ and Ca²⁺ concentrations. (A-B) Changes in serum Mg²⁺ and Ca²⁺ concentrations after 16 days, in mice receiving daily injections with Erlotinib or vehicle. (C-D) Effect of Erlotinib or vehicle on serum Mg²⁺ and Ca²⁺ concentrations after 23 days. Values are presented as means ± SEM (n = 9). *p<0.05 is considered statistically significant.

Upon sacrifice after 23 days of Erlotinib injections, similar results were found, namely a slight but significant decline in the serum Mg²⁺ concentration in the Erlotinib-injected group (p<0.05) (Figure 1C). Erlotinib did not affect the systemic Ca²⁺ concentration at day 23 (Figure 1D).

No difference was observed in the urinary excretion of Mg²⁺, (Figure 2A) and the urinary Ca²⁺ excretion (Figure 2B) after 23 days of Erlotinib administration. The glomerular filtration rate

Chapter 3

remained within normal limits (Figure 2C). Importantly, no change in the fractional excretion of Mg^{2+} was observed in mice receiving Erlotinib (Figure 2D). The fractional excretion of Ca^{2+} remained unchanged after chronic administration of Erlotinib (Figure 2E). These results suggest that Erlotinib-treated mice waste Mg^{2+} , as serum Mg^{2+} is decreased while a compensatory reduction in the fractional Mg^{2+} excretion is absent.

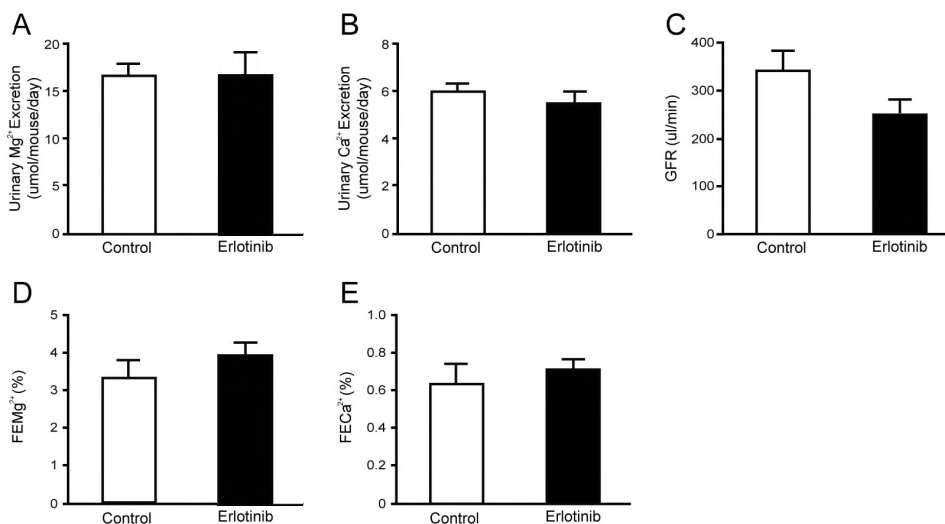


Figure 2. Functional data after 23 days of Erlotinib injections. (A-B) Daily urinary excretion of Mg^{2+} and Ca^{2+} in mice injected with Erlotinib for 23 days. (C) Creatinine clearance (estimated glomerular filtration rate) in Erlotinib- and vehicle- injected mice as well as (D-E) the corresponding fractional excretions of Mg^{2+} (FEMg) and Ca^{2+} (FECa). Values are presented as means \pm SEM (n = 9). * $p < 0.05$ is considered statistically significant.

Renal TRPM6 protein expression is unchanged in Erlotinib-injected mice

As mice injected with Erlotinib develop a modest reduction in serum Mg^{2+} , without appropriate compensation by the kidney, a possible effect could be on the expression level of TRPM6. Therefore, TRPM6 mRNA abundance was determined in the Erlotinib- and vehicle-injected mice. Chronic administration of Erlotinib caused a significant 0.67 fold decrease in the mRNA expression of TRPM6 ($p < 0.05$, $n = 9$) (Figure 3A). TRPM6 protein abundance was determined by semi-quantification of fluorescence, from anti-TRPM6 immunolabeled kidney sections. However, using this method no change in TRPM6 fluorescence was found ($p = 0.99$, $n = 9$) (Figure 3B). As

Erlotinib modulates TRPM6

TRPM6 is abundantly expressed in colon, the main site for active Mg^{2+} absorption in the intestine, the effect of Erlotinib on colonic TRPM6 mRNA expression was investigated. No change in the abundance of colonic TRPM6 was observed between Erlotinib- and vehicle- injected mice (Figure 3C).

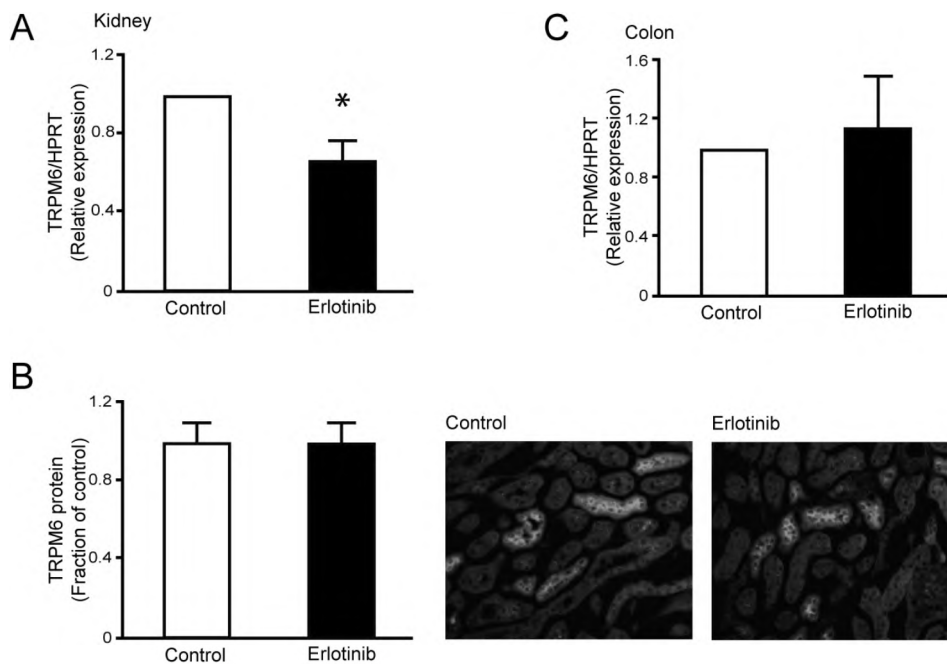


Figure 3. Effect of Erlotinib on mRNA and protein abundance of TRPM6. (A) Semi-quantitative real-time PCR was used to determine the abundance of TRPM6 mRNA extracted from kidney. (B) Histogram depicting TRPM6 protein abundance determined by computerized analysis of immunohistochemical images. Representative immunohistochemical pictures of TRPM6 in vehicle- and Erlotinib- injected mice. (C) Semi-quantitative real-time PCR determination of TRPM6 mRNA expression in colon. Data is presented as means \pm SEM. * $p < 0.05$ is considered statistically significant.

Renal EGFR expression is increased in mice injected with Erlotinib

To investigate whether changes in the renal EGF system were apparent after chronic administration of Erlotinib, renal mRNA expression of EGF and the EGFR was determined. A 1.6 fold increase in the mRNA abundance of the EGFR receptor was observed in Erlotinib-injected mice ($p < 0.05$, $n = 9$) (Figure 4A). Additionally, no change in renal mRNA expression of EGF was observed after injection of Erlotinib ($n = 9$) (Figure 4B). To evaluate changes in the secretion of EGF after administration of Erlotinib, the urinary excretion of EGF was measured in the

Chapter 3

experimental groups. No differences were observed in the total urinary excretion of EGF between vehicle- and Erlotinib-injected animals (Figure 4C). In addition, no changes were detected when the values were corrected for the urinary creatinine excretion (Figure 4D). As the colonic EGF system may be affected in a similar way, as observed in the kidney, the abundance of the EGFR and the EGF mRNA was investigated in samples extracted from colon. However, no differences in the colonic expression of the EGFR (n=9) (Figure 4E) and EGF (n=9) (Figure 4F) were detectable between vehicle- and Erlotinib-injected animals.

Supraphysiological concentrations of Erlotinib are necessary to inhibit TRPM6 channel activity

HEK293 cells expressing TRPM6 were subjected to whole cell patch-clamp analysis. Using this technique a TRPM6 specific outward current was detectable. Pretreatment with Erlotinib alone did not significantly affect channel currents from controls. Application of EGF (10 nM) significantly increased channel activity compared to control ($p < 0.05$) (Figure 5A-C). Pretreatment with Erlotinib (30 μM) completely prevented the EGF-induced increase in TRPM6 current density ($p < 0.05$). However, at lower Erlotinib concentrations (0.3 μM), Erlotinib did not significantly inhibit EGF-stimulated TRPM6 channel currents (Figure 5A-C). Tyrosine phosphorylation of the immunoprecipitated EGFR was evaluated under the same experimental conditions as aforementioned (Figure 5D). In the presence of EGF, tyrosine phosphorylation of the immunoprecipitated receptor was markedly increased. Preincubation of HEK293 cells with Erlotinib (30 μM) blunted the EGF-induced EGFR tyrosine phosphorylation. However, incubation with 0.3 μM of Erlotinib was not sufficient to effectively block EGFR phosphorylation. Cells incubated in the absence of EGF showed no detectable tyrosine phosphorylation of the EGFR.

Erlotinib modulates TRPM6

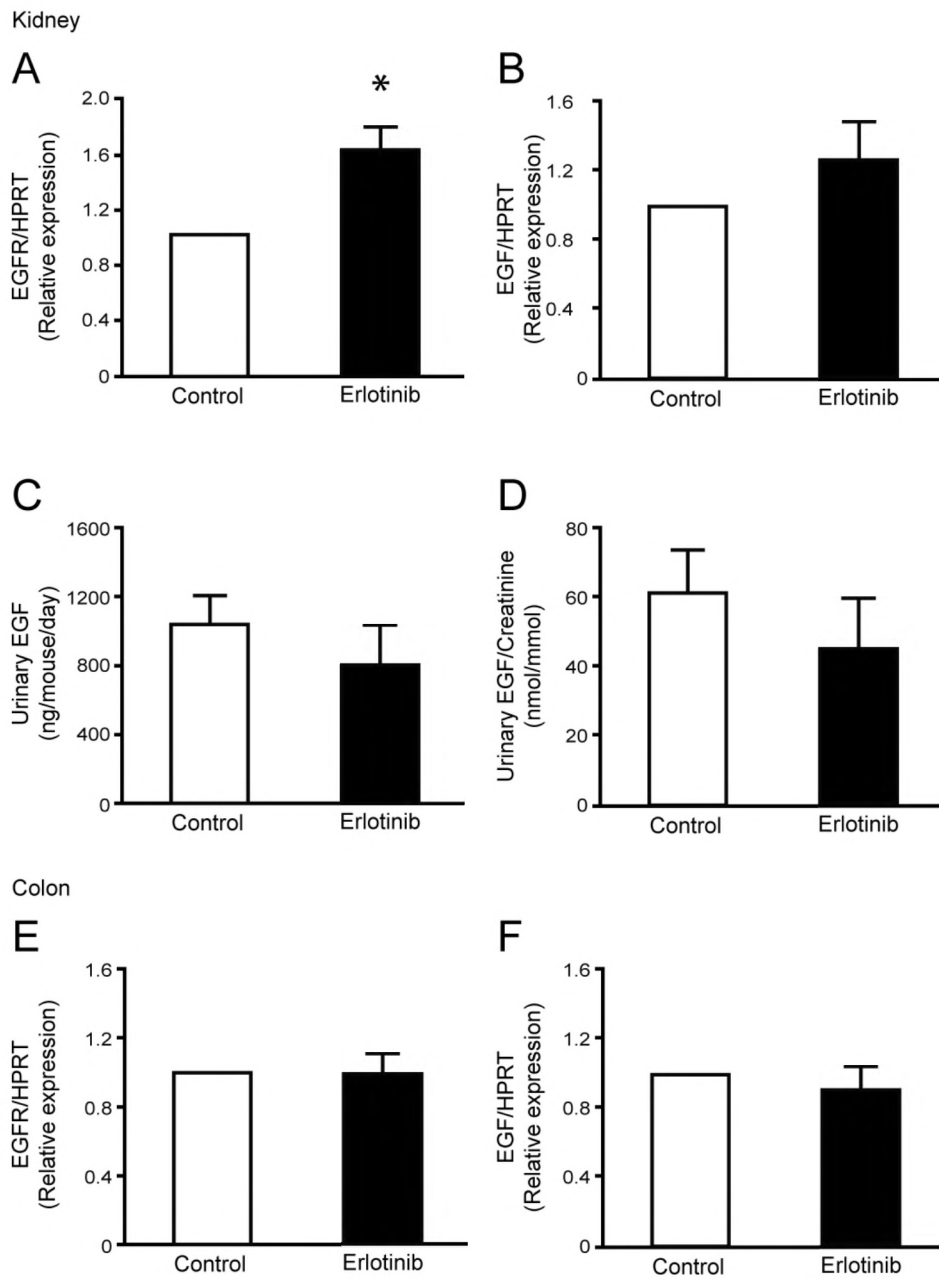


Figure 4. Erlotinib modulates EGFR mRNA expression. (A-B) Semi-quantitative determination of the mRNA abundance of EGFR and EGF in kidney of vehicle and Erlotinib-injected mice. (C-D) Measurements of urinary EGF excretion as well as the urinary EGF/creatinine ratio. (E-F) Colonic mRNA abundance of EGFR and EGF. Data is presented as means \pm SEM. * $p < 0.05$ is considered statistically significant.

Chapter 3

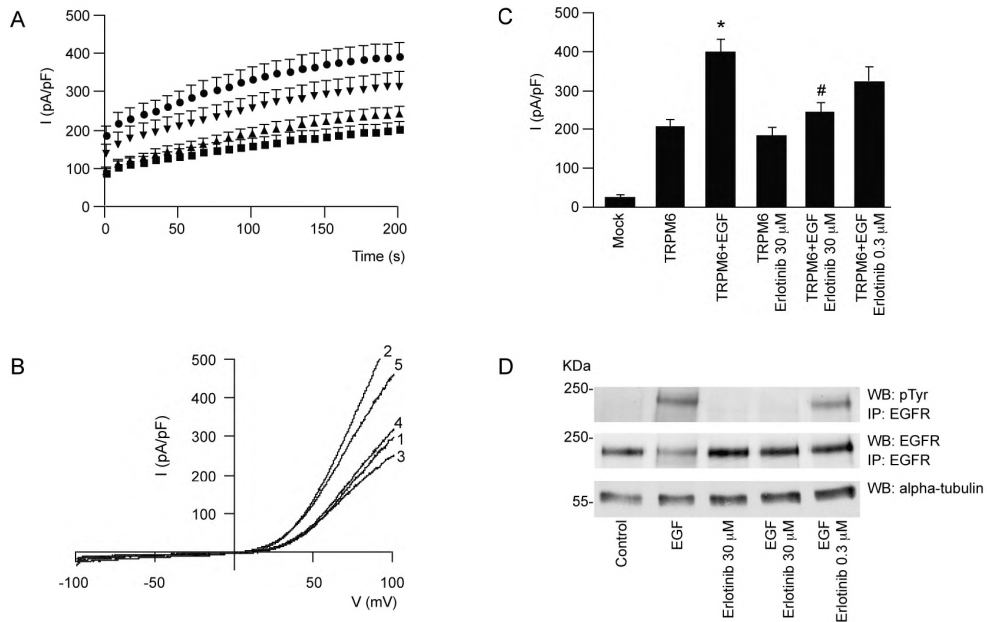


Figure 5. EGFR blockade by Erlotinib can prevent EGF-induced changes in TRPM6 current density. (A) Time course of the current development (pA/pF) at +80 mV of TRPM6 (■) transfected HEK293 cells, pretreated with EGF (●) and Erlotinib 30 μM (▲) or 0.3 μM (▼). (B) Current recorded after 200 sec stimulation by a voltage ramp between -100 and +100 mV of TRPM6 transfected HEK293 cells (1), pretreated with EGF (2) or Erlotinib (3) alone, or pretreated with EGF and Erlotinib 30 μM (4) / 0.3 μM (5). (C) Histogram summarizing the current density (pA/pF) at +80 of TRPM6 transfected HEK293 cells pretreated with EGF and/or Erlotinib as indicated. * indicates $p < 0.01$ compared to TRPM6 current ($n = 12-26$ cells). # indicates $p < 0.05$ compared to TRPM6 pretreated with EGF ($n = 12-26$ cells). (D) The immunoprecipitated EGFR was placed on Western blots for the detection of tyrosine phosphorylation (pTyr) as well as the EGFR itself. In addition, alpha-tubulin was detected in whole cell lysates as a control for total expression.

Erlotinib inhibits EGF-stimulated mobility of endomembrane TRPM6

Fluorescence recovery after photobleaching (FRAP) was used to estimate the mobility and mobile fraction of GFP-tagged TRPM6 channels in HEK293 cells. The electrophysiological properties of GFP-TRPM6 have previously been shown to display comparable currents to that of wild-type TRPM6 in the presence or absence of EGF (5). In line with this, an increase in the maximal recovery was found after EGF application ($p < 0.05$) (Figure 6 D-E). Pretreatment with Erlotinib (at 30 μM) prevented the EGF-stimulated increase in the mobile fraction of TRPM6 channels ($p < 0.05$) (Figure 6 D-E).

Erlotinib modulates TRPM6

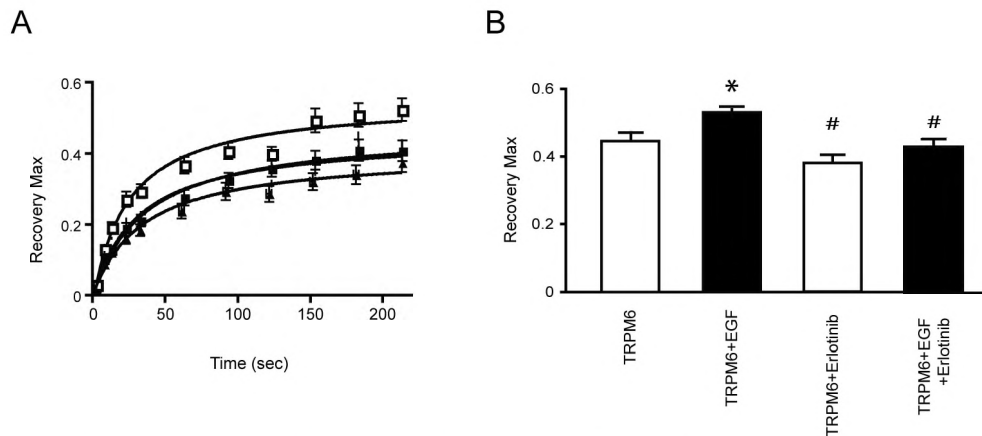


Figure 6. Erlotinib inhibits EGF-stimulated changes in the mobile fraction of TRPM6. (A) Fluorescence recovery kinetics as a function of time, measured in HEK293 cells transiently transfected with GFP-TRPM6. Cells were pre-incubated with Erlotinib (30 μ M, 30 min) alone (\blacktriangle) or prior to EGF application (10 nM, 30-60 min, \triangle), and compared to control (\blacksquare) or EGF-treated cells (\square). (B) Histogram representing the maximal recovery of fluorescence (estimated mobile fraction) in HEK293 cells expressing GFP-TRPM6 with or without application of Erlotinib, EGF, or both. Data is presented as means \pm SEM (n = 9). *p<0.05 is considered statistically significant from control. #p<0.05 statistically significant from EGF-treated.

Discussion

The current study shows Erlotinib is capable of affecting TRPM6 regulation and thereby altering Mg^{2+} handling. This conclusion is based on; 1) mice receiving supraphysiological doses of Erlotinib for 23 days develop a decrease in their serum Mg^{2+} concentration. 2) Erlotinib-injected mice fail to reduce the fractional renal excretion of Mg^{2+} in response to a decreased serum Mg^{2+} concentration. 3) Whole-cell patch clamp analysis in HEK293 cells shows that Erlotinib significantly inhibited EGF-stimulated TRPM6 channel activity.

Administration of 92 mg/kg Erlotinib (~2.3 mg/ 25 g mouse) intraperitoneally yielded a plasma concentration of approximately 40 μ M after 1 hr in mice (11). A virtually identical dose was employed in our mice study (2 mg/mouse/day), thus we can expect similar plasma concentrations of Erlotinib. HEK293 cells received dosages in the same range (30 μ M of Erlotinib). Given the moderate effects of Erlotinib *in vivo*, application of the compound could still block EGF-stimulated TRPM6 currents and routing in HEK293 cells. This can possibly be

Chapter 3

explained by the bioavailability of the compound. It has been estimated that 92-95% of the administered Erlotinib is bound to plasma proteins (12), thus the estimated free concentration in our mouse model would approximate 2-3 μM , a dose that likely would impose less inhibition on EGF-stimulated TRPM6 activity *in vitro*. Individuals receiving a single standard dose of Erlotinib (150 mg) show a maximal plasma concentration amounting to $2.65 \pm 2.02 \mu\text{M}$ (1.14 $\mu\text{g/ml}$) of the compound (12, 13), representing a ~10 times lower circulating concentration than the mouse model. Given that the free circulating concentration of Erlotinib is likely to be around 0.3 μM in human patients, we tested whether this concentration would be able to block the effect of EGF on TRPM6 currents. However, we could not detect any significant differences from EGF-stimulated cells. Evaluating EGF-induced tyrosine phosphorylation of its receptor substantiated these data. At Erlotinib concentrations of 30 μM , we were unable to detect any phosphorylation of the EGFR. At lower concentrations (0.3 μM), resembling the free concentration found in humans receiving standard doses of Erlotinib, EGFR phosphorylation was still present after application of EGF. Previous studies show that Erlotinib inhibits ligand-stimulated tyrosine autophosphorylation of the EGFR, with an IC_{50} of approximately 20 nM in cells. However, concentrations of at least a few hundred nM of Erlotinib are necessary to block more than 90% of the ligand-induced autophosphorylation (14, 15). The results obtained in this study fits well with the previous observations. Taken together, these data indicate that Erlotinib treatment in human patients is unlikely to induce severe hypomagnesemia as observed with EGFR-directed antibodies. However, it remains unclear whether the cellular concentration of Erlotinib, namely that obtained in the DCT, is similar to what is observed in plasma. Similarly, the bioavailability of monoclonal antibodies may explain why colorectal cancer patients receiving Cetuximab show a pronounced decrease in serum Mg^{2+} concentrations; to such a degree that hypomagnesemia develops.

We also find that inhibition of Mg^{2+} transport by Erlotinib is likely to occur via inhibition of TRPM6 routing, by preventing EGF-mediated changes in the mobile fraction of TRPM6 proteins.

Erlotinib modulates TRPM6

After application of Erlotinib, the EGF-stimulated fraction of TRPM6 channels becomes unresponsive. As previously shown, EGF does not only increase the mobile fraction, but also increases the plasma membrane expression of the channel, suggesting that EGF exerts its effect by redistributing TRPM6 from storage vesicles to the membrane (5). In the experimental animal, where physiological levels of EGF are present, blockade of the EGFR would be expected to retain a bigger fraction of TRPM6 channels in endomembrane compartments, thereby preventing plasma membrane trafficking and hence reduce Mg^{2+} influx. This hypothesis would also explain renal Mg^{2+} wasting, without concomitant changes in renal TRPM6 protein expression.

EGFR inhibition by Erlotinib influences Mg^{2+} handling, by decreasing serum Mg^{2+} content, without providing a compensatory decrease in the fractional renal Mg^{2+} excretion. These data are in good agreement with those obtained from patients receiving Cetuximab, although less pronounced (6, 7). Thus, the kidney is not able to effectively compensate for the reduction in serum Mg^{2+} concentration. Accordingly, the data insofar support tubular Mg^{2+} wasting, as a potential source of reducing serum Mg^{2+} concentration or at least in keeping serum Mg^{2+} lowered. Systemic and renal Ca^{2+} homeostasis remained unaffected during administration of Erlotinib, suggesting that EGF does not directly affect Ca^{2+} handling. Thus the changes in renal Mg^{2+} handling correlate well with impaired distal tubular transport, where Mg^{2+} transport is mechanistically separated from that of Ca^{2+} . Also, the lack of secondary changes in Ca^{2+} , which often accompany perturbations in Mg^{2+} homeostasis, may be explained by the modest decline in serum Mg^{2+} concentration observed in Erlotinib-injected animals. This is confirmed in patients treated with Cetuximab, as the appearance of hypocalcaemia was limited to individuals presenting with at least grade 2 hypomagnesemia (serum Mg^{2+} between 0.5 to 0.4 mM) (7). The underlying cause of the secondary hypocalcemia during severe hypomagnesemia remains incompletely understood, although impaired release of PTH from the parathyroid gland and desensitization of bone to PTH is likely implicated (16, 17).

Despite a significant decrease in renal TRPM6 mRNA abundance, semi-quantitative

Chapter 3

comparison of TRPM6 immunofluorescence could not detect a difference in protein expression. These findings may be explained by the observation that TRPM6 is retained in endomembrane vesicles, leading to a decreased degradation of the protein. In such an event, mRNA expression would be expected reduced, as the protein is retained in the cell. In fact, *in vitro* findings in this study support this observation, i.e. impaired mobility of TRPM6 after EGF-stimulation in the presence of Erlotinib.

No change was observed in colonic TRPM6 mRNA abundance. Due to difficulties detecting TRPM6 immunohistochemically in the colon, it is not possible to confirm whether TRPM6 protein abundance remains unchanged. Moreover, it cannot be excluded whether Erlotinib inhibits EGF-stimulated TRPM6 trafficking in the colon, as we observe in HEK293 cells. However, it is currently not possible to effectively estimate Mg^{2+} uptake in the intact animal using tracers, due to the very short half-life of the radioactive $^{28}Mg^{2+}$ isotope. In addition, one would expect an increased TRPM6 expression in the colon during conditions of lowered serum Mg^{2+} , an effect that is not observed here and elsewhere (3). It is currently unclear how colonic Mg^{2+} absorption is regulated. An increase was found in the renal EGFR mRNA expression, while in the colon no such change could be detected. This response may indicate that particularly in kidney, the EGF axis is affected after Erlotinib treatment. Additionally, the EGF mRNA abundance remained unchanged in both organs. Measurements of EGF in the urine supported these findings, suggesting that EGF secretion is not altered in response to Erlotinib.

The current study is to our knowledge the first to delineate the effects of Erlotinib on Mg^{2+} handling *in vivo*. Taken together, these findings suggest that Erlotinib can inhibit EGF-stimulated TRPM6 activity and consequently impair Mg^{2+} reabsorption in the kidney. Additionally, it provides an explanation about why hypomagnesemia has not been correlated with Erlotinib treatment in patients undergoing chemotherapy, as has been observed with Cetuximab. However, it should be noted that Erlotinib has the potential to modulate renal and systemic Mg^{2+} handling *in vivo*. Therefore, caution should be given when treating individuals prone to developing

Erlotinib modulates TRPM6

hypomagnesemia, and patients receiving combinational treatment with Mg^{2+} lowering compounds.

Materials and methods

Experimental protocol

C57BL/6 mice (10 weeks old, n=18) received intraperitoneal injections with Erlotinib or vehicle for 23 days. The animals were kept in a light- and temperature-controlled room with *ad libitum* access to food and water. Erlotinib (Tarceva®, generously provided by Roche Diagnostics GmbH, Penzberg, Germany) was dissolved in 10% dimethylsulfoxide (DMSO) v/v in saline with 0.1% Pluronic P105 v/v as previously described (11). The compound was delivered once daily at a dose of 2 mg/mouse/day. Controls received an identical vehicle solution. At day 16, blood was obtained by puncturing the vascular bundle located rear of the jawbone. During the last 24 hrs of the experimental period, mice were placed in metabolic cages and subsequently sacrificed under 1.5% v/v isoflurane anesthesia (Nicholas Piramal Limited, London, United Kingdom). Blood was withdrawn by perforating the orbital vessels and serum was extracted afterwards. Additionally, organs were dissected out and immediately frozen in liquid nitrogen. One half kidney was processed for immunohistochemistry by immersion fixation in 2% w/v periodate-lysine-paraformaldehyde (PLP), followed by overnight incubation in 15% w/v sucrose. The animal ethics board of Radboud University Nijmegen approved all experimental procedures.

Analytical procedures

Serum and urinary Mg^{2+} and Ca^{2+} concentrations were measured using a colorimetric assay kit according to the manufacturer's protocol (Roche Diagnostics, Almere, the Netherlands). Urinary mouse EGF was measured by an Enzyme-linked immunosorbent assay (R&D DuoSet® ELISA, DY2028, R&D systems Europe Ltd., United Kingdom). The wells were coated with anti-mouse

Chapter 3

EGF overnight, blocked with BSA (1 hour, room temperature) and washed with phosphate-buffered saline with 0.05% (v/v) Tween 20 (PBS-T). Urine samples and recombinant mouse EGF, used as standard (diluted in 0.5% (w/v) BSA), were added (2 hours, room temperature). After washing in PBS-T, biotinylated goat anti-mouse EGF was added, followed by horseradish peroxidase-conjugated streptavidin. Color was developed with OPD (o-Phenylenediamine) and stopped with H₂SO₄ (end concentration 0.33 M). Absorbance was measured at 492 nm (Varioskan, Thermo electron corporation, Waltham, USA); data were analyzed using SkanIt Software for Varioskan (Thermo electron corporation, Waltham, USA). Detection range of the ELISA was between 2-577 pg/ml.

Semi-quantitative Real-Time PCR Analysis

Tissue RNA was extracted using TriZol Total RNA Isolation Reagent (Life Technologies BRL, Breda, The Netherlands). After DNase treatment (Promega, Madison, WI), 1.5 µg of RNA was reverse transcribed by Molony-Murine Leukemia Virus-Reverse Transcriptase (Invitrogen) as described previously (18). The cDNA was mixed with Power SYBR® green PCR mastermix (Applied Biosystems, Foster City, CA, USA) and primers against TRPM6 (5'-AAAGCCATGCGAGTTATCAGC-3'; 5'-CTTCACAATGAAAACCTGCCC-3'), EGFR (5'-CAGAACTGGGCTTAGGGAAC-3'; 5'-GGACGATGTCCCTCCACTG-3'), EGF (5'-GAGAATCTACTGGACAGACAGTGG-3'; 5'-CTCGAGATTCTCTCCTGGATG-3') or the housekeeping gene hypoxanthine-guanine phosphoribosyl transferase (HPRT; 5'-TTATCAGACTGAAGAGCTACTGTAATGATC-3'; 5'-TTACCAGTGTCAATTATATCTTCAACAATC-3'). The mRNA expression levels were quantified using a single color real-time PCR detection system (MyiQ™, Biorad, Veenendaal, the Netherlands). Data analysis was carried out using the Relative Expression Software Tool (REST©(19)).

Immunohistochemistry

7 μm PLP fixed cryosections were prepared and stained with anti-TRPM6 (guinea pig antiserum), as described previously (4). Photographs of TRPM6 staining in kidney cortex were taken through a 25x objective on a Zeiss fluorescence microscope (Sliedrecht, The Netherlands) equipped with a digital photo camera (Nikon DMX1200). Semi-quantitative determination of TRPM6 protein expression was done using Image J (image processing program, NIH, USA), similar to previous publications (20).

Cell culture and transfection

Cells were maintained and transfected using Lipofectamine 2000 (Invitrogen-Life Technologies, Breda, The Netherlands) as previously described (21). Briefly, HEK293T cells were transiently transfected with a N-terminal HA-tagged TRPM6 in the pCINeo/IRES-GFP vector for patch clamp analysis (4). HEK293 cells were transfected with TRPM6 N-terminally conjugated to Green Fluorescent Protein (GFP) in the pCINeo vector for FRAP analysis (5). Experiments were performed 48–72 h post-transfection. Cells were preincubated at 37°C in the presence or absence Erlotinib (30 μM or 0.3 μM) for 60 minutes. Cells were also incubated with or without EGF (10 nM) for 30 minutes.

Electrophysiology

Electrophysiological recordings were made as previously described (4, 5). Briefly, whole-cell currents were determined in the tight seal whole-cell configuration using a patch clamp amplifier controlled by Patchmaster software (HEKA, Lambrecht, Germany). Cells were kept in an extracellular bath solution (150 mM NaCl, 10 mM HEPES/NaOH, 1 mM CaCl_2 , pH 7.4). Electrode resistances were between 2–4 $\text{M}\Omega$ after filling with standard pipette solution (150 mM NaCl, 10 mM EDTA and 10 mM HEPES/NaOH, pH 7.2). Capacitance and access resistances were continuously monitored using the automatic capacitance compensation of the Patchmaster

Chapter 3

software. A linear voltage ramp protocol from -100 to +100 mV (within 450 ms) was applied every 2 s from a holding potential of 0 mV. Extracting the current amplitudes at +80 and -80 mV from individual ramp current records assessed the temporal development of membrane currents. Current densities presented were determined by normalizing the current amplitude to the cell membrane capacitance. All experiments were performed at room temperature. The analysis and display of patch clamp data were performed using Igor Pro software (WaveMetrics, Lake Oswego, USA).

Western blotting and immunoprecipitation

HEK293T cells were incubated with EGF and Erlotinib as described above. Immunoprecipitation and western blotting was performed as previously described (22). Briefly, cells were incubated in lysis buffer (150 mM NaCl, 25 mM Tris/HCL pH=7.5, 1% Brij97 (Polyethylene Glycol Monooleyl Ether), 5 mM EDTA/NaOH pH=8.0, 1 mM Na₃VO₄, 1 mM NaF, 1 mM phenylmethylsulfonyl fluoride, 1 µg/ml leupeptin, 1 µg/ml aprotinin, 1 µg/ml pepstatin) and spun down at 1000 g for 10 min at 4°C. Lysates were incubated overnight with anti-EGFR directed mouse antibodies (sc-120, Santa Cruz Biotechnology, CA, UAS) coupled to protein A-Sepharose beads. Immunoprecipitates were run on SDS-PAGE gels and blotted onto membranes for detection of tyrosine phosphorylation (4G10, Millipore, MA, USA) and EGFR abundance (sc-03, Santa Cruz Biotechnology). Alpha-tubulin was detected in whole cell lysates and used as a housekeeping control (T6199, Sigma Aldrich, Zwijndrecht, the Netherlands).

Fluorescence recovery after photobleaching (FRAP)

The experiments were performed essentially as described previously (5). GFP-TRPM6 expressing HEK293 cells were plated onto glass Petri dish chambers (0.17 mm thick Wilco Wells, USA) and mounted on a confocal laser-scanning microscope (Zeiss LSM 510). Cells were kept in a standard solution (130 mM NaCl, 20 mM HEPES/Tris, 5 mM KCl, 5 mM glucose, 1 mM

Erlotinib modulates TRPM6

CaCl₂, 1 mM MgCl₂, pH 7.4). After defining two regions of interest (ROI) and subsequent recording two base-line fluorescence measurements, irreversible photobleaching of one ROI was initiated. Following photobleaching, fluorescence of both ROI's was measured over a 4 min period. Recovery in fluorescence was calculated from baseline measurements. The unbleached ROI was used to correct for photobleaching induced by image acquisition. The FRAP data was fitted by nonlinear regression analysis using previously published equations (23). Between 14-16 cells were measured in each experimental condition.

Statistical analysis

Values are presented as means ± SEM. Comparisons between two groups were made using an unpaired t-test. Statistical significance was determined by ANOVA in the patch clamp and FRAP experiments. $p < 0.05$ is considered statistically significant.

Acknowledgements

This work was supported by the Netherlands Organization for Scientific Research (ZonMw 9120.6110, 9120.8026), EURYI award from the European Science Foundation, and the Dutch Kidney foundation (C03.6017, C05.4106). We would like to thank Titia Woudenberg-Vrenken, Tom Nijenhuis, Henk Arnts, AnneMiete W.C.M van der Kemp, and Jeroen van Leeuwen for technical and scientific contributions to this work.

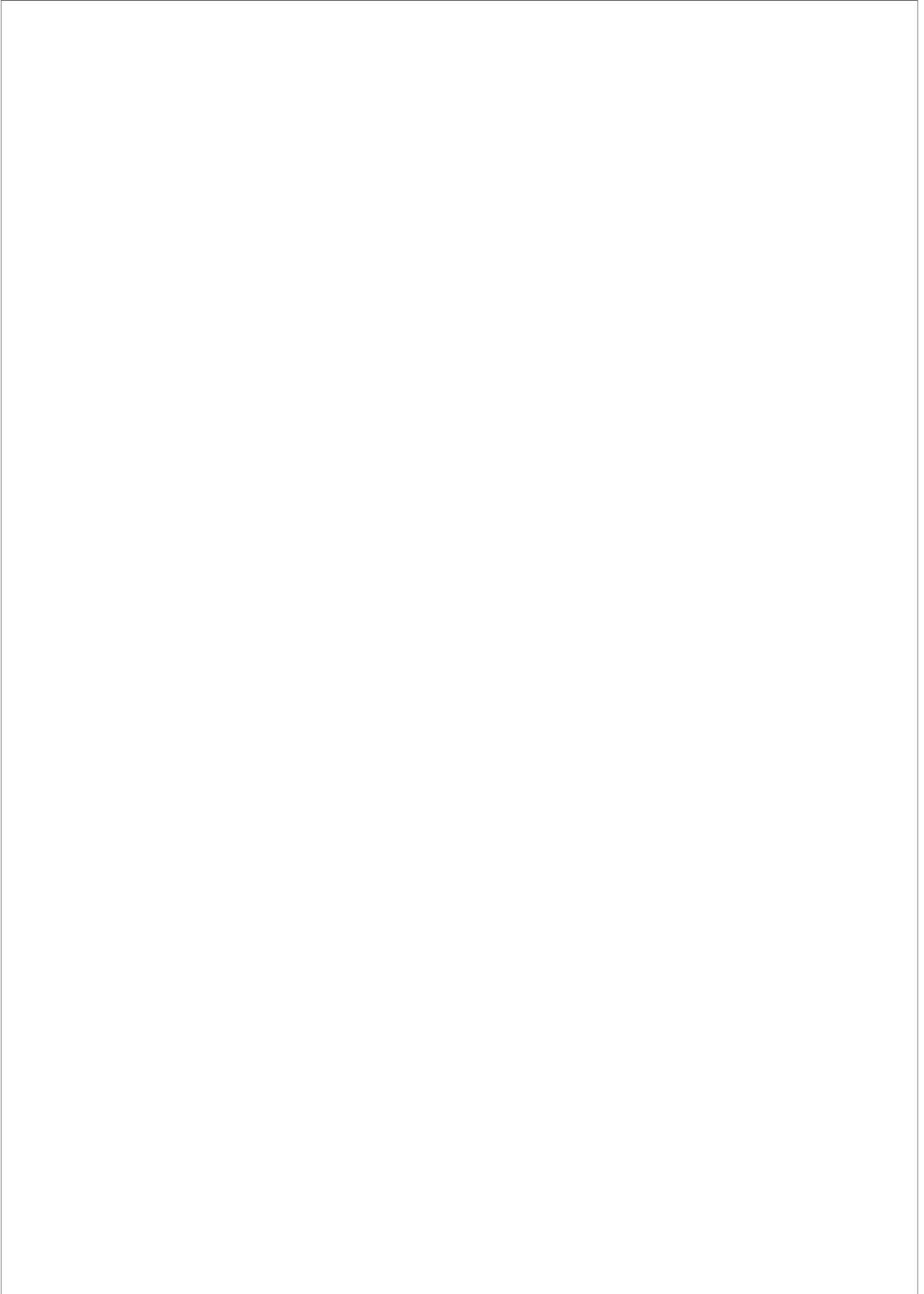
Chapter 3

References

1. Schlingmann KP, Weber S, Peters M, Niemann Nejsum L, Vitzthum H, Klingel K, Kratz M, Haddad E, Ristoff E, Dinour D, et al. Hypomagnesemia with secondary hypocalcemia is caused by mutations in TRPM6, a new member of the TRPM gene family. *Nat Genet.* 2002;31(2):166-170.
2. Walder RY, Landau D, Meyer P, Shalev H, Tsoia M, Borochowitz Z, Boettger MB, Beck GE, Englehardt RK, Carmi R, et al. Mutation of TRPM6 causes familial hypomagnesemia with secondary hypocalcemia. *Nat Genet.* 2002;31(2):171-174.
3. Groenestege WM, Hoenderop JG, van den Heuvel L, Knoers N, Bindels RJ. The epithelial Mg²⁺ channel transient receptor potential melastatin 6 is regulated by dietary Mg²⁺ content and estrogens. *J Am Soc Nephrol.* 2006;17(4):1035-1043.
4. Voets T, Nilius B, Hoefs S, van der Kemp AW, Droogmans G, Bindels RJ, Hoenderop JG. TRPM6 forms the Mg²⁺ influx channel involved in intestinal and renal Mg²⁺ absorption. *J Biol Chem.* 2004;279(1):19-25.
5. Thebault S, Alexander RT, Tiel Groenestege WM, Hoenderop JG, Bindels RJ. EGF increases TRPM6 activity and surface expression. *J Am Soc Nephrol.* 2009;20(1):78-85.
6. Groenestege WM, Thebault S, van der Wijst J, van den Berg D, Janssen R, Tejpar S, van den Heuvel LP, van Cutsem E, Hoenderop JG, Knoers NV, et al. Impaired basolateral sorting of pro-EGF causes isolated recessive renal hypomagnesemia. *J Clin Invest.* 2007;117(8):2260-2267.
7. Tejpar S, Piessevaux H, Claes K, Piront P, Hoenderop JG, Verslype C, Van Cutsem E. Mg²⁺ wasting associated with epidermal-growth-factor receptor-targeting antibodies in colorectal cancer: a prospective study. *Lancet Oncol.* 2007;8(5):387-394.
8. Schrag D, Chung KY, Flombaum C, Saltz L. Cetuximab therapy and symptomatic hypomagnesemia. *J Natl Cancer Inst.* 2005;97(16):1221-1224.
9. Mendelsohn J, Baselga J. Epidermal growth factor receptor targeting in cancer. *Semin Oncol.* 2006;33(4):369-385.
10. Gatzemeier U, Pluzanska A, Szczesna A, Kaukel E, Roubec J, De Rosa F, Milanowski J, Karnicka-Mlodkowski H, Pesek M, Serwatowski P, et al. Phase III study of erlotinib in combination with cisplatin and gemcitabine in advanced non-small-cell lung cancer: the Tarceva Lung Cancer Investigation Trial. *J Clin Oncol.* 2007;25(12):1545-1552.
11. Pollack VA, Savage DM, Baker DA, Tsaparikos KE, Sloan DE, Moyer JD, Barbacci EG, Pustilnik LR, Smolarek TA, Davis JA, et al. Inhibition of epidermal growth factor receptor-associated tyrosine phosphorylation in human carcinomas with CP-358,774: dynamics of receptor inhibition in situ and antitumor effects in athymic mice. *J Pharmacol Exp Ther.* 1999;291(2):739-748.
12. Hidalgo M, Bloedow D. Pharmacokinetics and pharmacodynamics: maximizing the clinical potential of Erlotinib (Tarceva). *Semin Oncol.* 2003;30(3 Suppl 7):25-33.

Erlotinib modulates TRPM6

13. Hidalgo M, Siu LL, Nemunaitis J, Rizzo J, Hammond LA, Takimoto C, Eckhardt SG, Tolcher A, Britten CD, Denis L, et al. Phase I and pharmacologic study of OSI-774, an epidermal growth factor receptor tyrosine kinase inhibitor, in patients with advanced solid malignancies. *J Clin Oncol*. 2001;19(13):3267-3279.
14. Moyer JD, Barbacci EG, Iwata KK, Arnold L, Boman B, Cunningham A, DiOrio C, Doty J, Morin MJ, Moyer MP, et al. Induction of apoptosis and cell cycle arrest by CP-358,774, an inhibitor of epidermal growth factor receptor tyrosine kinase. *Cancer Res*. 1997;57(21):4838-4848.
15. Schaefer G, Shao L, Totpal K, Akita RW. Erlotinib directly inhibits HER2 kinase activation and downstream signaling events in intact cells lacking epidermal growth factor receptor expression. *Cancer Res*. 2007;67(3):1228-1238.
16. Anast CS, Mohs JM, Kaplan SL, Burns TW. Evidence for parathyroid failure in Mg²⁺ deficiency. *Science*. 1972;177(49):606-608.
17. Rude RK, Oldham SB, Singer FR. Functional hypoparathyroidism and parathyroid hormone end-organ resistance in human Mg²⁺ deficiency. *Clin Endocrinol (Oxf)*. 1976;5(3):209-224.
18. Hoenderop JGJ, Hartog A, Stuiver M, Doucet A, Willems PHGM, Bindels RJM. Localization of the Epithelial Ca²⁺ Channel in Rabbit Kidney and Intestine. *J Am Soc Nephrol*. 2000;11(7):1171-1178.
19. Pfaffl MW, Horgan GW, Dempfle L. Relative expression software tool (REST) for group-wise comparison and statistical analysis of relative expression results in real-time PCR. *Nucleic Acids Res*. 2002;30(9):e36.
20. Nijenhuis T, Hoenderop JG, Bindels RJ. Downregulation of Ca²⁺ and Mg²⁺ transport proteins in the kidney explains tacrolimus (FK506)-induced hypercalciuria and hypomagnesemia. *J Am Soc Nephrol*. 2004;15(3):549-557.
21. Topala CN, Groenesteghe WT, Thebault S, van den Berg D, Nilius B, Hoenderop JG, Bindels RJ. Molecular determinants of permeation through the cation channel TRPM6. *Cell Calcium*. 2007;41(6):513-523.
22. Alwan HA, van Zoelen EJ, van Leeuwen JE. Ligand-induced lysosomal epidermal growth factor receptor (EGFR) degradation is preceded by proteasome-dependent EGFR de-ubiquitination. *J Biol Chem*. 2003;278(37):35781-35790.
23. Yguerabide J, Schmidt JA, Yguerabide EE. Lateral mobility in membranes as detected by fluorescence recovery after photobleaching. *Biophys J*. 1982;40(1):69-75.



CHAPTER 4

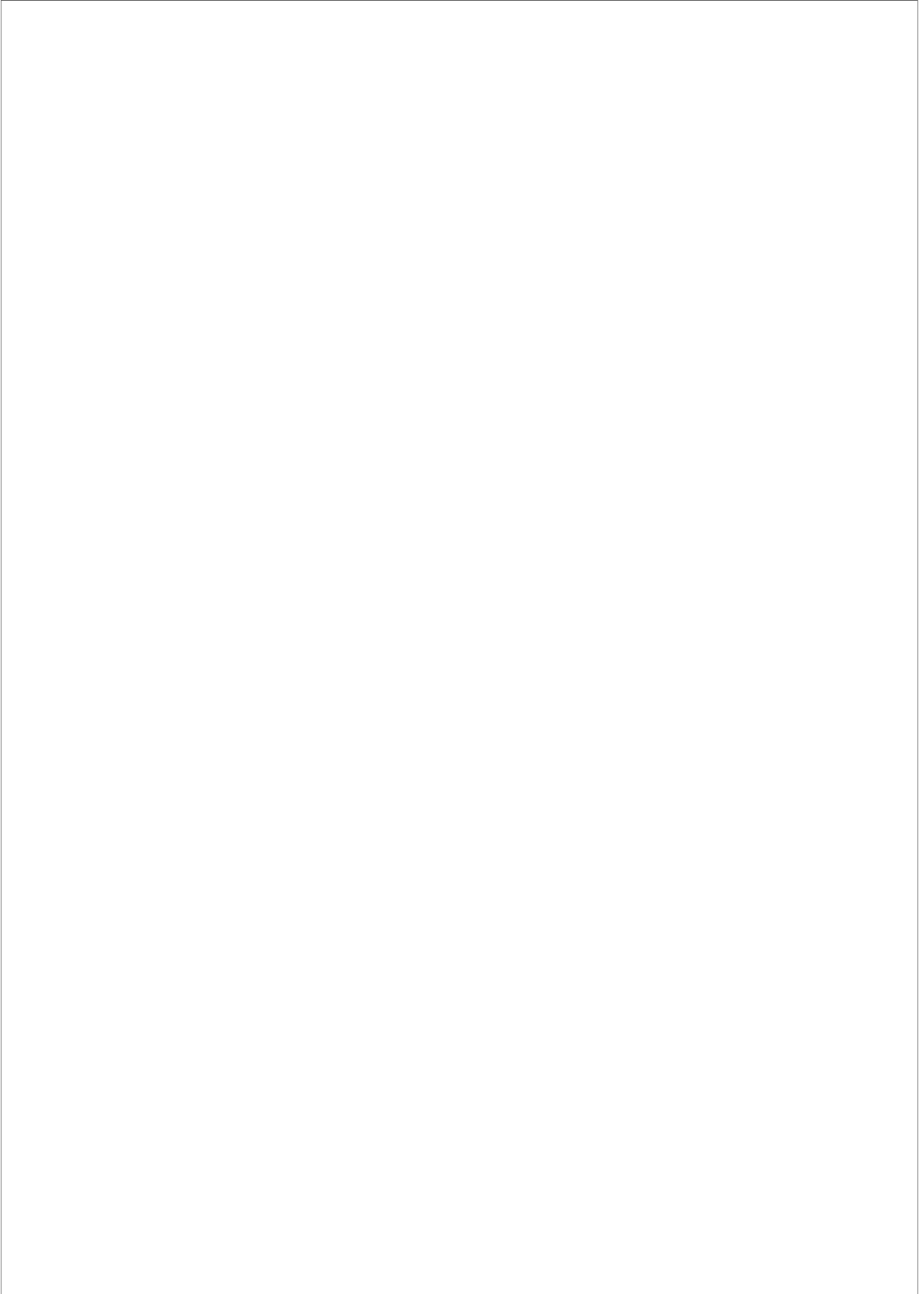
Testosterone increases urinary Ca²⁺ excretion and inhibits the expression of renal Ca²⁺ transport proteins

Henrik Dimke^{1*}, Yu-Juei Hsu^{1,2*}, Joost P.H. Schoeber¹, Shih-Che Hsu², Shih-Hua Lin², Pauling Chu², Joost G. Hoenderop¹, and René J. Bindels¹.

¹Department of Physiology, Radboud University Nijmegen Medical Centre, the Netherlands.

²Division of Nephrology, Department of Internal Medicine, Tri-Service General Hospital, Taipei, Taiwan.

*Authors contributed equally



Testosterone attenuates renal TRPV5 expression

Abstract

Gender differences in renal handling of Ca^{2+} have previously been reported. However, the overall contribution of androgens to these differences remains uncertain. The aim of this study was to determine whether testosterone affects active renal Ca^{2+} reabsorption by regulating the Ca^{2+} transport proteins Transient Receptor Potential Vanilloid-subtype 5 (TRPV5), calbindin- $\text{D}_{28\text{K}}$, the plasma membrane Ca^{2+} -ATPase, and the $\text{Na}^+/\text{Ca}^{2+}$ exchanger. Male mice, compared to females, had a higher urinary Ca^{2+} excretion accompanied by reduced renal expression of Ca^{2+} transporters. In addition, androgen deficient bilaterally orchidectomized (ORX) mice excreted less Ca^{2+} in their urine than sham-operated controls. ORX-induced hypocalciuria was normalized after testosterone replacement. Consistently, androgen deficiency resulted in augmentation of both renal mRNA and protein abundance of TRPV5 and calbindin- $\text{D}_{28\text{K}}$, which in turn was suppressed by testosterone treatment. Importantly, no significant differences in serum estrogen, parathyroid hormone or 1,25-dihydroxyvitamin D_3 levels were observed between control, ORX and testosterone-supplemented ORX mice. Moreover, incubation of primary rabbit connecting tubules and cortical collecting duct cells with the non-aromatizable androgen, dihydrotestosterone, reduced transcellular Ca^{2+} transport. In conclusion, this study demonstrates that sex differences in renal Ca^{2+} handling are in part mediated by the inhibitory actions of androgens on TRPV5-mediated active renal Ca^{2+} transport.

Introduction

Several studies have reported sex differences in the urinary Ca^{2+} excretion, showing a greater urinary Ca^{2+} loss in males than in females (1, 2). In addition, estrogens have been shown to increase the renal reabsorption of Ca^{2+} , which is in good agreement with the observed gender differences (3). Presently, it remains unclear whether androgens play an opposing role to estrogens in modulating renal Ca^{2+} reabsorption. The androgen receptor (AR) is expressed in

Chapter 4

renal epithelial cells (4), and a growing body of evidence points to sex differences in various functional characteristics of mammalian kidneys; for example, a higher glomerular filtration rate in the male rat kidney (possibly due to higher renal plasma flow and lower vascular resistance) (reviewed in (5)). However, the role of androgens in regulating renal Ca^{2+} handling remains poorly characterized.

In the kidney, Ca^{2+} re-enters the blood by passive paracellular as well as active transcellular reabsorption. The active Ca^{2+} reabsorptive component is restricted to the distal convoluted tubules (DCT) and the connecting tubules (CNT) (6-9). Here, Ca^{2+} enters the epithelial cell via the Ca^{2+} -selective ion channel Transient Receptor Potential Vanilloid-subtype 5 (TRPV5). Subsequently, Ca^{2+} is bound to calbindin- $\text{D}_{28\text{K}}$ that transports Ca^{2+} from the apical to the basolateral side where the $\text{Na}^+/\text{Ca}^{2+}$ -exchanger (NCX1) and the plasma membrane Ca^{2+} -ATPase (PMCA1b) extrude Ca^{2+} into the peritubular lumen (6).

Active renal Ca^{2+} reabsorption is critical in determining the final urinary Ca^{2+} excretion, and has been demonstrated to be regulated by calcitropic hormones, including parathyroid hormone (PTH) and 1,25-dihydroxyvitamin D_3 ($1,25(\text{OH})_2\text{D}_3$) (6, 10, 11). Estrogen has also been shown to affect active renal Ca^{2+} transport, although sex hormones are usually not considered as calcitropic factors (6, 12).

The present study aims to determine whether androgens contribute to the gender differences in renal Ca^{2+} handling by regulating the expression of Ca^{2+} transport proteins TRPV5, calbindin- $\text{D}_{28\text{K}}$, NCX1 and PMCA1b. Because changes in systemic androgen concentrations also affect bone mineralization via a long-term process (13), we evaluated the short-term effects of androgen deficiency in orchidectomized (ORX) mice and of testosterone resupplementation (ORX+T), on the expression of the renal Ca^{2+} transporters. In addition, to exclude possible effects of androgens on bone turnover, non-aromatizable dihydrotestosterone (DHT) was applied to an isolated cell system of primary renal connecting tubule (CNT) / cortical collecting duct cells (CCD).

Testosterone attenuates renal TRPV5 expression

Results

Gender differences in urinary Ca^{2+} excretion

To investigate whether sex differences could be noted in renal and intestinal Ca^{2+} handling, 24 h urinary Ca^{2+} excretion and intestinal absorption was determined in age-matched male and

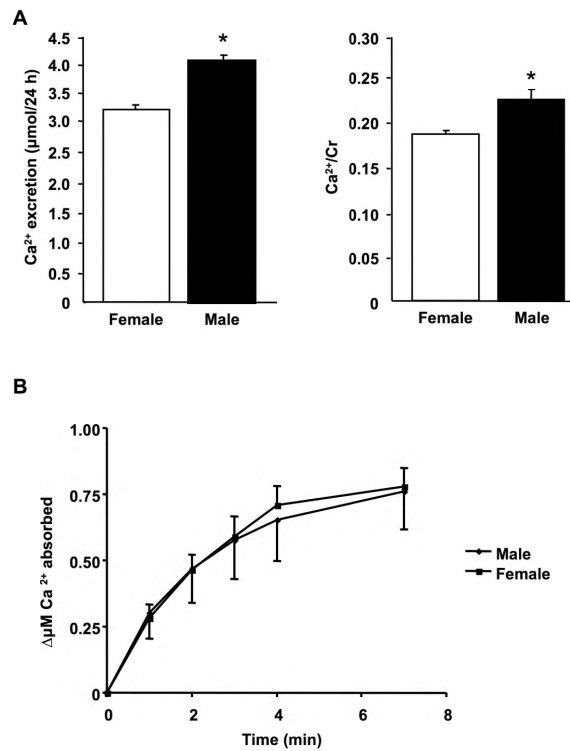


Figure 1. Mice sex differences in urinary Ca^{2+} excretion. (A) 24 h urine Ca^{2+} excretion and Ca^{2+}/Cr ratio were determined in both female and male mice. Data are presented as means \pm S.E.M. Cr, creatinine. * $p < 0.05$ male vs. female mice. $n = 8$ samples per group. (B) Intestinal $^{45}\text{Ca}^{2+}$ absorption into serum of male (\blacklozenge) and female (\blacksquare) mice after oral gavage. $n = 5$ animals per group.

female mice. Body weight (26.7 ± 0.8 in male vs. 25.4 ± 1.8 g in female) and diuresis (1.3 ± 0.5 in male vs. 1.1 ± 0.3 ml/24 h in female) was not significantly different between sexes. Male mice demonstrated a significant higher 24 h urinary Ca^{2+} excretion (4.1 ± 0.3 vs. 3.3 ± 0.2 $\mu\text{mol}/\text{day}$) and Ca^{2+}/Cr ratio (0.23 ± 0.03 vs. 0.18 ± 0.02), in comparison to females (Figure 1A). Male and

Chapter 4

female mice consumed similar amounts of food (3.30 ± 0.02 g vs. 3.24 ± 0.03 g, respectively) and hence ingested comparable amounts of Ca^{2+} (33.0 ± 0.2 mg vs. 32.4 ± 0.3 mg, respectively). In addition, intestinal radioactive Ca^{2+} tracer uptakes were performed in male and female mice. Intestinal Ca^{2+} absorption was determined by an *in vivo* absorption assay, measuring serum levels of radioactive $^{45}\text{Ca}^{2+}$ at several time points after oral gavage. The intestinal absorption of Ca^{2+} was similar in both males and females (Figure 1B).

Sex differences in renal expression of Ca^{2+} transporters

The increased urinary Ca^{2+} excretion and Ca^{2+}/Cr ratio in male mice, was paralleled by a significant decline in the renal mRNA expression of TRPV5, calbindin- $\text{D}_{28\text{K}}$, NCX1 and PCMA1b (Figure 2A,B). For calbindin- $\text{D}_{28\text{K}}$ abundance, this was confirmed by immunoblotting (Figure 3A). Densitometrical analysis of the immunoblots showed significantly less calbindin- $\text{D}_{28\text{K}}$ protein expression in male than in female mice (Figure 3B). Similarly, computerized analysis of immunohistochemical images revealed a significant decrease in TRPV5 and calbindin- $\text{D}_{28\text{K}}$ abundance in male mice as compared to female mice (Figure 4).

Localization of the androgen receptor in mouse kidney

Binding of the steroid hormone to the androgen receptor (AR) may regulate the expression of renal Ca^{2+} transporters. To investigate whether the AR is localized in TRPV5-expressing cells, immunohistochemical labeling of TRPV5 and the AR was performed using mouse kidney sections. As depicted in Figure 5, TRPV5 and the AR are co-expressed in DCT/CNT cells.

Effects of ORX and testosterone treatment on serum and urine parameters

To specifically address the effects of androgens on renal Ca^{2+} handling, urinary Ca^{2+} excretion was measured in sham-operated, ORX mice, and in ORX+T. Importantly, the body weight of

Testosterone attenuates renal TRPV5 expression

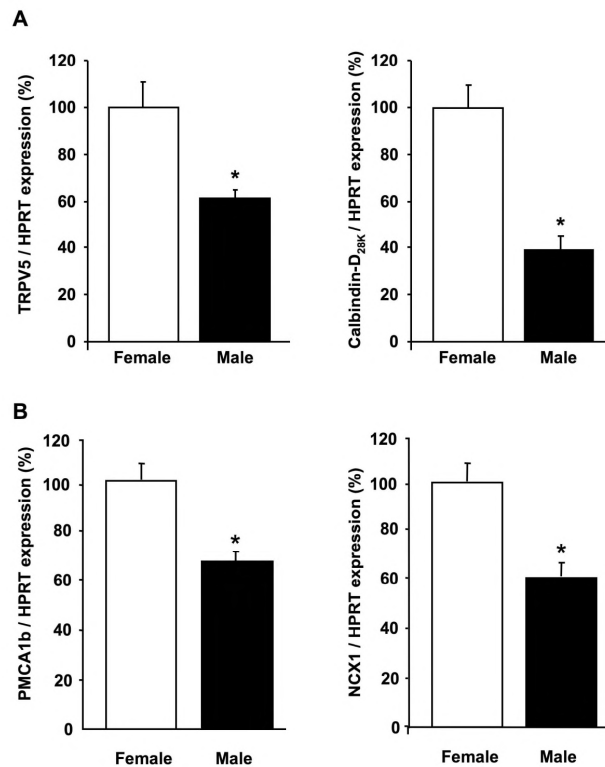


Figure 2. Mice sex differences in the expression of renal Ca²⁺ transporters. (A) renal mRNA expression of TRPV5 and calbindin-D_{28K} were determined by real-time quantitative RT-PCR analysis, expressed as the ratio of HPRT, and depicted as percentage of female mice. (B) Similarly, mRNA expression of PMCA1b and NCX1 was determined in kidney RNA isolates from male and female mice. mRNA expression was corrected for endogenous HPRT.

mice between sham-operated, ORX and ORX+T groups was not different (27.1 ± 0.7 , 26.1 ± 0.9 , and 26.9 ± 0.9 g, respectively). ORX significantly decreased urinary excretion of Ca²⁺ (4.4 ± 0.3 (sham-operated) vs. 2.3 ± 0.2 (ORX) $\mu\text{mol/day}$) and the Ca²⁺/creatinine (Cr) ratio (0.28 ± 0.05 (sham-operated) vs. 0.16 ± 0.03 (ORX)) (Figure 6). A change in renal transport was apparent, as the fractional Ca²⁺ excretion was significantly reduced (0.94 ± 0.12 (sham-operated) vs. 0.49 ± 0.04 (ORX) %). Testosterone supplementation of ORX mice restored renal Ca²⁺ excretion (4.3 ± 0.3 $\mu\text{mol/day}$) and the Ca²⁺/Cr ratio (0.25 ± 0.03) to values comparable with the sham-operated mice. Table 1 summarizes the effects of ORX and testosterone replacement

Chapter 4

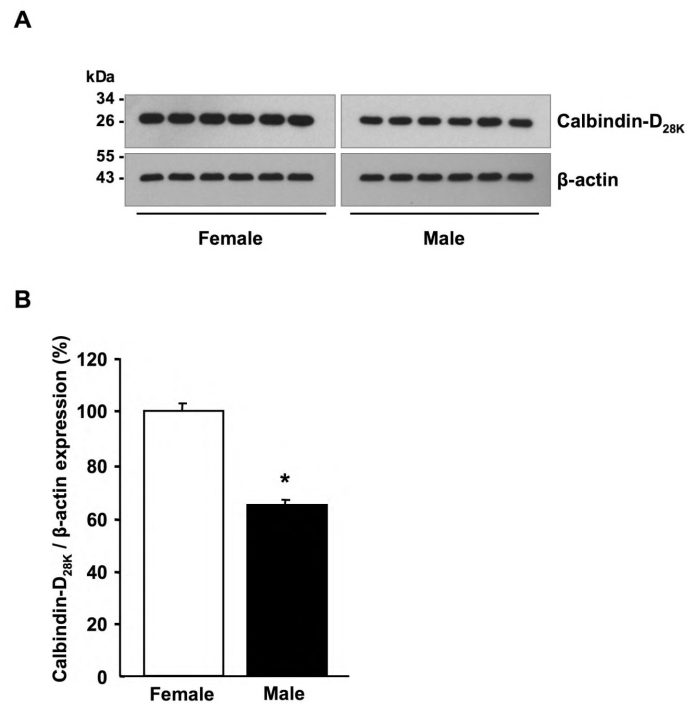


Figure 3. Mice sex differences in the expression of renal Ca²⁺ transporters. (A) Immunoblots of protein samples (10 μg each) from homogenates of kidney tissues were labeled with antibodies against calbindin-D_{28K} or β-actin. (B) Expression of calbindin-D_{28K} protein was quantified by computer-assisted densitometry analysis and presented as the ratio to β-actin expression levels, in relative percentages compared with female mice. Data are presented as means ± S.E.M. **p* < 0.05 male vs. female mice. *n* = 6 samples per group.

	Sham	ORX	ORX+T
Ca ²⁺ (mM)	2.8 ± 0.1	2.6 ± 0.1	2.5 ± 0.1
Testosterone (ng/dl)	499 ± 129	59 ± 11 ^a	1005 ± 291 ^{a, b}
Estrogen (pg/ml)	63 ± 16	36 ± 12	50 ± 10
PTH (pg/ml)	23.9 ± 6.5	20.7 ± 5.5	25.4 ± 7.4
1,25(OH) ₂ D ₃ (pmol/ml)	156 ± 19	130 ± 11	143 ± 17

Table 1. Effect of testosterone on serum Ca²⁺ and calcitropic hormones. Serum concentrations of Ca²⁺ and calcitropic hormones in sham-operated mice and ORX mice with or without testosterone replacement (Sustanon 250, 250 mg/kg/week subcutaneously, 2 weeks). PTH, parathyroid hormone; 1,25(OH)₂D₃, 1,25-dihydroxyvitamin D₃. ^a*p* < 0.05 vs. sham-operated mice; ^b*p* < 0.05 vs. ORX mice. *n* = 8 samples per parameter.

Testosterone attenuates renal TRPV5 expression

therapy on systemic Ca^{2+} handling, calciotropic hormones, and sex hormones. Serum testosterone levels were effectively reduced in untreated ORX mice, whereas supplementation with Sustanon 250 resulted in significantly higher serum testosterone levels. Importantly, serum PTH, $1,25(\text{OH})_2\text{D}_3$, and estrogen levels were not significantly different in ORX mice as compared to sham-operated and ORX+T mice.

Effects of ORX and testosterone treatment on the expression of renal Ca^{2+} transporters

To address the molecular mechanism responsible for the effect of testosterone on renal Ca^{2+} handling, the expression of TRPV5, calbindin- $\text{D}_{28\text{K}}$, PMCA1b and NCX1 were examined using real-time quantitative reverse transcriptase (RT) PCR, immunoblotting and immunohistochemistry. ORX mice demonstrated a 3.2-fold increase in TRPV5 and a 2.0-fold increase in calbindin- $\text{D}_{28\text{K}}$ mRNA expression as compared to sham-operated mice (Figure 7A). Conversely, administration of testosterone to ORX mice (ORX+T) resulted in a significant decrease of TRPV5 and calbindin- $\text{D}_{28\text{K}}$ mRNA expression (Figure 7A, dashed bars). Similarly, NCX1 was increased in the ORX group, while both PMCA1b and NCX1 were decreased in the ORX+T group (Figure 7B). As determined by semi-quantitative immunoblotting, protein abundance of calbindin- $\text{D}_{28\text{K}}$ was increased in ORX mice compared to sham-operated mice (Figure 8A, B). In accordance, calbindin- $\text{D}_{28\text{K}}$ protein abundance in ORX+T mice was comparable to the sham-operated controls (Figure 8A, B). In line with the above, semi-quantification of protein expression, the immunohistochemical labeling experiments revealed a significant up-regulation of TRPV5 (2.7-fold) and calbindin- $\text{D}_{28\text{K}}$ (1.5-fold) signal in ORX mice when compared to sham-operated mice (Figure 9). Furthermore, treatment of ORX mice with testosterone led to a significant decline in TRPV5 and calbindin- $\text{D}_{28\text{K}}$ signals (Figure 9).

Chapter 4

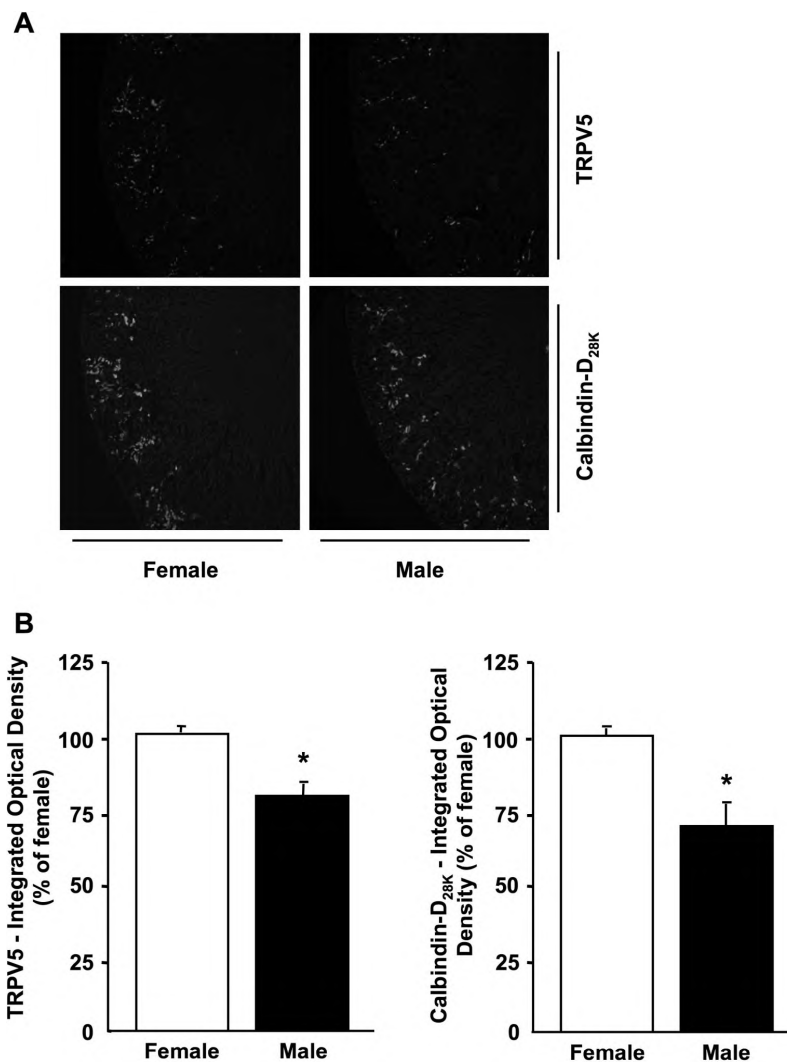


Figure 4. Gender differences in protein expression of Ca²⁺ transporters in mouse kidney. (A) Representative images of immunohistochemical staining of TRPV5 and calbindin-D_{28K} in male and female kidney cortex. (B) Semi-quantification of renal TRPV5 and calbindin-D_{28K} protein abundance was performed by computerized analysis of immunohistochemical images. Data were calculated as IOD (arbitrary units) and depicted as percentage of female mice. Data are presented as means \pm S.E.M. * $p < 0.05$ male vs. female mice. $n = 8$ samples per group.

Testosterone attenuates renal TRPV5 expression

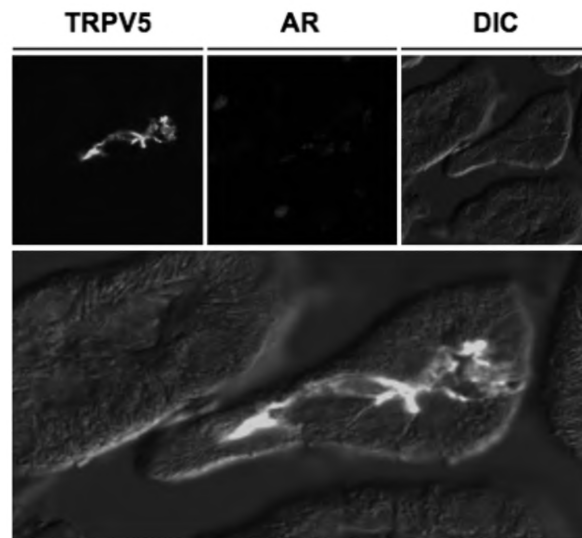


Figure 5. Characterization of AR localization in kidney. Confocal laser microscopy of double-labeled mouse kidney sections using guinea pig anti-TRPV5 (TRPV5, upper left panel) and rabbit anti-AR antibodies (AR, upper middle panel). Differential interference contrast (DIC, upper right panel) and overlay (lower panel) are also presented.

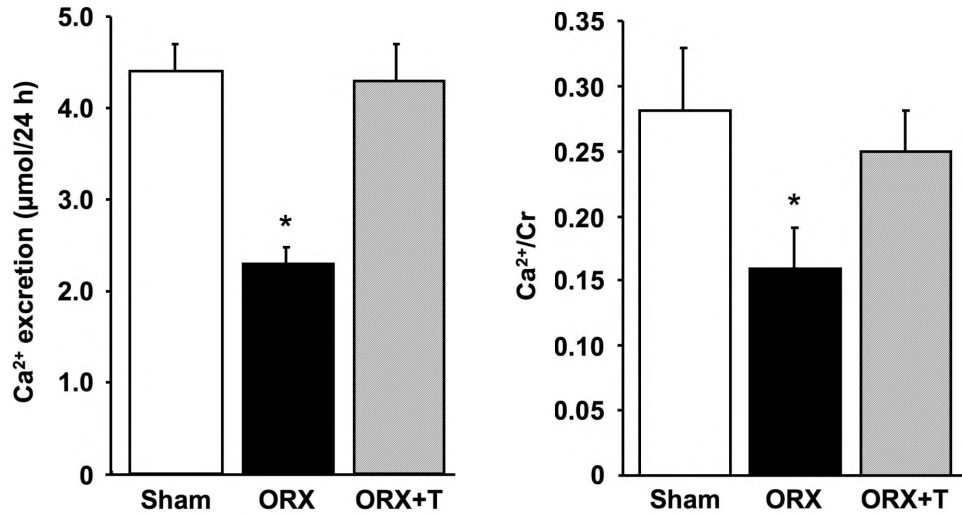


Figure 6. Differences in urinary Ca²⁺ excretion of Sham-operated, ORX and ORX+T mice. 24 h urine Ca²⁺ excretion and Ca²⁺/Cr ratio were determined in Sham-operated, ORX and ORX+T mice. Data are presented as means ± S.E.M. Cr, creatinine. * $p < 0.05$ male vs. female mice. $n = 8$ per group.

Chapter 4

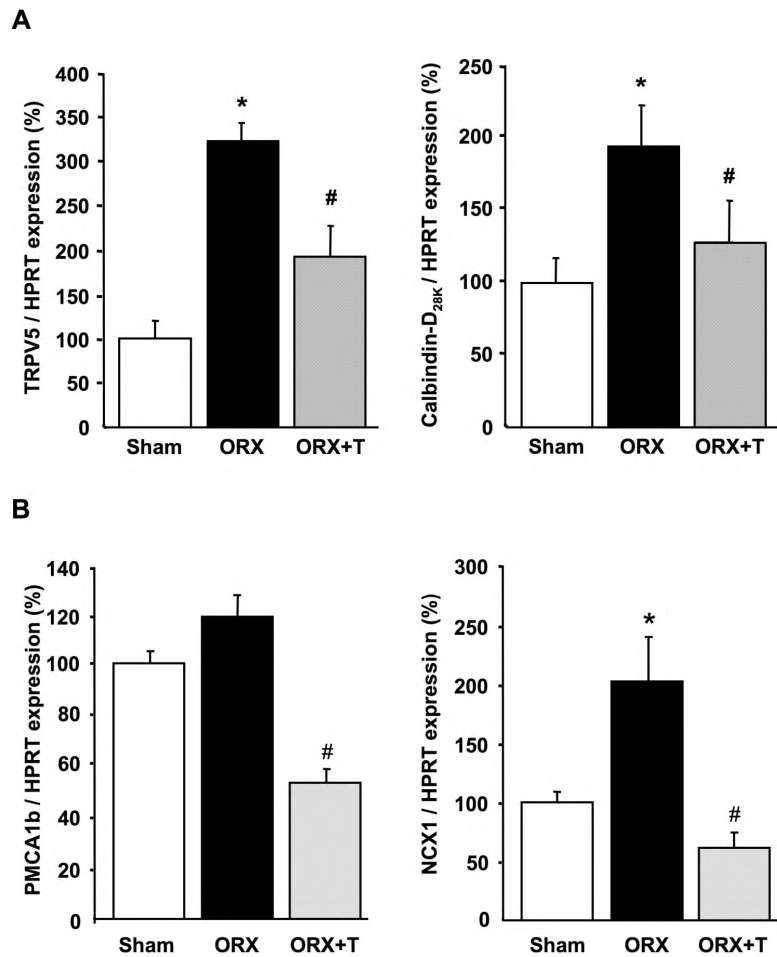


Figure 7. Effects of ORX and testosterone treatment on renal mRNA expression of Ca^{2+} transporters. (A) Renal mRNA expression of TRPV5 and calbindin- $\text{D}_{28\text{K}}$ in sham-operated, ORX and ORX+T mice were analyzed by quantitative real-time RT-PCR analysis, (B) Expression of PMCA1b and NCX1 in the kidney of sham, ORX, and ORX+T mice. In all cases expression was normalized to HPRT and depicted as percentage of sham-operated mice.

Effect of DHT on transcellular Ca^{2+} transport in rabbit kidney CNT and CCD primary cell cultures

The effect of androgen on renal Ca^{2+} handling in the ORX mice may be facilitated by the possible interference of other organs (e.g. bone). Therefore, the effect of androgen on TRPV5-mediated Ca^{2+} transport was studied in an isolated renal cell system. Primary cultures of rabbit CNT/CCD cells were grown to confluence on permeable supports. The cells were treated with DHT or

Testosterone attenuates renal TRPV5 expression

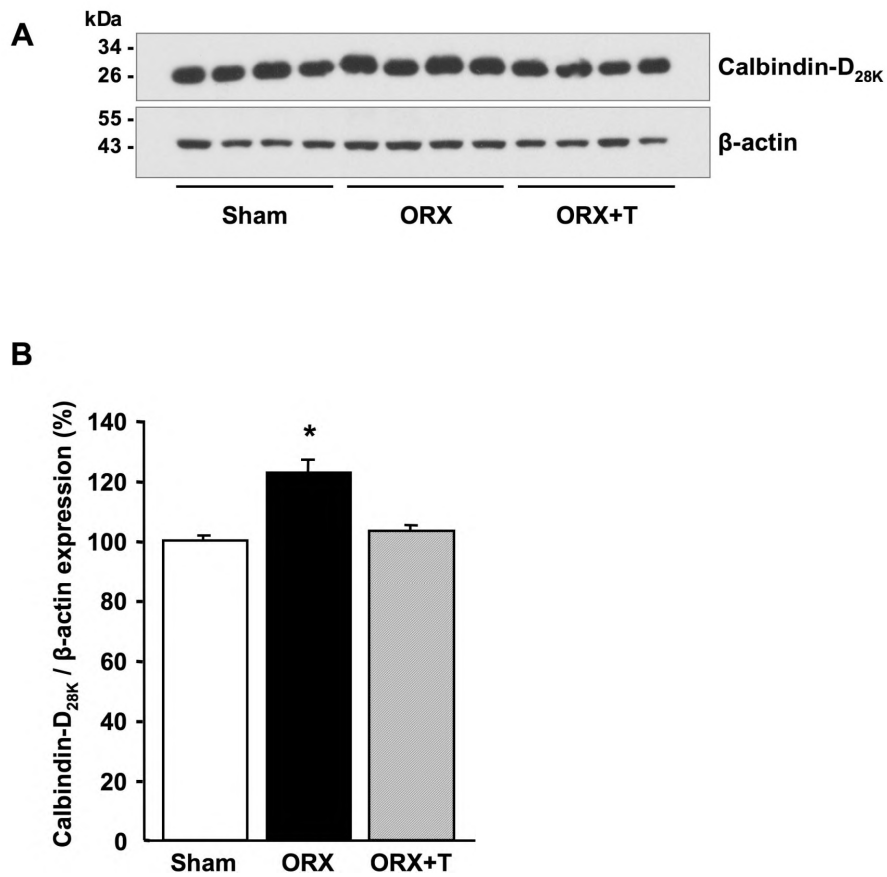


Figure 8. Effects of ORX and testosterone treatment on renal protein abundance of calbindin-D_{28K}. (A) Immunoblots of protein samples (10 μ g each) from homogenates of kidney tissue of sham-operated, ORX and ORX+T mice were labeled with antibodies against calbindin-D_{28K} or β -actin. (B) Expression of calbindin-D_{28K} protein was quantified by computer-assisted densitometry analysis and presented as the ratio to β -actin expression levels, in relative percentages compared with sham-operated mice. Data are presented as means \pm S.E.M. Sham, sham-operated mice; ORX, orchidectomized mice; ORX+T, orchidectomized mice treated with Sustanon 250 subcutaneously (250 mg/kg/week) for 2 weeks. * $p < 0.05$ vs. sham-operated mice. # $p < 0.05$ vs. ORX mice. $n = 8$ samples per group.

vehicle, and the rate of transepithelial Ca^{2+} transport was determined. Application of 10 nM DHT to the polarized confluent cell monolayers for 24 h significantly inhibited the net apical-to-basolateral transport of Ca^{2+} ($p < 0.02$) (Figure 10).

Chapter 4

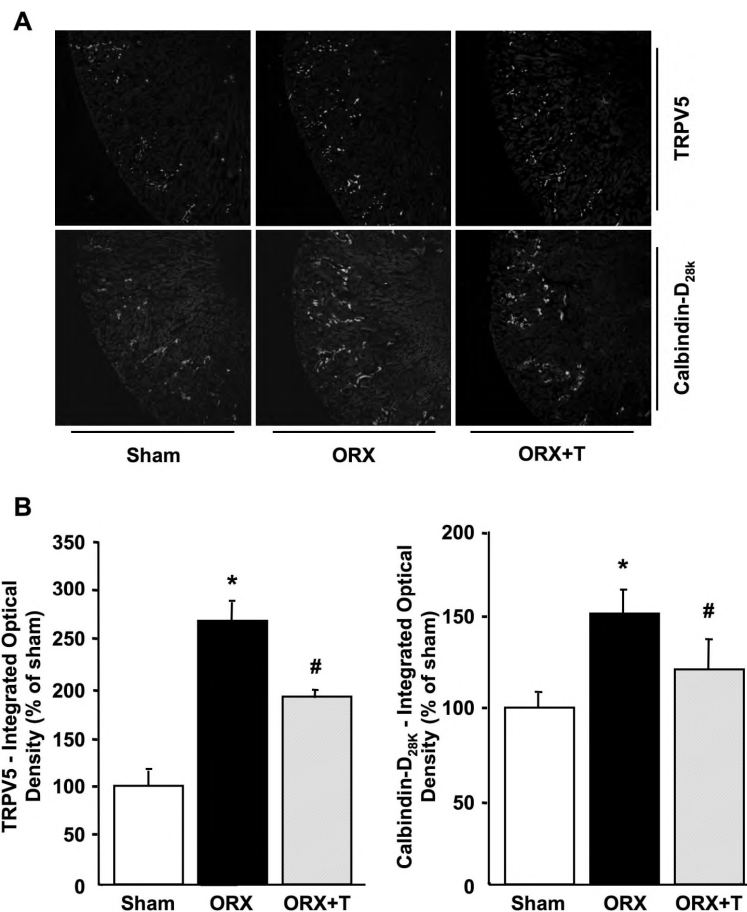


Figure 9. Immunohistochemical staining of renal Ca²⁺ transporters in sham-operated, ORX and ORX+T mice. (A) Representative images of immunohistochemical staining of TRPV5 and calbindin-D_{28K} in kidney cortex of sham-operated, ORX and ORX+T mice. **(B)** Semi-quantification of renal TRPV5 and calbindin-D_{28K} protein abundance was performed by computerized analysis of immunohistochemical images. Data were calculated as IOD (arbitrary units), depicted as percentage of sham-operated mice, and presented as means ± S.E.M. Sham, sham-operated mice; ORX, orchidectomized mice, ORX+T, orchidectomized mice treated with Sustanon 250 subcutaneously (250 mg/kg/week) for 2 weeks. * *p* < 0.05 vs. sham-operated mice. # *p* < 0.05 vs. ORX mice. *n* = 8 samples per group.

Discussion

The present study is to our knowledge the first to delineate the effect of androgens on renal handling of Ca²⁺ and TRPV5-mediated active Ca²⁺ transport. We find that testosterone contributes significantly to the sex differences observed in renal Ca²⁺ handling. This conclusion is based on the following observations: First, male mice have a greater urinary Ca²⁺ excretion

Testosterone attenuates renal TRPV5 expression

compared to females, a feature accompanied by a reduced renal expression of Ca^{2+} transport proteins. Second, androgen-deficient ORX mice show a significant decline in the urinary excretion of Ca^{2+} , which normalizes after testosterone replacement. Similar data was obtained when evaluating the fractional excretion of Ca^{2+} , suggesting that the testosterone-induced increase of urinary Ca^{2+} excretion is due to inhibition of tubular Ca^{2+} reabsorption. Forth, the mRNA and protein abundance of renal Ca^{2+} transporters was up-regulated in ORX mice, while the expression of renal Ca^{2+} transporters was suppressed by resupplying these mice with testosterone. Fifth, the serum $1,25(\text{OH})_2\text{D}_3$, PTH, and estrogen levels did not differ between the sham-operated, ORX and ORX+T mice, suggesting that androgens may affect the transcription of the renal Ca^{2+} transporters. Finally, inhibition of transcellular Ca^{2+} transport after DHT treatment was observed in rabbit kidney CNT/CCD primary cell cultures.

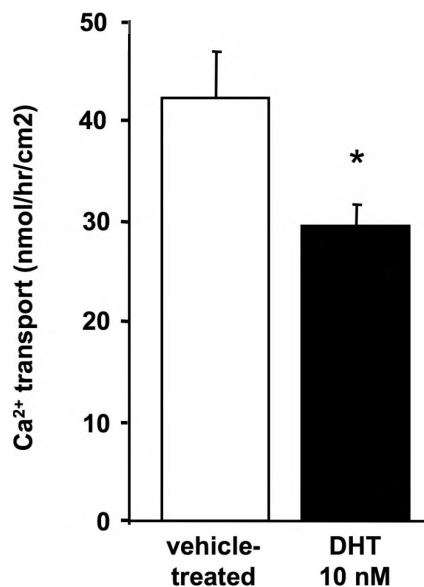


Figure 10. Effect of DHT on net apical to basolateral Ca^{2+} transport in primary cultures of rabbit CNT/CCD cells. Transepithelial Ca^{2+} transport across confluent monolayers was measured in the absence or presence of 10 nM DHT. At the end of the 90 minutes incubation period apical medium was collected to determine the amount of Ca^{2+} transport across the monolayer. Transepithelial Ca^{2+} transport is expressed nmol/h/cm². Data from 3 independent experiments ($n = 21$ per condition) was combined. * $p < 0.001$.

Chapter 4

Fe(male) sex hormones regulating Ca²⁺ transport

Our observation that male mice have an increased urinary Ca²⁺ excretion than females is in agreement with previous clinical studies evaluating gender differences in humans (1, 2). ORX induce hypocalciuria in male mice, while testosterone supplementation normalized their urinary Ca²⁺ excretion. This was accompanied by a decreased expression of renal Ca²⁺ transport proteins such as TRPV5, NCX1, PMCA1b and calbindin-D_{28k}. Previous studies evaluating the effect of estrogen on renal Ca²⁺ handling, demonstrated that the hormone exerts a direct effect on renal Ca²⁺ reabsorption via up-regulation of these Ca²⁺ transport proteins (3). Thus, both testosterone and estrogen have opposing regulatory properties in terms of renal expression of Ca²⁺ transporters. Similar sex differences have been found for the regulation of the thiazide-sensitive sodium-chloride cotransporter (NCC) expressed in the DCT. Chen *et al.* (14) demonstrated that the density of NCC (quantified by [³H]metolazone binding) was two-fold higher in female, than in male rats. Furthermore, ORX resulted in an increase in metolazone binding sites in males, whereas ovariectomy decreased the binding density in females (14).

Role of calcitropic hormones in androgen regulation?

In the present study serum 1,25(OH)₂D₃ and PTH did not vary between sham-operated, ORX, and ORX+T mice, suggesting that up-regulation of TRPV5 in ORX mice is not mediated by these calcitropic hormones. Conversely, androgens have previously been suggested to affect Ca²⁺ homeostasis by altering the regulation of calcitropic hormones. Some discrepancy has been reported in the literature; in a study by Nyomba *et al.* (15), the serum concentration of 1,25(OH)₂D₃ was shown to decrease after ORX in male rats, while testosterone replacement therapy restored serum 1,25(OH)₂D₃ to normal levels. In agreement with our data, a study by Hope *et al.* (16), reported that ORX performed in male rats could not be associated with any changes in active 1,25(OH)₂D₃ levels. Possible explanations for these discrepancies are currently unclear and may not exclude a contribution of 1,25(OH)₂D₃ to overall Ca²⁺ handling by

Testosterone attenuates renal TRPV5 expression

androgens.

Here, we showed that the AR is present in TRPV5-expressing cells, which is in line with earlier results demonstrating the presence of the AR in the distal part of the nephron (17). It is presently unclear whether the activated AR is directly or indirectly involved in decreasing the expression of the investigated Ca^{2+} transporters and hence a higher urinary Ca^{2+} excretion. We investigated this directly by expressing a 5 kb fragment (-5,000 to +1) of the mouse TRPV5 promoter coupled to the luciferase gene in androgen-responsive human prostate adenocarcinoma (LnCAP) cells (data not shown). However in these cells, we were not able to observe any effect of DHT on luciferase activity. Currently, it remains unclear how large the promoter fragment should be to adequately drive TRPV5 transcription in response to androgens. In addition, transcriptional regulators that could be necessary for the androgen-mediated inhibition may be absent in this cell system. The exact mechanism whereby testosterone alters TRPV5 expression remains to be clarified.

Short vs. long term effects of androgens on Ca^{2+} homeostasis

In this study, we aimed to evaluate the primary effect of androgens on renal Ca^{2+} handling. The inhibitory effect of testosterone on renal Ca^{2+} reabsorption seems at variance with the increased Ca^{2+} excretion found in elderly men with androgen deficiency, which is thought to be associated with male osteoporosis during aging (18-20). However, the short-term renal effects of androgen deficiency presented here should be separated from the long-term consequences of andropause in terms of bone remodeling. This issue was appropriately addressed in a study of Murras *et al.* (13). They studied young men who were made hypogonadal for different time periods by injection of a gonadotropin-releasing hormone agonist. The contribution of Ca^{2+} released from bone to urine losses was shown to remain unchanged for 4 weeks, but, thereafter, significantly increased upon 10 weeks after induction of hypogonadism. In our experiments, we studied the effects of androgen deficiency in mice within the time frame of 2 weeks, to avoid the possible

Chapter 4

interference of Ca^{2+} released from bone. We could clearly delineate a change in intrarenal Ca^{2+} transport. Furthermore, we substantiated our *in vivo* results by experiments in isolated rabbit kidney CNT/CCD primary cell cultures. These cells express endogenous TRPV5 and calbindin- $\text{D}_{28\text{K}}$, and are a consistent model to investigate active transepithelial Ca^{2+} transport *ex vivo* (11). Here, we found that incubation with the non-aromatizable androgen DHT (10 nM, which is in line with a physiological concentration of testosterone) for 24 h resulted in a marked inhibition of apical-to-basolateral Ca^{2+} transport. This finding further supports the inhibitory role of androgen on the regulation of renal active Ca^{2+} reabsorption *in vivo*.

In conclusion, this study provides evidence that androgens contribute to sex differences observed in renal Ca^{2+} handling via inhibiting the expression of renal Ca^{2+} transport proteins. Furthermore, this effect is independent of calcitropic hormones or estrogen.

Methods

Animal experiments

Experiment A: male ($n = 15$) and female ($n = 15$) C57BL6 mice, 12 weeks of age, were housed in a light and temperature-controlled room with ad libitum access to deionized drinking water and standard chow (0.28 % (wt/wt) NaCl, 1.00 % (wt/wt) Ca^{2+} , 0.22 % (wt/wt) Mg^{2+} ; LabDiet, USA). After acclimatization, mice were housed in couples in metabolic cages and 24 h urine was collected. Animals were sacrificed at the end of the experiment. Blood was collected and the kidneys dissected out and processed for further analyses.

Experiment B: male C57BL6 mice ($n = 36$), 12 weeks of age, were housed and fed as described for experiment A. After acclimatization, the mice were randomly allocated to either a sham or bilateral ORX operation under (1.5 %) halothane anesthesia and divided into three groups ($n = 12$ in each group): (i) sham-operated mice serving as control animals; (ii) ORX mice treated with vehicle; (iii) ORX mice treated with Sustanon 250 (ORX+T) subcutaneously (250

Testosterone attenuates renal TRPV5 expression

mg/kg/week; Sustanon 250 is a long-acting mixture of testosterone ester (21)) (Organon Laboratories Ltd, Cambridge, UK). The operation was performed under halothane anesthesia. After 2 weeks, these mice were housed in couples in metabolic cages and 24 h urine was collected. Thereafter, animals were sacrificed as in experiment A. The animal ethics boards of the National Defense Medical Center (Taipei, Taiwan) approved all animal experimental procedures.

Urine and serum analyses

Urine and serum concentrations of Cr and Ca^{2+} were determined using an automated analyzer (AU 5000 chemistry analyzer, Olympus, Tokyo, Japan). Serum $1,25(\text{OH})_2\text{D}_3$ levels were determined by an [^{125}I]1,25(OH) $_2\text{D}_3$ RIA assay (DiaSorin, Stillwater, MN, USA). Serum PTH concentrations were determined by IMMULITE PTH assay (Siemens Medical Solutions Diagnostics, Los Angeles, CA, USA). Both serum testosterone and estrogen concentrations were measured using chemiluminescence immunoassays (Siemens Medical Solutions Diagnostics, Tarrytown, NY, USA).

Determination of intestinal Ca^{2+} absorption

Male and female wild-type mice (7-8 weeks of age) breed off a C57Bl/6 strain, were used as previously described (22). Radioactive $^{45}\text{Ca}^{2+}$ was given by oral gavage, after an overnight fast. Intestinal absorption was determined by repeatedly measuring serum $^{45}\text{Ca}^{2+}$ content as described in detail (22). Briefly, the solution used to measure Ca^{2+} absorption contained 0.1 mM CaCl_2 , 125 mM NaCl, 17 mM Tris, 1.8 g/l fructose and 20 μCi $^{45}\text{CaCl}_2/\text{ml}$. Blood samples were obtained at 1, 2, 3, 4, and 7 min after oral gavage. Serum $^{45}\text{Ca}^{2+}$ content was determined by liquid scintillation counting. Changes in serum Ca^{2+} concentration was calculated from the $^{45}\text{Ca}^{2+}$ content of the serum samples and the specific activity of the administrated $^{45}\text{Ca}^{2+}$.

Chapter 4

Expression of renal Ca²⁺ transporters

To determine mRNA expression levels, total RNA was extracted from kidney using Trizol Total RNA Isolation Reagent (Sigma, St Louis, MO, USA). The obtained total RNA was subjected to DNase treatment to prevent genomic DNA contamination. Thereafter, 1.5 µg of total RNA was reverse transcribed by Moloney-murine leukemia virus-reverse transcriptase (Promega, Madison, WI, USA), as described previously (3). The obtained cDNA was used to determine TRPV5, calbindin-D_{28K}, NCX1 and PMCA1b mRNA levels in kidney cortex by real-time quantitative RT-PCR (ABI Prism 7700 Sequence Detection System, PE Biosystems, Rotkreuz, Switzerland). The expression level of the housekeeping gene hypoxanthine-guanine phosphoribosyl transferase (HPRT) was used as an internal control to normalize differences in RNA extractions and reverse transcription efficiencies. The primers and fluorescent probes used are as previously described (MDBIO, Taipei, Taiwan) (3, 23).

For protein expression quantification, total kidney lysates of the mice were prepared and analyzed as described previously (24). Briefly, proteins in kidney lysates were separated using SDS-PAGE and subsequent electro-transferred to polyvinylidene fluoride membranes (Immobilon-P, Millipore Corporation, Bedford, MA). Blots were incubated with rabbit anti-calbindin-D_{28K} (Sigma, St Louis, MO, USA) or rabbit β-actin (Sigma) polyclonal antibodies. Subsequently, the blots were incubated with a goat anti-rabbit peroxidase-labeled secondary antibody (Sigma). Immunoreactive protein was detected by the enhanced chemiluminescence method (Pierce, Rockford, IL, USA). Protein expression of the immunopositive bands was quantified by the use of pixel density scanning and computed calculation using the Molecular Analyst software of BioRad Laboratories (Hercules, CA, USA).

Immunohistochemical labeling of renal Ca²⁺ transporters

Kidneys were immersion-fixed in 1 % (wt/v) periodate-lysine-paraformaldehyde for 2 h at room temperature, and incubated overnight at 4 °C in phosphate-buffered saline containing 15 % (wt/v)

Testosterone attenuates renal TRPV5 expression

sucrose. Subsequently, 7 μm sections were cut from liquid nitrogen frozen kidney tissue samples for immunohistochemistry as described previously (25). For detection of TRPV5 protein abundance, kidney sections were stained with a guinea pig anti-TRPV5 antibody, as described (25), and a mouse anti-calbindin-D_{28K} antibody (Sigma). TRPV5 and calbindin-D_{28K} were visualized by staining those sections with goat anti-guinea pig and goat anti-mouse Alexa 488-conjugated anti-IgGs (Sigma), respectively. Next, to semi-quantify the TRPV5 protein expression, 5 digital images of each kidney section were taken with a Zeiss Axioskop microscope (Carl Zeiss, Inc., Thornwood, NY, USA) and the integrated optical density (IOD) was measured by computer analysis with the Image-Pro Plus version 3.0 software (Media Cybernetics, Silver Spring, MD).

Double staining using anti-TRPV5 and a rabbit anti-AR antibody (N-20, Santa Cruz Biotechnology, Santa Cruz, CA, USA) was performed using the TSA™ Plus Fluorescein amplification system (Perkin Elmer, Groningen, The Netherlands) for TRPV5 and a goat anti-rabbit IgG conjugated to Alexa 594 for visualization of the AR. Confocal pictures were acquired with an Olympus FV1000 laser scanning microscope (Center Valley, PA, USA). Differential interference contrast (DIC) was superimposed on the fluorescence images.

Primary cultures of rabbit CNT/CCD and determination of transepithelial Ca²⁺ transport

Rabbit kidney CNT and CCD cells were immunodissected from the kidney cortex of New Zealand White rabbits (5 weeks of age) using R2G9 antibodies and set in primary culture on permeable filter supports (0.33 cm²; Corning-Costar, Cambridge, MA, USA), as previously described in detail (26). The culture medium was a 1:1 mixture of Dulbecco's modified Eagle's medium and Ham's F12 (Gibco, Paisley, UK) supplemented with 5 % (v/v) decomplexed fetal calf serum, 10 $\mu\text{g}/\text{ml}$ ciproxin, 10 $\mu\text{l}/\text{ml}$ nonessential amino acids, 5 $\mu\text{g}/\text{ml}$ insulin, 5 $\mu\text{g}/\text{ml}$ transferrin, 50 nM hydrocortisone, 70 ng/ml prostaglandin E₁, 50 nM Na₂SeO₃, 5 pM triiodothyronine, and 5 μM indomethacin. Before incubation with DHT, the transepithelial

Chapter 4

resistance (R) was measured to assure the integrity of the cells. In all filters used, the R was greater than $400 \Omega \times \text{cm}^2$.

Five days after seeding, cells were incubated for 24 h with 10 nM (5 α ,17 β)-17-Hydroxy-androstan-3-one (dihydrotestosterone (DHT); Sigma), or vehicle (ethanol absolute), at the apical and basolateral compartments. Transport assays were performed on confluent monolayers the following day as described previously (26, 27). Briefly, Confluent monolayers were washed twice and pre-incubated in physiological salt solution (140 mM NaCl, 2 mM KCl, 1 mM K₂HPO₄, 1 mM MgCl₂, 1 mM CaCl₂, 5 mM glucose, 5 mM L-alanine, 5 μ M indometacin, and 10 mM HEPES-Tris (pH 7.4)) for 15 min at 37°C. The cell monolayers were subsequently incubated in physiological salt solution for another 90 min to measure transepithelial Ca²⁺ transport. During the transport assay 10 nM of DHT was added to both the apical and basolateral compartments. At the end of the experimental period, the apical medium was removed and assayed for total Ca²⁺ concentrations, using a colorimetric assay kit (Roche, Mannheim, Germany). Under these experimental conditions, net apical-to-basolateral Ca²⁺ transport is linear for at least 3 h. Transepithelial Ca²⁺ transport was determined as nmol/h/cm².

Statistical analyses

Values are expressed as means \pm S.E.M. Statistical significance ($p < 0.05$) between groups was determined by an unpaired Student's t-test (for comparisons between two individual groups), or by one-way analysis of variance (for multiple comparisons). All analyses were performed using the Statview Statistical Package Software (Power PC, version 4.51, Berkeley, CA, USA).

Acknowledgements

The authors thank A.W. van der Kemp for the primary rabbit CNT/CCD cell isolations, and T. Nijenhuis for critical reading of this manuscript. We also thank Minja Pfeiffer for helpful

Testosterone attenuates renal TRPV5 expression

discussion regarding experimental design. This work was supported by the National Science Council - Taiwan (NSC 96-2314-B-016-007-MY3), the Research Fund of Tri-Service General Hospital (TSGH-C97-81), the Netherlands Organization for Scientific Research (NWO-ALW 814.02.001), the Dutch Kidney Foundation (C05.4106), and the European Science Foundation (EURYI 2006 award to JH).

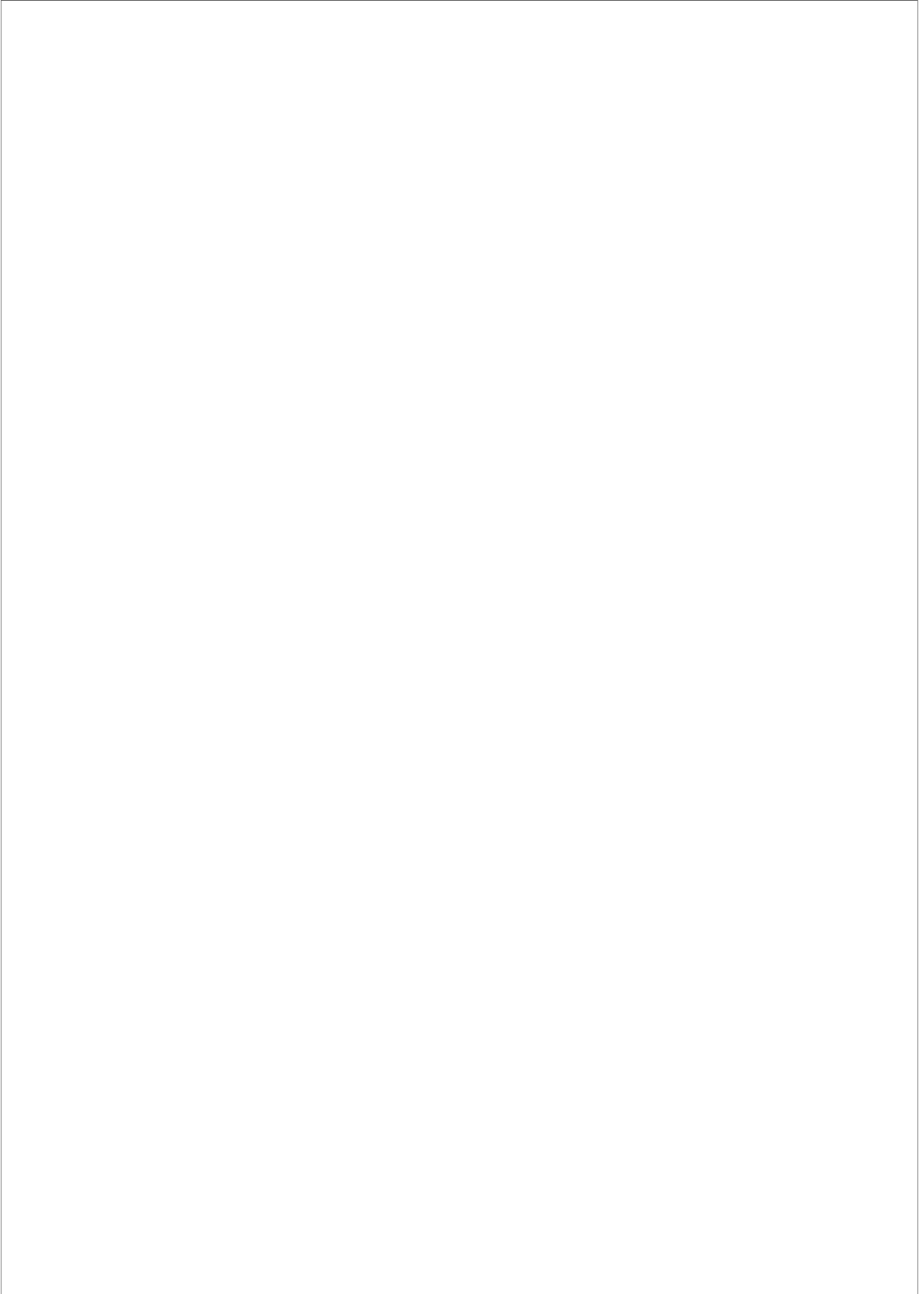
Chapter 4

References

1. Morgan B, Robertson WG. The urinary excretion of calcium. An analysis of the distribution of values in relation to sex, age and Ca^{2+} deprivation. *Clin Orthop Relat Res.* 1974;101):254-267.
2. Davis RH, Morgan DB, Rivlin RS. The excretion of Ca^{2+} in the urine and its relation to calcium intake, sex and age. *Clin Sci.* 1970;39(1):1-12.
3. Van Abel M, Hoenderop JG, Dardenne O, St Arnaud R, Van Os CH, Van Leeuwen HJ, Bindels RJ. 1,25-dihydroxyvitamin D_3 -independent stimulatory effect of estrogen on the expression of ECaC1 in the kidney. *J Am Soc Nephrol.* 2002;13(8):2102-2109.
4. Stefani S, Aguiari GL, Bozza A, Maestri I, Magri E, Cavazzini P, Piva R, del Senno L. Androgen responsiveness and androgen receptor gene expression in human kidney cells in continuous culture. *Biochem Mol Biol Int.* 1994;32(4):597-604.
5. Sabolic I, Asif AR, Budach WE, Wanke C, Bahn A, Burckhardt G. Gender differences in kidney function. *Pflugers Arch.* 2007;455(3):397-429.
6. Hoenderop JG, Nilius B, Bindels RJ. Ca^{2+} absorption across epithelia. *Physiol Rev.* 2005;85(1):373-422.
7. Bindels RJ. Ca^{2+} handling by the mammalian kidney. *J Exp Biol.* 1993;184(89-104).
8. Bindels RJ. Molecular pathophysiology of renal Ca^{2+} handling. *Kidney Blood Press Res.* 2000;23(3-5):183-184.
9. Hoenderop JG, Willems PH, Bindels RJ. Toward a comprehensive molecular model of active Ca^{2+} reabsorption. *Am J Physiol Renal Physiol.* 2000;278(3):F352-360.
10. Hoenderop JG, Muller D, Van Der Kemp AW, Hartog A, Suzuki M, Ishibashi K, Imai M, Sweep F, Willems PH, Van Os CH, et al. Calcitriol controls the epithelial Ca^{2+} channel in kidney. *J Am Soc Nephrol.* 2001;12(7):1342-1349.
11. van Abel M, Hoenderop JG, van der Kemp AW, Friedlaender MM, van Leeuwen JP, Bindels RJ. Coordinated control of renal Ca^{2+} transport proteins by parathyroid hormone. *Kidney Int.* 2005;68(4):1708-1721.
12. Hoenderop JG, Bindels RJ. Calcitropic and magnesiotropic TRP channels. *Physiology (Bethesda).* 2008;23(32-40).
13. Mauras N, Hayes VY, Vieira NE, Yergey AL, O'Brien KO. Profound hypogonadism has significant negative effects on Ca^{2+} balance in males: a calcium kinetic study. *J Bone Miner Res.* 1999;14(4):577-582.
14. Chen Z, Vaughn DA, Fanestil DD. Influence of gender on renal thiazide diuretic receptor density and response. *J Am Soc Nephrol.* 1994;5(4):1112-1119.
15. Nyomba BL, Bouillon R, De Moor P. Evidence for an interaction of insulin and sex steroids in the regulation of vitamin D metabolism in the rat. *J Endocrinol.* 1987;115(2):295-301.
16. Hope WG, Ibarra MJ, Thomas ML. Testosterone alters duodenal Ca^{2+} transport and

Testosterone attenuates renal TRPV5 expression

- longitudinal bone growth rate in parallel in the male rat. *Proc Soc Exp Biol Med.* 1992;200(4):536-541.
17. Takeda H, Chodak G, Mutchnik S, Nakamoto T, Chang C. Immunohistochemical localization of androgen receptors with mono- and polyclonal antibodies to androgen receptor. *J Endocrinol.* 1990;126(1):17-25.
 18. Khosla S, Melton LJ, 3rd, Atkinson EJ, O'Fallon WM. Relationship of serum sex steroid levels to longitudinal changes in bone density in young versus elderly men. *J Clin Endocrinol Metab.* 2001;86(8):3555-3561.
 19. Riggs BL, Khosla S, Melton LJ, 3rd. Sex steroids and the construction and conservation of the adult skeleton. *Endocr Rev.* 2002;23(3):279-302.
 20. Syed F, Khosla S. Mechanisms of sex steroid effects on bone. *Biochem Biophys Res Commun.* 2005;328(3):688-696.
 21. Nolan LA, Levy A. The effects of testosterone and oestrogen on gonadectomised and intact male rat anterior pituitary mitotic and apoptotic activity. *J Endocrinol.* 2006;188(3):387-396.
 22. Alexander RT, Woudenberg-Vrenken TE, Buurman J, Dijkman H, van der Eerden BC, van Leeuwen JP, Bindels RJ, Hoenderop JG. Klotho Prevents Renal Ca²⁺ Loss. *J Am Soc Nephrol.* 2009;20(11):2371-2379.
 23. van Abel M, Hoenderop JG, van der Kemp AW, van Leeuwen JP, Bindels RJ. Regulation of the epithelial Ca²⁺ channels in small intestine as studied by quantitative mRNA detection. *Am J Physiol Gastrointest Liver Physiol.* 2003;285(1):G78-85.
 24. Van Baal J, Yu A, Hartog A, Fransen JA, Willems PH, Lytton J, Bindels RJ. Localization and regulation by vitamin D of calcium transport proteins in rabbit cortical collecting system. *Am J Physiol.* 1996;271(5 Pt 2):F985-993.
 25. Hoenderop JG, Hartog A, Stuver M, Doucet A, Willems PH, Bindels RJ. Localization of the epithelial Ca²⁺ channel in rabbit kidney and intestine. *J Am Soc Nephrol.* 2000;11(7):1171-1178.
 26. Bindels RJ, Hartog A, Timmermans J, Van Os CH. Active Ca²⁺ transport in primary cultures of rabbit kidney CCD: stimulation by 1,25-dihydroxyvitamin D₃ and PTH. *Am J Physiol.* 1991;261(5 Pt 2):F799-807.
 27. Hoenderop JG, Hartog A, Willems PH, Bindels RJ. Adenosine-stimulated Ca²⁺ reabsorption is mediated by apical A1 receptors in rabbit cortical collecting system. *Am J Physiol.* 1998;274(4 Pt 2):F736-743.



CHAPTER 5

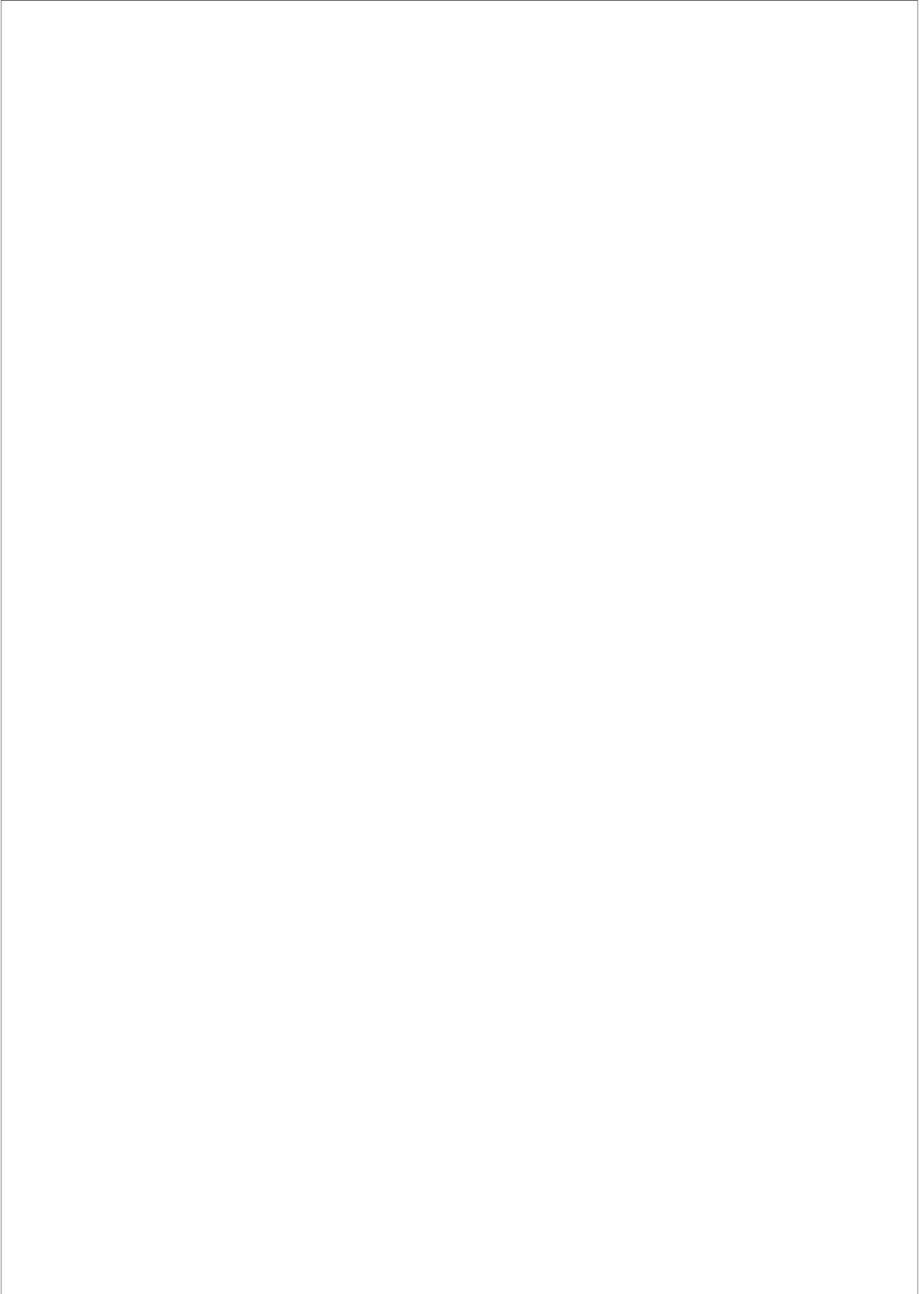
Calcitonin stimulated renal Ca^{2+} reabsorption occurs independently of TRPV5

Henrik Dimke^{1*}, Yu-Juei Hsu^{1,2*}, Joost G. Hoenderop¹, and René J. Bindels¹.

¹Department of Physiology, Radboud University Nijmegen Medical Centre, the Netherlands.

²Division of Nephrology, Department of Internal Medicine, Tri-Service General Hospital, Taipei, Taiwan.

*Authors contributed equally.



Calcitonin stimulates Ca²⁺ transport

Abstract

Calcitonin (CT) is known to affect renal Ca²⁺ handling. However, it remains unclear how CT affects Ca²⁺ transport in the distal convolutions. The aim of this study was to investigate the contribution of the renal epithelial Ca²⁺ channel, TRPV5, to renal Ca²⁺ handling in response to CT. C57BL/6 mice received a single bolus injection of CT, which significantly reduced the urinary Ca²⁺ excretion. In addition, urinary Na⁺ and K⁺ excretion also decreased after CT administration. No apparent changes in renal TRPV5 and calbindin-D_{28K} mRNA could be detected between CT- and vehicle-treated mice. To evaluate whether TRPV5 activity is needed for the CT-induced increase in Ca²⁺ reabsorption, mice with genetic ablation of TRPV5 (*Trpv5*^{-/-}), were employed. *Trpv5*^{-/-} mice as well as their wild type (*Trpv5*^{+/+}) controls, received three bolus injections of CT over a 40 hr study period. Overnight (16 hr) as well as the subsequent 24 hr urine was collected. Overnight urinary Ca²⁺ excretion was reduced in both *Trpv5*^{-/-} and *Trpv5*^{+/+} mice after a bolus injection of CT. The subsequent 24 hr urinary excretion of Ca²⁺ which was collected after the third bolus injection, showed no effect of CT on renal Ca²⁺ handling in either mice group. Accordingly, CT did not alter the intrarenal protein abundance of TRPV5 and Calbindin-D_{28K} after three bolus injections of CT. In conclusion, CT augments the renal reabsorptive capacity for Ca²⁺. This increase is likely to occur independently of TRPV5.

Introduction

Disturbances in the systemic Ca²⁺ concentration often result in instability of the neurological and cardiac systems (e.g. hypercalcemia causes fatigue, nausea, and abnormal heart rhythms (1)). Thus, maintenance of the serum Ca²⁺ concentration plays an important role in stabilizing these physiological processes. Several hormones have been known to affect the systemic Ca²⁺ concentration. Calcitonin (CT) is a 32 amino-acid peptide synthesized by posttranslational processing in the C cells of the thyroid gland in mammals (2). CT acts primarily by inhibiting

Chapter 5

osteoclast-mediated bone resorption and is secreted in response to increases in systemic Ca^{2+} concentration (2). Historically, CT has been extensively used in treating hypercalcemia, osteoporosis and Paget's disease (2). Throughout the kidney and elsewhere, CT acts primarily by activating the adenylate cyclase pathway (3, 4).

In the kidney, vectorial NaCl transport within the thick ascending limb (TAL) drives paracellular transport of Ca^{2+} . Administration of CT to rats increases the renal reabsorption of Ca^{2+} , which is in part achieved by increasing the reabsorption of Ca^{2+} in the TAL. Here application of CT also increases vectorial NaCl transport (5-7). Active transcellular Ca^{2+} transport is restricted to the distal convolutions. Here, luminal Ca^{2+} enters across the apical membrane via the epithelial Ca^{2+} channel, transient receptor potential vanilloid 5 (TRPV5) (8, 9). Studies in rabbit suggest that CT exerts its effect on Ca^{2+} reabsorption only in the distal convoluted tubule (DCT), while no stimulation occurs in the connecting tubule (CNT) (10). In addition, CT fails to stimulate cAMP accumulation in the CNT of rabbits (11). Our group has also been unable to show stimulatory effects of CT on cAMP production in rabbit primary CNT cultures (12). In the rabbit, TRPV5 localizes primarily to the CNT where CT does not affect Ca^{2+} reabsorption. However, in mouse, TRPV5 is highly expressed in apical membrane domains of particularly the late distal convoluted tubule (DCT2), with a gradual decrease along CNT and initial collecting duct (iCD) (13, 14), suggesting that TRPV5-mediated Ca^{2+} uptake predominates in the DCT2 segment. Similarly, in rat, immunohistochemical data suggests that TRPV5 expression appears in the DCT2 and is further observed in the CNT (15). The intrarenal distribution of TRPV5 in human is currently not known.

In comparison to rabbit, the boundaries defining the DCT/CNT/iCD regions in human, rat, and mouse are morphologically less well defined, with cell types from different segments intermingled. In the kidney of rats, the "bright" portion of the DCT retains responsiveness to CT, resulting in increased cAMP production (4). CT binding sites have been identified in the rat kidney, including the TAL and DCT (16). Detailed micropuncture studies performed by Elalouf *et*

Calcitonin stimulates Ca^{2+} transport

a/. investigated the effects of CT on electrolyte transport in the distal tubules of rats deprived of vasopressin, parathyroid hormone (PTH), and glucagon. Here they demonstrated that NaCl, as well as Ca^{2+} transport was increased by CT infusion (17). Other cAMP-elevating hormones such as PTH affect TRPV5-mediated Ca^{2+} transport. PTH supplementation to parathyroidectomized rats increases the expression of TRPV5, independent of serum 1,25-dihydroxyvitamin D_3 levels, suggesting that perhaps intracellular elevations in cAMP affect the abundance of TRPV5 (18). In addition, cAMP generation has been shown to increase TRPV5 single channel activity via a PKA-dependent mechanism (19). However, it is unclear whether there is a functional overlap between PTH and CT in the DCT2 regions of rats and mice and whether the CT-induced increase in cAMP could lead to a similar activation in the DCT2 segment as PTH.

In order to better understand the molecular actions of CT on overall renal Ca^{2+} balance and to delineate the potential effects of CT on TRPV5-dependent Ca^{2+} reabsorption, several experimental series were performed in wildtype and TRPV5-deficient mice. Due to the rapid action of CT we investigated the short-term effects by of CT on the renal Ca^{2+} excretion.

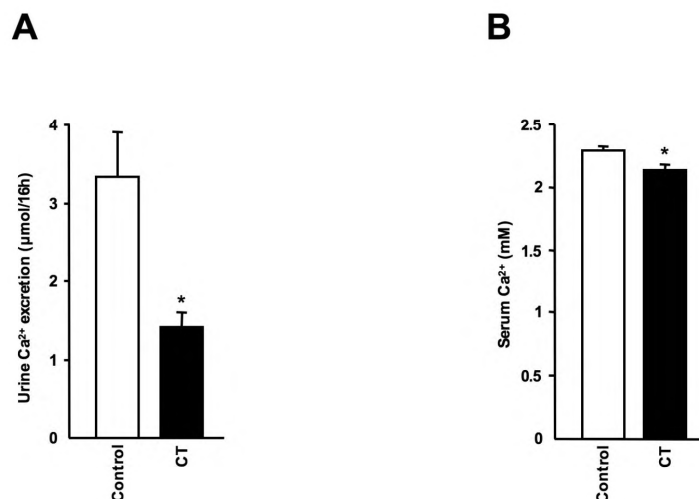


Figure 1. CT reduces urinary Ca^{2+} excretion. (A) Renal Ca^{2+} excretion and (B) serum Ca^{2+} concentration 16 hrs after a bolus injection CT. Data is presented as mean \pm SEM. * indicates statistical significance ($p < 0.05$).

Chapter 5

Results

CT increases renal Ca²⁺ reabsorption in mice

To assess the acute effects of CT, 16 hr urine from overnight collections was obtained following a bolus injection of the hormone (20U/100g bodyweight) or vehicle. The effect of overnight CT exposure on renal and systemic Ca²⁺ handling is depicted in Figure 1. Administration of CT resulted in a significant decrease in the urinary excretion of Ca²⁺ ($p < 0.05$). Serum Ca²⁺ concentrations were slightly reduced after overnight CT administration ($p < 0.05$). Urinary excretion of Na⁺ and K⁺ showed a significant decrease after CT injection (Table 1). In addition, the urinary Na⁺/K⁺ ratio remained unchanged excluding an effect on the collecting duct. These data are consistent with a primary effect of CT on electrolyte transport in the TAL and DCT (5-7, 17).

	Urine				Serum	
	Diuresis (ml)	Na ⁺ (μ mol)	K ⁺ (μ mol)	Na ⁺ /K ⁺ ratio	Na ⁺ (mM)	K ⁺ (mM)
Control	1.21 \pm 0.11	268 \pm 32	639 \pm 30	0.42 \pm 0.03	150 \pm 0.4	5.34 \pm 0.11
CT	0.98 \pm 0.18	132 \pm 16*	305 \pm 50*	0.44 \pm 0.02	152 \pm 0.5	5.30 \pm 0.03

Table 1. Serum concentrations and urinary excretion of Na⁺ and K⁺ after a bolus injection CT. Data is presented as mean \pm SEM. N=6 animals per group. * indicates statistical significance ($p < 0.05$ versus controls). CT, calcitonin.

CT does not change the renal mRNA expression of TRPV5 and Calbindin-D_{28K}

To evaluate whether the increased Ca²⁺ reabsorption could in part be due to transcriptional changes in Ca²⁺ transport proteins located in the distal convolutions, semi-quantitative PCR was

Calcitonin stimulates Ca^{2+} transport

used to estimate TRPV5 and Calbindin- $\text{D}_{28\text{K}}$ abundance. As can be seen in Figure 2, no changes were observed in the renal mRNA expression of either transcript. Although CT did not modulate the changes of TRPV5, it does not exclude the potential involvement of TRPV5. Therefore, we investigated the effect of CT in *Trpv5*^{+/+} and *Trpv5*^{-/-} mice after 1 and 3 injections of CT.

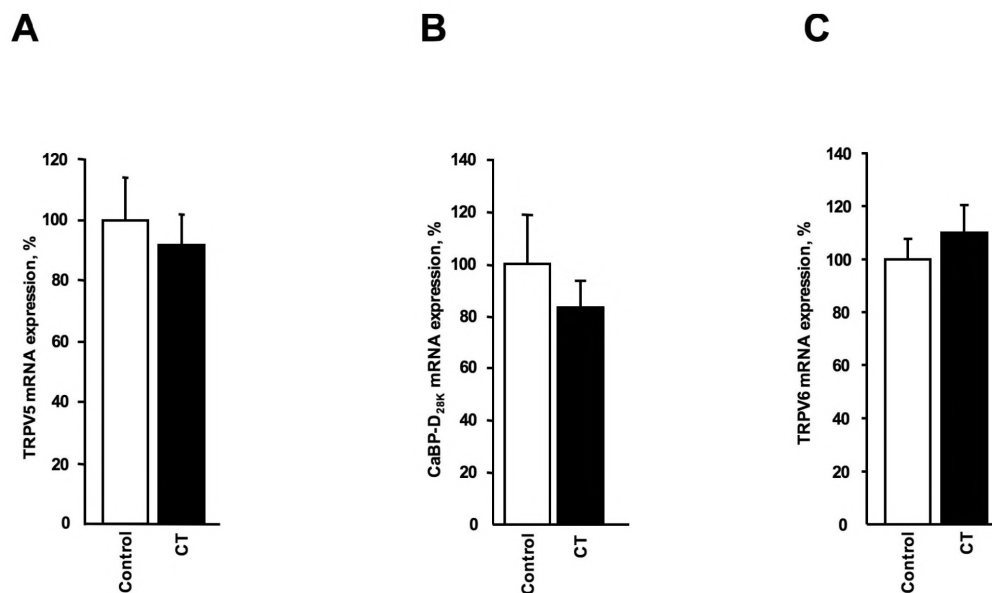


Figure 2. Semi-quantitative mRNA expression of TRPV5 and Calbindin- $\text{D}_{28\text{K}}$ after overnight bolus injection of CT. Representative histograms of mRNA expression of (A) TRPV5 and (B) Calbindin- $\text{D}_{28\text{K}}$ in kidney. Data are presented as mean \pm SEM.

*CT stimulates Ca^{2+} reabsorption in *Trpv5*^{-/-} mice*

Administration of CT to *Trpv5*^{+/+} and *Trpv5*^{-/-} mice resulted in a decreased overnight urinary Ca^{2+} excretion in both groups. However, after repeated administration of CT, the urinary Ca^{2+} excretion returned to normal in both *Trpv5*^{+/+} and *Trpv5*^{-/-} mice, as compared to their corresponding vehicle-injected controls (Figure 3). Serum Ca^{2+} concentrations were measured after 40 hrs, but no difference was observed after CT administration in either strain (Figure 3). This is in line with the observed rapid effect of CT.

Chapter 5

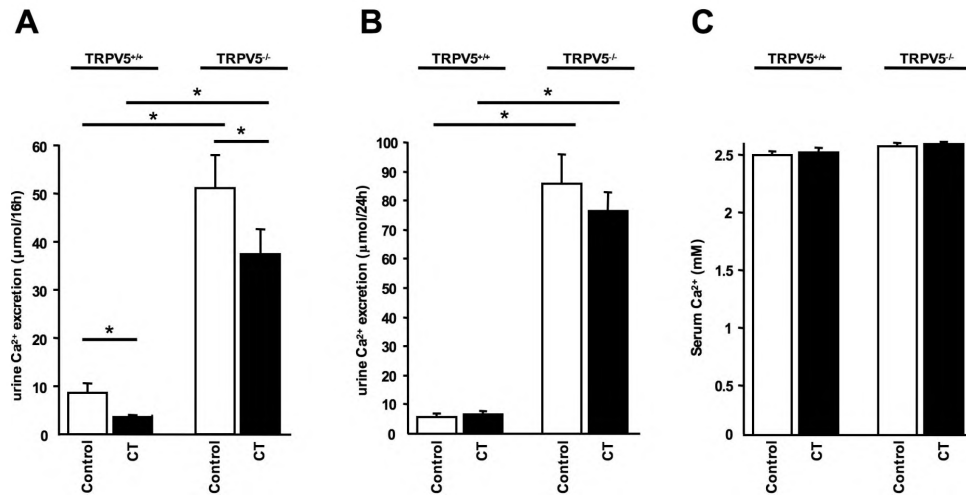


Figure 3. Renal Ca^{2+} excretion after 1 and 3 bolus injections spaced over 40 hrs in $Trpv5^{+/+}$ and $Trpv5^{-/-}$ mice. (A) 16 hrs urinary Ca^{2+} excretion after a single bolus injection of CT (B) and the consecutive 24 hrs of urinary Ca^{2+} excretion after 3 injections. (C) Serum Ca^{2+} concentrations after 3 CT bolus injections spaced over 40 hrs. Data is presented as mean \pm SEM. * $p < 0.05$ versus $Trpv5^{+/+}$ controls. # $p < 0.05$ versus $Trpv5^{-/-}$ controls.

Renal protein expression of Ca^{2+} transporters remains unaltered after 3 CT injections

Kidneys retrieved from $Trpv5^{+/+}$ and $Trpv5^{-/-}$ mice by the end of the experiment were used to assess the effects of CT on renal Ca^{2+} transporter expression. TRPV5 and Calbindin- D_{28K} protein abundance was semi-quantified by immunohistochemistry (Figure 4) and immunoblotting (Figure 5), respectively. Computerized analysis of immunohistochemical images did not reveal any changes in TRPV5 protein expression after CT administration in $Trpv5^{+/+}$ mice compared to their vehicle- injected control $Trpv5^{+/+}$ mice (Figure 4). This is in line with the observation that CT affects renal Ca^{2+} transport independent of TRPV5. In addition, the renal Calbindin- D_{28K} protein expression remained unchanged after CT administration in $Trpv5^{-/-}$ mice (Figure 4-5). The Calbindin- D_{28K} protein expression of $Trpv5^{-/-}$ mice was significantly reduced compared to $Trpv5^{+/+}$ mice (20) (Figure 4-5).

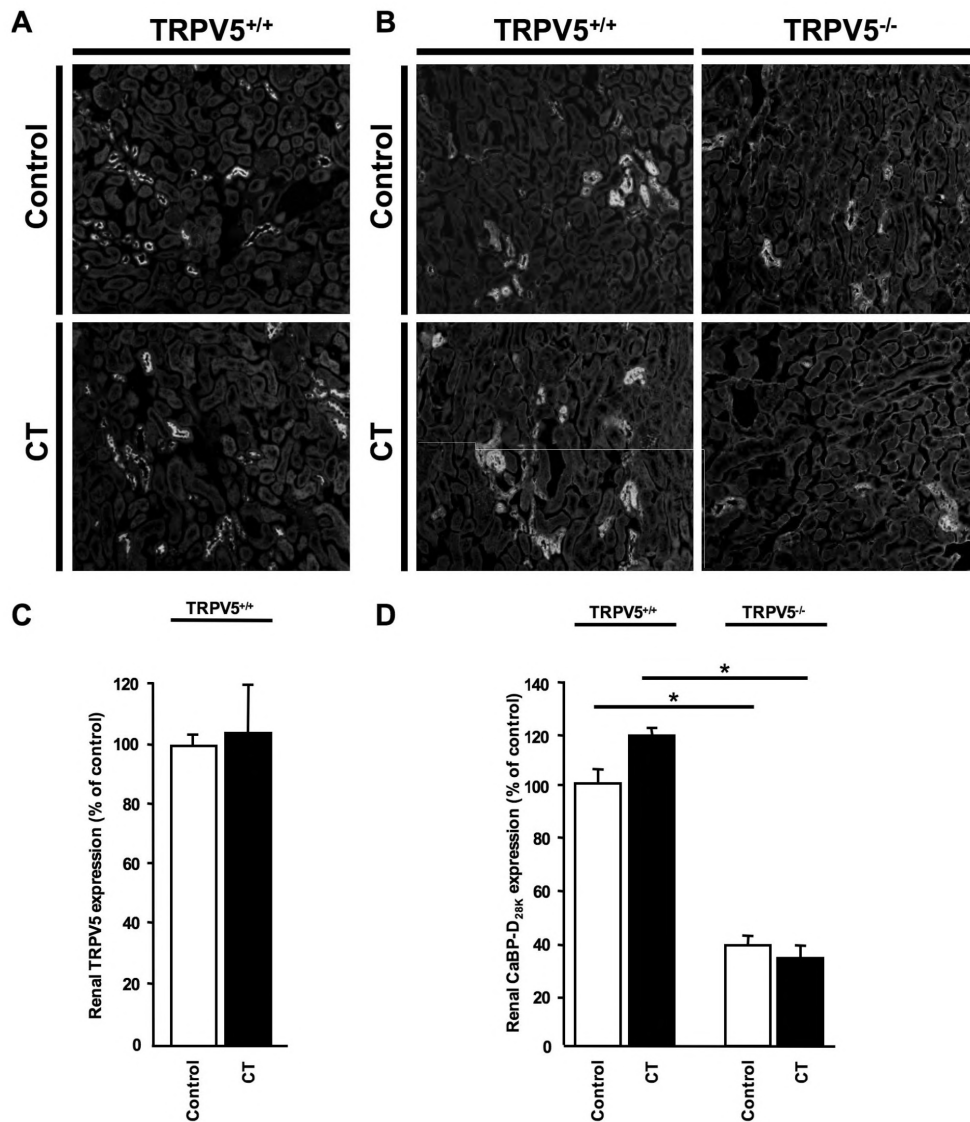


Figure 4. Immunohistochemical staining of renal Ca^{2+} transporters after 3 bolus injections in *Trpv5^{+/+}* and *Trpv5^{-/-}* mice. Representative images of immunohistochemical staining of (A) TRPV5 and (B) Calbindin-D_{28K} in kidney cortex. Semi-quantification of renal (C) TRPV5 and (D) Calbindin-D_{28K} protein abundance was performed by computerized analysis of immunohistochemical images. Data were calculated as integrated optical density (IOD; arbitrary units) and depicted as percentage of *Trpv5^{+/+}* controls. Data is presented as mean \pm SEM. * $p < 0.05$ versus *Trpv5^{+/+}* vehicle-injected controls. N=6 animals per group.

Chapter 5

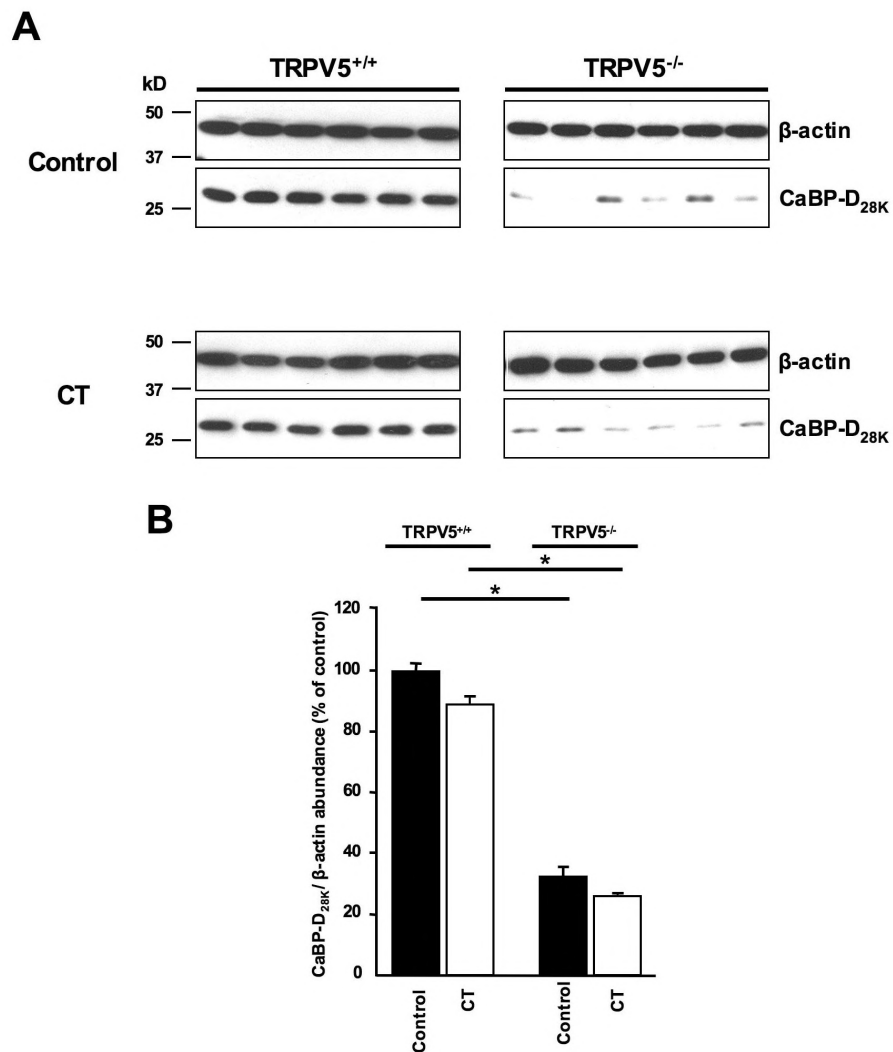


Figure 5. Effects of CT on renal Calbindin-D_{28K} protein expression in *Trpv5*^{+/+} and *Trpv5*^{-/-} mice. (A) Immunoblots of protein samples (10μg each) from homogenates of kidney tissue were labeled with antibodies against Calbindin-D_{28K}. (B) Expression of Calbindin-D_{28K} protein was quantified by computer-assisted densitometry analysis and presented as the ratio to β-actin expression levels in relative percentages. Data are presented as mean ± SEM. * indicates statistical significance (p<0.05) versus *Trpv5*^{+/+} controls. N=6 animals per group.

Discussion

A bolus injection of CT significantly reduced the urinary excretion of Ca²⁺ in wildtype mice. This decrease was associated with a reduction in the urinary Na⁺ and K⁺ excretion, leaving the urinary

Calcitonin stimulates Ca^{2+} transport

Na^+/K^+ ratio unchanged. These data are consistent with the previously reported effects of CT on stimulating TAL and DCT transport of NaCl and K^+ (6, 7, 17, 21). Earlier studies in the TAL of mice and rats have demonstrated that CT activates NaCl transport only in the cortical TAL (6, 21). This segment of the TAL is also thought to drive paracellular Ca^{2+} reabsorption in these species. Although never delineated in detail, CT is likely to activate a cAMP cascade leading to increased NKCC2 transport, perhaps via increased membrane trafficking and phosphorylation (5, 6, 22). Currently, it remains unknown which transporter CT stimulates in the DCT (17). One option is the thiazide-sensitive NCC transporter that resides there.

A significant, albeit small, change in serum Ca^{2+} concentrations was observed after overnight CT administration. Earlier reports showing that infusion of CT, depending on dose, acutely reduces serum Ca^{2+} concentrations, that frequently reverts to normal range within one day (23). In line with this, no change was observed in systemic Ca^{2+} concentrations after 3 injections of CT spaced over 40 hrs. One may suggest that the reduced excretion of Ca^{2+} in the presence of CT occurs to compensate for the acute surge in systemic Ca^{2+} concentrations normally associated with CT administration. However, in thyroparathyroidectomized (TPTX) rats, Ca^{2+} infusion prior to CT treatment was given in order to avoid hypocalcemia in the animals. In these TPTX rats, CT was still able to reduce the fractional excretion of Ca^{2+} despite normocalcemia (24). This is consistent with a direct effect of CT on the kidney. The effect of CT on urinary Ca^{2+} excretion is also absent after repeated administration of CT to either *Trpv5*^{+/+} or *Trpv5*^{-/-} mice. Reduced surface expression of CT receptors and decreased mRNA expression has been shown to explain such escape phenomena in other cell types (25). This may also explain why patients with a CT-secreting tumor frequently have normal systemic concentrations of Ca^{2+} (26).

The present study was initiated to investigate the potential effect of CT on TRPV5-mediated Ca^{2+} reabsorption. Injections of CT for 16 or 40 hrs did not change the renal abundance of TRPV5. In addition, *Trpv5*^{+/+} and *Trpv5*^{-/-} mice responded in a similar manner to

Chapter 5

CT administration. Given the data obtained in these experimental models, it is likely that the effect of CT on renal Ca^{2+} transport occurs independently of TRPV5. Although CT does not affect TRPV5-mediated Ca^{2+} reabsorption, it is clear from this study that CT strongly stimulates renal Ca^{2+} reabsorption. The stimulatory effect of CT is likely to occur primarily through changes in Ca^{2+} transport, as previously described (6, 7, 21). It should be stated that although the effects of CT on renal Ca^{2+} transport are present in *Trpv5^{+/+}* as well as in *Trpv5^{-/-}* mice, and that TRPV5 expression is unaltered after CT administration, does not fully exclude an effect upon TRPV5. Although unlikely, a lack of stimulation of CT on TRPV5 in *Trpv5^{-/-}* mice, may be masked due to the pronounced effect of CT in the TAL.

In the rat, CT has been shown to increase NaCl as well as Ca^{2+} transport in the DCT (17), thus vectorial transfer of Ca^{2+} does occur to a greater extent in the presence of CT. The present study suggests that these effects occur largely independent of TRPV5. In addition, microperfusion experiments in rabbits show that CT stimulates Ca^{2+} transport in the early DCT, where TRPV5 is not expressed (10). This raises the question, how does Ca^{2+} transport occurs in the early DCT and does it contribute significantly to overall renal Ca^{2+} handling? Further studies are needed to determine the potential effect of CT on electrolyte transporters in these segments.

In conclusion, overnight CT administration increases renal Ca^{2+} reabsorption in mice. This effect occurs independently of TRPV5 as no change can be detected in TRPV5 and Calbindin-D_{28K} expression and similar responses to CT is observed in *Trpv5^{+/+}* and *Trpv5^{-/-}* mice.

Methods

Experimental protocol 1

Male C57BL/6 mice (12 weeks of age) were housed in a light and temperature-controlled room with ad libitum access to deionized drinking water and standard chow (0.28 % (wt/wt) NaCl, 1.00

Calcitonin stimulates Ca²⁺ transport

% (wt/wt) Ca, 0.22 % (wt/wt) Mg; LabDiet, USA). Mice were injected with a single dose of CT 20U/100g bodyweight (Novartis Pharmaceuticals, Taiwan, n=6) or vehicle (n=6) and placed in metabolic cages. After 16 hrs, overnight urine was collected and the animals were sacrificed under halothane anesthesia. Blood was obtained via orbital puncture before cervical dislocation. The kidneys were dissected out and snap frozen for RNA extraction. The animal ethics boards of the National Defense Medical Center (Taipei, Taiwan) approved all animal experimental procedures.

Experimental protocol 2

Trpv5^{-/-} mice were generated by targeted ablation of the TRPV5 gene as described previously (20). After acclimatization, *Trpv5*^{+/+} and *Trpv5*^{-/-} mice were injected with CT (20U/100g body weight, n=6) or vehicle (n=6) in three subcutaneous bolus injections spaced over 40 hrs. During this period the mice were housed in metabolic cages. Overnight (16hr) urine was collected during the period between the first and second dose of CT. Subsequently, 24h urine was collected during the remainder of the study, where the mice received the last two injections. At the end of the experiment, animals were killed under halothane anesthesia, blood was removed and tissue samples were harvested for immunohistochemistry and Western blotting. The animal ethics board of the Radboud University Nijmegen approved the animal experimental procedures.

Urine and serum analyses

Urine and serum concentrations of Ca²⁺ were analyzed using a colorimetric assay kit (Roche, Mannheim, Germany). Urine and serum concentrations of Na⁺ and K⁺ were determined using an automated analyzer (AU 5000 chemistry analyzer, Olympus, Tokyo, Japan).

Chapter 5

RNA extraction and semi-quantitative PCR

Total RNA was extracted from kidney using Trizol Total RNA Isolation Reagent (Sigma, St Louis, MO, USA) as described previously (27). The obtained total RNA was subjected to DNase treatment to prevent genomic DNA contamination. Thereafter, 1.5 µg of total RNA was reverse transcribed by Moloney-murine leukemia virus-reverse transcriptase (Promega, Madison, WI, USA). The cDNA was used to determine intrarenal mRNA levels of TRPV5 and calbindin-D_{28K} in kidney cortex by real-time semi-quantitative polymerase chain reaction, using the ABI Prism 7700 Sequence Detection System (PE Biosystems, Rotkreuz, Switzerland). The expression level of the housekeeping gene hypoxanthine-guanine phosphoribosyl transferase (HPRT) was used as an internal control to normalize differences in RNA extractions and reverse transcription efficiencies. The primers and fluorescent probes used are as previously described (MDBIO, Taipei, Taiwan) (27, 28)

Immunohistochemistry

Kidney tissue was immersion fixed in 1 % (w/v) periodate-lysine-paraformaldehyde for 2 hours at room temperature, and subsequently incubated overnight at 4°C in phosphate-buffered saline (PBS) containing 15% (w/v) sucrose. The kidneys were snap frozen in liquid nitrogen and 7 µm sections cut on a cryostat microtome (HM 550, MICROM International GmbH, Germany). For immunohistochemical detection of TRPV5, kidney sections were stained with a guinea pig anti-TRPV5 antibody (1:50) (8) or mouse anti-Calbindin-D_{28K} antibody (1:1,000; Sigma). To visualize TRPV5 and Calbindin-D_{28K}, sections were stained with goat anti-guinea pig Alexa 488-conjugated anti-IgG (1:300; Sigma) and goat anti-mouse Alexa 488-conjugated anti-IgG (1:300; Sigma), respectively. TRPV5 protein expression was semi-quantified by taking 5 digital images of each kidney section on with a Zeiss Axioskop microscope (Carl Zeiss, Inc., Thornwood, NY, USA) and calculating the integrated optical density using Image-Pro Plus version 3.0 software (Media Cybernetics, Silver Spring, MD).

Calcitonin stimulates Ca²⁺ transport

Immunoblotting

Total mouse kidney lysates were prepared as described previously (29). The protein concentration of the homogenates was determined with the Bio-Rad protein assay (Bio-Rad, München, Germany). Samples were submitted to 12% (wt/vol) SDS-PAGE and blotted to polyvinylidene difluoride-nitrocellulose membranes (Immobilon-P, Millipore Corp., Bedford, MA). Blots were incubated overnight with a rabbit anti-Calbindin-D_{28K} polyclonal antibody (1:5,000; Sigma) at 4°C. Subsequently, blots were incubated with a goat anti-rabbit peroxidase-labeled secondary antibody (1 hr; 1:10,000; Sigma, St. Louis, MO). Immunoreactive protein was detected by the chemiluminescence method (Pierce, Rockford, IL). Immunopositive bands were scanned using an imaging densitometer (Bio-Rad Gs-690) to determine pixel density (Molecular Analyst Software; BioRad Laboratories, Hercules, CA).

Statistical analyses

Values are expressed as mean ± SEM. Statistical significance ($p < 0.05$) in experimental protocol 1 was determined using the student's t-test. In experimental group 2, significance was determined by a one-way ANOVA. In case of significance the Tukey-Kramer multiple comparisons test was applied. The analyses were performed using the Statview Statistical Package Software (Power PC, version 4.51, Berkeley, CA).

Acknowledgements

The authors thank Pedro San-Cristobal and Sjoerd Verkaart for helpful comments on the manuscript. This work was supported by the Netherlands Organization for Scientific (ZonMw 9120.6110), EURYI award from the European Science Foundation, the Dutch Kidney foundation (C05.2134, C03.6017), the National Science Council - Taiwan (NSC 96-2314-B-016-007-MY3), and the Research Fund of Tri-Service General Hospital (TSGH-C98-84).

Chapter 5

References

1. Bilezikian JP. Clinical review 51: Management of hypercalcemia. *J Clin Endocrinol Metab.* 1993;77(6):1445-1449.
2. Pondel M. Calcitonin and calcitonin receptors: bone and beyond. *Int J Exp Pathol.* 2000;81(6):405-422.
3. Chabardes D, Gagnan-Brunette M, Imbert-Teboul M, Gontcharevskaia O, Montegut M, Clique A, Morel F. Adenylate cyclase responsiveness to hormones in various portions of the human nephron. *J Clin Invest.* 1980;65(2):439-448.
4. Morel F. Sites of hormone action in the mammalian nephron. *Am J Physiol.* 1981;240(3):F159-164.
5. Vuillemin T, Teulon J, Geniteau-Legendre M, Baudouin B, Estrade S, Cassingena R, Ronco P, Vandewalle A. Regulation by calcitonin of Na⁺-K⁺-Cl⁻ cotransport in a rabbit thick ascending limb cell line. *Am J Physiol.* 1992;263(3 Pt 1):C563-572.
6. Di Stefano A, Wittner M, Nitschke R, Braitsch R, Greger R, Bailly C, Amiel C, Roinel N, de Rouffignac C. Effects of parathyroid hormone and calcitonin on Na⁺, Cl⁻, K⁺, Mg²⁺ and Ca²⁺ transport in cortical and medullary thick ascending limbs of mouse kidney. *Pflugers Arch.* 1990;417(2):161-167.
7. Elalouf JM, Roinel N, de Rouffignac C. ADH-like effects of calcitonin on electrolyte transport by Henle's loop of rat kidney. *Am J Physiol.* 1984;246(2 Pt 2):F213-220.
8. Hoenderop JG, Hartog A, Stuiver M, Doucet A, Willems PH, Bindels RJ. Localization of the epithelial Ca²⁺ channel in rabbit kidney and intestine. *J Am Soc Nephrol.* 2000;11(7):1171-1178.
9. Hoenderop JG, van der Kemp AW, Hartog A, van de Graaf SF, van Os CH, Willems PH, Bindels RJ. Molecular identification of the apical Ca²⁺ channel in 1, 25-dihydroxyvitamin D₃-responsive epithelia. *J Biol Chem.* 1999;274(13):8375-8378.
10. Shimizu T, Yoshitomi K, Nakamura M, Imai M. Effects of PTH, calcitonin, and cAMP on Ca²⁺ transport in rabbit distal nephron segments. *Am J Physiol.* 1990;259(3 Pt 2):F408-414.
11. Chabardes D, Imbert-Teboul M, Montegut M, Clique A, Morel F. Distribution of calcitonin-sensitive adenylate cyclase activity along the rabbit kidney tubule. *Proc Natl Acad Sci U S A.* 1976;73(10):3608-3612.
12. Bindels RJ, Hartog A, Timmermans J, Van Os CH. Active Ca²⁺ transport in primary cultures of rabbit kidney CCD: stimulation by 1,25-dihydroxyvitamin D₃ and PTH. *Am J Physiol.* 1991;261(5 Pt 2):F799-807.
13. Loffing J, Loffing-Cueni D, Valderrabano V, Klausli L, Hebert SC, Rossier BC, Hoenderop JG, Bindels RJ, Kaissling B. Distribution of transcellular Ca²⁺ and Na⁺ transport pathways along mouse distal nephron. *Am J Physiol Renal Physiol.* 2001;281(6):F1021-1027.
14. Hoenderop JG, Nilius B, Bindels RJ. Ca²⁺ absorption across epithelia. *Physiol Rev.*

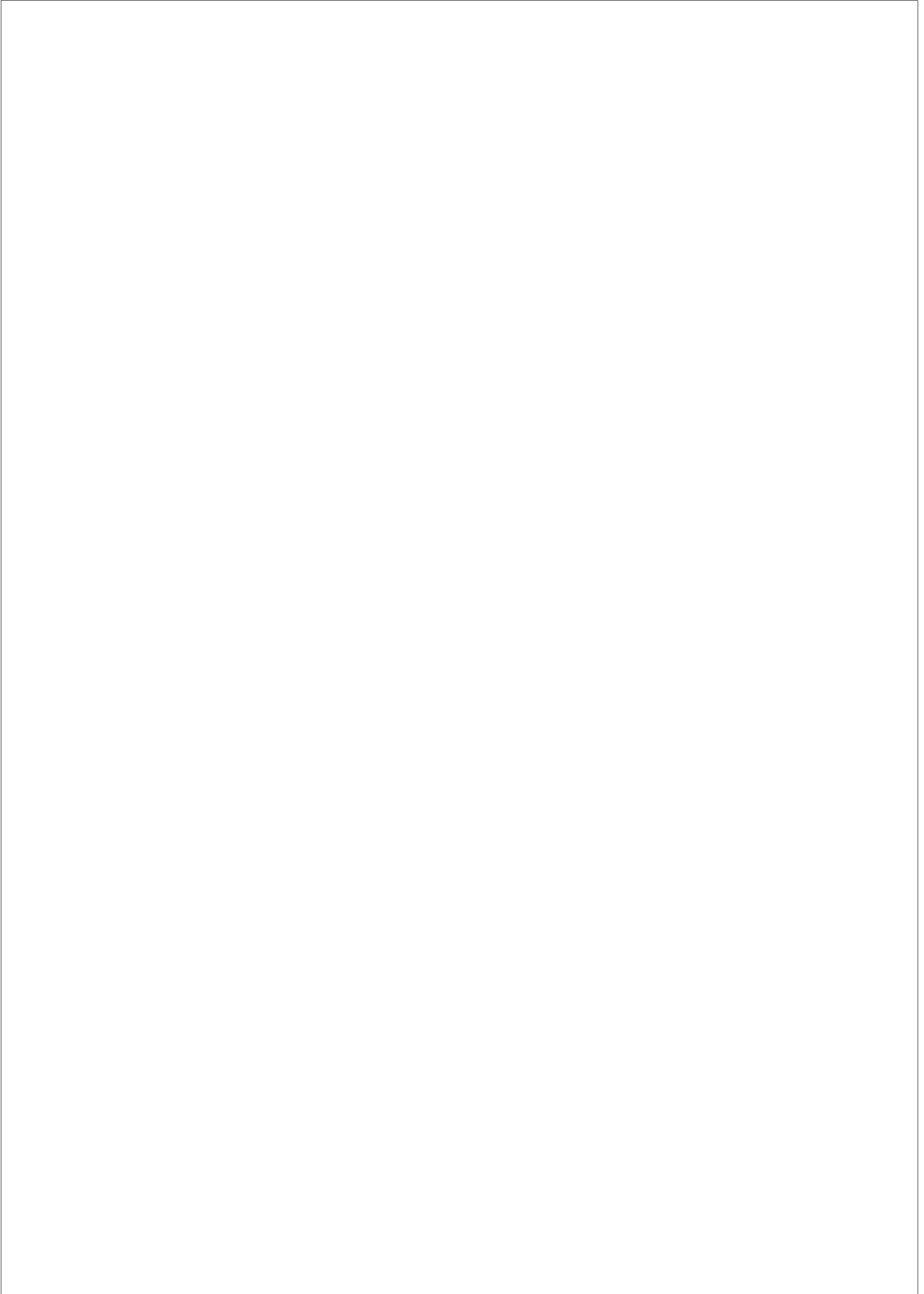
Calcitonin stimulates Ca²⁺ transport

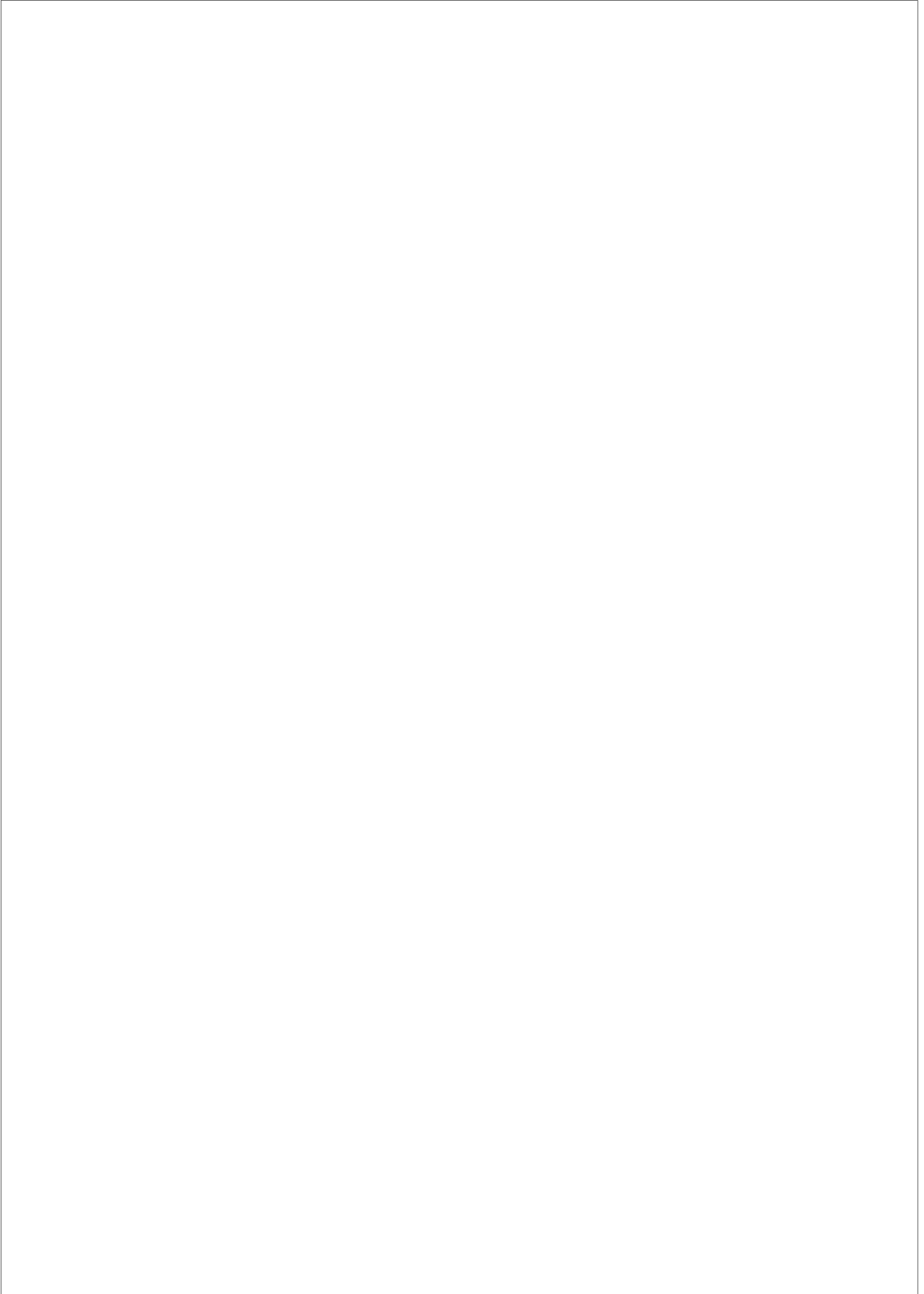
- 2005;85(1):373-422.
15. Hoenderop JG, Muller D, Van Der Kemp AW, Hartog A, Suzuki M, Ishibashi K, Imai M, Sweep F, Willems PH, Van Os CH, et al. Calcitriol controls the epithelial Ca²⁺ channel in kidney. *J Am Soc Nephrol*. 2001;12(7):1342-1349.
 16. Sexton PM, Adam WR, Moseley JM, Martin TJ, Mendelsohn FA. Localization and characterization of renal calcitonin receptors by in vitro autoradiography. *Kidney Int*. 1987;32(6):862-868.
 17. Elalouf JM, Roinel N, de Rouffignac C. Stimulation by human calcitonin of electrolyte transport in distal tubules of rat kidney. *Pflugers Arch*. 1983;399(2):111-118.
 18. van Abel M, Hoenderop JG, van der Kemp AW, Friedlaender MM, van Leeuwen JP, Bindels RJ. Coordinated control of renal Ca²⁺ transport proteins by parathyroid hormone. *Kidney Int*. 2005;68(4):1708-1721.
 19. de Groot T, Lee K, Langeslag M, Xi Q, Jalink K, Bindels RJ, Hoenderop JG. Parathyroid Hormone Activates TRPV5 via PKA-Dependent Phosphorylation. *J Am Soc Nephrol*. 2009;20(8):1693-1704
 20. Hoenderop JG, van Leeuwen JP, van der Eerden BC, Kersten FF, van der Kemp AW, Merillat AM, Waarsing JH, Rossier BC, Vallon V, Hummler E, et al. Renal Ca²⁺ wasting, hyperabsorption, and reduced bone thickness in mice lacking TRPV5. *J Clin Invest*. 2003;112(12):1906-1914.
 21. De Rouffignac C, Di Stefano A, Wittner M, Roinel N, Elalouf JM. Consequences of differential effects of ADH and other peptide hormones on thick ascending limb of mammalian kidney. *Am J Physiol*. 1991;260(6 Pt 2):R1023-1035.
 22. Ortiz PA. cAMP increases surface expression of NKCC2 in rat thick ascending limbs: role of VAMP. *Am J Physiol Renal Physiol*. 2006;290(3):F608-616.
 23. Lausson S, Tracqui P, Toubiana L, Milhaud G, Perault-Staub AM, Staub JF. Regulation of plasma Ca²⁺ and PO₃⁻ in calcitonin-infused rats. *Am J Physiol*. 1990;259(3 Pt 1):E370-377.
 24. Carney S, Thompson L. Acute effect of calcitonin on rat renal electrolyte transport. *Am J Physiol*. 1981;240(1):F12-16.
 25. Wada S, Udagawa N, Nagata N, Martin TJ, Findlay DM. Physiological levels of calcitonin regulate the mouse osteoclast calcitonin receptor by a protein kinase Alpha-mediated mechanism. *Endocrinology*. 1996;137(1):312-320.
 26. Hirsch PF, Baruch H. Is calcitonin an important physiological substance? *Endocrine*. 2003;21(3):201-208.
 27. Van Abel M, Hoenderop JG, Dardenne O, St Arnaud R, Van Os CH, Van Leeuwen HJ, Bindels RJ. 1,25-dihydroxyvitamin D₃-independent stimulatory effect of estrogen on the expression of ECaC1 in the kidney. *J Am Soc Nephrol*. 2002;13(8):2102-2109.
 28. van Abel M, Hoenderop JG, van der Kemp AW, van Leeuwen JP, Bindels RJ. Regulation

Chapter 5

of the epithelial Ca^{2+} channels in small intestine as studied by quantitative mRNA detection. *Am J Physiol Gastrointest Liver Physiol.* 2003;285(1):G78-85.

29. Van Baal J, Yu A, Hartog A, Fransen JA, Willems PH, Lytton J, Bindels RJ. Localization and regulation by vitamin D of Ca^{2+} transport proteins in rabbit cortical collecting system. *Am J Physiol.* 1996;271(5 Pt 2):F985-993.





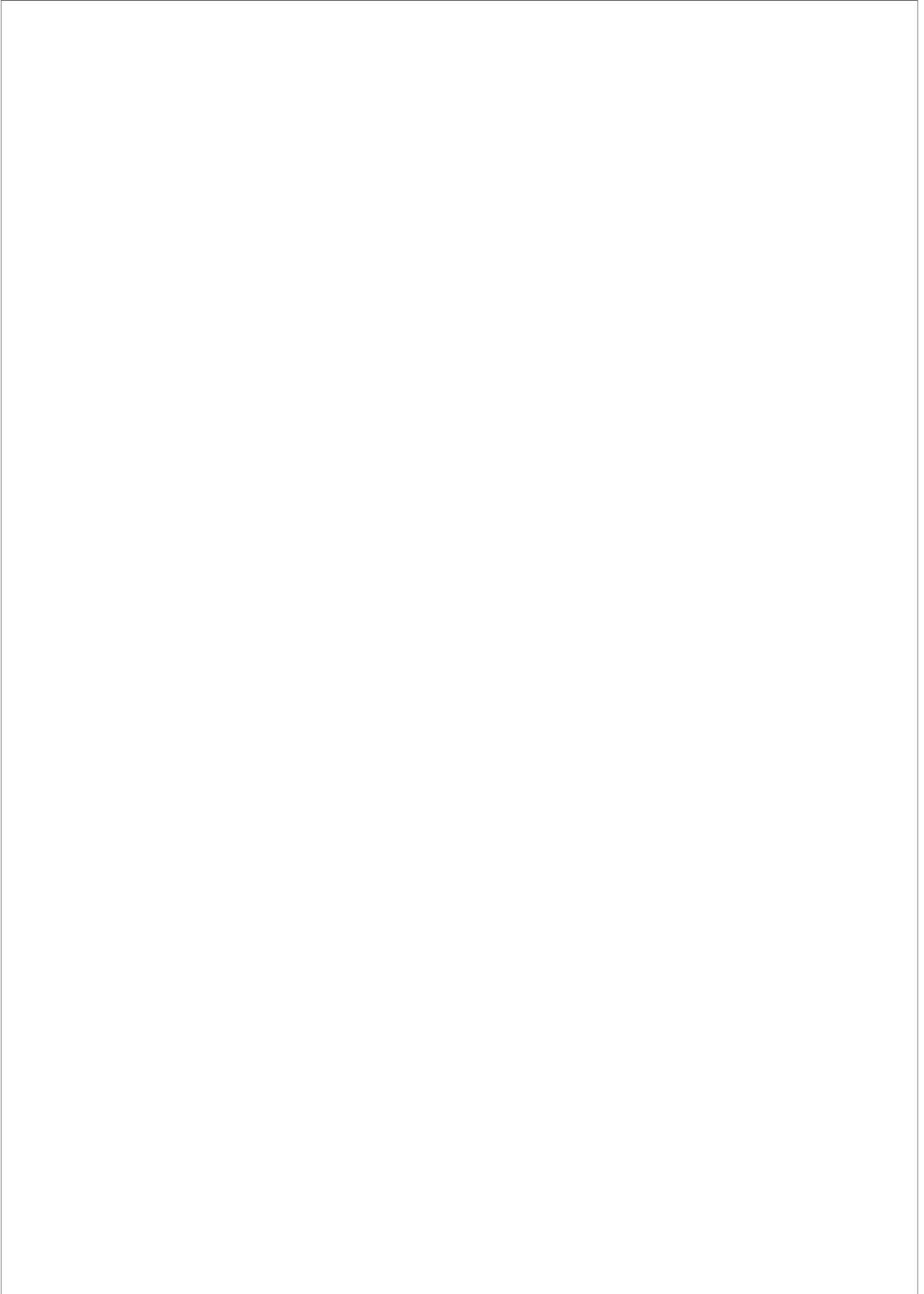
CHAPTER 6

Tissue transglutaminase inhibits TRPV5-dependent Ca²⁺ transport in a N-glycosylation-dependent manner

**Sandor Boros¹, Henrik Dimke¹, Qi Xi¹, AnneMiete W. van der Kemp¹, Sjoerd Verkaart¹,
Kyupil Lee¹, René J. Bindels¹, and Joost G. Hoenderop¹.**

¹Department of Physiology, Radboud University Nijmegen Medical Centre, the Netherlands.

Journal of the American Society of Nephrology, submitted 2010



tTG inhibits the activity of TRPV5

Abstract

Tissue transglutaminase (tTG) is a multifunctional Ca^{2+} -dependent enzyme, catalyzing the covalent crosslinking of proteins. Recent studies have shown that the transient receptor potential vanilloid (TRPV) family of cation channels can contribute to the regulation of TG activities in keratinocytes and hence skin barrier formation. In the kidney, where active transcellular Ca^{2+} transport via TRPV5 predominates, the potential effect of tTG remains untested. TRPV5 is regulated by a multitude of factors, many secreted into the urine, acting from the extracellular side. We detected tTG in mouse urine and in the apical medium of polarized cultures of rabbit connecting tubule and cortical collecting duct (CNT/CCD) cells. Importantly, extracellular application of tTG significantly reduced TRPV5 activity in human embryonic kidney (HEK293) cells transiently expressing the channel. Similar strong inhibition of transepithelial Ca^{2+} transport was observed after apical application of purified tTG to polarized rabbit CNT/CCD cells. tTG promoted the aggregation of the plasma membrane-associated fraction of TRPV5. Using (whole cell) patch clamp, we observed a clear reduction in the pore diameter after tTG treatment, suggesting distinct structural changes in TRPV5 upon crosslinking by tTG. As N-linked glycosylation of TRPV5 is a key step in regulating channel function, we determined the effect of tTG in the N-glycosylation-deficient TRPV5 mutant. In the absence of N-linked glycosylation, the TRPV5 channel was insensitive to tTG treatment. Taken together, these observations imply that tTG is a novel extracellular enzyme inhibiting the activity of TRPV5 via covalent crosslinking. The inhibition of TRPV5 occurs in an N-glycosylation-dependent manner, signifying a common final pathway by which different extracellular factors regulate the activity of the channel.

Introduction

Maintenance of the systemic Ca^{2+} concentration is essential for many physiological

Chapter 6

processes, ranging from enzyme activation to bone mineralization. As such, the kidney plays a key role in stabilizing serum Ca^{2+} , by changing the urinary excretion of Ca^{2+} in response to excess or depletion of the ion (1-3). In the kidney, most of the Ca^{2+} is reabsorbed via a passive paracellular pathway along the proximal tubule and the thick ascending loop of Henle (3). Approximately 10% of the Ca^{2+} load re-enters the bloodstream via an active transcellular transport process in the distal nephron (3, 4). The transient receptor potential vanilloid type 5 (TRPV5) cation channel facilitates the apical uptake of Ca^{2+} in these segments (5). In rabbit, TRPV5 is expressed predominantly in the collecting tubule (CNT), while in other species, such as mouse and rat, substantial expression of the channel is also observed in the distal convoluted tubule (DCT) (4, 6). Ablation of TRPV5 in mice (TRPV5^{-/-}) impairs transcellular Ca^{2+} reabsorption, resulting in robust hypercalciuria (7) and compensatory vitamin D-dependent hyperabsorption (7).

TRPV5 has unique electrophysiological characteristics, including the constitutive inward rectifying activity at low intracellular Ca^{2+} concentrations and physiological membrane potentials, Ca^{2+} -dependent inactivation and selectivity for Ca^{2+} (8). Monomers of TRPV5 associate into functional tetramers by facing each other with their pore-forming regions (9). Furthermore, a single conserved N-glycosylation site at an asparagine-358 (N358), harbored in the first extracellular loop is another important structural feature of TRPV5. Native TRPV5 has been shown to undergo N-glycosylation, resulting in high mannose and complex-glycosylated proteins (9). The activity of TRPV5 is controlled at multiple levels by an array of different factors, including calciotropic hormones (e.g. 1,25-dihydroxyvitamin- D_3) and extracellular factors (e.g. the glycosidase klotho) (10-12). Klotho, as an extracellular glycosidase (10, 13, 14), hydrolyzes oligosaccharide chains from the complex N-glycan of TRPV5. This extracellular modification results in delayed retrieval of the Ca^{2+} channel from the apical plasma membrane and subsequently increases Ca^{2+} transport (10, 13). The stimulatory effect of klotho is entirely dependent of the N-glycosylation of TRPV5, suggesting

tTG inhibits the activity of TRPV5

that the N-glycosylation status of TRPV5 is crucial for this type of extracellular regulation (10, 13).

Tissue transglutaminase (tTG, also known as TGase2) is a multifunctional protein catalyzing the Ca^{2+} -dependent covalent crosslinking of specific lysine (Lys) and glutamine (Gln) residues of substrate proteins (15, 16). Interestingly, several Ca^{2+} -binding proteins are known substrates of tTG. Calbindin- $\text{D}_{28\text{K}}$, an intracellular protein involved in Ca^{2+} binding playing a key role in transcellular Ca^{2+} transport, has been shown to be a substrate of tTG (17, 18). Furthermore, several members of the family of S100A EF-hand proteins are also substrates of tTG (19, 20). This includes S100A10, which is involved in forward trafficking of TRPV5 to the plasma membrane, (20, 21).

A recent elegant study by Cheng *et al.* showed that TRPV3, another member of the TRPV family, in part contributes to epidermal barrier function by affecting the activity of tTG (22). This is likely to occur via increased TRPV3-dependent Ca^{2+} influx and subsequent Ca^{2+} dependent activation of the enzyme. In addition to these observations, TGase1 expression has also been shown to be regulated by TRPV6 during Ca^{2+} -induced differentiation of keratinocytes (23). Transporters in the renal epithelium can be directly affected by extracellular factors found in the urine, secreted by the cells themselves or filtered by the glomerulus from the blood, constituting a unique environment. tTG is found in the intracellular compartment, but the enzyme is also secreted, indicating that in this epithelia, the enzyme could act from the urinary side. In terms of TRPV5-dependent transport, such a mechanism could suggest alternative mechanism of regulation, in comparison to what is observed in e.g. the skin barrier formation. Our experiments describe the identification of tTG as a novel molecular inhibitor of TRPV5. Furthermore, this study shows that the kidney secretes tTG into the pro-urine where it covalently crosslinks TRPV5 from the extracellular compartment and, thereby reducing the pore size of the channel in an N-glycosylation-dependent manner.

Chapter 6

Results

tTG is secreted into the pro-urine and into the apical medium of CNT/CCD cells

24-hour urine samples from wild-type mice were desalted, concentrated and the total amounts were subsequently analyzed for tTG expression by SDS-PAGE followed by tTG Western blotting. A band with a molecular size slightly above 75 kDa was observed in the urine samples (Fig. 1A), corresponding to the known 75-78 kDa size of tTG. Since tTG was detected in the 24-hour urine of mice, we next analyzed the expression levels of tTG in the CNT/CCD region. To this end, polarized primary cultures of rabbit CNT/CCD were used. Western blot analysis, wherein β -actin was used as loading control, revealed that polarized CNT/CCD cells abundantly express tTG (Figure 1B, upper panel) (n=3). In the apical conditioned media of primary CNT/CCD cells a significant amount of tTG could be detected (Figure 1C upper panel), In addition, tTG was also abundantly present in the basolateral compartment (Figure 1C lower panel).

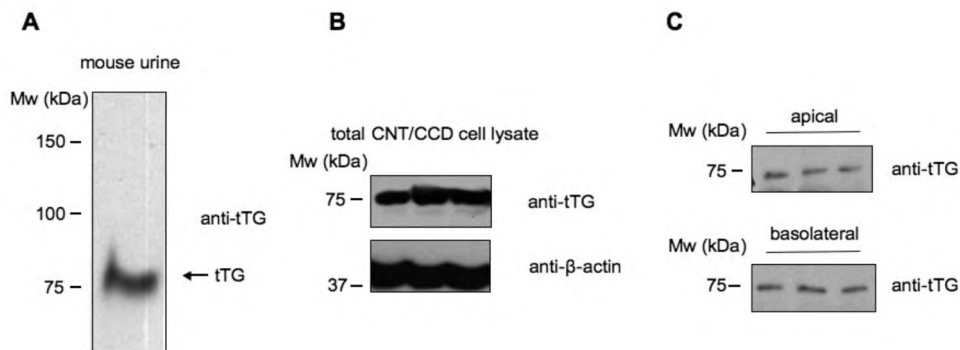


Figure 1. tTG is secreted into mouse urine and into the apical media of rabbit primary CNT/CCD cells. (A) Mice (n=3) were housed in metabolic cages and 24 hour urine samples were collected. Samples were concentrated and subsequently analyzed for tTG expression by SDS-PAGE followed by anti tTG Western blotting. (B) Isolated rabbit primary CNT/CCD cells were allowed to polarize on filter supports. Polarized monolayers (n=3) were probed for tTG expression by SDS-PAGE and subsequent immunoblot with anti-tTG (upper panel), and anti- β -actin antibodies (lower panels) respectively. (C) Apical and basolateral media from polarized CNT/CCD cells were collected and concentrated, and subsequently analyzed for tTG secretion.

tTG inhibits the activity of TRPV5

tTG inhibits the activity of TRPV5

Next, we investigated whether tTG can affect the activity of TRPV5. To this end, HEK293 cells transiently over-expressing the channel were treated with tTG (1 $\mu\text{g/ml}$), for 6 hours and subjected to patch clamp (whole cell configuration) analysis (Figure 2A). Heterologous overexpression of TRPV5 yielded a large, approximately 1500 pA/pF sodium current density (Figure 2A). Incubation with tTG for 6 hours resulted in a significant, 50 % reduction of the current density (Figure 2A). Additionally, the tTG inhibitor cadaverine (150 μM) prevented the tTG-mediated inhibition of TRPV5 (Figure 2A and 2B), without affecting the activity of TRPV5 (Figure 2A and 2B).

To address whether tTG reduces the number of channels at the plasma membrane, the action of tTG on TRPV5 was assessed by cell surface biotinylation studies. TRPV5, with molecular masses between approximately 70 and 85, representing the core and complex glycosylated monomers of the channel were detected in the plasma membrane fraction (Figure 2C). Compared to the control (-tTG), a decrease in the amount of TRPV5 monomers was observed after tTG treatment (Figure 2C). More importantly, after incubation with tTG, TRPV5 oligomers with a molecular mass of ~ 250 kDa were observed (Figure 2C).

The inhibitory effect of tTG was further investigated by transcellular Ca^{2+} transport assays in polarized rabbit primary CNT/CCD cell monolayers. The forskolin-stimulated transcellular Ca^{2+} transport was significantly reduced by tTG and this inhibitory effect of the enzyme could be prevented by the tTG blocker cadaverine (Figure 2D). Additionally, incubating the cells with cadaverine did not result in any detectable changes in transcellular Ca^{2+} transport (Figure 2D).

tTG decreases the pore diameter of TRPV5

To estimate whether tTG-induced aggregation of TRPV5 can affect the pore of the channel, the pore diameter was determined both in the absence and the presence of the enzyme. To

Chapter 6

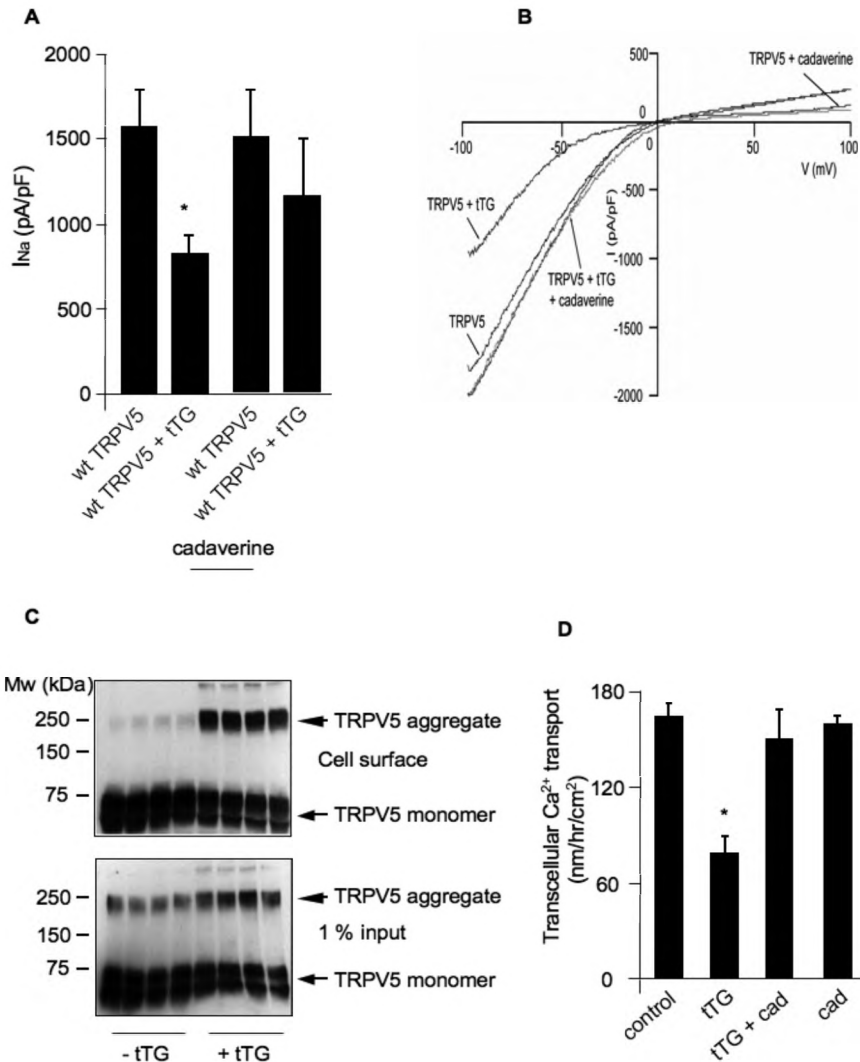


Figure 2. tTG inhibits TRPV5-mediated currents and transcellular Ca^{2+} transport in primary CNT/CCD cells. (A) Na^+ I/V relations were measured from TRPV5-transfected HEK293 cells. The cells were subjected to 6 hour tTG treatment (1 μ g/ml) in the presence and absence of cadaverine (150 μ M) before the current measurements. Data are shown as mean \pm S.E.M. * indicates significant difference from the cells expressing TRPV5 (n = 15; p < 0.05). (B) Representative Na^+ I/V relations of TRPV5 treated with transglutaminase in the absence or presence of cadaverine. (C) HEK293 cells were transiently transfected with pCINeo-HA-TRPV5/IRES-GFP and treated for 6 hours with 1 μ g/ml tTG. After treatment cells were subjected to cell surface biotinylation, followed by neutravidin pull-down. Lysates were separated on SDS-PAGE and blots were probed with an anti-HA antibody. (D) Polarized rabbit primary CNT/CCD cells were treated for 6 hours with 1 μ g/ml apically administered tTG and transport was measured as described previously (23). Data are shown as mean \pm S.E.M. * indicates significant difference from the control situation (n = 15; p < 0.05).

tTG inhibits the activity of TRPV5

this end, the permeability ratios of currents carried by organic monovalent cations of increasing size relative to Na^+ current were measured. When Na^+ was used as the sole charge carrier, the current reverted close to 0 mV with a clearly inward-rectifying shape (Figure 3A). Once all Na^+ ions from the extracellular solution were substituted by methyl-ammonium or its di-, tri- and tetra methyl derivatives (MA^+ , DMA^+ , TriMA^+ , TetMA^+) and finally by the larger organic cation *N*-methyl-D-glutamine (NMDG^+). To a lesser extent, these cations, were also able to permeate TRPV5, and the recorded currents were directly proportional to the size of each cation (Figure 3B). More importantly, incubation with tTG resulted in significantly smaller currents in the case of all cations (Figure 3B).

The permeability ratios, relative to Na^+ (P_x/P_{Na}), were calculated from the recorded bi-ionic reversal potentials for all five cations (MA^+ , DMA^+ , TriMA^+ , TetMA^+ and NMDG^+) for both untreated and tTG-treated HEK293 cells expressing TRPV5, and subsequently plotted against the estimated diameter of each cation. In the control situation the pore diameter for TRPV5 was calculated to be 6.44 ± 0.01 Å. Treatment with tTG resulted in a decreased pore size as the diameter was calculated to be 5.79 ± 0.02 Å (Figure 3C).

N-glycosylation of TRPV5 is important for tTG-mediated inhibition

HEK293 cells expressing the N-glycosylation-deficient mutant form of the channel (HA-TRPV5-N358Q) were treated with tTG and subjected to patch clamp and cell surface biotinylation analyses. Patch clamp recordings showed identical Na^+ currents for the untreated wild type and the mutant form of TRPV5 (Figure 4A). However, tTG incubation reduced the activity of the wild type channel, but not of TRPV5-N358Q (Figure 4A). Cell surface labeling of HEK293 cells expressing either the wild type TRPV5-N358Q showed abundant expression of both wild type and mutant TRPV5 at the plasma membrane (Figure 5B, upper panel). Treatment with tTG caused the aggregation of TRPV5 at the plasma membrane and concomitantly decreased the amount of wild type TRPV5 monomers (Figure

Chapter 6

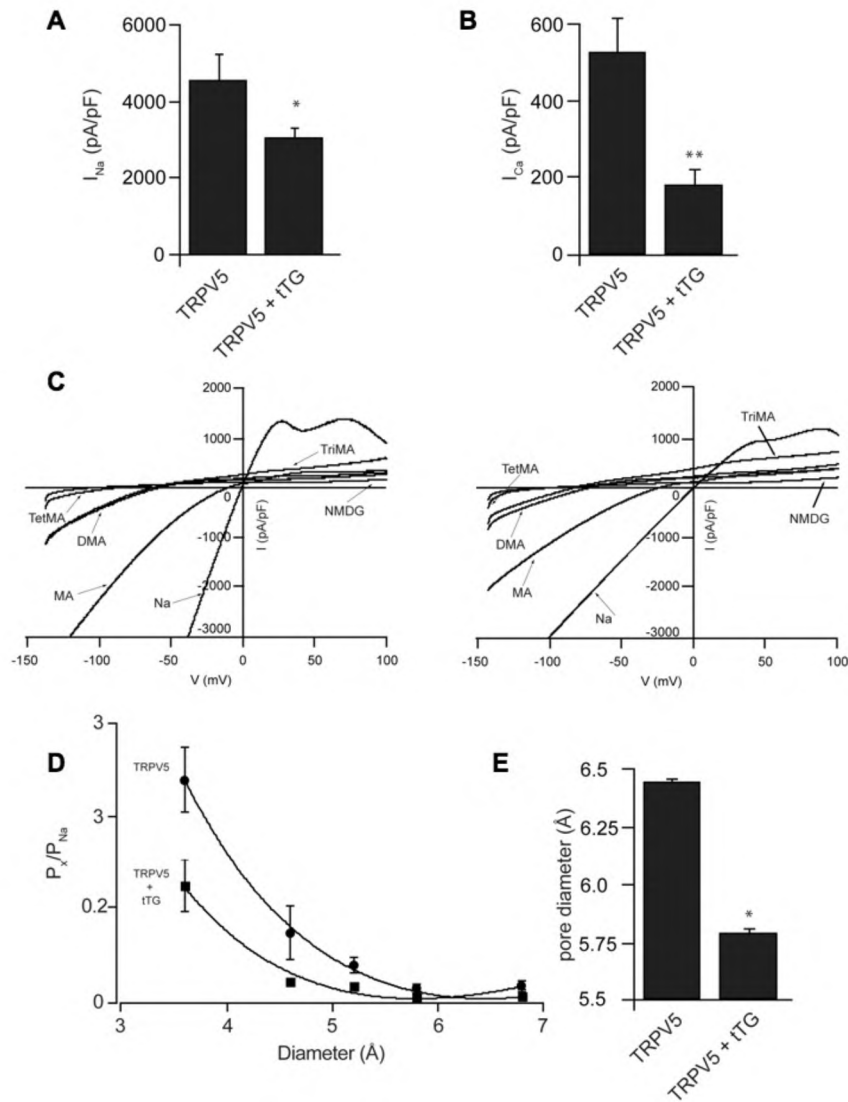
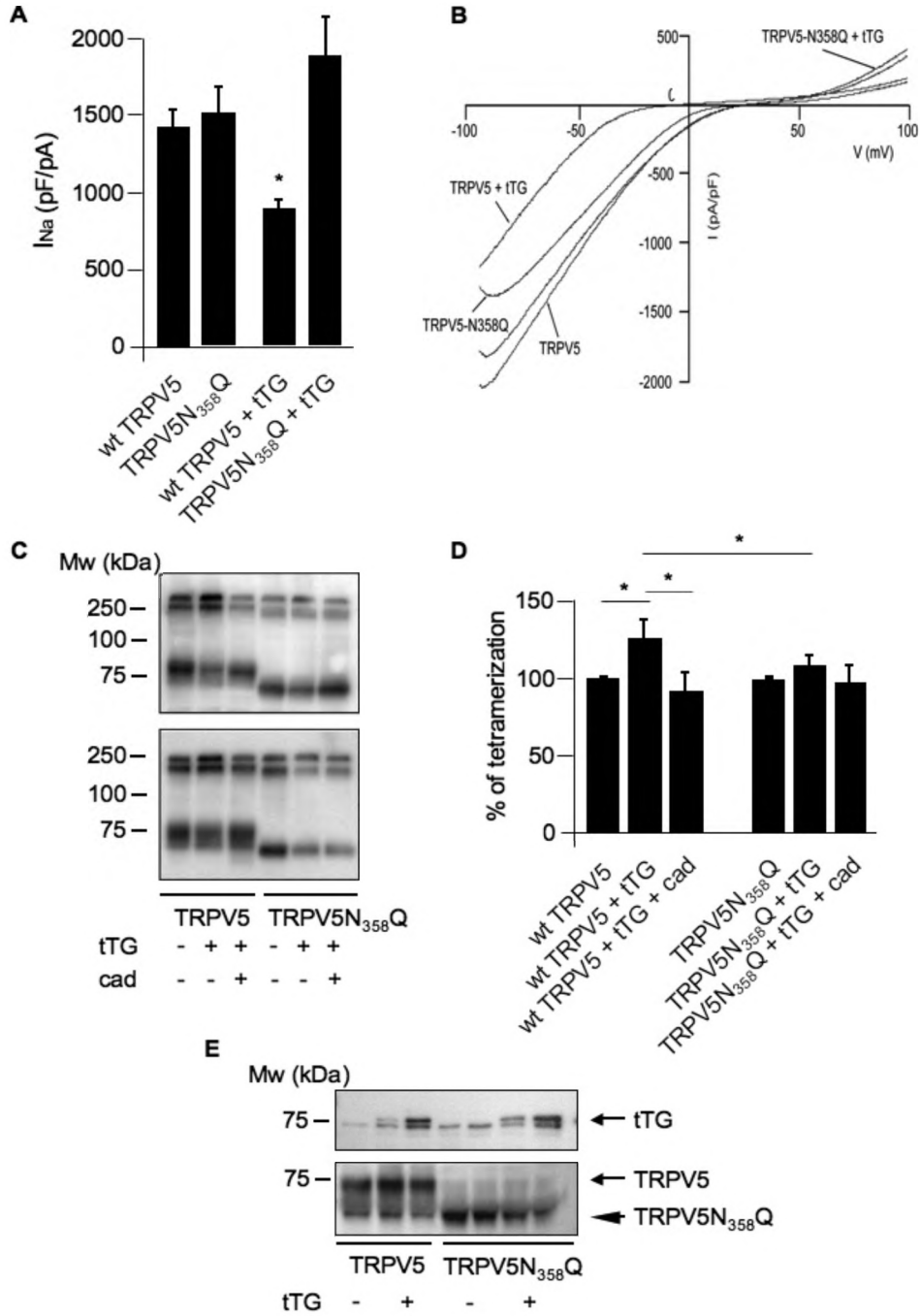


Figure 3. tTG decreases the pore diameter of TRPV5. (A) Na^+ traces and (B) Ca^{2+} traces. (C) The permeability ratios of currents carried by organic monovalent cations of increasing size relative to Na^+ current were measured in the absence and presence of tTG. The permeability of mono-, di-, tri- and tetra-methyl ammonium derivatives (MA^+ , DMA^+ , $TriMA^+$, $TetMA^+$) and of N-methyl-D-glutamine (NMDG) were measured using solutions in which Na^+ was substituted by the respective cations, and finally by the larger organic cation (NMDG $^+$). (D) Calculated relative permeability ratios of untreated and tTG treated TRPV5. (P_x/P_{Na}), were calculated from the recorded biionic reversal potentials for all five cations (MA^+ , DMA^+ , $TriMA^+$, $TetMA^+$ and NMDG $^+$) for both untreated and tTG-treated TRPV5 and subsequently plotted against the estimated diameter of each cation. For curve-fitting, the points from the graph plotting permeability ratios of the different organic cations (X) versus the estimated diameters, the excluded volume considering friction of the permeating ion Eq. $P_x/P_{Na} = k(1-a/d)^2/a$ was used where a is the organic cation diameter, k a constant factor and d is the minimal pore diameter. (E) Histogram representing change in pore diameter.

tTG inhibits the activity of TRPV5



Chapter 6

Figure 4. N-glycosylation-deficient mutant TRPV5 is insensitive to tTG-mediated inhibition. (A) Na^+ currents were measured from wild type TRPV5 and N-glycosylation-deficient TRPV5-N358Q mutant channels. The cells were subjected to 6 hour tTG treatment (1 $\mu\text{g}/\text{ml}$) before the current measurement. Data are shown as mean \pm S.E.M. * indicates significant difference from the cells expressing either wild type or N-glycosylation-deficient mutant TRPV5 (n =11; p < 0.05). (B) Representative Na^+ I/V relations of wild type TRPV5 and TRPV5N358Q in the absence or presence of purified transglutaminase. (C) Cell surface biotinylation of HEK293 cells transiently expressing HA-TRPV5 or HA-TRPV5-N358Q, after for 6 hours of tTG treatment (1 $\mu\text{g}/\text{ml}$) tTG. (D) Semi-quantitative analysis of C. (E) Wild type TRPV5 and TRPV5N358Q bind tTG with equal efficiency. HA-tagged wild type TRPV5 or TRPV5-N358Q was immunoprecipitated with HA-antibody from transiently transfected HEK 293 cells. The precipitated fractions were incubated over night at 4 °C with 1 $\mu\text{g}/\text{ml}$ purified tTG in EDTA-containing Ca^{2+} free buffer to prevent any enzymatic activity of tTG. The beads with TRPV5 and tTG were successively washed and subjected to SDS-PAGE followed by anti-tTG or anti-TRPV5 immunoblot, respectively.

4B, upper panel). However, this aggregation could not be observed in case of the mutant channel (Figure 4B, upper panel). Additionally, incubation with tTG did not alter the total expression of the wild type or the mutant form of TRPV5 (Figure 4B).

Finally, we investigated the binding capacity of tTG to wild type and the N-glycosylation deficient mutant Ca channels. The immunoprecipitated wild type and mutant TRPV5 were incubated with or without tTG at 4 °C in the absence of Ca^{2+} to reduce the enzymatic activity of tTG. These immuno-precipitation experiments revealed that tTG binds to both wild type and the mutant form of TRPV5 with equal affinity (Figure 4C).

Discussion

Active transcellular Ca^{2+} transport in the kidney takes place exclusively in the DCT/CNT segments of the nephron, where the epithelial Ca^{2+} channel TRPV5 controls the Ca^{2+} entry. In this study we identified tTG as a novel inhibitor of TRPV5 activity, acting from the extracellular side in a N-glycosylation-dependent manner. This conclusion is based on the following observations: 1) tTG is found in the urine in mice, in line with the expression and secretion of the enzyme in polarized primary CNT/CCD cells. 2) tTG decreases the activity of TRPV5 in transiently transfected HEK293 cells and inhibits transcellular Ca^{2+} transport in polarized primary CNT/CCD cells; 3) crosslinking of TRPV5 by tTG decreases the pore size of the channel; 4) the inhibitory effect of tTG depends on the N-glycosylation state of TRPV5

tTG inhibits the activity of TRPV5

as the N-glycosylation-deficient mutant is not susceptible to tTG-catalyzed modifications.

Increased expression and activity of tTG have been previously observed in renal disorders such as diabetic nephropathy or chronic kidney disease (24-29). In these diseases, tTG activity has been associated with tissue fibrosis and scar formation, taking place in the extracellular matrix (24, 30). However, whether tTG is secreted into the urine during these conditions, has not been tested. We established the presence of tTG in the urine of mice, which indicates the presence of tTG in the urine during normal physiological conditions. The fact that primary cultures of polarized rabbit CNT/CCD cells also secrete a large fraction of endogenously expressed tTG into the apical medium further corroborates this finding. The presence of tTG has been reported previously in the DCT region and in other nephron segments as well (24, 26, 30). Tubular secretion is therefore likely to contribute significantly to the amount of tTG found in the urine. These observations imply that tTG could function as a novel urinary factor, involved in regulating Ca^{2+} reabsorption in the distal nephron.

Patch clamp recordings of TRPV5 and transcellular transport assays in primary CNT/CCD cells showed a significant inhibitory effect of tTG on Ca^{2+} transport. Earlier studies have reported that tTG had the ability to modify the activity of the large conductance Ca^{2+} -activated K^+ (Maxi-K) channel (31). Using the non-hydrolyzable GTP analogue $\text{GTP}\gamma\text{S}$, these studies showed that the $\text{GTP}\gamma\text{S}$ -stimulated channel activity was decreased to control levels when cells were treated with an antibody against tTG (31). Such a G-protein like effect of tTG on TRPV5 is unlikely, as cadaverine, the inhibitor of the crosslinking activity of the enzyme, abolishes the effect of tTG. Next to the functional assays, cell surface biotinylation studies revealed the formation of SDS-resistant, probably covalently crosslinked TRPV5 aggregates in the plasma membrane upon tTG incubation. tTG is known to be externalized into the extracellular space where it crosslinks and therefore stabilizes the heteromeric assemblies of several matrix and basolateral membrane proteins (32-36). In case of the tTG substrate small heat shock proteins (αB -crystallin, Hsp27, Hsp20 and HspB2), crosslinking

Chapter 6

between different small heat shock proteins has been demonstrated to be more efficient when they interact with each other in the same macromolecular assembly (37). These observations suggested that tTG-substrate proteins in close proximity to each other are more prone to crosslinking than those of existing in different complexes. The functional TRPV5 exists in a homotetrameric form, as four monomers need to associate into operational tetramers prior to plasma membrane insertion (9). Furthermore, it also harbors several glutamine and lysine residues facing the extracellular environment. Since the extracellular environment as well as the pro-urine contains sufficient amount of Ca^{2+} for the activation of tTG, the tTG-mediated aggregation of TRPV5 monomers could take place from the extracellular side.

tTG did not change the protein stability, membrane expression or trafficking/recycling properties of TRPV5. Instead, we found that extracellular addition of tTG results in a decreased pore size of TRPV5. TRPV5 harbors several glutamines and two lysines in the first extracellular loop, which are the potential substrate sites for tTG. Crosslinking these sites could introduce extra rigidity or tension into the structure of the membrane-inserted TRPV5 in such a way that it results in pore deformation and subsequent reduction in ion permeability. Previously, acidification of both the intra- and extracellular environment has been shown to decrease the pore diameter of TRPV5 intracellular pH (38). Our observations suggest that not only pH changes, but also tTG could inhibit the activity of TRPV5 by reducing its pore size.

N-glycosylation of TRPV5 is crucial for the extracellular regulation of the channel by klotho (10, 13). Surprisingly, tTG had no inhibitory effect on TRPV5-N358Q, suggesting that the presence of the sugar tree is critical for tTG action. Negatively charged glycosaminoglycans such as heparin are known to bind tTG (39-41). We speculated that the sialic acid containing, and therefore negatively charged N-glycan of TRPV5 may bind tTG, providing better accessibility to the substrate sites located in the vicinity of the N-glycan.

tTG inhibits the activity of TRPV5

However, co-immunoprecipitation experiments showed that tTG equally binds to both the wild type and to the N-glycosylation-deficient TRPV5 mutant. Because of the equal binding efficiency, the substrate site exposure is more likely to depend on the N-glycosylation status of TRPV5. Klotho (as well as other glycosidases) can hydrolyze sugar residues from the N-glycan of TRPV5 and thereby increase the activity of the channel (10, 13, 14). The fact that these different enzymes require intact N-glycosylation of TRPV5 for their actions could imply a central role for the N-glycan in the extracellular regulation of the channel. Thus, a cross-talk between the tTG-mediated inhibition and the activating mechanism by klotho could also be speculated. Modification of the N-glycan by klotho might safeguard TRPV5 from the tTG-mediated inhibition. However, further experiments should clarify the presence of such cross-talk between klotho and tTG.

Taken together, our observations suggest that the apically secreted tTG functions as an inhibitor of TRPV5 and thereby contributes to the regulation of body Ca^{2+} homeostasis. Currently, it remains unclear whether an increased urinary tTG concentration is observed in conditions related to defective Ca^{2+} handling. One could envision several pathological conditions in which tTG reaches higher urinary concentrations, due to increased tissue damage or secretion of the enzyme. As such, rats with experimentally-induced diabetes and diabetic nephropathy have increased renal tTG expression and activity resulting in abnormal extracellular crosslinking.

Here, we delineate a potential molecular mechanism by which tTG inhibits TRPV5 channel activity by changing the pore diameter. The change is functionally coupled with crosslinking of the channel and seems to occur in a N-glycosylation dependent manner. Further studies are needed to establish the physiological role of tTG in regulating TRPV5-dependent Ca^{2+} transport.

Chapter 6

Materials and methods

DNA constructs

The pCINeo/IRES-GFP plasmid encoding HA-TRPV5 was generated as described previously (21). HA-TRPV5-N358Q was obtained by *in vitro* mutagenesis of HA-TRPV5-pCINeo/IRES-GFP cDNA according to the manufacturer's instructions (Stratagene, La Jolla, CA, USA) (10). All constructs were verified by DNA sequence analysis.

Cell lines and transfections

Human embryonic kidney (HEK293) cells were cultured in Dulbecco's modified essential medium (DMEM) supplemented with 10 % v/v fetal calf serum and 2 mM L-glutamine. For cell surface biotinylation experiments, cells were transiently transfected in petri dishes, using polyethylene-imine (PEI).

Collection and concentration of pre-conditioned culture medium

CNT/CCD cells were isolated from New Zealand White rabbits as described previously (42) and grown to confluence on 0.33 cm² permeable filter supports (Corning-Costar, Cambridge, MA, USA). Apical and basolateral media were collected after seeding the cells on permeable supports. All collected media were concentrated 3 times (Millipore), and salts and proteins < 30 kDa were removed by using centriprep ultracel YM-30 columns (Millipore corporation, Bedford, MA, USA) as described (10).

Immunoblotting, and protein concentration determination

TRPV5 protein expression was determined by SDS-PAGE followed by immunoblotting, using anti-HA (Cell Signaling, Danvers, USA) and peroxidase-labeled goat anti-guinea pig IgG (Sigma-Aldrich, St. Louis, MO, USA) antibodies. Protein concentration was measured by using the bicinchoninic acid protein assay kit (Thermo Scientific, Rockford, IL, USA),

tTG inhibits the activity of TRPV5

according to the manufacturer's manual.

Plasma membrane biotinylation

HEK293 cells were transfected with HA-TRPV5 or HA-TRPV5-N358Q in pCINeo/IRES-GFP, or the empty vector (mock). One day after transfection, cells were re-seeded on poly-L-lysine-coated (0.1 mg/ml) culture dishes and incubated with tTG (1 µg/ml, Sigma-Aldrich, St. Louis, MO, USA) for 6 hours at 37 °C, respectively. Subsequently, cells were biotinylated, and TRPV5 was precipitated from the cell lysates with neutravidin beads (Pierce, Etten-leur, The Netherlands) as described previously (10). Briefly, cells were collected from the plates and disrupted in 1 ml lysis buffer (1 % v/v Triton-X100, 150 mM NaCl, 5 mM EDTA, 50 mM Tris (pH 7.5 adjusted with HCl), PMSF 1 mM, leupeptin 5 µg/ml, aprotinin 5 µg/ml, pepstatin-A 1 µg/ml), immediately after biotinylation. Cells were subsequently washed with ice-cold PBS, and homogenized in 1 ml lysis buffer, followed by precipitation using neutravidin beads. TRPV5 protein expression at the cell surface and in total cell lysates was measured as described above.

Electrophysiology

Whole-cell currents were measured with an EPC-10 (HEKA electronic, Lambrecht, Germany) amplifier using Patch master V2.20 software. The borosilicate glass electrode resistance was between 2.5 and 4 MΩ. The ramp protocol for measuring the current-voltage (*I/V*) relationship of Na⁺ consisted of linear voltage ramps from -100 to +100 mV within 450 milliseconds repeated every 5 seconds. The step protocol for measuring the Ca²⁺ current consisted of a 10 seconds long voltage step applied from +70 to -100 mV. Current traces were sampled at 0.5 ms for the ramp and 2 ms for the step protocol. Current densities were calculated from the current at -80 mV during the ramp protocol. The standard extracellular solution contained 150 mM NaCl, 6 mM CsCl, 10 mM HEPES, 50 µM EDTA and 10 mM glucose, (pH 7.4 adjusted

Chapter 6

with NaOH) for divalent free Na^+ , and 10 mM CaCl_2 was supplemented for the Ca^{2+} measurement. The internal (pipette) solution contained 20 mM CsCl, 100 mM Cs-aspartate, 1 mM MgCl_2 , 10 mM BAPTA, 4 mM NaCl, 2 mM ATP and 10 mM HEPES (pH 7.2 adjusted with CsOH). Data was analyzed using Igor-pro software (WaveMetrics, Oswego, OR, USA).

Pore measurements

The standard pipette solution contained Tris-HCl buffered 150 mM NaCl, 10 mM EDTA and 10 mM HEPES (pH 7.2 adjusted with Tris-HCl) whereas the extracellular solution contained 150 mM NaCl and 10 mM HEPES (pH 7.4 adjusted with Tris-HCl) The relative permeabilities (P_X/P_{Na}) of mono-, di-, tri- and tetra-methyl ammonium derivatives and of N-methyl-D-glutamine chloride (NMDG) were measured using solutions in which Na^+ was substituted by the respective cations. Reversal potentials were calculated from the bi-ionic reversal potentials furthermore, all potentials were corrected for possible liquid junction potentials calculated according to Barry et al (43). In these permeation experiments, the standard pipette solution was used as intracellular solution. For the ammonium derivatives, the following compound diameters were used (in nm): 0.36, 0.46, 0.52, 0.58 and 0.68 for monomethylammonium (MA^+) dimethylammonium (DMA^+), trimethylammonium (TriMA^+), tetramethylammonium (TetMA^+) and for NMDG⁺ (all compounds obtained from Sigma), respectively. For curve-fitting, the points from the graph plotting permeability ratios of the different organic cations (X) versus the estimated diameters, the excluded volume considering friction of the permeating ion Eq. $P_X/P_{\text{Na}} = k(1-a/d)^2/a$ was used (43) where a is the organic cation diameter, k the constant factor and d is the minimal pore diameter.

Statistical analysis

In all experiments, the data were expressed as mean \pm S.E.M. Statistical significance ($p < 0.05$) was determined by analysis of variance (ANOVA) and a Bonferroni post-hoc test.

References

1. Hoenderop JG, Bindels RJ. Calcitropic and magnesiotropic TRP channels. *Physiology (Bethesda)*. 2008;23(32-40).
2. Suzuki Y, Landowski CP, Hediger MA. Mechanisms and regulation of epithelial Ca²⁺ absorption in health and disease. *Annu Rev Physiol*. 2008;70(257-271).
3. van de Graaf SF, Bindels RJ, Hoenderop JG. Physiology of epithelial Ca²⁺ and Mg²⁺ transport. *Rev Physiol Biochem Pharmacol*. 2007;158(77-160).
4. Hoenderop JG, Nilius B, Bindels RJ. Ca²⁺ absorption across epithelia. *Physiol Rev*. 2005;85(1):373-422.
5. Hoenderop JG, van der Kemp AW, Hartog A, van de Graaf SF, van Os CH, Willems PH, Bindels RJ. Molecular identification of the apical Ca²⁺ channel in 1, 25-dihydroxyvitamin D₃-responsive epithelia. *J Biol Chem*. 1999;274(13):8375-8378.
6. Loffing J, Loffing-Cueni D, Valderrabano V, Klausli L, Hebert SC, Rossier BC, Hoenderop JG, Bindels RJ, Kaissling B. Distribution of transcellular Ca²⁺ and Na⁺ transport pathways along mouse distal nephron. *Am J Physiol Renal Physiol*. 2001;281(6):F1021-1027.
7. Hoenderop JG, van Leeuwen JP, van der Eerden BC, Kersten FF, van der Kemp AW, Merillat AM, Waarsing JH, Rossier BC, Vallon V, Hummler E, et al. Renal Ca²⁺ wasting, hyperabsorption, and reduced bone thickness in mice lacking TRPV5. *J Clin Invest*. 2003;112(12):1906-1914.
8. Nilius B, Prenen J, Vennekens R, Hoenderop JG, Bindels RJ, Droogmans G. Modulation of the epithelial Ca²⁺ channel, ECaC, by intracellular Ca²⁺. *Cell Ca*. 2001;29(6):417-428.
9. Hoenderop JG, Voets T, Hoefs S, Weidema F, Prenen J, Nilius B, Bindels RJ. Homo- and heterotetrameric architecture of the epithelial Ca²⁺ channels TRPV5 and TRPV6. *Embo J*. 2003;22(4):776-785.
10. Chang Q, Hoefs S, van der Kemp AW, Topala CN, Bindels RJ, Hoenderop JG. The beta-glucuronidase klotho hydrolyzes and activates the TRPV5 channel. *Science*. 2005;310(5747):490-493.
11. Okano T, Tsugawa N, Morishita A, Kato S. Regulation of gene expression of epithelial Ca channels in intestine and kidney of mice by 1,25-dihydroxyvitamin D₃. *J Steroid Biochem Mol Biol*. 2004;89-90(1-5):335-338.
12. van de Graaf SF, Boullart I, Hoenderop JG, Bindels RJ. Regulation of the epithelial Ca²⁺ channels TRPV5 and TRPV6 by 1alpha,25-dihydroxy Vitamin D₃ and dietary Ca²⁺. *J Steroid Biochem Mol Biol*. 2004;89-90(1-5):303-308.
13. Cha SK, Ortega B, Kurosu H, Rosenblatt KP, Kuro OM, Huang CL. Removal of sialic acid involving Klotho causes cell-surface retention of TRPV5 channel via binding to galectin-1. *Proc Natl Acad Sci U S A*. 2008;105(28):9805-9810.

Chapter 6

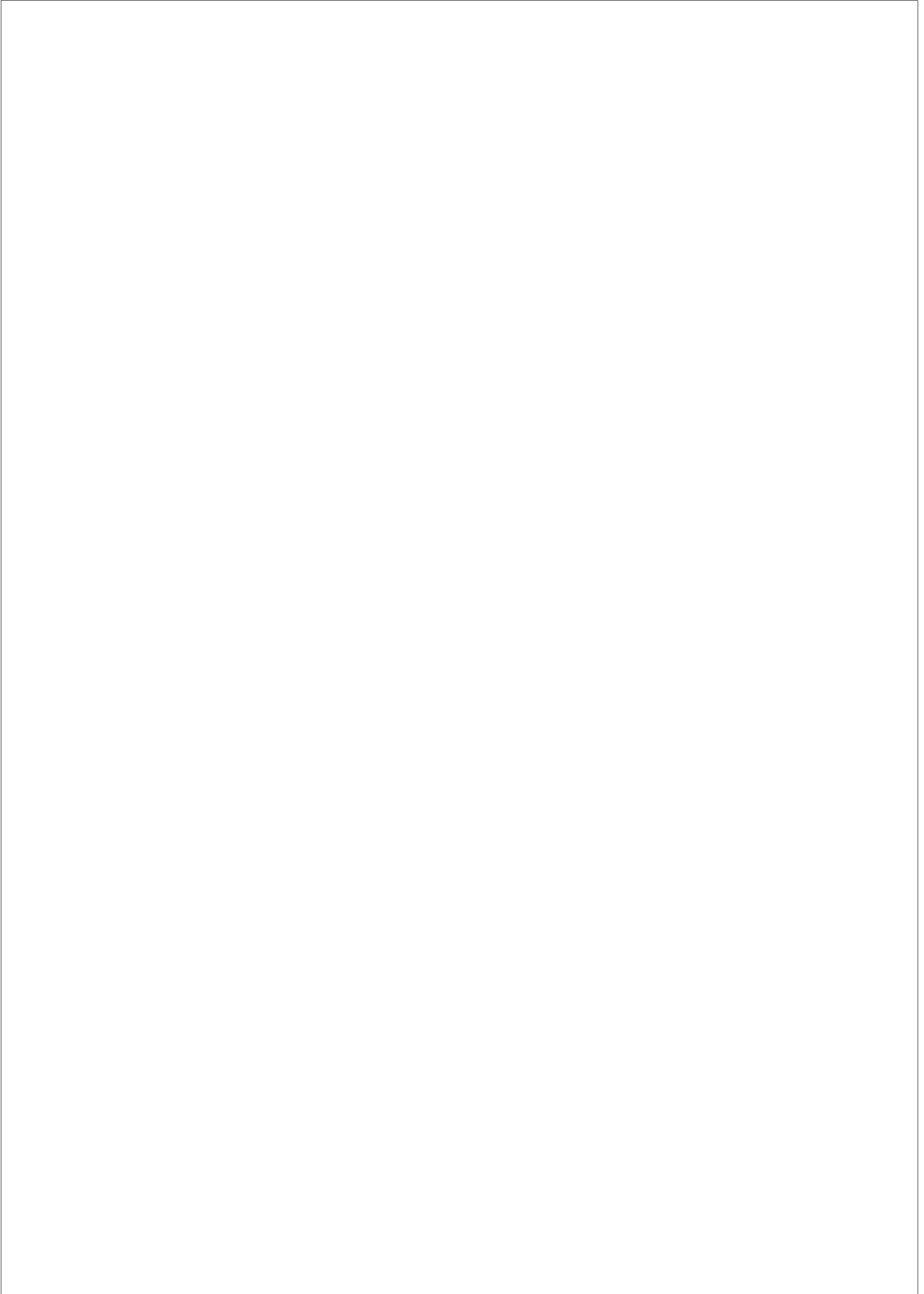
14. Lu P, Boros S, Chang Q, Bindels RJ, Hoenderop JG. The β -glucuronidase klotho exclusively activates the epithelial Ca^{2+} channels TRPV5 and TRPV6. *Nephrol Dial Transplant*. 2008.
15. Fesus L, Piacentini M. Transglutaminase 2: an enigmatic enzyme with diverse functions. *Trends Biochem Sci*. 2002;27(10):534-539.
16. Lorand L, Graham RM. Transglutaminases: crosslinking enzymes with pleiotropic functions. *Nat Rev Mol Cell Biol*. 2003;4(2):140-156.
17. D'Souza DR, Wei J, Shao Q, Hebert MD, Subramony SH, Vig PJ. Tissue transglutaminase crosslinks ataxin-1: possible role in SCA1 pathogenesis. *Neurosci Lett*. 2006;409(1):5-9.
18. Vig PJ, Wei J, Shao Q, Hebert MD, Subramony SH, Sutton LT. Role of tissue transglutaminase type 2 in calbindin- $\text{D}_{28\text{K}}$ interaction with ataxin-1. *Neurosci Lett*. 2007;420(1):53-57.
19. Broome AM, Ryan D, Eckert RL. S100 protein subcellular localization during epidermal differentiation and psoriasis. *J Histochem Cytochem*. 2003;51(5):675-685.
20. Ruse M, Lambert A, Robinson N, Ryan D, Shon KJ, Eckert RL. S100A7, S100A10, and S100A11 are transglutaminase substrates. *Biochemistry*. 2001;40(10):3167-3173.
21. van de Graaf SF, Hoenderop JG, Gkika D, Lamers D, Prenen J, Rescher U, Gerke V, Staub O, Nilius B, Bindels RJ. Functional expression of the epithelial Ca^{2+} channels (TRPV5 and TRPV6) requires association of the S100A10-annexin 2 complex. *Embo J*. 2003;22(7):1478-1487.
22. Cheng X, Jin J, Hu L, Shen D, Dong XP, Samie MA, Knoff J, Eisinger B, Liu ML, Huang SM, et al. TRP channel regulates EGFR signaling in hair morphogenesis and skin barrier formation. *Cell*. 2010;141(2):331-343.
23. Lehen'kyi V, Beck B, Polakowska R, Charveron M, Bordat P, Skryma R, Prevarskaya N. TRPV6 is a Ca^{2+} entry channel essential for Ca^{2+} -induced differentiation of human keratinocytes. *J Biol Chem*. 2007;282(31):22582-22591.
24. El Nahas AM, Abo-Zenah H, Skill NJ, Bex S, Wild G, Griffin M, Johnson TS. Elevated epsilon-(gamma-glutamyl)lysine in human diabetic nephropathy results from increased expression and cellular release of tissue transglutaminase. *Nephron Clin Pract*. 2004;97(3):c108-117.
25. Huang L, Haylor JL, Hau Z, Jones RA, Vickers ME, Wagner B, Griffin M, Saint RE, Coutts IG, El Nahas AM, et al. Transglutaminase inhibition ameliorates experimental diabetic nephropathy. *Kidney Int*. 2009;76(4):383-394.
26. Ikee R, Kobayashi S, Hemmi N, Saigusa T, Namikoshi T, Yamada M, Imakiire T, Kikuchi Y, Suzuki S, Miura S. Involvement of transglutaminase-2 in pathological changes in renal disease. *Nephron Clin Pract*. 2007;105(3):c139-146.

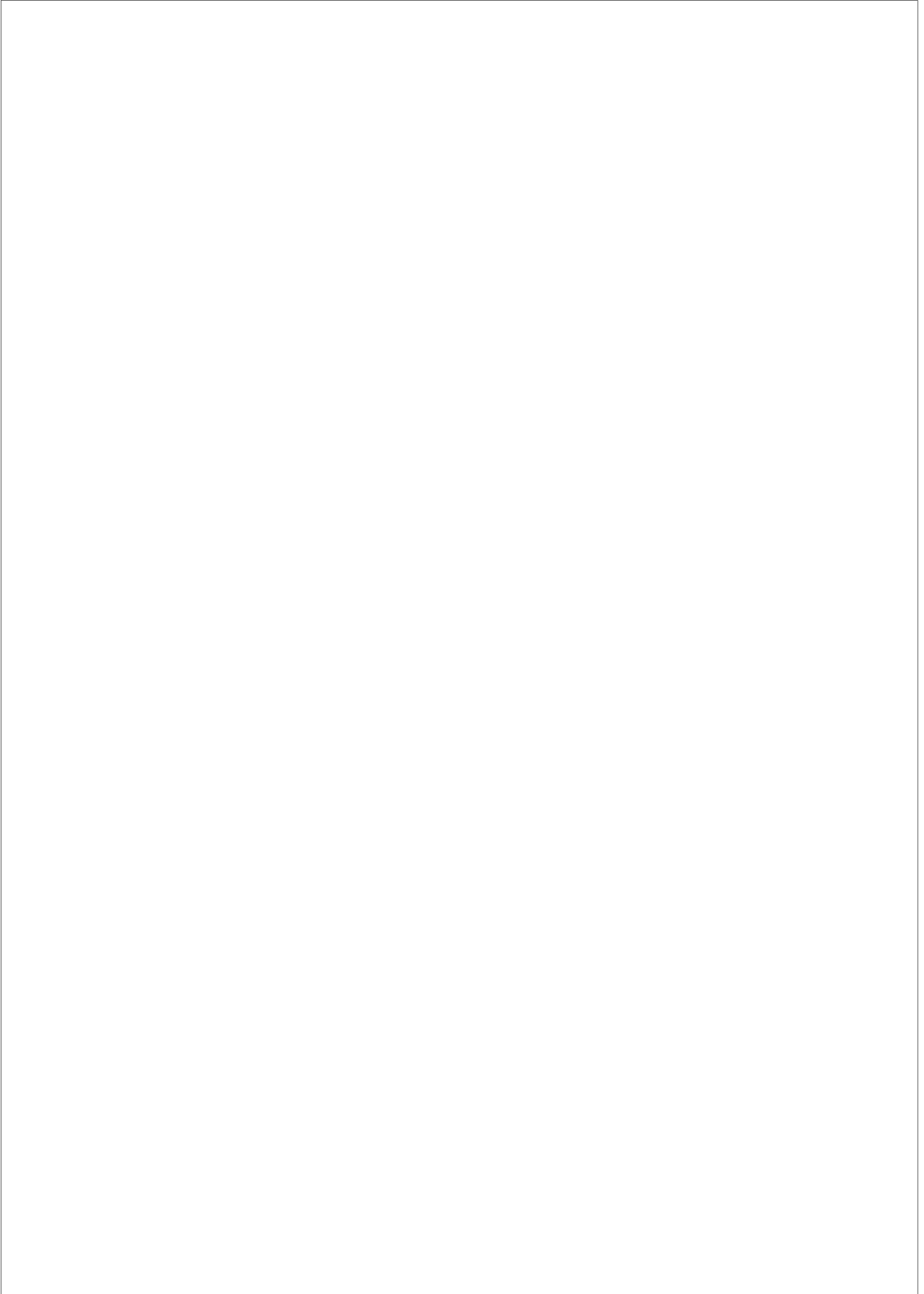
tTG inhibits the activity of TRPV5

27. Liu SY, Huang HC, Li XM. [Tissue transglutaminase and renal fibrosis]. *Sheng Li Ke Xue Jin Zhan*. 2005;36(4):314-318.
28. Shweke N, Boulos N, Jouanneau C, Vandermeersch S, Melino G, Dussaule JC, Chatziantoniou C, Ronco P, Boffa JJ. Tissue transglutaminase contributes to interstitial renal fibrosis by favoring accumulation of fibrillar collagen through TGF-beta activation and cell infiltration. *Am J Pathol*. 2008;173(3):631-642.
29. Skill NJ, Johnson TS, Coutts IG, Saint RE, Fisher M, Huang L, El Nahas AM, Collighan RJ, Griffin M. Inhibition of transglutaminase activity reduces extracellular matrix accumulation induced by high glucose levels in proximal tubular epithelial cells. *J Biol Chem*. 2004;279(46):47754-47762.
30. Skill NJ, Griffin M, El Nahas AM, Sanai T, Haylor JL, Fisher M, Jamie MF, Mould NN, Johnson TS. Increases in renal epsilon-(gamma-glutamyl)-lysine crosslinks result from compartment-specific changes in tissue transglutaminase in early experimental diabetic nephropathy: pathologic implications. *Lab Invest*. 2001;81(5):705-716.
31. Lee MY, Chung S, Bang HW, Baek KJ, Uhm D. Modulation of large conductance Ca²⁺-activated K⁺ channel by Galphah (transglutaminase II) in the vascular smooth muscle cell. *Pflugers Arch*. 1997;433(5):671-673.
32. Aeschlimann D, Paulsson M. Cross-linking of laminin-nidogen complexes by tissue transglutaminase. A novel mechanism for basement membrane stabilization. *J Biol Chem*. 1991;266(23):15308-15317.
33. Beninati S, Senger DR, Cordella-Miele E, Mukherjee AB, Chackalaparampil I, Shanmugam V, Singh K, Mukherjee BB. Osteopontin: its transglutaminase-catalyzed posttranslational modifications and cross-linking to fibronectin. *J Biochem*. 1994;115(4):675-682.
34. Kaartinen MT, El-Maadawy S, Rasanen NH, McKee MD. Tissue transglutaminase and its substrates in bone. *J Bone Miner Res*. 2002;17(12):2161-2173.
35. Priglinger SG, May CA, Neubauer AS, Alge CS, Schonfeld CL, Kampik A, Welge-Lussen U. Tissue transglutaminase as a modifying enzyme of the extracellular matrix in PVR membranes. *Invest Ophthalmol Vis Sci*. 2003;44(1):355-364.
36. Raghunath M, Hopfner B, Aeschlimann D, Luthi U, Meuli M, Altermatt S, Gobet R, Bruckner-Tuderman L, Steinmann B. Cross-linking of the dermo-epidermal junction of skin regenerating from keratinocyte autografts. Anchoring fibrils are a target for tissue transglutaminase. *J Clin Invest*. 1996;98(5):1174-1184.
37. Boros S, Kamps B, Wunderink L, de Bruijn W, de Jong WW, Boelens WC. Transglutaminase catalyzes differential crosslinking of small heat shock proteins and amyloid-beta. *FEBS Lett*. 2004;576(1-2):57-62.
38. Cha SK, Jabbar W, Xie J, Huang CL. Regulation of TRPV5 single-channel activity by intracellular pH. *J Membr Biol*. 2007;220(1-3):79-85.

Chapter 6

39. Gambetti S, Dondi A, Cervellati C, Squerzanti M, Pansini FS, Bergamini CM. Interaction with heparin protects tissue transglutaminase against inactivation by heating and by proteolysis. *Biochimie*. 2005;87(6):551-555.
40. Scarpellini A, Germack R, Lortat-Jacob H, Muramatsu T, Billett E, Johnson T, Verderio EA. Heparan sulfate proteoglycans are receptors for the cell-surface trafficking and biological activity of transglutaminase-2. *J Biol Chem*. 2009;284(27):18411-18423.
41. Verderio EA, Telci D, Okoye A, Melino G, Griffin M. A novel RGD-independent cell adhesion pathway mediated by fibronectin-bound tissue transglutaminase rescues cells from anoikis. *J Biol Chem*. 2003;278(43):42604-42614.
42. Bindels RJ, Hartog A, Timmermans J, Van Os CH. Active Ca^{2+} transport in primary cultures of rabbit kidney CCD: stimulation by 1,25-dihydroxyvitamin D_3 and PTH. *Am J Physiol*. 1991;261(5 Pt 2):F799-807.
43. Barry PH. JPCalc, a software package for calculating liquid junction potential corrections in patch-clamp, intracellular, epithelial and bilayer measurements and for correcting junction potential measurements. *J Neurosci Methods*. 1994;51(1):107-116.





CHAPTER 7

A mouse model for autosomal dominant hypercalciuria due to a mutation in the epithelial Ca²⁺ channel, TRPV5

Nellie Y. Loh¹, Henrik Dimke², Liz Bentley³, Sjoerd Verkaar², Paolo Tammaro⁴, Michael J. Stechman¹, Bushra N. Ahmad¹, Fadil Hannan¹, Tertius A. Hough⁵, William D. Fraser⁵, Joost G. Hoenderop², Frances M. Ashcroft⁴, René J. Bindels², Steve D. M. Brown³, Roger D. Cox³, Rajesh V. Thakker¹

¹Academic Endocrine Unit, Nuffield Department of Medicine, University of Oxford, Oxford Centre for Diabetes, Endocrinology and Metabolism, Churchill Hospital, Headington, Oxford, U.K.

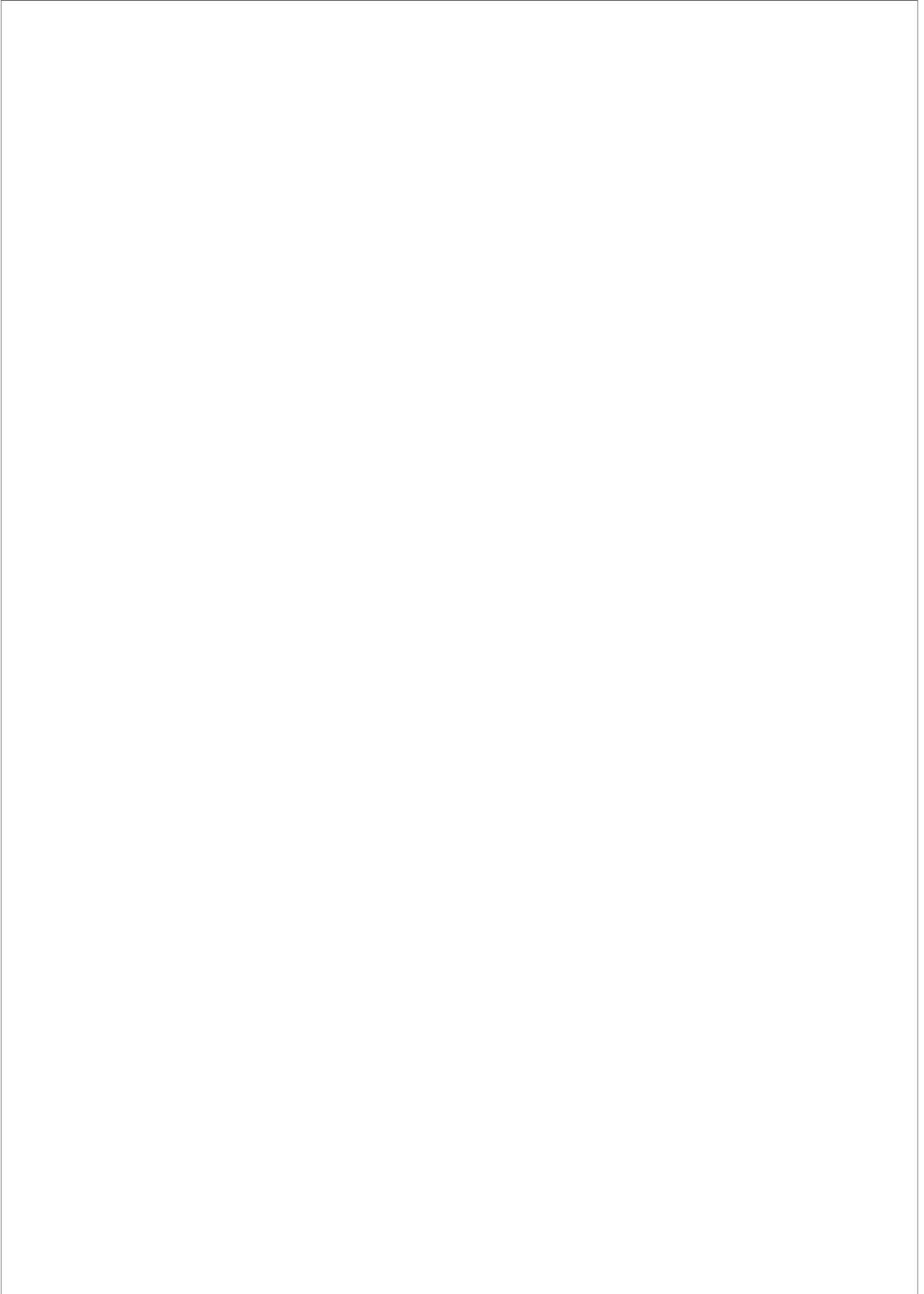
²Department of Physiology, Radboud University Nijmegen Medical Centre, the Netherlands.

³MRC Mammalian Genetics Unit and Mary Lyon Centre, Medical Research Council, Oxfordshire, Oxfordshire, U.K.

⁴Department of Physiology, Anatomy and Genetics, University of Oxford, U.K.

⁵Unit of Clinical Chemistry, School of Clinical Sciences, University of Liverpool, Liverpool, U.K.

In preparation



TRPV5 and autosomal dominant hypercalciuria

Abstract

Nephrolithiasis is a highly prevalent clinical condition that increases with age. Hypercalciuria remains a major risk factor for kidney stone formation. Twin and family studies indicate a genetic basis for hypercalciuria. To investigate novel genetic defects underlying hypercalciuria, we established Hcalc1, a mouse model with autosomal dominant hypercalciuria by screening mice from a N-ethyl-N-nitrosourea mouse mutagenesis resource. Linkage studies mapped the locus to chromosome 6. Candidate gene sequence analysis revealed a T>C transition in codon 682 of the transient receptor potential cation vanilloid 5 (TRPV5) gene, converting a conserved serine to a proline (S682P). Heterozygous and homozygous Hcalc1 mice had a ~10-25-fold higher urinary Ca^{2+}/Cr ratio than their wild-type littermates. Furthermore, histological examination showed that ~10% of Hcalc1 male mice had primary tubulointerstitial nephritis, consistent with urinary reflux. Immunostaining of Hcalc1 kidneys revealed a loss of TRPV5 from the distal convoluted tubules (DCT), with a selective decrease in TRPV5 positive DCT cells in kidneys of *Trpv5*^{682P/+} and *Trpv5*^{682P/682P} mice (100 ± 13%, 56 ± 6% and 27 ± 5% for wild-type, *Trpv5*^{682P/+} and *Trpv5*^{682P/682P}, respectively, $P < 0.05$ compared to wild-type). Furthermore, a reduction in calbindin-D_{28K} expression was observed by semi-quantitative immunohistochemical analysis in kidneys of *Trpv5*^{682P/682P} mice (100 ± 11%, 108% ± 32 and 8 ± 2% for wild-type, *Trpv5*^{682P/+} and *Trpv5*^{682P/682P}, respectively, $P < 0.05$ compared to wild-type). This reduction was also observed by western blot, albeit less prominent (100 ± 6%, 120 ± 13% and 52 ± 3% for wild-type, *Trpv5*^{682P/+} and *Trpv5*^{682P/682P}, respectively, $P < 0.05$ compared to wild-type). This is in line with a defect in TRPV5-mediated renal Ca^{2+} reabsorption. In support of this, transient expression studies of wild-type and mutant TRPV5 in human embryonic kidney 293 cells using the Ca^{2+} -binding dye Fura-2 revealed a lower baseline intracellular Ca^{2+} concentration in the TRPV5-S682P mutant expressing cells (0.77 ± 0.06 and 0.51 ± 0.02 for TRPV5-wild-type and TRPV5-S682P, respectively, $P < 0.05$). Thus, the Hcalc1 mouse with a TRPV5 S682P mutation represents a novel model for autosomal dominant hypercalciuria.

Chapter 7

Introduction

Kidney stone disease (nephrolithiasis) is a global health problem that affects 12% of men and 5% of women by the seventh decade of life and has a recurrence rate of ~10% per annum (1). Ca^{2+} stones, comprising Ca^{2+} oxalate and/or Ca^{2+} phosphate, account for up to 80% of kidney stones and hypercalciuria is the most common and correctable metabolic abnormality found in Ca^{2+} stone formers (1, 2). Hypercalciuria and kidney stone disease are strongly influenced by genetic factors. Between 35-65% of patients with hypercalciuric stone disease have affected family members (2) and twin studies have estimated the heritability of kidney stones and urine Ca^{2+} excretion to be 56% (3) and 52% (4), respectively. In addition, hypercalciuria and kidney stone disease are genetically heterogeneous disorders that may be inherited as polygenic quantitative traits, or as monogenic disorders of autosomal dominant, autosomal recessive or X-linked recessive modes of transmission (2, 5).

The etiology of hypercalciuria is complex. In the body, extracellular free ionized Ca^{2+} concentrations are maintained by a balance between intestinal absorption of dietary Ca^{2+} , renal Ca^{2+} reabsorption and excretion, and bone turnover. Thus, a disturbance in Ca^{2+} handling in any of these three organs could result in hypercalciuria. The pathophysiology of hypercalciuria has been classified as absorptive, renal, or resorptive hypercalciuria, depending on whether the primary defect is due to intestinal hyperabsorption, impaired renal tubular reabsorption, or increased bone resorption (6). In addition, hypercalciuria may occur in association with other metabolic or renal tubular disturbances, thus confounding efforts to identify the genetic factors underlying familial hypercalciuria and Ca^{2+} stone disease (5, 7). Past successes include one study in 3 families with severe absorptive hypercalciuria that linked haplotypes on chromosome 1 to the disorder and identified a candidate gene, the human soluble adenylyl cyclase (8, 9). A recent genome wide association study in Icelandic and Dutch populations also identified susceptibility risk variants in the *CLDN14* gene for hypercalciuric kidney stone disease (10), although the underlying mechanisms have not been elucidated. Furthermore, studies of rare

TRPV5 and autosomal dominant hypercalciuria

monogenic disorders associated with hypercalciuric stone disease such as Dent's disease, Bartter's syndrome and autosomal dominant hypocalcaemia with hypercalciuria, have given us much insight into the receptors, channels and transporters important in Ca^{2+} homeostasis and kidney stone formation (2, 11, 12). However, large extended families needed for such studies are limited.

We have utilized a N-ethyl-N-nitrosourea (ENU) mouse mutagenesis resource (13, 14) in a phenotype-driven screen, to identify new genetic models of hypercalciuria. ENU is a chemical mutagen that causes random point mutations by alkylation of nucleic acids, which leads to mispairing and subsequent single base substitutions during DNA replication. The resulting mutations can lead to loss-of-function, hypomorphic, hypermorphic or dominant-negative changes in protein function (14). Its ability to produce single base pair mutations in mouse has made the ENU mouse mutagenesis program an ideal resource for uncovering new genes involved in disease phenotypes, novel function to known genes, and in identifying amino acid residues crucial for protein function that is not possible in a whole gene deletion approach (14).

Here we report the identification of a mouse, designated Hcalc1, with severe autosomal dominant hypercalciuria. This defect is caused by a novel missense S682P mutation in the TRPV5 gene. The present study delineates the identification and functional characterization of this gene defect.

Results

Phenotype-driven screen, genetic mapping and mutational analysis in Hcalc1 mice

The Hcalc1 founder mouse was identified from a urine and plasma biochemical screen of 598 F1 male mice derived from matings of ENU-mutagenised C57BL/6J (B6J) male mice and wild-type C3H/HeH (C3H) female mice. This single founder mouse had a urine Ca^{2+} /creatinine (Ca^{2+}/Cr) value that was >10 SD above the mean of age-matched control males at an age of 16 weeks

TRPV5 and autosomal dominant hypercalciuria

test whether the observed value deviates significantly from the expected value of a given null hypothesis, in this case, whether the number of offspring for the *Hcalc1* founder that are hypercalciuric and normocalciuric (observed value) deviates significantly from the expected numbers if the phenotype were inherited in an autosomal dominant manner (null hypothesis). Df (degree of freedom) is calculated as $n-1$, in which n =the number of groups or observations (in this case $n=2$ for hypercalciuric and normocalciuric mice). We accepted the null hypothesis that the phenotype is inherited in an autosomal dominant manner, since $P=0.53$ (Figure 1A).

A genome wide scan using DNA from 10 hypercalciuric mice and 3 normocalciuric littermates identified co-segregation of the *Hcalc1* locus with B6J alleles of 3 SNPs on chromosome 6 (LOD score = 3.91, 0% recombination). Haplotype analysis of all 23 G2 mice and a further 66 G2 offspring (29 hypercalciuric, 37 normocalciuric) derived by IVF, using additional chromosome 6 markers, mapped the *Hcalc1* locus to a ~11.94-Mbp interval on chromosome 6B1/B2, between *rs13478709* and *rs30110406*, with a peak LOD score = 26.8 at 0% recombination (Figure 1B). This interval contains 176 genes, including those for *Trpv5* and *TRPV6*

Sequence analysis of the entire coding region of *Trpv5* and *TRPV6* using DNA from a hypercalciuric G2 mouse and wild-type BL6 and C3H mice did not identify a mutation in *TRPV6*. However, a heterozygous T>C transition in codon 682 of *Trpv5* was found in the hypercalciuric mouse that is predicted to alter a wild-type serine (S) to a mutant proline (P) (Figure 1C). This mutation results in a gain of a *Bsa*II restriction enzyme site, which was used to confirm the presence of the mutation in all hypercalciuric mice, and its absence in all normocalciuric mice (Figure 1C). This S682 residue, which is located in the cytoplasmic carboxyl-terminal region of TRPV5, is conserved across species and in TRPV6 (Figure 1D). S682 is not predicted to be phosphorylated based on phospho-database prediction servers nor is it located in a known functional or protein-binding domain.

Chapter 7

Urine and plasma biochemistry of *Hcalc1* mice

TRPV5 is an epithelial Ca^{2+} channel highly expressed in the DCT and connecting tubule (CNT), and is vital to active renal Ca^{2+} reabsorption (15, 16). To further characterize the *Hcalc1* phenotype, urine and plasma chemistry were assessed in wild-type, heterozygous (*Trpv5*^{682P/+}) and homozygous mutant (*Trpv5*^{682P/682P}) mice. *Trpv5*^{682P/682P} mice were generated from

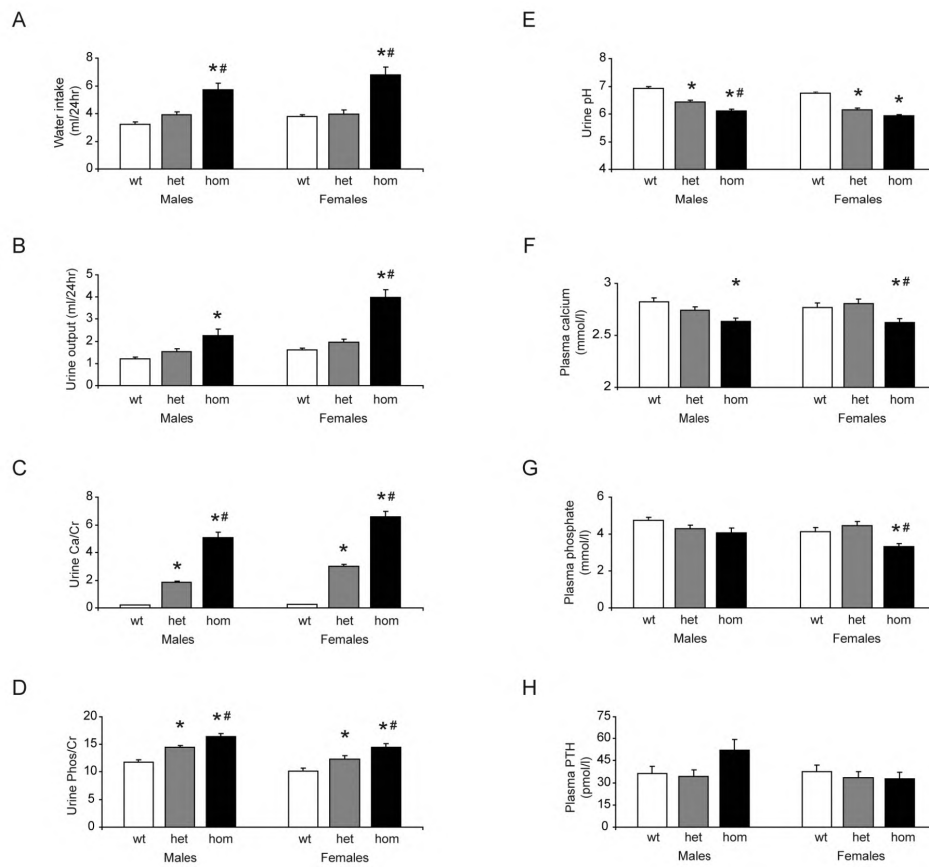


Figure 2. Phenotypic characterization of *Hcalc1* mice. (A-B) Water intake and urine output of wild-type (wild-type), *Trpv5*^{682P/+} (het) and *Trpv5*^{682P/682P} (hom) mice individually housed in metabolic cages for 24 hours (N=17-72 mice/group). (C-E) Analysis of Ca^{2+}/Cr and Phos/Cr ratios, and pH of urine samples from wild-type (wild-type), *Trpv5*^{682P/+} (het) and *Trpv5*^{682P/682P} (hom) mice (N= 17-72 mice/group). (F-H) Analysis of plasma Ca^{2+} , phosphate (N=15-50 mice/group), and PTH (N=17-22 mice/group) of wild-type (wild-type), *Trpv5*^{682P/+} (het) and *Trpv5*^{682P/682P} (hom) mice. All data are presented as means \pm SEM. * $P < 0.05$, significantly different from wild-type mice. # $P < 0.05$, significantly different from *Trpv5*^{682P/+} mice, with Bonferroni correction for multiple comparisons.

(*Trpv5*^{682P/+} \times *Trpv5*^{682P/+}) crosses, and are viable, fertile and outwardly indistinguishable from

TRPV5 and autosomal dominant hypercalciuria

their wild-type and *Trpv5*^{682P/+} littermates. Mice aged between 12-20 weeks of age were housed in metabolic cages for 24 hours and urine samples collected for biochemical analysis. *Trpv5*^{682P/682P} mice of both genders were polydipsic and polyuric compared with wild-type mice (Figure A-B). Biochemical analysis of urine samples revealed that the mean urine Ca²⁺/Cr of *Trpv5*^{682P/+} and *Trpv5*^{682P/682P} mice were ~9- and ~24-fold greater for males, and ~10- and ~27-fold greater for females, compared with their gender matched controls ($P < 0.05$, Figure 2C). In addition, the hypercalciuria in *Trpv5*^{682P/682P} mice was significantly greater than that in *Trpv5*^{682P/+} mice ($P < 0.05$, Figure 2C). *Trpv5*^{682P/+} and *Trpv5*^{682P/682P} mice also had elevated urine phosphate/creatinine ratios (Phos/Cr) compared with wild-type mice indicating hyperphosphaturia (Figure 2D). Furthermore, urine samples of both *Trpv5*^{682P/+} and *Trpv5*^{682P/682P} mice were significantly more acidic than those from wild-type littermates (Figure 2E).

To determine if the observed increased urinary Ca²⁺ and phosphate excretion in *Hcalc1* mice is accompanied by alterations in systemic Ca²⁺ and phosphate levels, plasma samples were obtained from mice aged 18-25 weeks old for analysis. Plasma Ca²⁺ and phosphate were not significantly different between gender-matched *Trpv5*^{682P/+} and wild-type mice (Figure 2F-G). However, *Trpv5*^{682P/682P} mice had significantly lower plasma Ca²⁺ concentrations compared with gender-matched wild-type mice (Figure 2F). Furthermore, plasma phosphate concentrations in *Trpv5*^{682P/682P} female mice were significantly lower compared with female wild-type and *Trpv5*^{682P/+} mice (Figure 2G). Plasma PTH for *Trpv5*^{682P/+} and *Trpv5*^{682P/682P} mice were not significantly different from wild-type mice (Figure 2H).

Renal histopathology

We examined kidneys dissected from wild-type, *Trpv5*^{682P/+} and *Trpv5*^{682P/682P} mice between the age of 17 and 25 weeks for the presence of renal abnormalities. Histological analysis of

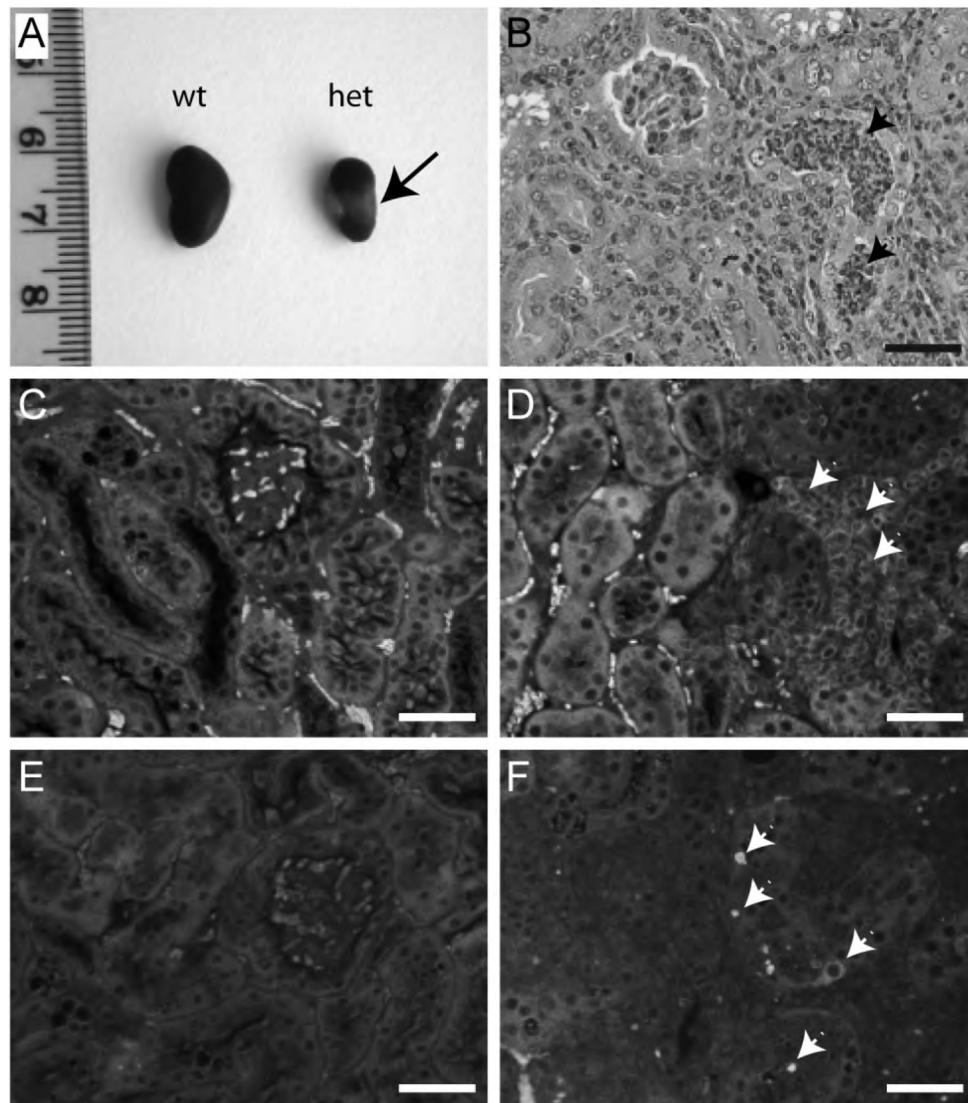


Figure 3. Tubulointerstitial nephritis in kidneys of *Trpv5*^{682P/+} and *Trpv5*^{682P/682P} male mice. (A) Left kidneys from a wild-type male mouse (wild-type), and a *Trpv5*^{682P/+} mutant (het) male mouse with renal scarring (arrowed). Representative images of: (B) H&E staining of the renal cortex of an affected *Hcalc1* male mouse showing interstitial infiltrations of mononuclear cells and dilated tubular lumen filled with cells and cell debris (arrowheads), (C-D) anti-CD3-labelling (green) of the renal cortex of a wild-type male (C) and an affected *Hcalc1* male (D) mouse. A large number of T-lymphocytes were present in the interstitial regions of the affected *Hcalc1* mouse kidney (D, arrowheads), (E-F) TUNEL-labelling (green) of the renal cortex of a wild-type (E) and an affected *Hcalc1* (F) male showing the presence of tubular cell apoptosis in the *Hcalc1* mouse kidney (F, arrowheads). DAPI (blue) labels nuclei (C-F). Scale bar = 50 μ m.

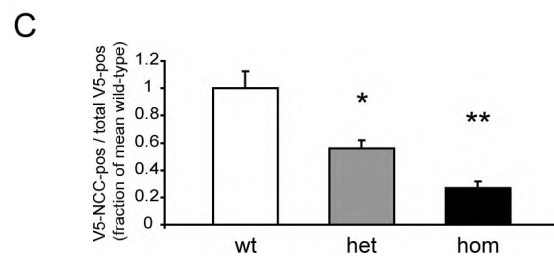
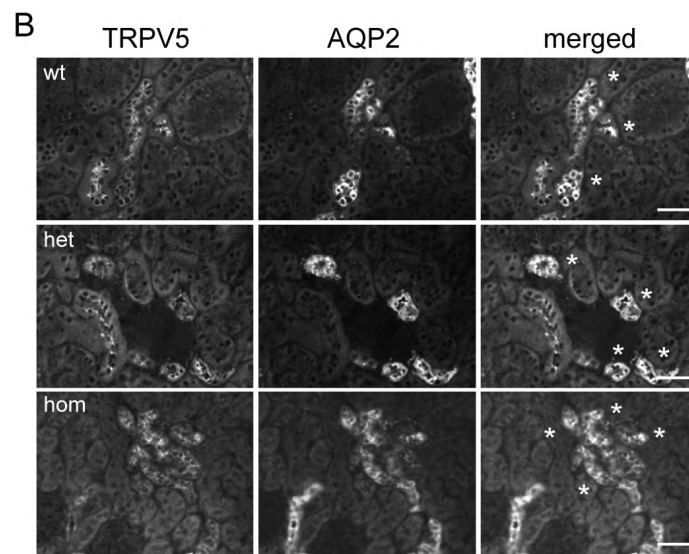
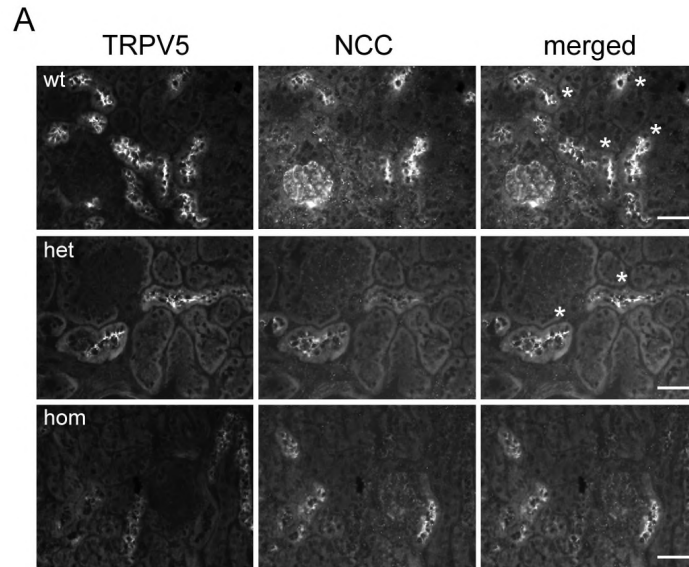
TRPV5 and autosomal dominant hypercalciuria

kidney sections using von Kossa staining which detects Ca^{2+} deposits, revealed the occasional interstitial calcification (one or more calcified foci/ renal cross-section) in the renal cortex in a number of hypercalciuric mice (26% G2 mice). However, such calcification was also present in wild-type littermates (24% G2 mice), and thus not considered to be associated with the hypercalciuric phenotype in *Hcalc1* mice. Interestingly, kidneys from ~9% (6/66) of *Trpv5*^{682P/+} and 13% (3/23) *Trpv5*^{682P/682P} male mice were grossly abnormal with the appearance of renal scarring (Figure 3A). Histological examination of these kidneys revealed the presence of inflammatory cell infiltrates, tubular dilatation, flattening of tubular epithelia and the presence of numerous cells and/or cell debris within the dilated lumen of some cortical tubules (Figure 3B). Immunohistochemical staining with antibodies against CD3, which forms part of the T-cell receptor complex, confirmed an abundance of T-lymphocytes within the interstitial regions of the renal cortex of affected mice that was not present in wild-type mice (Figure 3C-D). In addition, TUNEL-staining showed apoptosis of renal tubular cells in affected kidneys that were not observed in wild-type kidneys (Figure 3E-F). Glomeruli and blood vessels appeared normal. These features are consistent with primary tubulointerstitial nephritis, which could result from vesicoureteral reflux (VUR) or urinary flow obstruction that may be compounded by the increased volume of urine produced in these mice. Obstruction of urine flow can occur as a result of obstruction of tubular lumen by renal calculi. However, histological examination of these kidneys revealed only an occasional, but not generalized presence of calcification within renal tubular lumen, indicating that renal tubular obstruction by Ca^{2+} phosphate crystals is unlikely to be the cause of tubulointerstitial nephritis in these mice.

Assessment of Trpv5 and calbindin-D_{28K} expression in wild-type and mutant kidneys

To assess the effect of the S682P mutation on TRPV5 expression in the kidney, 8- μm kidney

Chapter 7



TRPV5 and autosomal dominant hypercalciuria

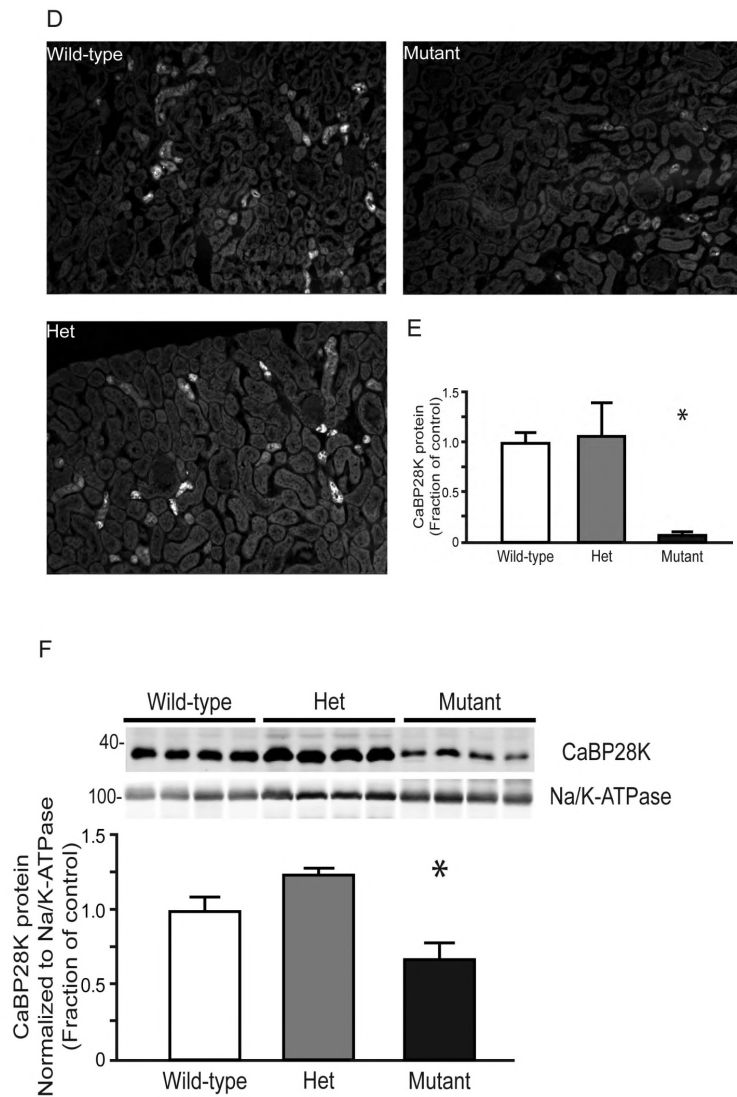


Figure 4. Effect of TRPV5-S682P mutation on TRPV5 and calbindin-D_{28K} expression in kidney. (A-B) Representative immunohistochemical images of kidney sections from wild-type (wild-type), *Trpv5*^{682P/+} (het) and *Trpv5*^{682P/682P} (hom) mice, co-stained for (A) TRPV5 and NCC, and (B) TRPV5 and AQP2. * denotes co-localisation. Scale bar = 50µm. (C) Histogram depicting the ratio of the number of TRPV5-NCC co-positive cells to the total number of TRPV5-positive cells (N=5 mice/group). (D) Representative immunohistochemical images of calbindin-D_{28K} (CaBP28K) stained kidney sections from wild-type (wild-type), *Trpv5*^{682P/+} (het) and *Trpv5*^{682P/682P} (hom) mice. Scale bar = 200µm (E) Histogram depicting calbindin-D_{28K} protein abundance determined by computerized analysis of immunohistochemical images (N=4-6 mice/group) (F) Semi-quantitative western blotting of calbindin-D_{28K} in kidney. The α -1 subunit of the Na/K-ATPase was used as a housekeeping gene to normalize for equal loading. All histogram data are presented as means \pm SEM. **P*<0.05, ***P*<0.01 are considered significantly different from wild-type mice.

Chapter 7

cryosections were co-stained with anti-TRPV5 antibodies, and antibodies against the thiazide-sensitive sodium/chloride co-transporter (NCC) or aquaporin-2 (AQP2) to distinguish the expression of TRPV5 in the DCT2 and CNT, respectively. In the adult mouse kidney, NCC is expressed at the apical regions of DCT cells, with a slight decrease in expression towards the most distal part of the DCT segment (16), whereas AQP2-expression begins at the CNT and extends throughout the collecting ducts (17, 18). In kidneys of wild-type mice, immunostaining of TRPV5 was observed in the apical regions of the second half of the DCT (DCT2), and in the cytoplasmic regions of CNT cells (Figure 4A-B), as previously described (16). By contrast, in kidneys of *Trpv5*^{682P/682P} mice, overall TRPV5-immunofluorescence was greatly reduced, especially in NCC-positive (AQP2-negative) tubular cells. In these cells, TRPV5-staining was absent or appeared diffusely cytoplasmic (Figure 4A-B). Overall TRPV5-immunofluorescence in *Trpv5*^{682P/+} kidneys appeared to be unaffected compared with wild-type kidneys (Figure 4A-B), although a functional effect on renal Ca²⁺ excretion was still apparent. Careful examination of TRPV5-NCC co-stained sections revealed that in *Trpv5*^{682P/+} kidneys, TRPV5-expression appeared confined to the most distal portion of the DCT2 where NCC-immunostaining was weakest (Figure 4A). To test this observation, the number of TRPV5-positive and TRPV5-NCC co-positive cells in wild-type, *Trpv5*^{682P/+} and *Trpv5*^{682P/682P} mice were counted in a minimum of 3 different fields per kidney section and the % of TRPV5-positive cells that were NCC co-positive was determined (N=5 mice/group). Our results showed that TRPV5-NCC co-positive cells in kidneys of *Trpv5*^{682P/+} and *Trpv5*^{682P/682P} mice were reduced in comparison to wild-type kidneys (100% ± 13%, 56% ± 6% and 27% ± 5% for wild-type, *Trpv5*^{682P/+} and *Trpv5*^{682P/682P}, respectively, *P*<0.05 compared to wild-type) (Figure 4C).

The intracellular vitamin D-regulated Ca²⁺-binding protein calbindin-D_{28K} is co-expressed with TRPV5 in the DCT2/CNT. We therefore investigated calbindin-D_{28K} expression in *Trpv5*^{682P/+} and *Trpv5*^{682P/682P} kidneys by semi-quantitative immunohistochemistry and Western blot analysis. Expression levels of calbindin-D_{28K} in *Trpv5*^{682P/+} kidneys were not significantly different from

TRPV5 and autosomal dominant hypercalciuria

wild-type kidneys (Figure 4D-F). However, semi-quantitative immunohistochemical analysis of *Trpv5*^{682P/682P} kidneys revealed that calbindin-D_{28K}-expression was significantly decreased ($100 \pm 11\%$, $108\% \pm 32$ and $8 \pm 2\%$ for wild-type, *Trpv5*^{682P/+} and *Trpv5*^{682P/682P}, respectively, $P < 0.05$ compared to wild-type). This observation was confirmed by Western blot ($100 \pm 6\%$, $120 \pm 13\%$ and $52 \pm 3\%$ for wild-type, *Trpv5*^{682P/+} and *Trpv5*^{682P/682P}, respectively, $P < 0.05$ compared to wild-type). (Figure 4D-F).

Functional assessment of Trpv5-S682P channels

We next investigated the effect of the S682P mutation on TRPV5 function in intact cells. Human Embryonic Kidney (HEK) 293 cells were transiently transfected with constructs encoding enhanced green fluorescent protein (eGFP)-tagged wild-type mouse TRPV5 (mTRPV5-wild-type), mouse TRPV5 with the S682P mutation (mTRPV5-S682P), or the empty mock vector. eGFP positive cells were monitored for changes in intracellular Ca^{2+} ($[\text{Ca}^{2+}]_i$) in response to changes in extracellular Ca^{2+} ($[\text{Ca}^{2+}]_o$) using the Ca^{2+} -sensing dye, Fura-2. Transient expression of mTRPV5-wild-type resulted in an elevated basal $[\text{Ca}^{2+}]_i$ level compared to mock-transfected cells, due to increased Ca^{2+} permeability of the cell. When the cells were superfused with Ca^{2+} -free medium, the $[\text{Ca}^{2+}]_i$ in TRPV5-expressing cells dropped to levels similar to mock-transfected cells. Reapplication of 1.4 mM Ca^{2+} solution induced a rapid increase of $[\text{Ca}^{2+}]_i$ followed by a gradual decrease back to basal levels (Figure 5A). No significant changes in $[\text{Ca}^{2+}]_i$ were observed in mock-transfected cells (Figure 5A). By comparison, cells transfected with mTRPV5-S682P showed a lower basal $[\text{Ca}^{2+}]_i$ than mTRPV5-wild-type transfected cells ($N=24/\text{group}$, $P < 0.05$, Figure 5A-B). The mTRPV5-S682P transfected cells had a similar response in $[\text{Ca}^{2+}]_i$ to Ca^{2+} depletion and Ca^{2+} reapplication as that observed in mTRPV5-wild-type transfected cells. These data strongly suggest that the S682P mutation in TRPV5 affects Ca^{2+} permeability of the cell, a feature consistent with the hypercalciuric phenotype observed in *Trpv5*^{682P/+} and *Trpv5*^{682P/682P} mice.

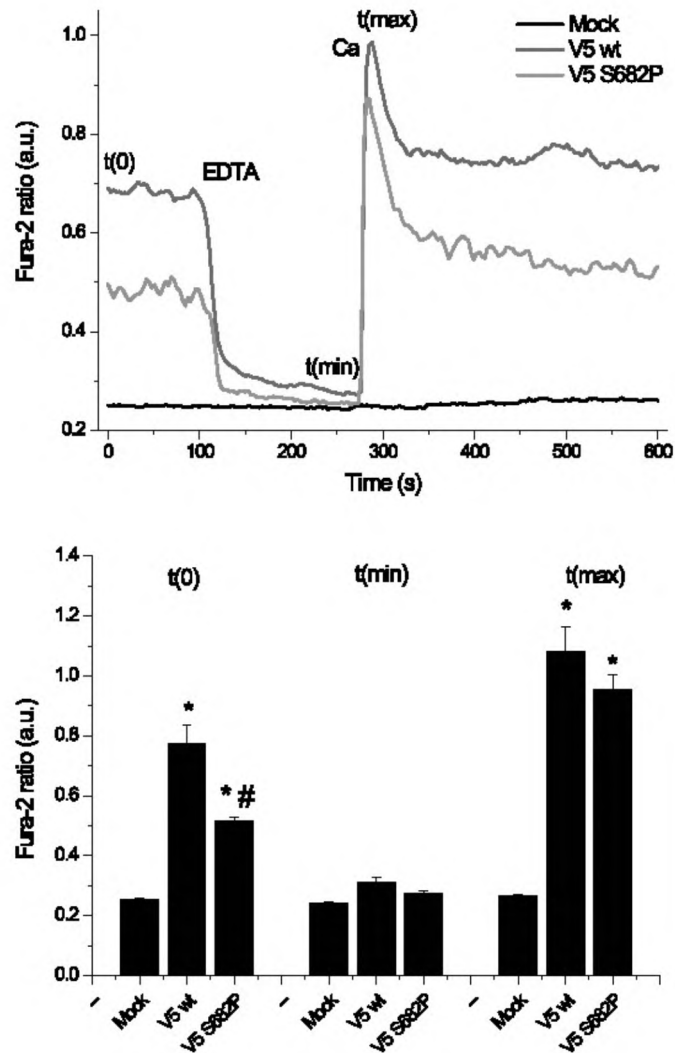


Figure 5. Monitoring TRPV5 activity using Fura-2. (A) Representative trace of Fura-2 ratio in HEK293 cells transiently transfected with an empty EGFP vector (mock), or EGFP-tagged mTRPV5-wild-type (V5-wild-type) or mTRPV5-S682P (V5-S682P). Cells expressing EGFP were selected and monitored for changes in intracellular Ca²⁺ levels when extracellular Ca²⁺ concentrations were varied from 1.4 mM Ca²⁺ to 2mM EDTA and 1.4mM Ca²⁺ which was facilitated by superfusion. (B) Fura-2 levels under resting conditions (t_0), minimal Fura-2 ratio after EGTA treatment (t_{\min}) and peak level (t_{\max}) upon administration of 1.4mM Ca²⁺ after EGTA treatment. Average data of cells transfected with the empty vector (N=7), mTRPV5-wild-type (N=24) and mTRPV5-S682P (N=24) from at least three independent experiments. * $P < 0.05$ is considered significantly different from cells transfected with empty vector. # $P < 0.05$ is considered significantly different from mTRPV5-wild-type transfected cells.

TRPV5 and autosomal dominant hypercalciuria

Discussion

Our studies have identified a novel mouse model, *Hcalc1*, for autosomal dominant hypercalciuria and increased susceptibility to primary tubulointerstitial nephritis. Importantly, we have provided evidence that the mutation in the mouse TRPV5 gene underlies the observed hypercalciuria. This is based on the following observations: *i*) The T>C substitution in codon 682 of mouse TRPV5 results in substitution of a highly conserved serine residue, making it unlikely to be simply a silent polymorphism (Figure 1); *ii*) Expression of TRPV5 in *Trpv5*^{682P/+} and *Trpv5*^{682P/682P} kidneys was altered, particularly in the DCT2 segment (Figure 4A-C); *iii*) Renal calbindin-D_{28K}-expression in *Trpv5*^{682P/682P} mouse kidneys was greatly reduced, further supporting a specific defect in TRPV5-mediated Ca²⁺ reabsorption (Figure 4D-F); *iv*) The alteration from S682 to a proline leads to a reduced basal [Ca²⁺]_i level in HEK293 cells transfected with mTRPV5-S682P, indicating a defect in the TRPV5-mediated Ca²⁺ permeability of the cell (Figure 5).

Hcalc1 is the first reported genetic model with autosomal dominant hypercalciuria due to a mutation in TRPV5. *Hcalc1* mice are hypercalciuric, hyperphosphaturic, polyuric, polydipsic and have a low urine pH. However, despite extreme calciuresis, renal calcification was only very occasionally found in *Hcalc1* kidneys, and this was not different from wild-type mice. These features are similar to the reported phenotype in *Trpv5*^{-/-} mice (7). It has been postulated that polyuria and low urine pH reduce the risk of Ca²⁺ phosphate precipitations in hypercalciuric mice (7, 19). Indeed, studies in *Trpv5*^{-/-} mice have shown that increased luminal Ca²⁺ activates the apical Ca²⁺-sensing receptor in collecting duct cells. This, in turn, leads to the downregulation of the AQP2 water channel and increased activity of the proton pump H⁺-ATPase, resulting in polyuria and increased acid secretion into the urine, respectively (19). Abolishment of this compensatory urinary acidification in *Trpv5*^{-/-} mice by genetic ablation of the B1 subunit of the H⁺-ATPase resulted in severe Ca²⁺ phosphate precipitation in the renal medulla (19). Similar mechanisms may occur in *Hcalc1* mice for reducing the risk of Ca²⁺ precipitation in the presence

Chapter 7

of hypercalciuria.

Although TRPV5 is a major protein involved in active Ca^{2+} reabsorption in the kidney, to date, no TRPV5 mutation has been identified in patients with hypercalciuric kidney stone disease (20, 21). However, in a recent paper investigating the functional significance of common TRPV5 SNPs in African Americans who have lower urine Ca^{2+} excretion and reduced risk of kidney stones compared with white Americans, the TRPV5 A563T and L712F variants were shown to exhibit an increased Ca^{2+} influx in *Xenopus laevis* oocyte assays compared with the reference TRPV5, suggesting that these alleles may contribute to the superior ability of African Americans to conserve Ca^{2+} (20). More importantly, this increase in TRPV5 Ca^{2+} uptake in the A563T variant was observed even under experimental conditions mimicking compound heterozygous state, or in combination with other TRPV5 nonsynonymous SNP variations (20). Interestingly, the L712F residue, like our S682P mutation, is located in the cytoplasmic C-terminal tail of TRPV5, although the basis of the increased efficiency of this variant was not investigated.

The TRPV5 S682P mutation identified in the Hcalc1 mice was shown in heterologous expression studies to result in reduced TRPV5-mediated Ca^{2+} permeability (Figure 5). Transient expression of mTRPV5-S682P into HEK293 cells revealed a lower $[\text{Ca}^{2+}]_i$, than observed in the mTRPV5-wild-type-transfected cells. This observation is in agreement with a reduction in cellular Ca^{2+} transport in the S682P mutant. Changing the extracellular Ca^{2+} concentration (from depletion to reapplication) in HEK293 cells, leads to an overshoot of $[\text{Ca}^{2+}]_i$ followed by a gradual decrease in $[\text{Ca}^{2+}]_i$, which likely reflects Ca^{2+} -dependent inactivation of the channel. This feature has been described in detail previously (22). As the response to Ca^{2+} depletion and Ca^{2+} reapplication was similar between the mTRPV5-S682P and mTRPV5-wild-type transfected cells, it is unlikely that the mutation directly affects the Ca^{2+} -induced channel inactivation. The intracellular C-terminal region of TRPV5 contains several protein-binding and regulatory motifs, including three predicted protein kinase C phosphorylation sites and binding domains for the Na^+/H^+ exchanger regulatory factors 2 and 4 and Rab11a, that have been shown to regulate the

TRPV5 and autosomal dominant hypercalciuria

subcellular localization and trafficking of TRPV5 (23-25). Although S682 is not a predicted phosphorylated residue and does not form part of a known protein interaction or regulatory domain, it is possible that the alteration from a serine to a proline could result in protein misfolding which may alter protein binding and/or regulatory sites, and in turn affect TRPV5 channel function and/or trafficking to the apical membrane. A phosphorylation site has been reported close to the C-terminal end (T709), which affects the single-channel activity of the TRPV5 channel. Whether this mutation could influence phosphorylation kinetics remains to be determined (26).

Despite the presence of a wild-type TRPV5 allele in *Trpv5*^{682P/+} mice, the observed hypercalciuria in *Trpv5*^{682P/+} mice is at least as severe as that reported for the *Trpv5*^{-/-} mice (Figure 2C) (7). This suggests that in *Trpv5*^{682P/+} mice, the TRPV5-S682P protein is exerting a dominant-negative or antagonistic effect on the wild-type TRPV5 protein. This can be explained by the fact that the TRPV5 channel comprises four TRPV5 monomers that form a central pore (15). Thus in *Trpv5*^{682P/+} DCT/CNT, there would be a 1 in 16 probability that a TRPV5 tetramer comprising four wild-type subunits is formed, and a 15 in 16 probability that an assembled TRPV5 tetramer comprises at least one mutant subunit. A TRPV5 channel comprising at least one TRPV5-S682P subunit would be predicted to be less efficient than one comprising four wild-type TRPV5 subunits. The hypercalciuria in *Trpv5*^{682P/682P} mice is much more pronounced than that observed in *Trpv5*^{682P/+} mice and *Trpv5*^{-/-} mice (Figure 2C) (7), suggesting a dosage effect of the mutated allele. TRPV6 is co-expressed with TRPV5 in the DCT2/CNT of wild-type mouse kidney (17). It has been previously shown by heterologous expression studies in HEK293 cells that TRPV5 and TRPV6 can form functional heterotetrameric complexes and that the electrophysiological properties of the resulting channel depend on the combination/ratio of TRPV5/TRPV6 subunits that make up the tetramer (7). Whilst studies in *Trpv5*^{-/-} mice have shown that expression of TRPV6 in DCT2/CNT is not sufficient to compensate for the loss of TRPV5 in the mouse kidney, in *Trpv5*^{682P/682P} mice, heteromerisation of TRPV5-S682P with the

Chapter 7

endogenous TRPV6 monomers would be predicted to result in TRPV5/TRPV6 complexes with lower Ca^{2+} permeability, thereby leading to an even more severe phenotype.

The reduction in Ca^{2+} permeability of mTRPV5-S682P-transfected HEK293 cells (Figure 5), however, does not fully explain the degree of hypercalciuria observed in *Trpv5*^{682P/+} and *Trpv5*^{682P/682P} mice (Figure 2). Immunofluorescence studies in *Trpv5*^{682P/+} and *Trpv5*^{682P/682P} kidneys have shown that TRPV5-expression is greatly reduced from the apical membrane of DCT2 cells, suggesting that the S682P mutation could be affecting TRPV5 trafficking or regulation in these cells. While TRPV5 primarily localizes to the CNT in rabbit, this protein is highly expressed in apical membrane domains of the DCT2 cells in the mouse. Here, a gradual decrease in TRPV5 expression is observed from the DCT2 towards the CNT, suggesting that the majority of TRPV5-mediated Ca^{2+} transport occurs in the DCT2 segment (15, 16). It is not known why TRPV5-expression in DCT2 cells of *Trpv5*^{682P/+} and *Trpv5*^{682P/682P} kidneys appeared more affected than TRPV5-expression in the CNT, but this could be due to potential TRPV5 regulatory/interacting proteins present in DCT2 cells that are not expressed in the CNT. These findings underscore the importance of the DCT2 in active Ca^{2+} uptake, as strong TRPV5-expression in the CNT alone is not sufficient to prevent hypercalciuria in *Trpv5*^{682P/+} mice.

Expression of the vitamin D-regulated calbindin-D_{28K} protein was also found to be significantly reduced, but only in the *Trpv5*^{682P/682P} mice. Such reductions have previously been observed in models with defective Ca^{2+} influx via TRPV5, such as the *Trpv5*^{-/-} and *Klotho*^{-/-} mice (7, 27). It is interesting that calbindin-D_{28K}-expression is reduced in these animals, as they have severe hypervitaminosis D₃, a feature that is likely to exist in the *Hcalc1* model as well. This observation suggests that cellular Ca^{2+} concentration is an important regulator of calbindin-D_{28K} expression, overriding the stimulatory effects of vitamin D. Indeed, previous experiments in primary cultures of immuno-isolated rabbit CNT cells have demonstrated that inhibiting Ca^{2+} influx via TRPV5 using the channel blocker, ruthenium red, significantly reduces calbindin-D_{28K} abundance (28). This may also explain why a change in calbindin-D_{28K} expression in *Trpv5*^{682P/+}

TRPV5 and autosomal dominant hypercalciuria

mice was not observed, as some Ca^{2+} influx is still expected, via the wild-type TRPV5 channel. Thus, our data are in line with previously published observations, suggesting a functional defect in TRPV5-mediated Ca^{2+} transport in our mice.

One unexpected finding in our *Hcalc1* model was that ~9% of *Trpv5*^{682P/+} and ~13% of *Trpv5*^{682P/682P} male mice developed primary tubulointerstitial nephritis by the age of 25 weeks (Figure 3). Primary tubulointerstitial nephritis may result from urinary reflux due to possible obstruction by kidney stones or VUR, which would be compounded by the polyuria in these mice. However, histological examination of kidneys from these mice indicate that Ca^{2+} precipitation within tubular lumen were uncommon and therefore unlikely to be the cause of the tubulointerstitial nephritis. In a recent study of 11 inbred mouse strains for susceptibility to VUR, C57BL/6J mice were found to be VUR-resistant, while the C3H/HeJ inbred mouse was identified as a VUR-susceptible strain without kidney malformations (29). The authors showed that the predisposition of C3H/HeJ mice to reflux was as a result of a defective uretero-vesical junction characterized by a short intravesical ureter. This phenotype was shown to be inherited in an autosomal recessive manner and the VUR locus (*Vurm1*) was mapped to mouse chromosome 12 (29). Since the *Hcalc1* model was generated on a mixed B6J/C3H genetic background, it is possible that the tubulointerstitial nephritis in this subset of *Trpv5*^{682P/+} and *Trpv5*^{682P/682P} male mice is a result of an increased susceptibility to VUR from a combination of uretero-vesical junction defect and polyuria. Tubulointerstitial nephritis has not been previously been reported in *Trpv5*^{-/-} mice, although special focus has not been placed on this feature (7). This difference between the *Trpv5*^{-/-} mice and our hypercalciuric model is likely to be due to the difference in the genetic background of these two models, since the *Trpv5*^{-/-} mice were generated on a 129/Sv background (7), a mouse strain that is resistant to VUR (29).

In summary, *Hcalc1* is the first model reported to have dominant hypercalciuria and a missense mutation in TRPV5. Our model will prove useful in understanding the interplay between TRPV5 and other factors regulating Ca^{2+} homeostasis and factors underlying

Chapter 7

susceptibility to tubulointerstitial nephritis.

Methods

Experimental Animals

All studies were performed in accordance with guidelines provided by the UK Home Office Project license. All animals were maintained in specific pathogen-free facilities, in individual ventilated cages and a 12 hrs light-dark cycle, with free access to food and water. Mice were fed on Rat and Mouse No.3 diet containing 1.15% (w/w) Ca^{2+} , 0.82% (w/w) total phosphorus and approx. 4,100 units/kg of vitamin D (Special Diets Services, Wytham, Essex, UK).

Generation of mutant mice

ENU-mutagenesis of C57BL/6J (B6J) male mice was performed as described in detail previously (13). F1 mice were obtained by crossing ENU-mutagenised B6J male mice with C3H/HeH (C3H) female mice. G2 mice were subsequently obtained by mating the founder male mouse with C3H female mice, or by *in vitro* fertilization of C3H eggs using sperm from the founder male. These mice were used for inheritance testing and mapping studies. Homozygous mutant mice ($\text{Trpv5}^{682P/682P}$) mice were generated by intercrossing heterozygous ($\text{Trpv5}^{682P/+}$) male and female mice.

Phenotype screen

16-week old F1 male mice were kept in metabolic cages (Techniplast, Kettering, UK) for 24 hrs with free access to food and water. Bodyweight was determined before and after the experiment. Food and water intake was also monitored. 24 hrs urine samples were collected in the presence of NaN_3 and stored at -70°C . Blood samples were collected from the tail vein using lithium heparin-coated Microvette tubes (Sarstedt, Leicester, UK). Urine and plasma chemistry were

TRPV5 and autosomal dominant hypercalciuria

measured using an Olympus AU400 multi-channel analyser. Urine parameters were calculated as a ratio of sample creatinine, and plasma Ca^{2+} was adjusted for plasma albumin concentration using the formula: Plasma Ca^{2+} (mM) – [(plasma albumin (g/L) – 30) × 0.017], as previously described (30).

Urine and plasma chemistry

Urine samples were collected in metabolic cages as above. Blood samples were collected following terminal anesthesia from the internal jugular vein in lithium heparin Microvette tubes as previously described (30). Urine and plasma chemistry were performed as above.

Genetic mapping

DNA was isolated from ear or tail biopsies using the Gentra PureGene DNA isolation kit (QIAGEN, Crawley, UK). A genome wide scan was performed on 13 mice by Pyrosequencing on the PSQ HS 96A Instrument (QIAGEN), using a panel of ~60 informative SNPs, distributed at 20-30cM intervals across 19 autosomes (<http://www.pyrosequencing.com/>). Further mapping was carried out using more mice and additional informative SNPs across the candidate interval.

DNA sequence analysis

Exons and the corresponding intron-exon boundaries of the mouse *Trpv5* and *TRPV6* genes were amplified by PCR using gene specific primers. DNA sequences were determined by semi-automated DNA sequencing. The DNA sequence abnormality identified was confirmed by *Bsa*JI restriction enzyme digest of PCR products.

Chapter 7

Kidney histology and immunohistochemistry

Kidneys were cut in half, immersion-fixed in 10% (w/v) formalin overnight, and subsequently embedded in paraffin. 4- μ m-sections were prepared and stained with H&E, and von Kossa to evaluate the presence of renal calcifications as described previously (31). TUNEL-staining for detection of apoptotic cells was performed using the ApopTag Fluorescein *In Situ* Apoptosis Detection kit (Millipore, Watford, UK) according to the manufacturer's instructions. The presence of T-lymphocytes was detected using rabbit anti-CD3 monoclonal antibodies (ab16669, Abcam, Cambridge, UK), and subsequently visualized by secondary detection using Alexa Fluor 488-conjugated donkey anti-rabbit (Molecular Probes, Invitrogen, Paisley, UK). Stained sections were mounted in a mounting medium containing DAPI (Vector Labs, Peterborough, UK).

For TRPV5 detection, dissected kidneys were cut in half and embedded in OCT embedding medium on liquid nitrogen-cooled isopentane. 8- μ m kidney cryosections were co-stained with rabbit anti-TRPV5 (ACC-035, Alomone Labs, Jerusalem, Israel) and goat anti-AQP2 (sc-9882, Santa Cruz, Insight Biotechnology, Wembley, UK) polyclonal antibodies, or with goat anti-TRPV5 (sc-23379, Santa Cruz) and rabbit anti-NCC polyclonal antibodies, followed by the appropriate Alexa Fluor 488- or 594-conjugated secondary antibodies (Molecular Probes). Photographs of TRPV5 stained sections were taken on a Nikon Eclipse E400 microscope equipped with a Nikon DXM1200C digital camera. Images of kidney sections stained for each antibody were photographed under identical exposure conditions for all mice. The NIS-Elements BR 3.0 software was used to count the number of TRPV5-positive and TRPV5-NCC co-positive cells.

For calbindin-D_{28K} detection, kidneys were immersion fixed in 2% (w/v) periodate-lysine-paraformaldehyde (PLP), followed by overnight incubation in 15% (w/v) sucrose. 7- μ m cryosections were prepared and stained with rabbit anti-calbindin-D_{28K}. Photographs of calbindin-D_{28K} staining in kidney cortex were taken through a 10x objective on a Zeiss fluorescence microscope (Sliedrecht, The Netherlands) equipped with a digital photo camera

TRPV5 and autosomal dominant hypercalciuria

(Nikon DMX1200). Semi-quantitative determination of calbindin- D_{28K} protein expression was done using Image J (image processing program, NIH, USA), similar to previous publications (32).

Western blot analysis of renal calbindin- D_{28K}

For quantification of renal calbindin- D_{28K} protein expression, mouse total kidney lysates were prepared and analyzed as described previously (33). Briefly, proteins in kidney lysates were separated using SDS-PAGE and subsequently electro-transferred to polyvinylidene fluoride membranes (Immobilon-P, Millipore Corporation, Bedford, MA, USA). Blots were incubated overnight with rabbit anti-calbindin- D_{28K} polyclonal antibodies (Sigma, St Louis, MO, USA) and mouse anti-Na/K-ATPase α 1-subunit monoclonal antibodies (generously provided by Professor Michael J. Caplan, Yale University School of Medicine, New Haven, CT, USA). Subsequently, the blots were incubated with Alexa Fluor 680-conjugated goat anti-rabbit (Molecular Probes, Invitrogen) and IRDye 800CW conjugated goat anti-mouse (LI-COR Biosciences GmbH, Bad Homburg, Germany) secondary antibodies. Immunoreactive protein was detected using the Odyssey infrared detection system (Westburg, Leusden, The Netherlands). Densitometric analysis was done using Image J.

Video imaging of $[Ca^{2+}]_i$ using Fura-2-AM

Functional studies were performed using cDNAs encoding full-length wild-type (wild-type) and mutant (S682P) mouse TRPV5 that were cloned in-frame with EGFP in the mammalian vector pCINeo/IRES-EGFP. HEK293 cells were seeded on fibronectin-coated coverslips (\varnothing 25 mm) and transfected with the appropriate pCINeo/IRES-EGFP vector. After 24hr, cells were loaded with 3 μ M Fura-2-AM (Molecular Probes) and (0.01% v/v) pluronic F-129 (Molecular Probes) in DMEM medium at 37°C for 20 min. After loading, cells were washed twice with PBS and allowed to equilibrate at 37°C for another 10 min in HEPES-Tris buffer (132.0 mM NaCl, 4.2 mM KCl, 1.4

Chapter 7

mM CaCl₂, 1.0 mM MgCl₂, 5.5 mM D-glucose and 10 mM HEPES, titrated to pH 7.4 with Tris). For Ca²⁺ free conditions, a similar buffer composition was used in which Ca²⁺ was substituted with 2 mM EGTA.

After Fura-2 loading, cells were placed in an incubation chamber and attached to the stage of an inverted microscope (Axiovert 200M, Carl Zeiss, Jena, Germany). Extracellular Ca²⁺ was changed using a perfusion system and resulting changes in cytosolic Ca²⁺ levels were monitored with Fura-2 excited at 340 and 380 nm using a monochromator (Polychrome IV, TILL Photonics, Gräfelfing, Germany). Fluorescence emission light was directed by a 415DCLP dichroic mirror (Omega Optical Inc., Brattleboro, VT, USA) through a 510WB40 emission filter (Omega Optical Inc.) onto a CoolSNAP HQ monochrome CCD-camera (Roper Scientific, Vianen, the Netherlands). The integration time of the CCD-camera was set at 200msec with a sampling interval of 3sec. All hardware was controlled with Metafluor 6.0 software (Universal Imaging Corporation, Downingtown, PA, USA). Quantitative image analysis was performed with Metamorph 6.0 (Molecular Devices Corporation, Sunnyvale, CA, USA). For each wavelength, the mean fluorescence intensity was monitored in an intracellular region and, for purpose of background correction, an extracellular region of identical size. After background correction, the fluorescence emission ratio of 340 nm and 380 nm excitation was calculated to determine the intracellular Ca²⁺ concentration. All measurements were performed at room temperature. Numerical results were visualized using Origin Pro 7.5 (OriginLab Corp., Northampton, MA, USA).

Statistical analysis

Data are presented as mean ± SEM unless otherwise stated. Statistical significance between two groups was determined by pair-wise comparisons using a two-tailed unpaired Student's *t*-test. For comparisons of parameters between wild-type, *Trpv5*^{682P/+} and *Trpv5*^{682P/682P} mice, ANOVA analysis with Bonferroni's correction for multiple comparisons was used.

TRPV5 and autosomal dominant hypercalciuria

Acknowledgements

We thank Kan-Pai Chiev for plasma and urine biochemistry, Caroline Barker for histology and Michelle Stewart for maintaining the mouse colony. This research was funded by grants from the European Union, EuReGene FP6 (NYL, LB, RDC, RVT), the Medical Research Council UK (LB, TAH, RDC, SDMB, RVT), Kidney Research UK (MJS), the Wellcome Trust (BNA, RVT), Glaxo SmithKline, and the University of Oxford (NYL), European Young Investigator award (JGH) and the Dutch Kidney foundation C05.2134 (HD).

Chapter 7

References

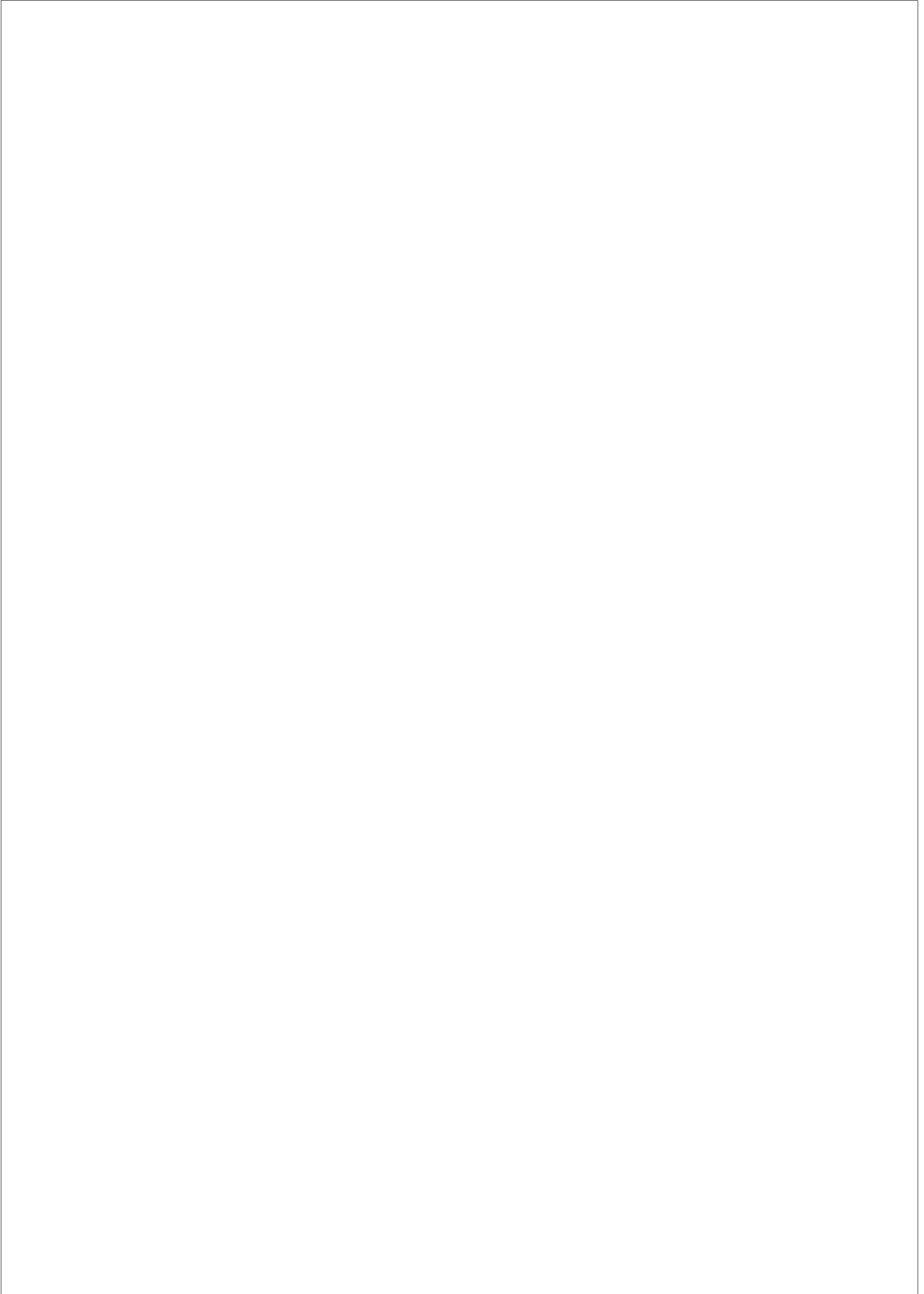
1. Coe FL, Evan A, Worcester E. Kidney stone disease. *J Clin Invest.* 2005;115(10):2598-2608.
2. Stechman MJ, Loh NY, Thakker RV. Genetic causes of hypercalciuric nephrolithiasis. *Pediatr Nephrol.* 2009;24(12):2321-2332.
3. Goldfarb DS, Fischer ME, Keich Y, Goldberg J. A twin study of genetic and dietary influences on nephrolithiasis: a report from the Vietnam Era Twin (VET) Registry. *Kidney Int.* 2005;67(3):1053-1061.
4. Hunter DJ, Lange M, Snieder H, MacGregor AJ, Swaminathan R, Thakker RV, Spector TD. Genetic contribution to renal function and electrolyte balance: a twin study. *Clin Sci (Lond).* 2002;103(3):259-265.
5. Moe OW, Bonny O. Genetic hypercalciuria. *J Am Soc Nephrol.* 2005;16(3):729-745.
6. Pak CY, Kaplan R, Bone H, Townsend J, Waters O. A simple test for the diagnosis of absorptive, resorptive and renal hypercalciurias. *N Engl J Med.* 1975;292(10):497-500.
7. Hoenderop JG, van Leeuwen JP, van der Eerden BC, Kersten FF, van der Kemp AW, Merillat AM, Waarsing JH, Rossier BC, Vallon V, Hummler E, et al. Renal Ca^{2+} wasting, hyperabsorption, and reduced bone thickness in mice lacking TRPV5. *J Clin Invest.* 2003;112(12):1906-1914.
8. Reed BY, Gitomer WL, Heller HJ, Hsu MC, Lemke M, Padalino P, Pak CY. Identification and characterization of a gene with base substitutions associated with the absorptive hypercalciuria phenotype and low spinal bone density. *J Clin Endocrinol Metab.* 2002;87(4):1476-1485.
9. Reed BY, Heller HJ, Gitomer WL, Pak CY. Mapping a gene defect in absorptive hypercalciuria to chromosome 1q23.3-q24. *J Clin Endocrinol Metab.* 1999;84(11):3907-3913.
10. Thorleifsson G, Holm H, Edvardsson V, Walters GB, Styrkarsdottir U, Gudbjartsson DF, Sulem P, Halldorsson BV, de Veigt F, d'Ancona FC, et al. Sequence variants in the CLDN14 gene associate with kidney stones and bone mineral density. *Nat Genet.* 2009;41(8):926-930.
11. Lloyd SE, Pearce SH, Fisher SE, Steinmeyer K, Schwappach B, Scheinman SJ, Harding B, Bolino A, Devoto M, Goodyer P, et al. A common molecular basis for three inherited kidney stone diseases. *Nature.* 1996;379(6564):445-449.
12. Pearce SH, Williamson C, Kifor O, Bai M, Coulthard MG, Davies M, Lewis-Barned N, McCredie D, Powell H, Kendall-Taylor P, et al. A familial syndrome of hypocalcemia with hypercalciuria due to mutations in the Ca^{2+} -sensing receptor. *N Engl J Med.* 1996;335(15):1115-1122.
13. Nolan PM, Peters J, Strivens M, Rogers D, Hagan J, Spurr N, Gray IC, Vizor L, Brooker D, Whitehill E, et al. A systematic, genome-wide, phenotype-driven mutagenesis

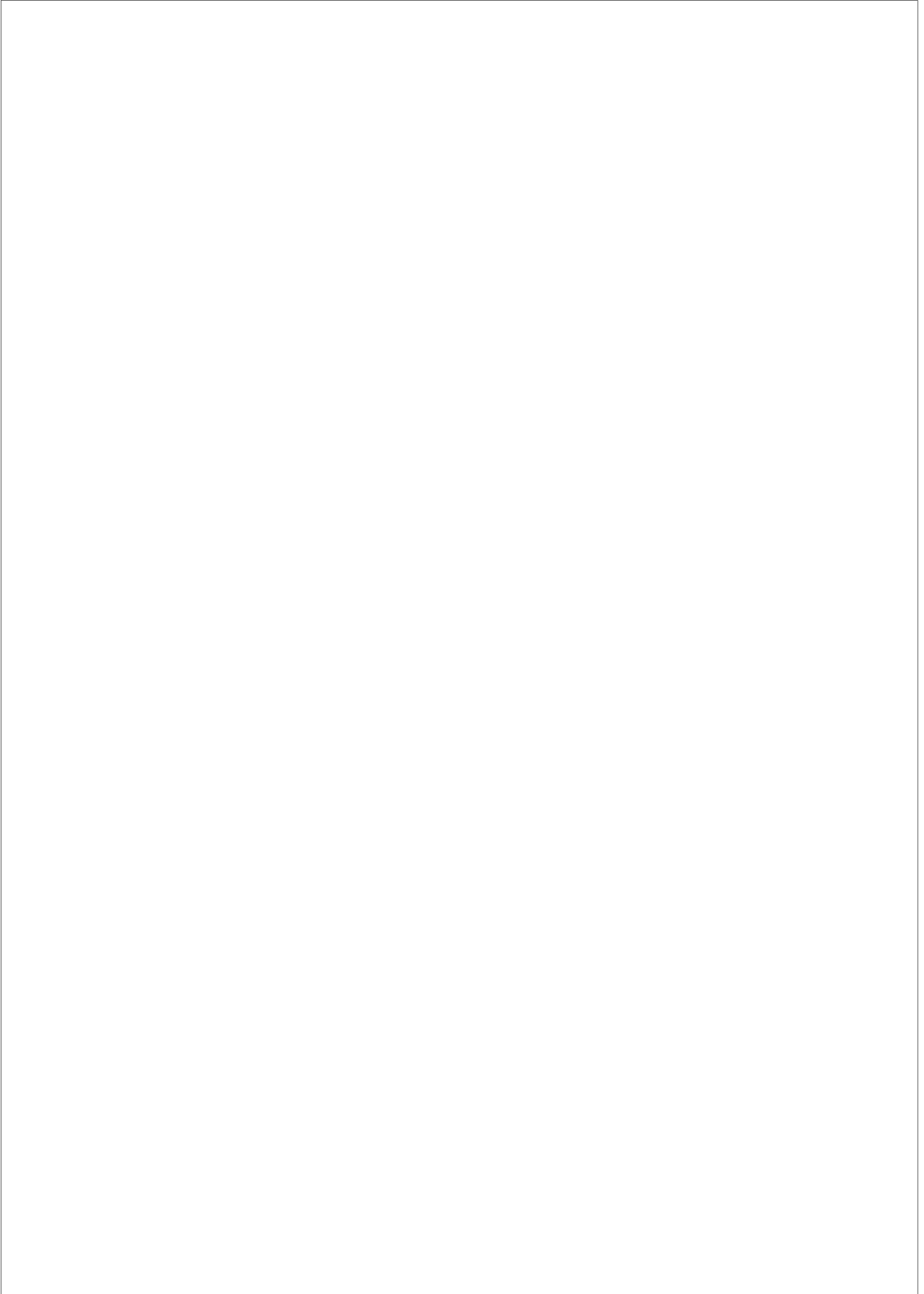
TRPV5 and autosomal dominant hypercalciuria

- programme for gene function studies in the mouse. *Nat Genet.* 2000;25(4):440-443.
14. Noveroske JK, Weber JS, Justice MJ. The mutagenic action of N-ethyl-N-nitrosourea in the mouse. *Mamm Genome.* 2000;11(7):478-483.
 15. Hoenderop JG, Nilius B, Bindels RJ. Ca^{2+} absorption across epithelia. *Physiol Rev.* 2005;85(1):373-422.
 16. Loffing J, Loffing-Cueni D, Valderrabano V, Klausli L, Hebert SC, Rossier BC, Hoenderop JG, Bindels RJ, Kaissling B. Distribution of transcellular Ca^{2+} and Na^{+} transport pathways along mouse distal nephron. *Am J Physiol Renal Physiol.* 2001;281(6):F1021-1027.
 17. Nijenhuis T, Hoenderop JG, van der Kemp AW, Bindels RJ. Localization and regulation of the epithelial Ca^{2+} channel TRPV6 in the kidney. *J Am Soc Nephrol.* 2003;14(11):2731-2740.
 18. Coleman RA, Wu DC, Liu J, Wade JB. Expression of aquaporins in the renal connecting tubule. *Am J Physiol Renal Physiol.* 2000;279(5):F874-883.
 19. Renkema KY, Velic A, Dijkman HB, Verkaart S, van der Kemp AW, Nowik M, Timmermans K, Doucet A, Wagner CA, Bindels RJ, et al. The Ca^{2+} -sensing receptor promotes urinary acidification to prevent nephrolithiasis. *J Am Soc Nephrol.* 2009;20(8):1705-1713.
 20. Na T, Zhang W, Jiang Y, Liang Y, Ma HP, Warnock DG, Peng JB. The A563T variation of the renal epithelial Ca^{2+} channel TRPV5 among African Americans enhances Ca^{2+} influx. *Am J Physiol Renal Physiol.* 2009;296(5):F1042-1051.
 21. Renkema KY, Lee K, Topala CN, Goossens M, Houillier P, Bindels RJ, Hoenderop JG. TRPV5 gene polymorphisms in renal hypercalciuria. *Nephrol Dial Transplant.* 2009.
 22. Vennekens R, Hoenderop JG, Prenen J, Stuiver M, Willems PH, Droogmans G, Nilius B, Bindels RJ. Permeation and gating properties of the novel epithelial Ca^{2+} channel. *J Biol Chem.* 2000;275(6):3963-3969.
 23. Embark HM, Setiawan I, Poppendieck S, van de Graaf SF, Boehmer C, Palmada M, Wieder T, Gerstberger R, Cohen P, Yun CC, et al. Regulation of the epithelial Ca^{2+} channel TRPV5 by the NHE regulating factor NHERF2 and the serum and glucocorticoid inducible kinase isoforms SGK1 and SGK3 expressed in *Xenopus* oocytes. *Cell Physiol Biochem.* 2004;14(4-6):203-212.
 24. Gkika D, Topala CN, Chang Q, Picard N, Thebault S, Houillier P, Hoenderop JG, Bindels RJ. Tissue kallikrein stimulates Ca^{2+} reabsorption via PKC-dependent plasma membrane accumulation of TRPV5. *Embo J.* 2006;25(20):4707-4716.
 25. van de Graaf SF, Chang Q, Mensenkamp AR, Hoenderop JG, Bindels RJ. Direct interaction with Rab11a targets the epithelial Ca^{2+} channels TRPV5 and TRPV6 to the plasma membrane. *Mol Cell Biol.* 2006;26(1):303-312.
 26. de Groot T, Lee K, Langeslag M, Xi Q, Jalink K, Bindels RJ, Hoenderop JG. Parathyroid hormone activates TRPV5 via PKA-dependent phosphorylation. *J Am Soc Nephrol.*

Chapter 7

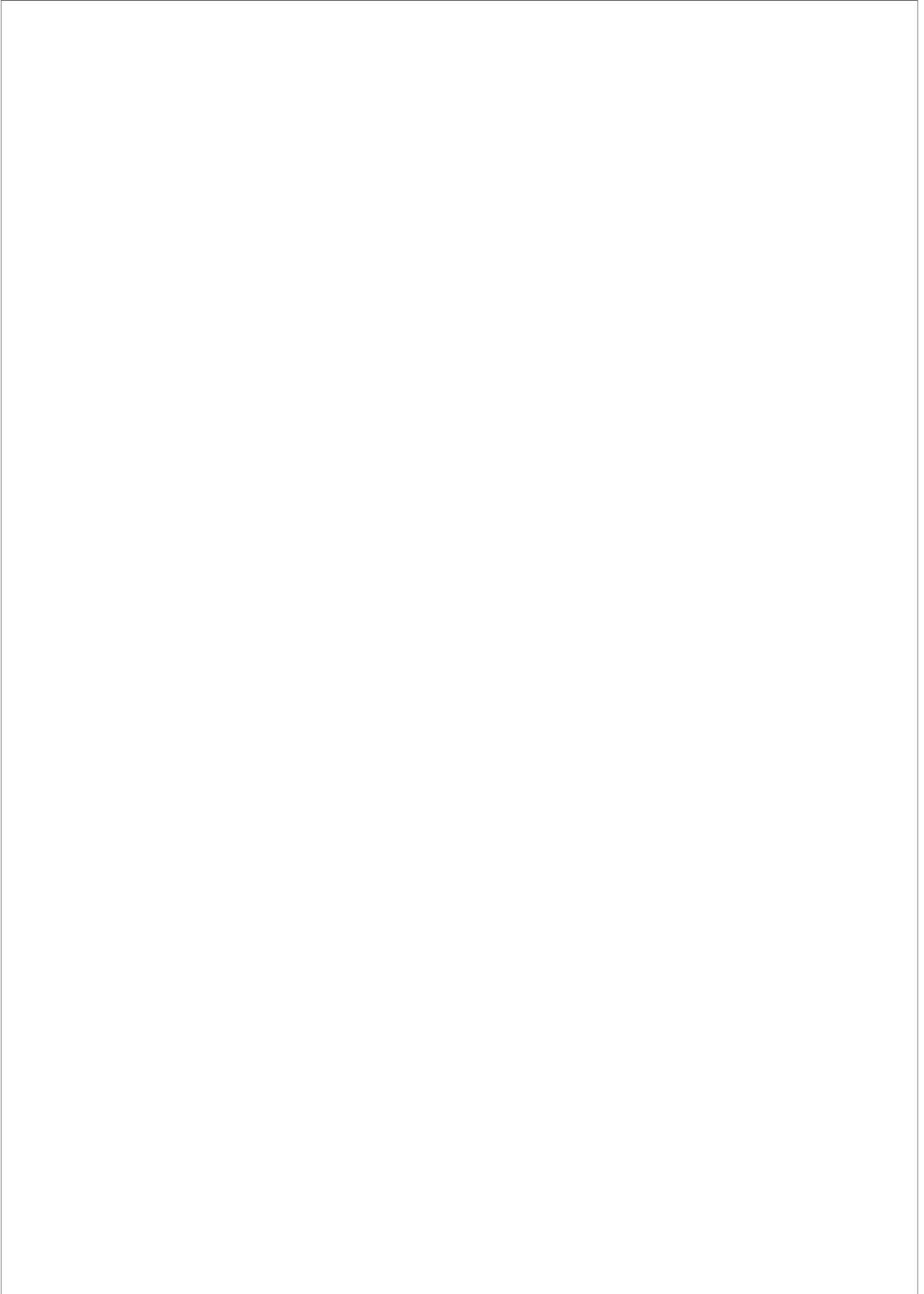
- 2009;20(8):1693-1704.
27. Alexander RT, Woudenberg-Vrenken TE, Buurman J, Dijkman H, van der Eerden BC, van Leeuwen JP, Bindels RJ, Hoenderop JG. Klotho Prevents Renal Ca^{2+} Loss. *J Am Soc Nephrol*. 2009.
 28. van Abel M, Hoenderop JG, van der Kemp AW, Friedlaender MM, van Leeuwen JP, Bindels RJ. Coordinated control of renal Ca^{2+} transport proteins by parathyroid hormone. *Kidney Int*. 2005;68(4):1708-1721.
 29. Murawski IJ, Maina RW, Malo D, Guay-Woodford LM, Gros P, Fujiwara M, Morgan K, Gupta IR. The C3H/HeJ inbred mouse is a model of vesico-ureteric reflux with a susceptibility locus on chromosome 12. *Kidney Int*.
 30. Stechman MJ, Ahmad BN, Loh NY, Reed AA, Stewart M, Wells S, Hough T, Bentley L, Cox RD, Brown SD, et al. Establishing normal plasma and 24-hour urinary biochemistry ranges in C3H, BALB/c and C57BL/6J mice following acclimatization in metabolic cages. *Lab Anim*.
 31. Hough TA, Bogani D, Cheeseman MT, Favor J, Nesbit MA, Thakker RV, Lyon MF. Activating Ca^{2+} -sensing receptor mutation in the mouse is associated with cataracts and ectopic calcification. *Proc Natl Acad Sci U S A*. 2004;101(37):13566-13571.
 32. Nijenhuis T, Hoenderop JG, Bindels RJ. Downregulation of Ca^{2+} and Mg^{2+} transport proteins in the kidney explains tacrolimus (FK506)-induced hypercalciuria and hypomagnesemia. *J Am Soc Nephrol*. 2004;15(3):549-557.
 33. Van Baal J, Yu A, Hartog A, Fransen JA, Willems PH, Lytton J, Bindels RJ. Localization and regulation by vitamin D of Ca^{2+} transport proteins in rabbit cortical collecting system. *Am J Physiol*. 1996;271(5 Pt 2):F985-993.





CHAPTER 8

General discussion and summary



Introduction

The kidney stabilizes the systemic electrolyte concentrations within normal ranges. This is achieved by amending the renal reabsorptive capacity for these electrolytes. The distal convoluted tubule (DCT), the connecting tubule (CNT), and the initial collecting duct (CD) (1)) plays a central role in reabsorbing Na^+ , Cl^- , Mg^{2+} , and Ca^{2+} from the renal ultrafiltrate. As such, NaCl transport within these segments contributes greatly to the maintenance and adjustment of blood pressure. Reabsorption of divalent cations by the distal convoluted tubule allows the maintenance of adequate plasma levels of Mg^{2+} and Ca^{2+} , which are essential for many physiological processes, such as neuronal excitability, muscle contraction, and bone formation. The distal convoluted tubule is under intense hormonal regulation to balance the urinary excretion of electrolytes in response to systemic changes in these ions. Thus, understanding the molecular pathways that regulate ion transport in the distal convoluted tubule, contributes importantly to the understanding of the physiology and pathophysiology of these aforementioned processes. As such, dysregulation of electrolyte transport in these segments (as exemplified by monogenic disorders affecting the distal convoluted tubule) may impose a shift or even completely blunt the renal reabsorptive capacity for these ions. Therefore, the overall aim of this thesis was to gain more knowledge about the regulation of electrolyte transport processes that are involved in the vectorial movement of Na^+ , Cl^- , Mg^{2+} , and Ca^{2+} across the distal convoluted tubule.

The distal convoluted tubule is composed of several cell types, which each are important for the transport of Na^+ , Cl^- , Mg^{2+} , and Ca^{2+} . Thiazide-sensitive NaCl transport occurs in the DCT cells, while amiloride-sensitive Na^+ transport predominates in the CNT and CD. The DCT2 is a segment in which the thiazide- and amiloride-sensitive Na^+ transport co-exists. Additionally, Mg^{2+} transport is localized exclusively in the DCT, while the cells of DCT2, CNT, and initial CD transport Ca^{2+} . The thiazide-sensitive NaCl cotransporter (NCC) localizes to the DCT1 and DCT2 segments. NCC colocalizes with the Transient Receptor Potential Melastin 6 channel (TRPM6),

Chapter 8

a divalent cation channel important for the apical uptake of Mg^{2+} in the DCT. In the DCT2, CNT and CD, the amiloride-sensitive epithelial Na^+ channel (ENaC) transports Na^+ from the filtrate. Similarly, the transient receptor potential vanilloid 5 channel (TRPV5), co-localizes with ENaC in the distal convoluted tubule and play an instrumental role in the apical uptake of Ca^{2+} . The distribution of electrolyte transport systems in the distal convoluted tubule is depicted in Figure 1.

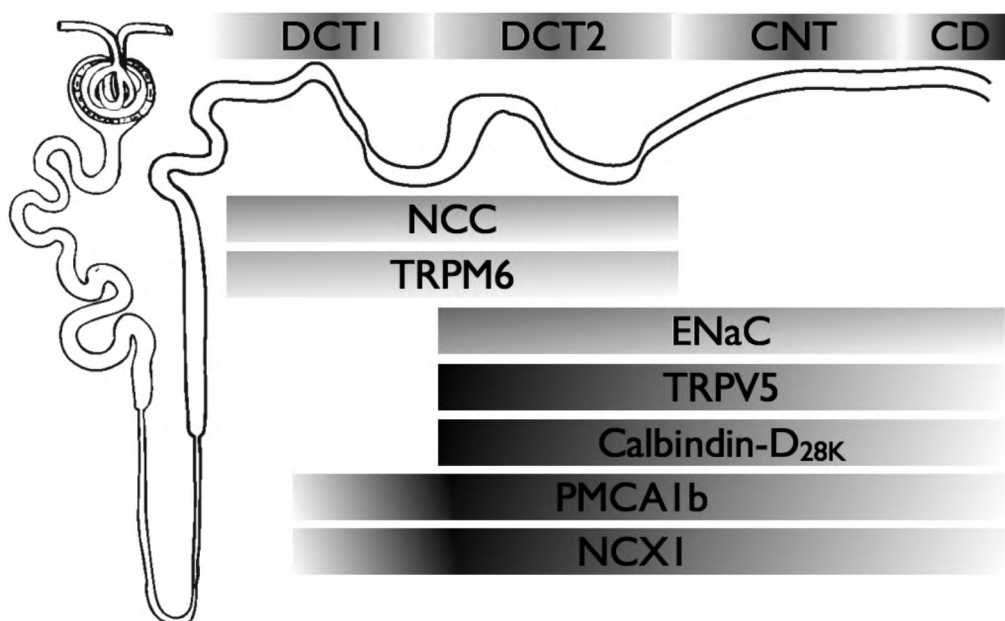


Figure 1. Distribution of electrolyte transport pathways in the distal convoluted tubule. NCC, thiazide-sensitive NaCl cotransporter; TRPM6, transient receptor potential melastatin 6 Mg^{2+} channel; ENaC, epithelial Na^+ channel; TRPV5, transient receptor potential vanilloid 5 Ca^{2+} channel. PMCA1b, plasma membrane Ca^{2+} ATPase 1b; NCX1, Na^+/Ca^{2+} exchanger. DCT, distal convoluted tubule; CNT, connecting tubule; CD, collecting duct.

NCC and γ -adducin

Hypertension remains a key player in the development of cardiovascular complications and chronic renal failure. NCC is of crucial importance for the reabsorption of NaCl by the distal convoluted tubule, thus influencing arterial pressure. In addition, thiazides that block NCC-dependent

General discussion

NaCl reabsorption are frequently prescribed for the treatment of hypertension. A better understanding of how NaCl transport is regulated via NCC may ultimately increase our understanding of how blood pressure is maintained and the etiology underlying primary hypertension. **Chapter 2** aimed to identify novel interactors of NCC, which could be involved in modulating its function. As the amino (N)-terminal domain has been shown to play an important role in activating the transporter, we performed pull down experiments using the N-terminal domain of NCC as bait. Mouse kidney lysates were screened and precipitates were subsequently sent for mass spectrometry analysis. Here we identified γ -adducin as a novel auxiliary factor interacting with NCC. The adducin gene family had previously been implicated in arterial hypertension. As such, one single nucleotide polymorphism (SNP) in the γ -adducin gene has been described, which is involved in systolic pressure regulation in certain individuals (2). Thus, γ -adducin was an interesting candidate gene for the regulating of NCC.

Our study identified γ -adducin as a strong interactor of the N-terminal domain of NCC. Using $^{22}\text{Na}^+$ uptakes in *Xenopus laevis* oocytes injected with NCC in the presence and absence of γ -adducin, we found that γ -adducin markedly stimulated the activity of the transporter. siRNA directed against the endogenous *Xenopus laevis* γ -adducin reduced NCC-dependent $^{22}\text{Na}^+$ uptake. Competition with increasing amounts of the N-terminal part of NCC completely reverted the stimulatory action of γ -adducin on thiazide-sensitive $^{22}\text{Na}^+$ transport. In addition, the γ -adducin binding site is mapped to the exact region encompassing three phosphorylation sites in the cotransporter. NCC forms lacking phosphorylatable sites in the N-terminus do not exhibit increased $^{22}\text{Na}^+$ transport rates when co-injected with γ -adducin. Moreover, γ -adducin dissociates from NCC when the phospho-residues are converted to aspartates, mimicking a constitutively active phosphorylated state of the transporter. Based on the data generated in **Chapter 2**, we could generate a model predicting the role of γ -adducin in activating NCC. γ -Adducin may stimulate NCC activity by anchoring a kinase, likely members of the STE20 family (encompassing the Ste20-related proline-alanine-rich kinase (SPAK) and oxidative stress

Chapter 8

response 1 (OSR1)) to the dephosphorylated transporter. Subsequently, the kinase increases the phosphorylation level of NCC, thereby stimulating the activity of the transporter. After the kinase-mediated phosphorylation event, γ -adducin dissociates from NCC and may also facilitate the release of the associated kinase. Dephosphorylation of the transporter reduces the activity of NCC to its basal state. The data obtained in **Chapter 2** strongly suggest that γ -adducin may contribute importantly to the regulation of NCC and hence blood pressure maintenance.

The role of the WNK family in the maintenance of ambient blood pressure has been firmly established as pseudohypoaldosteronism type II, due to defects in the *WNK1* and *WNK4* genes results in an augmented renal reabsorption of NaCl and an increased arterial pressure (3, 4). Moreover, renal NaCl wasting and secondary hypokalemic metabolic alkalosis is observed in Gitelman patients with a defect in the *SLC12A3* gene encoding NCC (5, 6). Gitelman patients have been reported with mutations in one of the phosphorylation sites (threonine 60 converted to methionine) (7), further solidifying the need for intact NCC phosphorylation sites in ambient blood pressure maintenance and renal NaCl reabsorption. These observations also suggest that changes in γ -adducin function could influence the arterial pressure, by a skewed regulation of the NCC phosphorylation state. Interestingly, one intronic SNP has been described in the γ -adducin gene, which correlates with systolic pressure, but only in individuals that also harbor the G460W polymorphism in α -adducin (2). These observations suggest that γ -adducin can affect blood pressure, potentially by altering the phosphorylation level of NCC, however in order to be visible clinically, arterial pressure needs to be perturbed by the G460W polymorphism in α -adducin. The findings of **Chapter 2** may aid in the understanding of the complex cascade regulating NCC activity in the distal convoluted tubule and may help elucidate the molecular events underlying the formation of primary hypertension.

Figure 2 depicts the complex interplay between the different factors regulating NCC. It also attempts to place these previously known findings in the context of γ -adducin. Phosphorylation of the N-terminal domain in NCC seems to be a common final pathway by which

General discussion

several stimuli converge to regulate the activity of the transporter. As such, SPAK and OSR1 have both been shown to modulate the direct phosphorylation of NCC (8, 9). Also both With-No-Lysine (WNK) kinases 1 and 4 regulate the phosphorylation level of NCC by modulating the STE20 kinases (8, 10). The positive effect of WNK4 on NCC phosphorylation, occurs only in the presence of angiotensin II, via activating phosphorylation upon sites in the STE20 family of

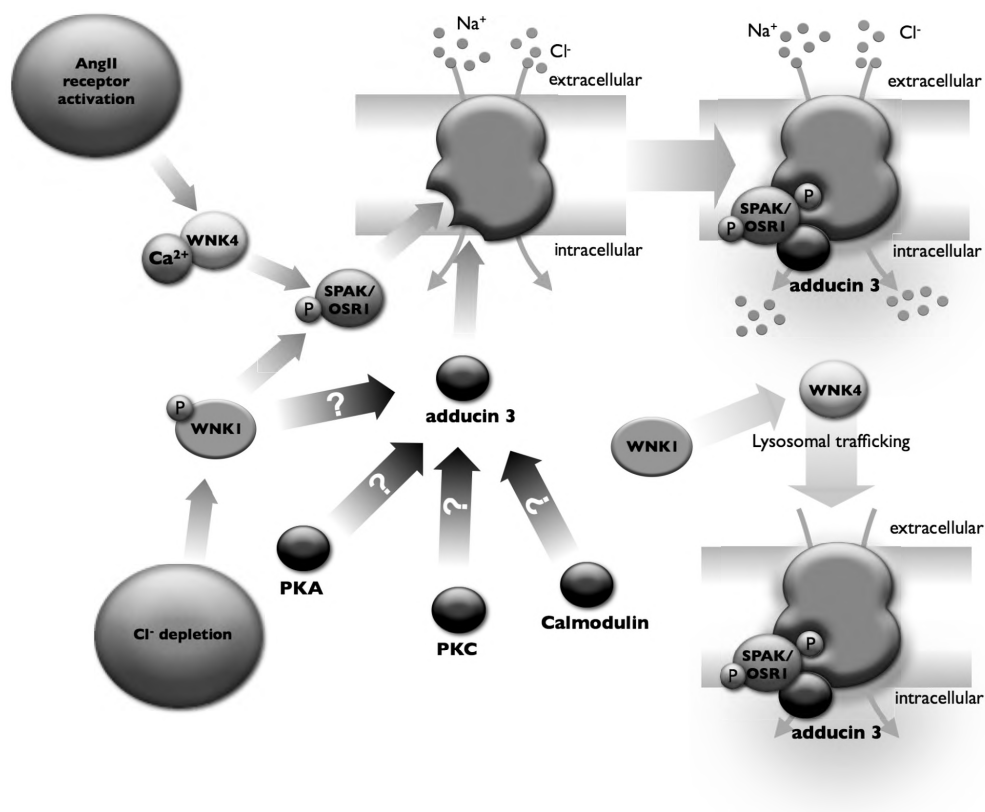


Figure 2. Proposed model depicting the complex regulation of NCC and the potential role of γ -adducin. AngII, angiotensin II; WNK, with-no-lysine, SPAK, Ste20-related proline-alanine-rich kinase; OSR1, oxidative stress response 1; PKA, protein kinase A; PKC, protein kinase C.

kinases (10). It is likely the intracellular Ca²⁺ concentration that dictates whether WNK4 acts as an activator of NCC. Thus, when the angiotensin II type I receptor is activated, intracellular

Chapter 8

elevations in Ca^{2+} causes WNK4 to act as an activator of NCC, by modulating phosphorylation. In the absence of angiotensin II-dependent increases in intracellular Ca^{2+} , WNK4 functions by removing NCC from the membrane, diverting it to the lysosomal compartment (11, 12). As several of the mutations in WNK4 which are observed in PHAII are located near a putative Ca^{2+} binding site, it may be that these mutations mimic Ca^{2+} binding, hence leading to increased phosphorylation of NCC and hypertension. γ -Adducin reverted the inhibitory effect of WNK4 on NCC in its basal state (i.e. without activation of the angiotensin II receptor). Moreover, our data suggest that γ -adducin stimulates a process occurring before the lysosomal removal of NCC, namely phosphorylation. It is currently unclear whether WNK4 can stimulate or interact with γ -adducin in its angiotensin II activated state, a matter for future studies. Another, and perhaps even more interesting point which could be addressed experimentally is the potential involvement of WNK1 in the phosphorylation cascade, leading to NCC activation. WNK1 increases the transport activity and phosphorylation level of NCC during Cl^- -depleted conditions, due to activation of SPAK and OSR1 (8). Whether a potential additional effect could be on γ -adducin remains to be determined, but should be considered likely. As will be discussed below, several other kinases can activate the adducin family leading either to changes in its localization or function. WNK1 also plays an additional role in NCC trafficking, as the protein can block the lysosomal shuttling of NCC mediated by WNK4, via interaction with the kinase (11, 13).

The adducin family of kinases contains several phosphorylation sites, making them substrates for protein kinases A (PKA) and protein kinase C (PKC). In addition, the adducin's also bind calmodulin, another Ca^{2+} -activated protein (14). PKA-dependent phosphorylation of adducin causes a reduced affinity for spectrin-F-actin complexes (14). Moreover, phosphorylation of adducin by PKC has been shown crucial for platelet activation and for the localization of the protein (15-17). It is currently difficult to translate potential changes in the phosphorylation level of γ -adducin by either PKA or PKC into functional changes in NCC. However, it has been shown that NCC is phosphorylated upon vasopressin dependent PKA

General discussion

activation (18). Moreover, both PKA and PKC phosphorylation at certain sequences leads to inhibition of calmodulin-binding in the β -adducin subunit. Whether, this is also occurring in the γ -adducin subunit remains unclear. It is however noteworthy that calmodulin, similarly to WNK4, is activated by elevations in intracellular Ca^{2+} (14). Future experiments are necessary to dissect whether there is a functional overlap between these signaling pathways and the coordinated function of γ -adducin and NCC.

Another pathway potentially activating γ -adducin deserves mentioning. Aldosterone is an important hormone involved in blood pressure maintenance and potassium secretion. These actions are in part mediated by increasing transport capacity in the DCT. Aldosterone has been shown to affect NCC phosphorylation as blockade of the mineralocorticoid receptor by spironolactone prevents phosphorylation of NCC during dietary Na^+ restriction (19). The expression of the serum- and glucocorticoid-inducible kinase 1 (SGK1) is increased by aldosterone, leading to several of the so-called early responses of aldosterone. Lack of SGK1 in mice has recently been shown to attenuate the increase in NCC phosphorylation, normally observed after dietary Na^+ deprivation (20). Interestingly, γ -adducin contains a predicted SGK1 site at serine 42. Given the available data of aldosterone on NCC activation, the potential involvement of this putative SGK1 phosphorylation site deserves further investigation.

Erlotinib and EGF-stimulated TRPM6 activity

TRPM6 is critically involved in active Mg^{2+} reabsorption in the distal convoluted tubule, acting as the apical entry step for Mg^{2+} in the DCT. Thus, the regulation of TRPM6 determines the final concentration of Mg^{2+} in the blood. Overall maintenance of plasma Mg^{2+} concentrations is essential for many cellular processes, including adequate function of neurological and cardiovascular systems. Therefore, factors affecting TRPM6 may cause e.g. neuromuscular dysfunction (tetany, muscle cramps and weakness as well as cardiac arrhythmias and

Chapter 8

tachycardia) in certain pathological states. Anti-cancer treatments with Cetuximab, a monoclonal antibody targeting the epidermal growth factor receptor (EGFR), causes hypomagnesemia in patients with colorectal cancer (21). However, numerous patient groups suffering from cancer receive tyrosine kinase inhibitors, such as Erlotinib (see figure 3 for summarized mechanisms of action). There are no published clinical reports detailing the potential effect of tyrosine kinase inhibitors on systemic and renal Mg^{2+} handling. **Chapter 3** shows that Erlotinib is capable of affecting TRPM6 regulation and thereby altering Mg^{2+} handling. We observed that mice, which received supraphysiological doses of Erlotinib for 23 days, developed a decrease in their serum Mg^{2+} concentration. In addition, these Erlotinib-injected mice failed to reduce the fractional renal excretion of Mg^{2+} in response to a decreased serum Mg^{2+} concentration. Whole-cell patch clamp analysis can be used to determine the cellular permeability of an ion, generated by one or more channels. Using this technique in human embryonic kidney (HEK) 293 cells, we found that Erlotinib significantly inhibited EGF-stimulated TRPM6 channel activity. The HEK293 cells received dosages in the same range as the expected plasma concentration in mice (30 μ M of Erlotinib). Although moderate effects of Erlotinib were observed *in vivo*, application of the compound could still block EGF-stimulated TRPM6 currents and routing in HEK293 cells. Given that the free circulating concentration of Erlotinib is likely to be around 0.3 μ M in human patients, we tested whether this concentration would be able to block the effect of EGF on TRPM6 currents. Here we could not detect any significant differences from EGF-stimulated cells. Evaluating EGF-induced tyrosine phosphorylation of its receptor substantiated these data. In addition, the inhibitory effect of Erlotinib on Mg^{2+} transport is likely to occur via inhibition of TRPM6 routing, by preventing EGF-mediated changes in the mobile fraction of TRPM6 proteins.

As many as 97% of colorectal cancer patients treated with the monoclonal antibody EGFR inhibitors such as Cetuximab develop hypomagnesemia to varying degree (21). These compounds are currently being considered as first-line treatment for metastatic colorectal cancer. However, side-effects due to these drugs are largely unexplored. It is now becoming increasingly

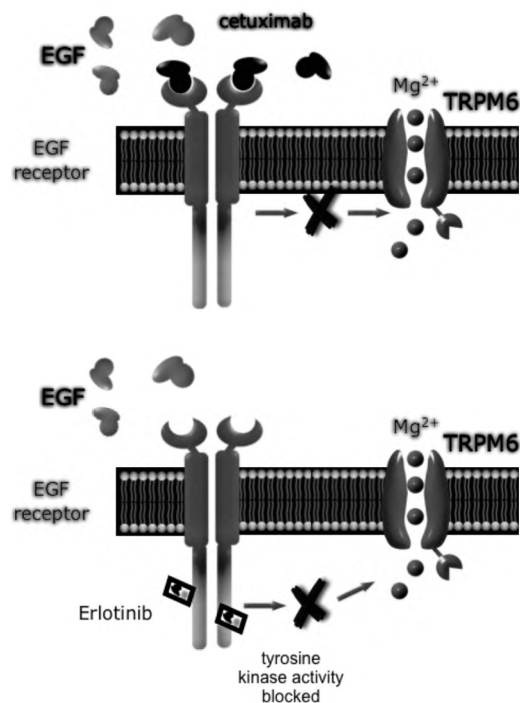


Figure 3. EGFR blockade by Erlotinib and Cetuximab can prevent EGF-induced changes in TRPM6 channel activity. (top) The blocking effects of Cetuximab on EGFR activity. The antibody binds with a 10 times higher affinity to the EGFR, as compared to EGF, thereby preventing EGFR dimerization and activation. (bottom) Erlotinib binds to the ATP binding pocket on the EGFR. This blocks tyrosine kinase activity and hence EGFR signalling. These effects are likely not observed at the dosages given to humans.

clear that hypomagnesemia is one of the most commonly reported side-effects. **Chapter 3** is the first to delineate the effects of Erlotinib on Mg²⁺ handling *in vivo*. The effect on the systemic Mg²⁺ concentration seems less potent than that observed with antibody-based EGFR inhibitors. Still, clinical data detailing the effect of Erlotinib on Mg²⁺ handling is lacking. However, based on the doses given to cancer patients it is unlikely that Erlotinib severely affects serum Mg²⁺ concentrations in these individuals. As a result of mutations, the EGFR is overexpressed in many types of cancer, presumably leading to uncontrolled cell division. Blocking the receptor either using monoclonal antibodies or tyrosine kinase inhibitors would therefore slow cancer progression. However, while Erlotinib blocks the EGFR by binding to the ATP pocket, Cetuximab

Chapter 8

binds the receptor with almost 10 times higher affinity than that of EGF. One could envision that while Erlotinib only blocks the overexpressed EGFR often found in tumors, due to its affinity for the receptor and overall circulating levels in the body, this inhibitor is unlikely to interfere with the normal functions of the EGFR, such as the reabsorption of Mg^{2+} in the distal convolution. However, due to the high affinity of the Cetuximab compound, hypomagnesemia might develop. Many patients undergoing chemotherapy are receiving combination therapy with nephrotoxic and potential Mg^{2+} -wasting drugs such as Cisplatinum. It should be noted that Erlotinib has the potential to modulate renal and systemic Mg^{2+} handling *in vivo*. Therefore, caution should be given when treating individuals prone to developing hypomagnesemia, such as patients receiving combinational treatment with Mg^{2+} lowering compounds.

Androgens and TRPV5-dependent Ca^{2+} transport

Active renal Ca^{2+} reabsorption in the distal convolution is critical in determining the final urinary Ca^{2+} excretion. Mice with a targeted deletion of the *TRPV5* gene show augmented renal Ca^{2+} loss, due to a blunted Ca^{2+} reabsorption in the distal convolution (22). The Ca^{2+} transport capacity in this segment is regulated by calcitropic hormones, such as parathyroid hormone (PTH) and 1,25-dihydroxyvitamin D_3 (23-25). In addition, estrogen has been shown to affect active renal Ca^{2+} transport (23, 26). Studies have previously addressed the impact of gender on the expression of renal transport proteins and consequently renal electrolyte handling. For instance, the density of NCC (quantified by 3H -metolazone binding) was two-fold higher in female, than in male rats (27). Furthermore, orchidectomy (ORX) resulted in an increase in 3H -metolazone binding sites in males, whereas ovariectomy decreased the binding density in females (27). In terms of the maintenance of overall Ca^{2+} balance, several gender differences exist. Males have greater urinary Ca^{2+} losses than females (28, 29). In addition, estrogens have been shown to increase the renal reabsorption of Ca^{2+} , in agreement with the observed gender

General discussion

differences (30). Presently, it remains unclear whether androgens play an opposing role to estrogens in modulating renal Ca^{2+} reabsorption. Thus, in **Chapter 4** we elucidated whether androgens contribute to the gender differences in renal Ca^{2+} handling. As such, we investigated its ability to regulate the expression of renal Ca^{2+} transport proteins, in particular the Ca^{2+} channel, TRPV5. The study showed that testosterone contributes significantly to the sex differences observed in renal Ca^{2+} handling. Male mice had a greater urinary Ca^{2+} excretion compared to females, which is accompanied by a reduced renal expression of Ca^{2+} transport proteins. Androgen-deficient ORX mice showed a significant reduction in the urinary excretion of Ca^{2+} . This reduction in urinary Ca^{2+} excretion was reverted after testosterone replacement. Similar data was obtained when evaluating the fractional excretion of Ca^{2+} , suggesting that the testosterone-induced increase of urinary Ca^{2+} excretion is due to inhibition of tubular Ca^{2+} reabsorption. Renal mRNA and protein abundance of Ca^{2+} transporters was up-regulated in ORX mice, a feature which was normalized when the mice were resupplied with testosterone. In addition, inhibition of transcellular Ca^{2+} transport after dihydrotestosterone treatment was observed in rabbit kidney CNT/cortical CD (CCD) primary cell cultures.

Chapter 4 provides evidence that androgens contribute to the gender differences in renal Ca^{2+} handling. These effects occur by inhibiting the expression of renal Ca^{2+} transport proteins and independent of changes in calciotropic hormones or estrogen. Thus, as the role of estrogens on overall Ca^{2+} metabolism and Ca^{2+} storage in bone are well known. It is also widely accepted that the presence or absence of estrogen is critically involved in setting the urinary excretion of Ca^{2+} as well as determining the bone mineral density. However, the effect of androgens on mineral metabolism have only now been delineated and one has to reconsider previous gender differences relating to the effect of estrogen alone, and perhaps reevaluate these gender differences, not only as a result of estrogen levels, but also in part due to differences in the circulating levels of androgens. In that respect, males have larger urinary Ca^{2+} excretion than females as well as higher incidence for the development of kidney stones (31). The exact

Chapter 8

contribution of androgens to the development of kidney stones in males (or absence thereof in females) remains to be studied in detail, but based on the observations made in **Chapter 4**, it is likely that androgens contribute importantly to the differences observed between males and females.

It seems that the distal convoluted tubule is a target for sex hormones and that the regulation of the different transporters is highly dependent on gender. We as well as others have now shown that key transporters in this segment are regulated by not only estrogens, but also by androgens.

Calcitonin and renal Ca²⁺ transport

Active transcellular Ca²⁺ transport is restricted to the distal convoluted tubule. Studies in rabbit suggested that calcitonin (CT) exerted its effect on Ca²⁺ reabsorption only in DCT, while no stimulation occurs in the CNT (32). In addition, CT fails to stimulate cAMP accumulation in the CNT of rabbits (33). In the rabbit, TRPV5 localizes primarily to the CNT where CT does not affect Ca²⁺ reabsorption. However, in rats and mice, TRPV5 is highly expressed in apical membrane domains of particularly the DCT2 segment, with a gradual decrease along CNT and initial CD (23, 34). The intrarenal distribution of TRPV5 in human is currently not known, however the structure of the distal convoluted tubule is similar to that of mouse. The bright portion of the DCT retains responsiveness to CT in the rat kidney, resulting in increased cAMP production (35). In addition, binding sites for CT have been identified in the rat kidney, including the thick ascending limb and DCT (36). Other cAMP-elevating hormones including PTH affect TRPV5-mediated Ca²⁺ transport by modulating expression and channel activity (25, 37). Currently, it is unclear whether there is a functional overlap between PTH and CT in the DCT2 regions of rats and mice and whether the CT-induced increase in cAMP could lead to a similar activation in the DCT2 segment as PTH.

Chapter 5 determined the molecular actions of CT on overall renal Ca²⁺ balance and

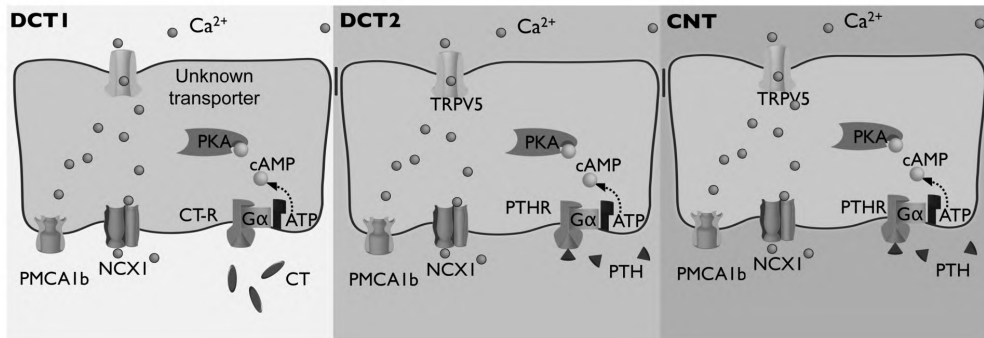
General discussion

delineates the potential effects of CT on TRPV5 dependant Ca^{2+} reabsorption in the distal convoluted tubule. Injections of CT for 16 or 40 hrs did not change the renal abundance of TRPV5. In addition, wild-type ($\text{TRPV5}^{+/+}$) and TRPV5 deficient ($\text{TRPV5}^{-/-}$) mice responded in a similar manner to CT administration. Given the data obtained in these experimental models, it is likely that the effect of CT on renal Ca^{2+} transport occurs independently of TRPV5. Although CT does not affect TRPV5-mediated Ca^{2+} reabsorption, it is clear from this study that CT strongly stimulates renal Ca^{2+} reabsorption. The stimulatory effect of CT is likely to occur primarily through changes in Ca^{2+} transport in the thick ascending limb, as previously described (38-40) and in the DCT via an unknown mechanism (41). In conclusion, CT augments the renal reabsorptive capacity for Ca^{2+} . This increase is likely to occur independently of TRPV5.

The distribution of electrolyte transport pathways and receptor signaling systems in the distal convoluted tubule is still being explored. It is difficult to separate experimentally the actions of DCT1, DCT2, and CNT cells without a detailed knowledge of the transport systems located in these segments and their pharmacological inhibition profile. In the rat, CT increases Ca^{2+} transport in the DCT (41), while the present study suggests that these effects occur largely independent of TRPV5. In rabbit, CT stimulates Ca^{2+} transport in the early DCT, where TRPV5 is not expressed (32). This raises the question of how Ca^{2+} transport occurs in the early DCT. Weak immunostaining for the $\text{Na}^+/\text{Ca}^{2+}$ exchanger (NCX1) and the plasma membrane Ca^{2+} pump (PMCA1b) has been observed in DCT1 segments of the mouse, suggesting that perhaps transepithelial Ca^{2+} transport also occurs in these cells (23, 34). Earlier studies in non-polarized immortalized mouse DCT cells, have demonstrated that CT increases chloride conductance resulting in membrane hyperpolarization, thereby driving Ca^{2+} entry through dihydropyridine-sensitive Ca^{2+} channels (42). TRPV5 mediated transport has been shown to be dihydropyridine-insensitive (43). L-type Ca^{2+} channels are particularly sensitive to dihydropyridine. Other voltage-dependent Ca^{2+} channels also exist including the T, N, and P

Chapter 8

Mouse



Rabbit

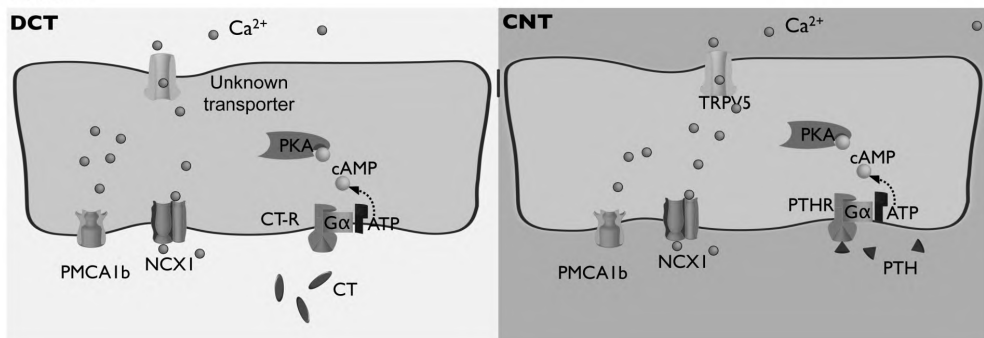


Figure 4. Distribution of cAMP-dependent Ca^{2+} transport mechanisms in the distal convoluted of the mouse and rabbit. PMCA1b, plasma membrane Ca^{2+} ATPase 1b; NCX1, $\text{Na}^+/\text{Ca}^{2+}$ exchanger; TRPV5, transient receptor potential vanilloid 5 Ca^{2+} channel; PTH, parathyroid hormone; PTHR, parathyroid hormone receptor; CT, calcitonin; CTR, calcitonin receptor. Adapted from T. de Groot (37).

types which show different electrophysiological characteristics and pharmacological inhibition profiles (44). Voltage-dependent Ca^{2+} channels have previously been located to the kidney. A gene encoding the pore-forming alpha 1-subunit was identified in kidney and found expressed predominantly in the DCT (45). In addition, a pore-forming alpha (1G) subunit with T-type characteristics has been detected in apical membrane domains of the DCT (46). However, how much such a mechanism would contribute to overall Ca^{2+} transport in the distal convoluted and within the kidney remains entirely unclear. Future studies are needed to further evaluate the role of potential Ca^{2+} transporting proteins in this segment. A schematic model predicting the

General discussion

segmentation of receptor systems and electrolyte transporters in the distal convoluted tubule, can be found in figure 4.

Tissue Transglutaminase and inhibition of TRPV5-mediated Ca^{2+} transport

Transport in the distal convoluted tubule is tightly regulated, by a large variety of molecular factors, hormones, and other signaling molecules. A group of regulating factors acting from the extracellular side, has recently been described to modulate the function of electrolyte transporters within the distal convoluted tubule. Several extracellular proteases have been shown to modulate the transport of Na^+ via ENaC expressed in the distal convoluted tubule and the remaining CD. In terms of Ca^{2+} , several factors have been shown to affect channel function from the luminal side. Tissue Kallikrein (TK) is one of the major proteins synthesized within the distal convoluted tubule and secreted into the tubular fluid. TK has been shown to stimulate Ca^{2+} reabsorption via protein kinase C-dependent plasma membrane accumulation of TRPV5 (47). Similarly, Klotho is another protein that acts from the extracellular side, removing oligosaccharides from the complex N-glycan of TRPV5. This extracellular modification results in delayed retrieval of the Ca^{2+} channel from the apical plasma membrane and subsequently increased Ca^{2+} transport (48). The stimulatory effect of Klotho was entirely dependent on the N-glycosylation of TRPV5. Extracellular protons have also been shown to alter the plasma membrane recruitment of TRPV5 and hence the activity of the channel. **Chapter 6** describes the identification of Tissue Transglutaminase (tTG) as a novel molecular inhibitor of TRPV5, acting from the extracellular side in a N-glycosylation-dependent manner.

tTG is a multifunctional Ca^{2+} -dependent enzyme, catalyzing the covalent crosslinking of proteins. tTG is an intracellular enzyme, which is also secreted by cells, suggesting that in kidney, the enzyme could act from the urinary side. tTG has been shown to be regulated by TRPV channels, in other epithelia (49, 50). In terms of TRPV5-dependent transport, it is not known

Chapter 8

whether this Ca^{2+} -activated enzyme affects Ca^{2+} transport in the distal convoluted tubule. We found that tTG is secreted into the urine in mice, expressed in polarized primary CNT/CCD cells from rabbit, and secreted into the apical medium of these cells. In addition, tTG decreases the activity of TRPV5 in HEK293 cells and inhibits transcellular Ca^{2+} transport in polarized primary CNT/CCD cells. This process likely occurs via covalent crosslinking of TRPV5 monomers, effectively decreasing the pore size of the channel. The inhibitory effect of tTG depends on the N-glycosylation state of TRPV5 as the N-glycosylation-deficient mutant is not susceptible to tTG-catalyzed modifications.

The findings in **Chapter 6** suggest a possible crosstalk between these two molecular factors (Klotho and tTG), both acting from the extracellular side, affecting TRPV5 transport in a N-glycosylation dependent manner, but via two distinct molecular mechanisms. Thus, while Klotho can cleave the N-glycan of TRPV5 and stimulate transport, tTG needs the N-glycan to exert its covalent cross-linked inhibition. Such an observation also suggests that Klotho could have the ability to overrule the effect of tTG, by cleaving the sugar tree of TRPV5. However, before such conclusions can be drawn firmly, two important experiments have to be performed. One that tests the effect of Klotho on tTG mediated inhibition of TRPV5 and one that tests whether Klotho can access the sugar tree, when tTG is present in sufficient quantity to normally inhibit TRPV5 transport. So although not fully delineated in detail yet, such a cross talk would be a novel mechanism by which several extracellular factors can interact via a common structure on the extracellular side of the protein. It is likely that future studies will uncover more of such factors, potentially secreted by the cells in the distal convoluted tubule, acting on channels and transports in these segments.

Autosomal dominant hypercalciuria due to a missense mutation in TRPV5

Ca^{2+} transport in the distal convoluted tubule contributes greatly to the total amount of Ca^{2+} reabsorbed

General discussion

by the kidney. This is evident as absence of TRPV5 leads to an elevated amount of Ca^{2+} in the urine of mice with a targeted deletion of the TRPV5 gene. Hypercalciuria can lead to kidney stone disease (nephrolithiasis). Nephrolithiasis is a major health problem affecting approximately 10% of elderly in their seventh decade of life (51). As many as 80% of kidney stones formed are Ca^{2+} based (51, 52). In addition, hypercalciuria is the most common metabolic abnormality found in Ca^{2+} stone formers. Hypercalciuria and nephrolithiasis are strongly influenced by genetic factors and between 35-65% of patients with hypercalciuric stone disease have affected family members (52). In order to investigate the possible genetic influence on hypercalciuria, and hence the generation of nephrocalcinosis and nephrolithiasis, we utilized a *N*-ethyl-*N*-nitrosourea (ENU) mouse mutagenesis resource in a phenotype-driven screen, to identify new genetic models of hypercalciuria. **Chapter 7** reports the identification of a mouse with severe autosomal dominant hypercalciuria. This defect was caused by a novel missense S682P mutation in the *TRPV5* gene. The study delineates the identification and functional characterization of this gene defect. We found that the expression of TRPV5 in *Trpv5*^{682P/+} and *Trpv5*^{682P/682P} kidneys is altered. In the *Trpv5*^{682P/+} mice, expression of TRPV5 is affected only in DCT2, while TRPV5 expression is reduced in both the DCT2 and CNT in the *Trpv5*^{682P/682P} mice. In addition, renal calbindin-D_{28k}-expression in *Trpv5*^{682P/682P} mouse kidneys was greatly reduced, further supporting a specific defect in TRPV5-mediated Ca^{2+} reabsorption. The alteration from serine 682 to a proline resulted in a reduced basal intracellular Ca^{2+} level in HEK293 cells transfected with the TRPV5 mutant, indicating a defect in the TRPV5-mediated Ca^{2+} permeability of the cell. In addition, approximately 10% of the male mice develop primary tubulointerstitial nephritis, consistent with urinary reflux.

TRPV5 is highly expressed in apical membrane domains of the DCT2 cell with a gradual decrease in TRPV5 expression is observed along the CNT and CD in the mouse, suggesting that the majority of TRPV5-mediated Ca^{2+} transport occurs in the DCT2 segment of the distal convoluted. **Chapter 7** supports this observation as selective loss of TRPV5 from the DCT2

Chapter 8

results in hypercalciuria in the *Trpv5*^{682P/+} mice. The reason for this type of selective loss remains unexplored. Potentially, this could be due to proteins regulating TRPV5, that are expressed only in DCT2 cells, but not in the CNT segment. Thus, this observation further underscores the axial heterogeneity within the distal convolution.

The hypercalciuria in these mice is inherited in an autosomal dominant fashion. This can be explained by the observation that the TRPV5 channel comprises four TRPV5 monomers that form a central pore. Thus, it is likely that the TRPV5-S682P protein is exerting a dominant-negative effect on the wild-type TRPV5 protein. No syndromes of hypercalciuria resulting in mutations of TRPV5 have previously been described. However, a recent paper found that SNPs in the *TRPV5* gene correlates with increased Ca²⁺ transport via TRPV5, potentially explaining the lower urine Ca²⁺ excretion and reduced risk of kidney stones in African Americans compared with white Americans (53).

It should also be noted that these mice do not display nephrolithiasis, as would be expected in conditions of hypercalciuria. The reason for this has been delineated in mice with a targeted deletion of the *TRPV5* gene (54). Due to the elevated loss of Ca²⁺ in these mice, the Ca²⁺-sensing receptor becomes activated. This leads to an increased H⁺ excretion acidifying the urine and a downregulation of the aquaporin 2 water channel causing polyuria. Disrupting these processes in part by deleting the collecting duct-specific B1 subunit of H⁺-ATPase in TRPV5 deficient mice, eliminates urinary acidification and results in tubular precipitations of Ca²⁺ stones in the renal medulla (54). The *Trpv5*^{682P/682P} mouse is the first model reported to have dominant hypercalciuria and a missense mutation in TRPV5. This model may therefore prove useful in understanding the interplay between TRPV5 in the distal convolution and other factors potentially involved in the underlying genetic basis of hypercalciuria and perhaps nephrolithiasis.

General discussion

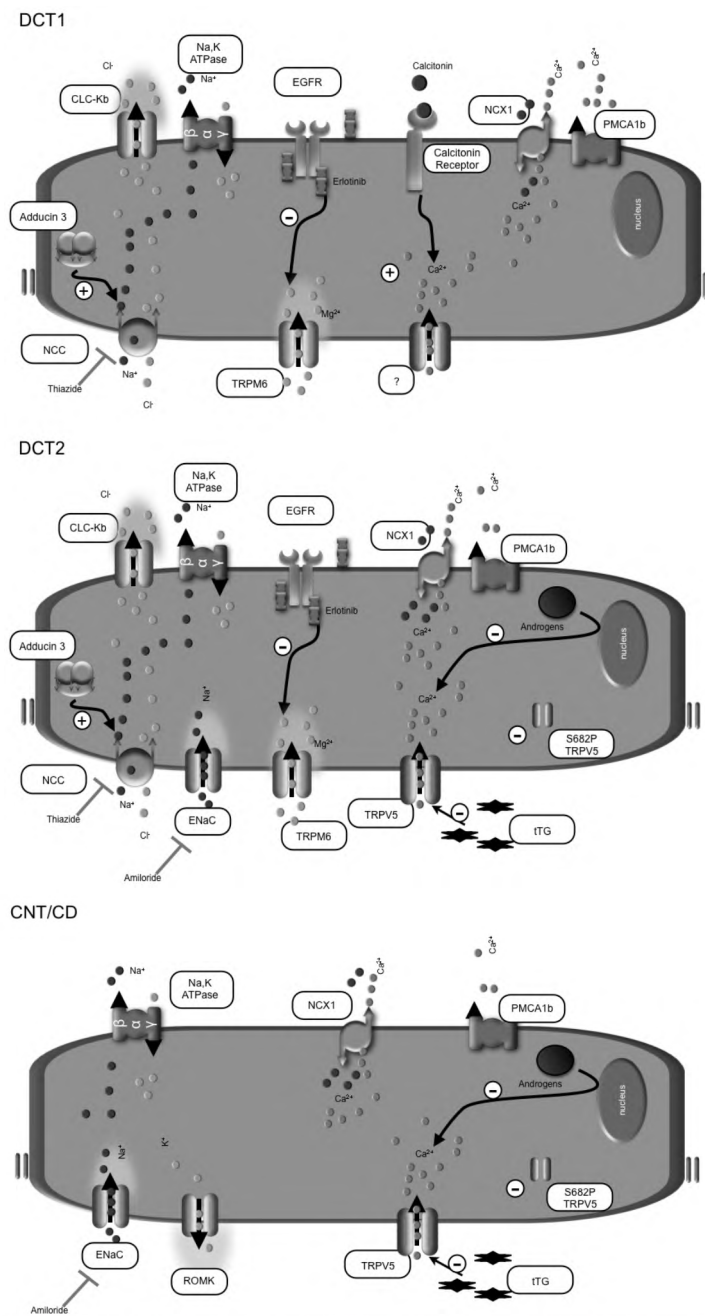


Figure 5. Schematic model of newly identified regulatory pathways within the distal convoluted tubule. NCC, thiazide-sensitive NaCl cotransporter; CLC-Kb, Cl⁻ channel Kb; TRPM6, transient receptor potential melastatin 6 Mg²⁺ channel; EGFR, epidermal growth factor receptor. Na⁺, K⁺-ATPase consisting of α , β , and γ subunits. ENaC, epithelial Na⁺ channel; ROMK, renal outer medullary K⁺ channel; TRPV5, transient receptor potential vanilloid 5 Ca²⁺ channel. PMCA1b, plasma membrane Ca²⁺-ATPase 1b; NCX1, Na⁺/Ca²⁺ exchanger.

Chapter 8

Conclusion

The overall aims of this thesis were to elucidate the molecular pathways that govern electrolyte transport in the distal convoluted tubule. The thesis investigated in detail the molecular regulation of NCC, TRPM6, and TRPV5 in an effort to understand how the transport of electrolyte by these carriers can be affected. The necessity of maintaining the systemic concentrations of electrolytes such as Na^+ , Cl^- , Ca^{2+} , and Mg^{2+} within normal limits is evident, as disturbances in these ions affect many important physiological processes. The detailed characterization of the molecular mechanisms regulating these transport systems, may aid in providing sufficient knowledge to treat or manage diseases related to defective renal electrolyte transport within the distal convoluted tubule.

The findings of this thesis are summarized in figure 5. As outlined in the figure, γ -adducin regulates the activity of NCC, which is expressed exclusively in the DCT1 and DCT2 segments within the kidney. Furthermore, Erlotinib can inhibit the EGF-stimulated activity of TRPM6, a protein co-localizing to the DCT1 and DCT2 with NCC. As calcitonin stimulates Ca^{2+} transport in the early distal segment (DCT1), but does not seem to affect TRPV5, we can assume that it potentially activates another carrier for Ca^{2+} . However, the physiological relevance of such a transport system remains incompletely understood. In the DCT2 and CNT, androgens inhibit the expression of Ca^{2+} proteins, including TRPV5. Moreover, tTG also impose an inhibition of TRPV5 in these segments, by chemically crosslinking the channel monomers and changing pore diameter. In the *Trpv5*^{682P/+} mice, selective loss of TRPV5 from the DCT2 segment is observed, while in the *Trpv5*^{682P/682} homozygotes loss of TRPV5 occurs from both the DCT2 and CNT segments.

Future perspectives

In recent years, many studies have elucidated new roles for the distal convoluted tubule in renal electrolyte transport and regulation thereof. This has contributed importantly to the understanding of the physiology and pathophysiology of the distal convoluted tubule. The new regulatory pathways found in this thesis will further help in expanding this understanding. We showed that γ -adducin regulates the activity of the NCC cotransporter. A future goal involves identifying the possible involvement of the α -adducin family member, which also is expressed within the kidney, in addition to the many kinases involved in NCC regulation. We elucidated the molecular effect of Erlotinib and its potential relation to clinical hypomagnesemia. Thereby, an alternative treatment could be suggested in some forms of cancer where there is an often occurrence of hypomagnesemia due to anti-EGFR therapy. We identified new molecular and physiological regulators of TRPV5, including tTG, and the androgenic hormones. Furthermore, we found that calcitonin was unable to stimulate TRPV5 dependent Ca^{2+} transport. Future studies directed at identifying the overall contributions of these factors to Ca^{2+} homeostasis by regulating transport within the distal convoluted tubule are needed. Also, the potential regulation of these newly identified regulators by other calciotropic factors may help to further solidify their roles in renal Ca^{2+} handling. Finally, the S682P mutations in the TRPV5 gene confer a phenotype resembling that of the TRPV5 deficient animals, although in a dominant negative fashion. New studies should aim at elucidating the molecular mechanism by which Ca^{2+} permeability and expression of TRPV5 is impaired due to this missense mutation.

Chapter 8

References

1. Kriz W, Bankir L. A standard nomenclature for structures of the kidney. The Renal Commission of the International Union of Physiological Sciences (IUPS). *Kidney Int.* 1988;33(1):1-7.
2. Cwynar M, Staessen JA, Ticha M, Nawrot T, Citterio L, Kuznetsova T, Wojciechowska W, Stolarz K, Filipovsky J, Kawecka-Jaszcz K, et al. Epistatic interaction between alpha- and gamma-adducin influences peripheral and central pulse pressures in white Europeans. *J Hypertens.* 2005;23(5):961-969.
3. Gordon RD. The syndrome of hypertension and hyperkalemia with normal glomerular filtration rate: Gordon's syndrome. *Aust N Z J Med.* 1986;16(2):183-184.
4. Wilson FH, Disse-Nicodeme S, Choate KA, Ishikawa K, Nelson-Williams C, Desitter I, Gunel M, Milford DV, Lipkin GW, Achard JM, et al. Human hypertension caused by mutations in WNK kinases. *Science.* 2001;293(5532):1107-1112.
5. Gitelman HJ, Graham JB, Welt LG. A new familial disorder characterized by hypokalemia and hypomagnesemia. *Trans Assoc Am Physicians.* 1966;79(221-235).
6. Simon DB, Nelson-Williams C, Bia MJ, Ellison D, Karet FE, Molina AM, Vaara I, Iwata F, Cushner HM, Koolen M, et al. Gitelman's variant of Bartter's syndrome, inherited hypokalaemic alkalosis, is caused by mutations in the thiazide-sensitive NaCl cotransporter. *Nat Genet.* 1996;12(1):24-30.
7. Lin SH, Shiang JC, Huang CC, Yang SS, Hsu YJ, Cheng CJ. Phenotype and genotype analysis in Chinese patients with Gitelman's syndrome. *J Clin Endocrinol Metab.* 2005;90(5):2500-2507.
8. Richardson C, Rafiqi FH, Karlsson HK, Moleleki N, Vandewalle A, Campbell DG, Morrice NA, Alessi DR. Activation of the thiazide-sensitive NaCl cotransporter by the WNK-regulated kinases SPAK and OSR1. *J Cell Sci.* 2008;121(Pt 5):675-684.
9. Rafiqi FH, Zuber AM, Glover M, Richardson C, Fleming S, Jovanovic S, Jovanovic A, O'Shaughnessy KM, Alessi DR. Role of the WNK-activated SPAK kinase in regulating blood pressure. *EMBO Mol Med.* 2010;2(2):63-75.
10. San-Cristobal P, Pacheco-Alvarez D, Richardson C, Ring AM, Vazquez N, Rafiqi FH, Chari D, Kahle KT, Leng Q, Bobadilla NA, et al. Angiotensin II signaling increases activity of the renal NaCl cotransporter through a WNK4-SPAK-dependent pathway. *Proc Natl Acad Sci U S A.* 2009;106(11):4384-4389.
11. Yang CL, Angell J, Mitchell R, Ellison DH. WNK kinases regulate thiazide-sensitive NaCl cotransport. *J Clin Invest.* 2003;111(7):1039-1045.
12. Zhou B, Zhuang J, Gu D, Wang H, Cebotaru L, Guggino WB, Cai H. WNK4 Enhances the Degradation of NCC through a Sortilin-Mediated Lysosomal Pathway. *J Am Soc Nephrol.* 2009.
13. Yang CL, Zhu X, Ellison DH. The thiazide-sensitive NaCl cotransporter is regulated by a

General discussion

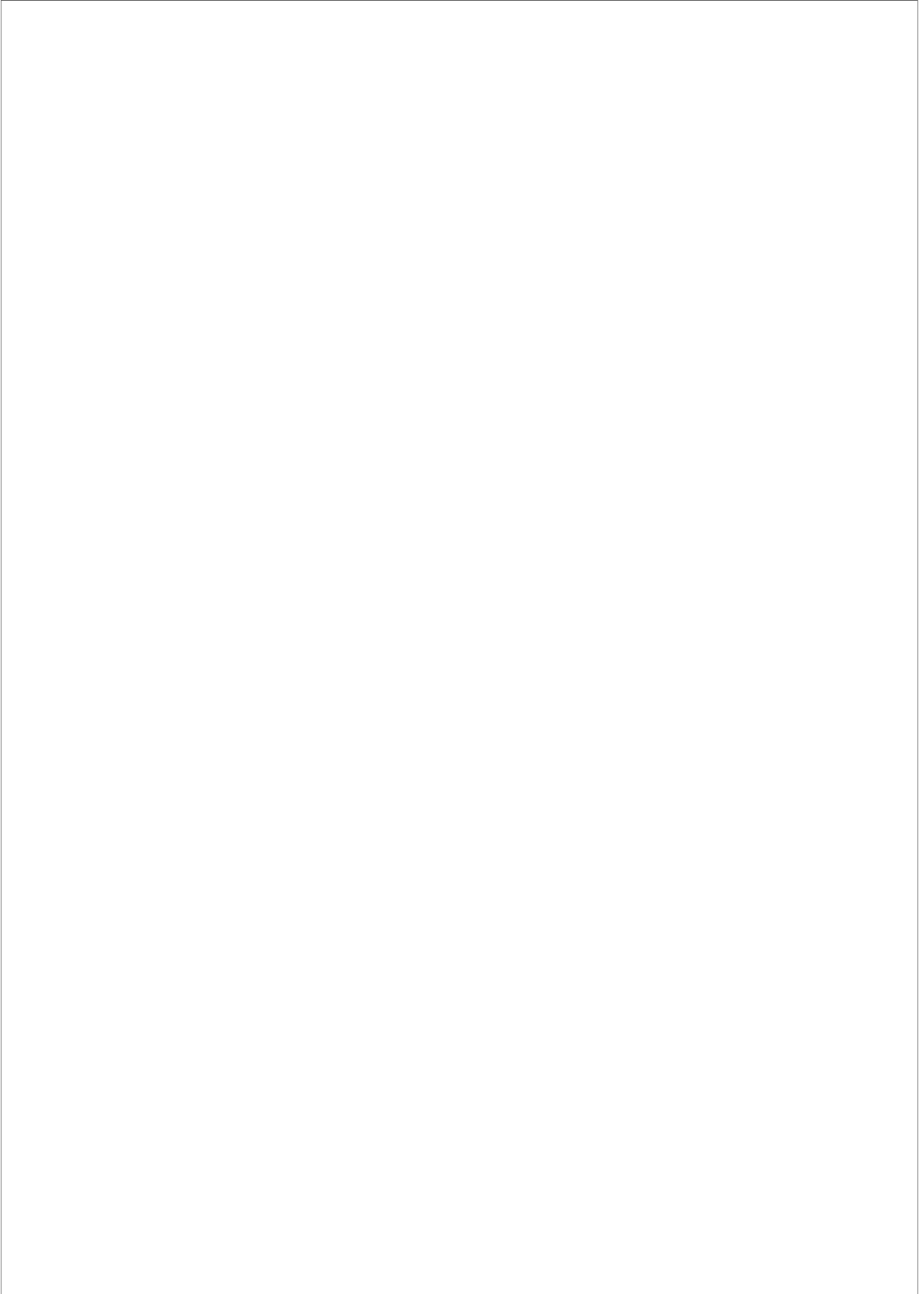
- WNK kinase signaling complex. *J Clin Invest.* 2007;117(11):3403-3411.
14. Matsuoka Y, Hughes CA, Bennett V. Adducin regulation. Definition of the calmodulin-binding domain and sites of phosphorylation by protein kinases A and C. *J Biol Chem.* 1996;271(41):25157-25166.
 15. Fowler L, Dong L, Bowes RC, 3rd, van de Water B, Stevens JL, Jaken S. Transformation-sensitive changes in expression, localization, and phosphorylation of adducins in renal proximal tubule epithelial cells. *Cell Growth Differ.* 1998;9(2):177-184.
 16. Fowler L, Everitt J, Stevens JL, Jaken S. Redistribution and enhanced protein kinase C-mediated phosphorylation of alpha- and gamma-adducin during renal tumor progression. *Cell Growth Differ.* 1998;9(5):405-413.
 17. Barkalow KL, Italiano JE, Jr., Chou DE, Matsuoka Y, Bennett V, Hartwig JH. Alpha-adducin dissociates from F-actin and spectrin during platelet activation. *J Cell Biol.* 2003;161(3):557-570.
 18. Pedersen NB, Hofmeister MV, Rosenbaek LL, Nielsen J, Fenton RA. Vasopressin induces phosphorylation of the thiazide-sensitive NaCl cotransporter in the distal convoluted tubule. *Kidney Int.*
 19. Chiga M, Rai T, Yang SS, Ohta A, Takizawa T, Sasaki S, Uchida S. Dietary salt regulates the phosphorylation of OSR1/SPAK kinases and the NaCl cotransporter through aldosterone. *Kidney Int.* 2008;74(11):1403-1409.
 20. Vallon V, Schroth J, Lang F, Kuhl D, Uchida S. Expression and phosphorylation of the Na⁺-Cl⁻ cotransporter NCC in vivo is regulated by dietary NaCl, K⁺, and SGK1. *Am J Physiol Renal Physiol.* 2009;297(3):F704-712.
 21. Tejpar S, Piessevaux H, Claes K, Piront P, Hoenderop JG, Verslype C, Van Cutsem E. Magnesium wasting associated with epidermal-growth-factor receptor-targeting antibodies in colorectal cancer: a prospective study. *Lancet Oncol.* 2007;8(5):387-394.
 22. Hoenderop JG, van Leeuwen JP, van der Eerden BC, Kersten FF, van der Kemp AW, Merillat AM, Waarsing JH, Rossier BC, Vallon V, Hummler E, et al. Renal Ca²⁺ wasting, hyperabsorption, and reduced bone thickness in mice lacking TRPV5. *J Clin Invest.* 2003;112(12):1906-1914.
 23. Hoenderop JG, Nilius B, Bindels RJ. Ca²⁺ absorption across epithelia. *Physiol Rev.* 2005;85(1):373-422.
 24. Hoenderop JG, Muller D, Van Der Kemp AW, Hartog A, Suzuki M, Ishibashi K, Imai M, Sweep F, Willems PH, Van Os CH, et al. Calcitriol controls the epithelial Ca²⁺ channel in kidney. *J Am Soc Nephrol.* 2001;12(7):1342-1349.
 25. van Abel M, Hoenderop JG, van der Kemp AW, Friedlaender MM, van Leeuwen JP, Bindels RJ. Coordinated control of renal Ca²⁺ transport proteins by parathyroid hormone. *Kidney Int.* 2005;68(4):1708-1721.
 26. Hoenderop JG, Bindels RJ. Calcitropic and magnesiotropic TRP channels. *Physiology*

Chapter 8

- (Bethesda). 2008;23(32-40).
27. Chen Z, Vaughn DA, Fanestil DD. Influence of gender on renal thiazide diuretic receptor density and response. *J Am Soc Nephrol*. 1994;5(4):1112-1119.
 28. Morgan B, Robertson WG. The urinary excretion of Ca^{2+} . An analysis of the distribution of values in relation to sex, age and Ca^{2+} deprivation. *Clin Orthop Relat Res*. 1974;101:254-267.
 29. Davis RH, Morgan DB, Rivlin RS. The excretion of Ca^{2+} in the urine and its relation to Ca^{2+} intake, sex and age. *Clin Sci*. 1970;39(1):1-12.
 30. Van Abel M, Hoenderop JG, Dardenne O, St Arnaud R, Van Os CH, Van Leeuwen HJ, Bindels RJ. 1,25-dihydroxyvitamin D_3 -independent stimulatory effect of estrogen on the expression of ECaC1 in the kidney. *J Am Soc Nephrol*. 2002;13(8):2102-2109.
 31. Robertson WG, Peacock M, Heyburn PJ, Hanes FA. Epidemiological risk factors in Ca^{2+} stone disease. *Scand J Urol Nephrol Suppl*. 1980;53(15-30).
 32. Shimizu T, Yoshitomi K, Nakamura M, Imai M. Effects of PTH, calcitonin, and cAMP on Ca^{2+} transport in rabbit distal nephron segments. *Am J Physiol*. 1990;259:F408-414.
 33. Chabardes D, Imbert-Teboul M, Montegut M, Clique A, Morel F. Distribution of calcitonin-sensitive adenylate cyclase activity along the rabbit kidney tubule. *Proc Natl Acad Sci U S A*. 1976;73(10):3608-3612.
 34. Loffing J, Loffing-Cueni D, Valderrabano V, Klausli L, Hebert SC, Rossier BC, Hoenderop JG, Bindels RJ, Kaissling B. Distribution of transcellular Ca^{2+} and sodium transport pathways along mouse distal nephron. *Am J Physiol Renal Physiol*. 2001;281(6):F1021-1027.
 35. Morel F. Sites of hormone action in the mammalian nephron. *Am J Physiol*. 1981;240(3):F159-164.
 36. Sexton PM, Adam WR, Moseley JM, Martin TJ, Mendelsohn FA. Localization and characterization of renal calcitonin receptors by in vitro autoradiography. *Kidney Int*. 1987;32(6):862-868.
 37. de Groot T, Lee K, Langeslag M, Xi Q, Jalink K, Bindels RJ, Hoenderop JG. Parathyroid Hormone Activates TRPV5 via PKA-Dependent Phosphorylation. *J Am Soc Nephrol*. 2009; 20(8):1693-1704,
 38. De Rouffignac C, Di Stefano A, Wittner M, Roinel N, Elalouf JM. Consequences of differential effects of ADH and other peptide hormones on thick ascending limb of mammalian kidney. *Am J Physiol*. 1991;260(6 Pt 2):R1023-1035.
 39. Di Stefano A, Wittner M, Nitschke R, Braitsch R, Greger R, Bailly C, Amiel C, Roinel N, de Rouffignac C. Effects of parathyroid hormone and calcitonin on Na^+ , Cl^- , K^+ , Mg^{2+} and Ca^{2+} transport in cortical and medullary thick ascending limbs of mouse kidney. *Pflugers Arch*. 1990;417(2):161-167.
 40. Elalouf JM, Roinel N, de Rouffignac C. ADH-like effects of calcitonin on electrolyte

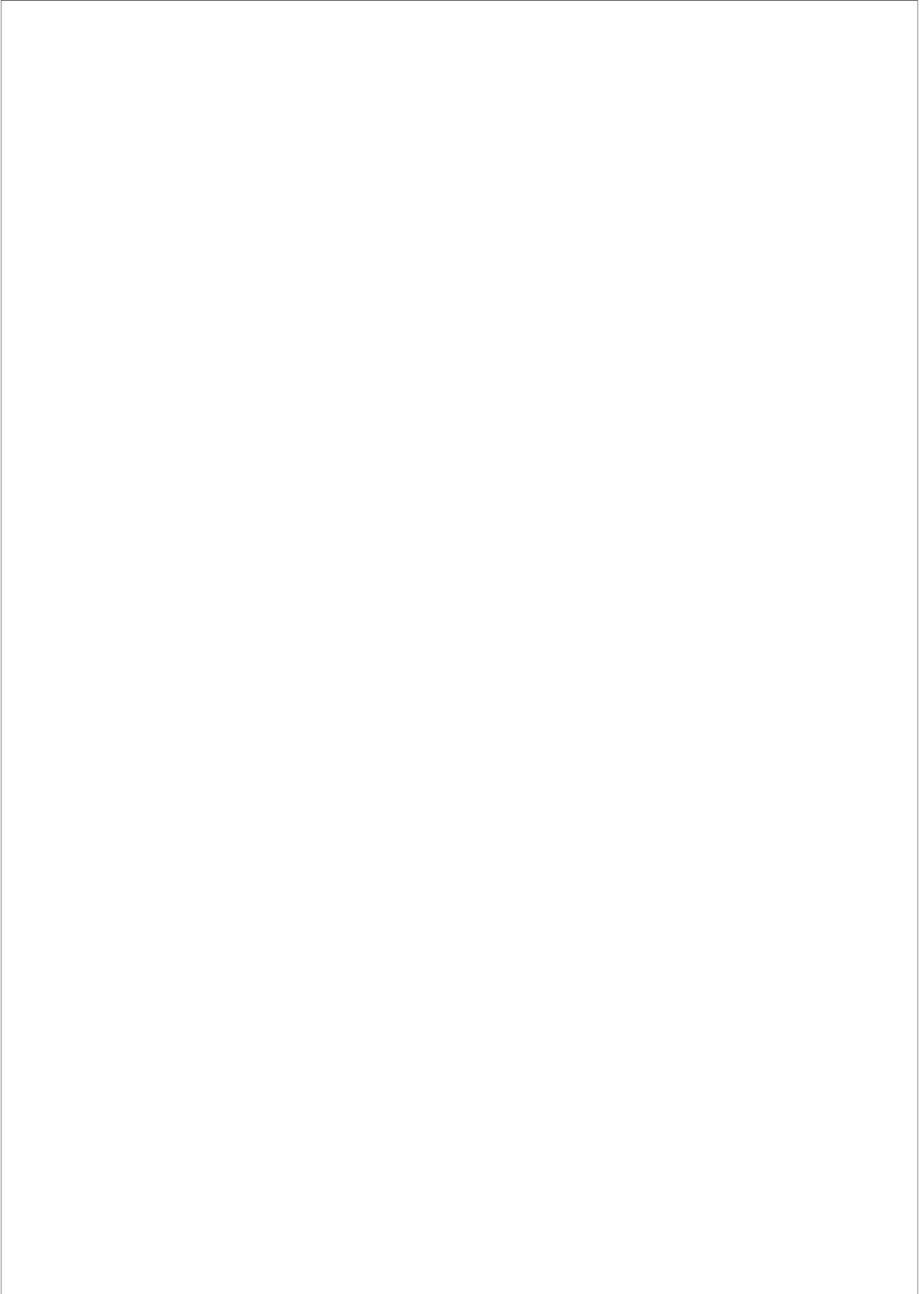
General discussion

- transport by Henle's loop of rat kidney. *Am J Physiol.* 1984;246(2 Pt 2):F213-220.
41. Elalouf JM, Roinel N, de Rouffignac C. Stimulation by human calcitonin of electrolyte transport in distal tubules of rat kidney. *Pflugers Arch.* 1983;399(2):111-118.
 42. Gesek FA, Friedman PA. Calcitonin stimulates Ca^{2+} transport in distal convoluted tubule cells. *Am J Physiol.* 1993;264(4 Pt 2):F744-751.
 43. Hoenderop JG, van der Kemp AW, Hartog A, van de Graaf SF, van Os CH, Willems PH, Bindels RJ. Molecular identification of the apical Ca^{2+} channel in 1, 25-dihydroxyvitamin D_3 -responsive epithelia. *J Biol Chem.* 1999;274(13):8375-8378.
 44. Hess P. Ca^{2+} channels in vertebrate cells. *Annu Rev Neurosci.* 1990;13: 337-356.
 45. Yu AS, Hebert SC, Brenner BM, Lytton J. Molecular characterization and nephron distribution of a family of transcripts encoding the pore-forming subunit of Ca^{2+} channels in the kidney. *Proc Natl Acad Sci U S A.* 1992;89(21):10494-10498.
 46. Andreasen D, Jensen BL, Hansen PB, Kwon TH, Nielsen S, Skott O. The alpha(1G)-subunit of a voltage-dependent Ca^{2+} channel is localized in rat distal nephron and collecting duct. *Am J Physiol Renal Physiol.* 2000;279(6):F997-1005.
 47. Gkika D, Topala CN, Chang Q, Picard N, Thebault S, Houillier P, Hoenderop JG, Bindels RJ. Tissue kallikrein stimulates Ca^{2+} reabsorption via PKC-dependent plasma membrane accumulation of TRPV5. *Embo J.* 2006;25(20):4707-4716.
 48. Chang Q, Hoefs S, van der Kemp AW, Topala CN, Bindels RJ, Hoenderop JG. The beta-glucuronidase Klotho hydrolyzes and activates the TRPV5 channel. *Science.* 2005;310(5747):490-493.
 49. Cheng X, Jin J, Hu L, Shen D, Dong XP, Samie MA, Knoff J, Eisinger B, Liu ML, Huang SM, et al. TRP channel regulates EGFR signaling in hair morphogenesis and skin barrier formation. *Cell.* 141(2):331-343.
 50. Lehen'kyi V, Beck B, Polakowska R, Charveron M, Bordat P, Skryma R, Prevarskaya N. TRPV6 is a Ca^{2+} entry channel essential for Ca^{2+} -induced differentiation of human keratinocytes. *J Biol Chem.* 2007;282(31):22582-22591.
 51. Coe FL, Evan A, Worcester E. Kidney stone disease. *J Clin Invest.* 2005;115(10):2598-2608.
 52. Stechman MJ, Loh NY, Thakker RV. Genetic causes of hypercalciuric nephrolithiasis. *Pediatr Nephrol.* 2009;24(12):2321-2332.
 53. Na T, Zhang W, Jiang Y, Liang Y, Ma HP, Warnock DG, Peng JB. The A563T variation of the renal epithelial Ca^{2+} channel TRPV5 among African Americans enhances Ca^{2+} influx. *Am J Physiol Renal Physiol.* 2009;296(5):F1042-1051.
 54. Renkema KY, Velic A, Dijkman HB, Verkaart S, van der Kemp AW, Nowik M, Timmermans K, Doucet A, Wagner CA, Bindels RJ, et al. The Ca^{2+} -sensing receptor promotes urinary acidification to prevent nephrolithiasis. *J Am Soc Nephrol.* 2009;20(8):1705-1713.



CHAPTER 9

Samenvatting/Sammendrag



Samenvatting

De nier zorgt voor stabilisatie van de systemische elektrolytenconcentraties binnen de normaalwaarden. Dit wordt bereikt door continue aanpassingen van de renale reabsorptiecapaciteit voor deze elektrolyten. Het distaal convoluut speelt een centrale rol in de reabsorptie van Na^+ , Cl^- , Mg^{2+} en Ca^{2+} uit het renale ultrafiltraat. Als zodanig draagt het NaCl -transport binnen dit segment aanzienlijk bij aan de stabilisatie en regulatie van de bloeddruk. Reabsorptie van tweewaardige kationen door het distaal convoluut zorgt voor de handhaving van adequate plasmaspiegels van Mg^{2+} en Ca^{2+} , ionen die essentieel zijn voor vele fysiologische processen zoals zenuwexcitatie, spiercontracties en botvorming. Zodoende draagt kennis over de moleculaire mechanismen betrokken bij de regulatie van het iontransport in het distaal convoluut in hoge mate bij aan het begrip van de fysiologie en pathofysiologie van deze bovengenoemde processen. Als zodanig kan de ontregeling van het elektrolyttransport in dit segment (zoals wordt geïllustreerd door monogene erfelijke aandoeningen waarbij het distaal convoluut aangedaan is, zoals Gitelman syndroom en pseudohypoaldosteronisme) zorgen voor een verlaging of zelfs gehele afwezigheid van de totale renale reabsorptiecapaciteit voor deze ionen. Het algemene doel van dit proefschrift was daarom om meer inzicht te krijgen in de regulatie van processen betrokken bij het transport van Na^+ , Cl^- , Mg^{2+} en Ca^{2+} in het distaal convoluut.

Hypertensie speelt een sleutelrol in de ontwikkeling van cardiovasculaire complicaties en chronische nierinsufficiëntie. De thiazide-gevoelige cotransporter (NCC) is van cruciaal belang voor de reabsorptie van NaCl in het distaal convoluut waardoor de arteriële bloeddruk beïnvloedend. Meer kennis over de regulatie van NaCl -transport via NCC zal leiden tot een beter inzicht in de bloeddruk-handhaving en de etiologie van primaire hypertensie. Het doel van **hoofdstuk 2** was het identificeren van nieuwe interactiepartners van NCC, die betrokken zouden kunnen zijn bij het moduleren van de functie van NCC. Aangezien van het amino-terminale domein is aangetoond dat het een belangrijke rol speelt bij de activatie van de

Chapter 9

transporter, werden pull-down experimenten uitgevoerd met behulp van dit domein van NCC, en werden lysaten van een muizennier gescreend voor mogelijke interactiepartners van de transporter. Met behulp van massaspectrometrie werd γ -adducin geïdentificeerd als een nieuwe interactiepartner van NCC. Ons onderzoek laat zien dat γ -adducin een sterke interactie aangaat met de amino-terminus van NCC. Met behulp van $^{22}\text{Na}^+$ -opnames in NCC-geïnjecteerde *Xenopus laevis* oöcyten in de aan- en afwezigheid van γ -adducin werd aangetoond dat γ -adducin aanzienlijk de activiteit van de transporter verhoogt. siRNA gericht tegen endogeen *Xenopus laevis* γ -adducin verlaagde de NCC-afhankelijke $^{22}\text{Na}^+$ -opname. Competitie met grotere hoeveelheden van de amino-terminus van NCC remde volledig de stimulerende werking van γ -adducin op het thiazide-gevoelige $^{22}\text{Na}^+$ -transport. Daarnaast werd aangetoond dat de bindingsplaats van γ -adducin zich bevindt in de amino-terminus van NCC, waar zich drie eerder beschreven fosforyleringsplaatsen bevinden. In mutanten waarbij de fosforyleringsplaatsen constitutief inactief werden gemaakt verhoogde γ -adducin het thiazide-gevoelige Na^+ -transport niet. Bovendien bond γ -adducin niet aan NCC wanneer de fosforyleerbare residuen waren vervangen door aspartaatresiduen, wat een constitutief actieve gefosforyleerde toestand nabootst. Deze gegevens uit **hoofdstuk 2** suggereren dat γ -adducin de NCC-activiteit stimuleert door de verankering van een kinase, waarschijnlijk een STE20-kinase, aan de gedefosforyleerde transporter. Vervolgens zorgt het kinase voor een toename van de NCC-fosforylering, wat vervolgens resulteert in een toename in de transporter-activiteit. Na de kinase-gemedieerde fosforylering wordt de binding tussen γ -adducin en NCC verbroken, en faciliteert γ -adducin mogelijk ook het loslaten van het geassocieerde kinase. Defosforylering van de transporter verlaagt de activiteit van NCC tot het basale niveau. De gegevens in **hoofdstuk 2** geven sterke aanwijzingen dat γ -adducin in belangrijke mate bijdraagt aan de regulatie van NCC en hierdoor ook aan de bloeddrukregulatie.

Het epitheliale kanaal voor tweewaardige kationen, Transient Receptor Potential Melastatin 6 (TRPM6), is verantwoordelijk voor de apicale influx van Mg^{2+} in het distaal convuluut

Samenvatting/Sammendrag

en speelt zo een belangrijke rol bij de actieve Mg^{2+} -reabsorptie in dit segment. Op deze manier bepaalt de regulatie van TRPM6 de uiteindelijke Mg^{2+} -concentratie in het bloed. Het is bekend dat behandeling van colonkanker met Cetuximab, een monoklonaal antilichaam tegen de epidermale groeifactorreceptor (EGFR), hypomagnesiëmie veroorzaakt bij de behandelde patiënten. Echter, veel patiënten die lijden aan kanker krijgen tyrosine-kinaseremmers, zoals Erlotinib. Er zijn geen klinische onderzoeken gepubliceerd over het potentiële effect van tyrosine-kinaseremmers op de systemische en renale Mg^{2+} -huishouding. **Hoofdstuk 3** toont aan dat TRPM6 wordt gereguleerd door Erlotinib wat leidt tot een veranderde Mg^{2+} -huishouding. Muizen die gedurende 23 dagen suprafysiologische doseringen Erlotinib kregen ontwikkelden een daling in de serum Mg^{2+} -concentratie. Bovendien slaagden deze Erlotinib-geïnjecteerde muizen er niet in de fractionele renale uitscheiding van Mg^{2+} te verminderen als reactie op de verlaagde serum Mg^{2+} -concentratie. Om het effect van Erlotinib op TRPM6 verder te onderzoeken is het belangrijk om de transportactiviteit van het kanaal te meten. Whole-cell patch-clamp is een techniek die kan worden gebruikt om de cellulaire permeabiliteit voor een ion te bepalen, gegenereerd door één of meer kanalen in het celmembraan. Gebruikmakend van deze techniek in humane embryonale nier (HEK) 293 cellen, werd aangetoond dat Erlotinib aanzienlijk de activiteit remt van het EGF-gestimuleerde TRPM6-kanaal. De HEK293 cellen werden blootgesteld aan doseringen in dezelfde orde van grootte (30 μ M Erlotinib gedurende 1 uur) als de verwachte plasma-concentratie in muizen. Hoewel matige effecten van Erlotinib werden waargenomen *in vivo*, kon het medicijn wel EGF-gestimuleerde TRPM6-stromen en routing van TRPM6 in HEK293 cellen blokkeren. Gezien het feit dat de vrij circulerende concentratie van Erlotinib ongeveer 0.3 μ M is in patiënten, onderzochten we of ook deze concentratie in staat zou zijn om het effect van EGF op TRPM6-stromen te blokkeren. Hierbij konden we echter geen effect op EGF-gestimuleerde cellen waarnemen. Het remmende effect van Erlotinib op Mg^{2+} -transport gaat waarschijnlijk via remming van TRPM6-routing, door het voorkomen van EGF-gemedieerde veranderingen in de

Chapter 9

mobiele fractie van de TRPM6-eiwitten.

Actieve Ca^{2+} -reabsorptie in het distaal convoluut is van cruciaal belang bij het bepalen van de uiteindelijke Ca^{2+} -excretie in de urine. De transportcapaciteit in dit segment wordt geregeld door calciotrope hormonen, zoals parathyroïd hormoon (PTH) en 1,25-dihydroxyvitamine D_3 . Mannen hebben een groter Ca^{2+} -verlies via de urine dan vrouwen. In overeenstemming met dit verschil is aangetoond dat oestrogenen de renale reabsorptie van Ca^{2+} verhogen. Het is niet bekend of androgenen een tegengesteld effect hebben ten opzichte van oestrogenen in de modulatie van renale Ca^{2+} -reabsorptie. Daarom hebben we in **hoofdstuk 4** onderzocht of androgenen bijdragen aan het verschil tussen de geslachten in de renale Ca^{2+} -homeostase. Als zodanig onderzochten we het vermogen van androgenen om de expressie van Ca^{2+} -transporteurs in de nier te veranderen, in het bijzonder het Transient Receptor Potential Vallinoid 5 (TRPV5) Ca^{2+} -kanaal. Het onderzoek toonde aan dat testosteron aanzienlijk bijdraagt aan de waargenomen geslachtsverschillen in de renale Ca^{2+} -huishouding. Mannelijke muizen hadden een hogere Ca^{2+} -excretie in de urine vergeleken met vrouwelijke muizen, en een verminderde expressie van Ca^{2+} -transporteurs in de nier. Androgeen-deficiënte muizen waarbij de testes waren verwijderd (ORX muizen) bleken een significant verminderde Ca^{2+} -uitscheiding in de urine te hebben. Deze vermindering van de Ca^{2+} -excretie werd opgeheven door toediening van testosteron. Vergelijkbare gegevens werden verkregen bij de beoordeling van de fractionele Ca^{2+} -excretie, hetgeen suggereert dat de testosteron-geïnduceerde stijging van de Ca^{2+} -excretie in de urine het gevolg is van de remming van de tubulaire Ca^{2+} -reabsorptie. De hoeveelheid mRNA en eiwit van Ca^{2+} -transporteurs in de nier was toegenomen in ORX-muizen, hetgeen werd genormaliseerd wanneer de muizen testosteron kregen toegediend. Bovendien zorgde dihydrotestosteron-behandeling voor een remming van het transcellulaire Ca^{2+} -transport in primaire celweken van verbindingsbuizen / corticale verzamelbuizen uit de konijnennier.

Een ander calciotroop hormoon betrokken bij de regulatie van de Ca^{2+} -huishouding is

Samenvatting/Sammendrag

calcitonine (CT). In ratten en muizen komt TRPV5 hoog tot expressie in het apicale membraan van met name cellen in het tweede deel van het distaal convoluut (DCT2), met een geleidelijke afname in de verbindingsbuis en het eerste deel van de verzamelbuis. De exacte lokalisatie van TRPV5 in de humane nier is momenteel niet bekend, maar de structuur van het distaal convoluut is gelijk aan die van de muis. Het "lichte" gedeelte van het distaal convoluut reageert op CT in nieren van de rat, wat resulteert in een verhoogde productie van cAMP. Andere cAMP-stimulerende hormonen, waaronder PTH beïnvloeden TRPV5-gemedieerd Ca^{2+} -transport door het moduleren van de expressie en de activiteit van het kanaal. Momenteel is het onduidelijk of er een functionele overlap is tussen PTH en CT in de DCT2 regio's van ratten en muizen, en of de CT-geïnduceerde toename van cAMP kan leiden tot een soortgelijke activering in het DCT2-segment zoals PTH.

In **Hoofdstuk 5** is het effect van CT bestudeerd op de totale Ca^{2+} -balans in de nier en zijn de mogelijke effecten van CT onderzocht op de TRPV5-afhankelijke Ca^{2+} -reabsorptie in het distaal convoluut. Injecties van muizen met CT gaven binnen 16 of 40 uur na toediening geen verandering in de expressie van TRPV5 in de nier. Bovendien was er geen verschil in de CT-respons tussen wild-type (TRPV5^{+/+}) en TRPV5-deficiënte (TRPV5^{-/-}) muizen. Gezien de gegevens die zijn verkregen in deze experimentele modellen, is het waarschijnlijk dat het effect van CT op het Ca^{2+} -transport in de nier onafhankelijk is van TRPV5. Hoewel CT geen invloed heeft op TRPV5-gemedieerde Ca^{2+} -reabsorptie, blijkt uit dit onderzoek dat CT de Ca^{2+} -reabsorptie in de nier in hoge mate stimuleert. De stimulerende werking van CT kan mogelijk worden verklaard door veranderingen in het Ca^{2+} -transport in het dikke opstijgende been van de lis van Henle, zoals eerder beschreven, en in het distaal convoluut via een nog onbekend mechanisme. Concluderend kan gesteld worden dat CT de reabsorptie-capaciteit vergroot voor Ca^{2+} in de nier.

Recent is er een groep van regulerende factoren beschreven die vanuit de extracellulaire zijde de functie van de elektrolyttransporteurs binnen het distaal convoluut

Chapter 9

moduleert. Klotho is zo'n eiwit dat werkt door het afsplitsen van oligosacchariden uit de complexe N-glycaan van TRPV5. Deze extracellulaire modificatie resulteert in een vertraagde internalisatie van het Ca^{2+} -kanaal vanuit het apicale plasmamembraan wat vervolgens leidt tot een verhoogd Ca^{2+} -transport. De stimulerende werking van klotho wordt bepaald door de N-glycosylering van TRPV5. Tissue transglutaminase (tTG) wordt net als klotho uitgescheiden in de urine en komt daardoor in direct contact met TRPV5 vanuit de pro-urine zijde. **Hoofdstuk 6** beschrijft de ontdekking van tTG als een nieuwe remmer van TRPV5, handelend vanuit de extracellulaire zijde in een N-glycosylering-afhankelijke manier.

tTG is een multifunctioneel Ca^{2+} -afhankelijk enzym dat de covalente binding van eiwitten katalyseert. tTG is een intracellulair enzym dat echter ook wordt uitgescheiden door cellen, wat suggereert dat in de nieren het enzym zou kunnen werken vanuit de urinezijde. In ander epitheel is aangetoond dat tTG wordt gereguleerd door TRPV-kanalen. Het is niet bekend of dit Ca^{2+} -geactiveerde enzym Ca^{2+} -transport in het distaal convoluut via TRPV5 beïnvloedt. Ons onderzoek toonde aan dat tTG wordt uitgescheiden in de urine van muizen, tot expressie komt in gepolariseerde cellen uit de verbindingsbuizen / corticale verzamelbuizen van het konijn, en werd uitgescheiden in het apicale medium van deze cellen. tTG remt het transculturele Ca^{2+} -transport in deze cellen en vermindert de activiteit van TRPV5 in HEK293-cellen. Dit proces gebeurt via covalente binding van TRPV5 monomeren, waardoor de poriegrootte van het kanaal kleiner wordt. Het remmend effect van tTG is afhankelijk van de N-glycosylering van TRPV5 aangezien de N-glycosylering-deficiënte mutant niet gevoelig is voor tTG-gekatalyseerde modificaties.

Ca^{2+} -transport in het distaal convoluut draagt sterk bij aan de totale hoeveelheid Ca^{2+} die wordt gereabsorbeerd door de nieren. Dat blijkt uit een verhoogde hoeveelheid Ca^{2+} in de urine van muizen met een geïnactiveerd TRPV5-gen. Hypercalciurie is de bekendste risicofactor voor verkalking van de nieren. Voor het onderzoeken van een mogelijke genetische invloed op hypercalciuria, en dus het ontstaan van nierverskalking en nierstenen, hebben we gebruik

Samenvatting/Sammendrag

gemaakt van N-ethyl-N-nitrosourea (ENU)-mutagenese muizen in een fenotype-gerichte screening, om zo nieuwe genetische modellen van hypercalciurie te identificeren. **Hoofdstuk 7** beschrijft de identificatie van een muis met een ernstige autosomaal dominante hypercalciurie. Dit defect werd veroorzaakt door een nieuwe S682P missense mutatie in het TRPV5-gen. De studie bevat de identificatie en functionele karakterisatie van dit gedefect. Ons onderzoek liet zien dat de expressie van TRPV5 in de nieren van $Trpv5^{682P/+}$ en $Trpv5^{682P/682P}$ muizen is veranderd. In de $Trpv5^{682P/+}$ muizen is de expressie van TRPV5 alleen aangedaan in het tweede gedeelte van het distaal convoluut, terwijl TRPV5-expressie in de $Trpv5^{682P/682P}$ muizen zowel in de het tweede deel van het distaal convoluut als in de verbindingsbuis is afgenomen. Bovendien was de calbindine-D_{28K}-expressie in $Trpv5^{682P/682P}$ muizenieren sterk verminderd, wat een specifiek defect in TRPV5-gemedieerde Ca^{2+} -reabsorptie bevestigt. De verandering van de serine 682 naar een proline resulteerde in een verlaagd basaal intracellulair Ca^{2+} -niveau in HEK293 cellen getransfecteerd met de TRPV5 mutant, hetgeen wijst op een defect in de TRPV5-gemedieerde Ca^{2+} -permeabiliteit van de cel. Daarnaast ontwikkelt ongeveer 10% van de mannelijke muizen primaire tubulo-interstitiële nefritis, waarschijnlijk veroorzaakt door urinaire reflux.

De algemene doelstelling van dit proefschrift was het ophelderen van de moleculaire mechanismen die het elektrolyttransport regelen in het distaal convoluut. Daarom onderzochten we in detail de moleculaire regulatie van de NCC, TRPM6 en TRPV5 om te begrijpen hoe het transport van elektrolyten door deze transporteurs kan worden beïnvloed. De noodzaak van het behoud van de plasmaspiegels van elektrolyten zoals Na^+ , Cl^- , Ca^{2+} en Mg^{2+} binnen de normale grenzen is duidelijk, aangezien een verstoring hierin invloed heeft op tal van belangrijke fysiologische processen. De gedetailleerde karakterisatie van de moleculaire mechanismen die deze transportsystemen reguleren, kan bijdragen aan het verkrijgen van kennis voor de behandeling of genezing van ziekten gerelateerd aan een defect elektrolyttransport in het distaal convoluut van de nier.

Chapter 9

Sammendrag

Nyren stabiliserer de systemiske koncentrationer af elektrolytter ved at ændre nyrens reabsorptive kapacitet for disse ioner. Den distal bøjede del (anatomisk struktur som inkluderer den distal bøjede tubuli (DCT), samle tubulien (CNT), samt starten af samle røret (CD)) spiller en central rolle i reabsorptionen af Na^+ , Cl^- , Mg^{2+} , and Ca^{2+} fra det renale ultrafiltrat. NaCl transport i disse segmenter bidrager signifikant til opretholdelsen og reguleringen af blodtrykket. Reabsorption af divalente kationer i den distal bøjede del er også vigtig for opretholdelse af stabile serum koncentrationer af Mg^{2+} og Ca^{2+} , der spiller en vigtig rolle i mange fysiologiske processer, såsom neuronal excitabilitet, muskel kontraktioner, og knogle dannelse. En bedre forståelse af de molekylære signalveje som regulerer ion transporten i den distal bøjede del, kan også hjælpe til at forstå den distal bøjede dels indflydelse på nyrens funktion i forskellige fysiologiske og patofysiologiske tilstande. For eksempel, fejl-regulering af elektrolyt transport i disse segmenter (som ses i monogene sygdomme der rammer den distal bøjede del) kan ændre eller ligefrem ødelægge nyrens reabsorptive kapacitet for disse ioner. Det overordnede formål med denne afhandling er at øge forståelsen omkring de elektrolyt transport processer som deltager i at flytte Na^+ , Cl^- , Mg^{2+} , and Ca^{2+} over den distal bøjede del.

Arteriel hypertension er en vigtig faktor i udviklingen af hjerte-kar sygdomme og kronisk nyresvigt. Den thiazid-følsomme cotransporter (NCC) er af afgørende betydning for reabsorptionen af NaCl i den distal bøjede del. En bedre forståelse af, hvordan NaCl transport reguleres via NCC kan i sidste ende øge vores forståelse af, hvordan blodtryk opretholdes og ætiologien bag den primære hypertension. **Kapitel 2** omhandler identifikationen af nye bindingspartnere til NCC, som kunne være involveret i at regulere denne transporters funktion. Eftersom det er blevet påvist at den N-terminale del af proteinet spiller en vigtig rolle for aktiveringen af transporteren, udførte vi pull down eksperimenter med dette domæne af NCC og nyre lysater fra mus. Masse spektrometri identificerede γ -adducin som en ny bindingspartner til NCC. Ved brug af $^{22}\text{Na}^+$ uptake eksperimenter i *Xenopus laevis* oocytter injiceret med NCC,

Samenvatting/Sammendrag

med eller uden γ -adducin, kunne vi vise at γ -adducin stimulerede NCC transporteren. siRNA rettet mod den endogene *Xenopus Laevis* γ -adducin reducerede det NCC afhængige Na^+ optag i oocytterne. Konkurrence med stigende mængder af den N-terminal del af NCC, fjernede helt den stimulerende effekt af γ -adducin på den thiazid følsomme $^{22}\text{Na}^+$ transport. Desuden fandt vi at γ -adducin bandt til præcis den region som tidligere havde været vist at indeholde tre fosforylerings sekvenser i transporteren. NCC transporterer som mangler fosforylerbare sekvenser i deres N-terminale del øger ikke deres $^{22}\text{Na}^+$ transport aktivitet når de co-injiceres sammen med γ -adducin. Ydermere, γ -adducin dissociere fra NCC når den N-terminale fosfosekvenser er omdannet til aspartater.

Baseret på data det blev genereret i **Kapitel 2**, foreslår vi at γ -adducin stimulerer NCC aktiviteten ved binde en kinase, sandsynligvis medlemmer af STE20 familien til den defosforylerede transporter. Derefter kan kinasen øge NCCs fosforylerings niveau og således stimulere aktiviteten for transporteren. Efter det kinase medierede fosforylering event, dissocierer γ -adducin fra NCC og kan måske også få stimulere frigivelsen af den associerende kinase. Defosforyleringen af transporteren reducerer NCCs aktivitet tilbage til det basale niveau. De observationer som bliver lavet i **Kapitel 2** indikerer kraftigt at γ -adducin kan bidrage væsentligt til regulering af NCC og dermed til vedligeholdelsen af det arterielle blodtryk.

Den divalente kation kanal Transient Receptor Potential Melastatin 6 (TRPM6), er en vigtig komponent i den aktive Mg^{2+} reabsorption i den distal bøjede struktur, hvor den danner den apikale Mg^{2+} pore i DCT segmentet. Reguleringen af TRPM6 bestemmer derfor også den endelige koncentration af Mg^{2+} i blodet. Kræftbekæmpende behandlinger med Cetuximab, et monoklonalt antistof mod den epidermal growth factor receptor (EGFR), er årsag til hypomagnesemi hos mange patienter med kolorektal kræft. Imidlertid er der mange patientgrupper der lider af kræft som modtager behandling med de såkaldte tyrosin kinase inhibitorer såsom f. eks. Erlotinib. Der findes ingen offentliggjort kliniske revisionsrapporter om de potentielle bivirkninger af tyrosin kinase inhibitorer på den systemiske og renale Mg^{2+}

Chapter 9

håndtering. **Kapitel 3** viser, at Erlotinib kan påvirke reguleringen af TRPM6 og derved ændre Mg^{2+} håndteringen i nyren. Vi observerede at mus, som modtog suprafysiologiske doser af Erlotinib i 23 dage, reducerede deres serum koncentration af Mg^{2+} . De Erlotinib-injicerede mus havde en uændret fraktionel renal udskillelse af Mg^{2+} , selvom der var et fald i serum Mg^{2+} koncentrationen, hvilket indikere at nyren ikke reagerer normalt. Patch-clamp analyse kan anvendes til bestemmelse af den cellulære permeabilitet af et ion, skabt af en eller flere kanaler. Ved brug af denne teknik i humane embryoniske nyre celler (HEK293), kunne vi vise at Erlotinib inhiberede den EGF stimulerede TRPM6 aktivitet. HEK293 cellerne modtog en dosis af samme størrelsesorden (30 μM af Erlotinib) som den forventede plasma koncentration i mus. Selv om en moderat effekt af Erlotinib blev observeret *in vivo*, kunne denne dosis fuldstændig blokere EGF inducerede øgning i TRPM6 aktiviteten *in vitro*. Eftersom den frie plasma koncentration af Erlotinib sandsynligvis vil være omkring 0,3 μM i mennesker, testede vi om denne koncentration var i stand til at blokere virkning af EGF på aktiviteten af TRPM6. Her kunne vi ikke påvise en betydelige forskel fra de EGF stimulerede celler. Den inhiberende virkning af Erlotinib på Mg^{2+} transporten i den distal bøjede del sker sandsynligvis igennem inhibering af TRPM6 routing, ved at blokere EGF stimulerede øgninger i den mobile fraktion af TRPM6 proteiner.

Den aktive renale Ca^{2+} reabsorption som foregår i det distal bøjede del spiller en kritisk rolle i den totale renale Ca^{2+} transport. Transport kapaciteten i dette segment er reguleret af calciotropiske hormoner som f. eks. parathyridea hormonet og 1,25-dihydroxyvitamin D_3 . Mænd har et større Ca^{2+} tab i urinen end kvinder. Man har ydermere påvist at østrogen kan øge den aktive renale Ca^{2+} transport, hvilket er i overensstemmelse med de kendte kønsforskelle. Det forholder sig uklart om androgener kan spille en opponerende rolle til østrogen ved at regulere den renale Ca^{2+} udskillelse. I **Kapitel 4** undersøgte vi om androgener kunne bidrage til de kønsforskelle som ses i den mængde af Ca^{2+} der udskilles af nyren af mænd og kvinder. Her undersøgte vi om androgener kunne regulere mængden af de renale Ca^{2+} transport proteiner, især Ca^{2+} kanalen Transient Receptor Potential Vallinoid 5 (TRPV5). Studiet viser at testosteron

Samenvatting/Sammendrag

spiller en væsentlig rolle i de kønsforskelle som der ses i den renale Ca^{2+} udskillelse i mus. Hanner havde en øget Ca^{2+} udskillelse i forhold til hunnerne, hvilket sammenfaldt med en reduceret mængde af Ca^{2+} transport proteiner. Kastrede hanner uden cirkulerende androgener (ORX) viste en signifikant reduktion i den urinære udskillelse af Ca^{2+} , hvilket blev normaliseret efter musene fik testosteron injiceret (ORX^T). Lignende observationer sås for den fraktionelle renale udskillelse af Ca^{2+} , hvilket indikerer at den testosteron induceret øgning i den urinære Ca^{2+} udskillelse, skyldes hæmning af Ca^{2+} transport i nyren. Mængden af renalt Ca^{2+} transporter mRNA og protein var øget i ORX mus, men normaliseret i ORX^T musene. Derudover observerede vi at den transcellulære Ca^{2+} transport var inhiberet i isolerede kanin tubuli fra CNT og de corticale CD (CCD) segmenter efter behandling med dihydrotestosterone.

Calcitonin (CT) er et vigtigt hormon involveret i Ca^{2+} metabolismen. Studier i kaniner har vist at CT kun øger Ca^{2+} transporten i DCT, imens hormonet ikke kan stimulere transporten af Ca^{2+} i CNT. I overensstemmelse med disse observationer er det blevet vist at CT ikke kan stimulere cAMP produktionen i kaniners CNT. I kaniner findes TRPV5 i de apikale membraner af CNT, hvor CT ikke har nogen effekt. I rotter og mus derimod er TRPV5 højt udtrykt i de apikale domæner i DCT, og mindre udtrykt i CNT og CD. Den intrarenale distribution af TRPV5 i mennesker kendes ikke, men strukturen af deres distal bøjede del ligner den som findes i mus. Den lyse del af DCT er responsiv til CT i rotter, hvilket resulterer i en øget cAMP produktion i dette segment når de behandles med hormonet. Ydermere, findes der bindings steder for CT i rotte nyre i både TAL og DCT. Andre cAMP øgende hormoner såsom PTH påvirker TRPV5 medieret transport ved at øge mængden og aktiviteten af kanalen. Det er på nuværende tidspunkt uklart om der er et overlap imellem PTH og CT i DCT2 regionen af rotter og mus.

Kapitel 5 undersøgte de molekulære mekanismer som CT bruger til at øge den renale Ca^{2+} reabsorption, samt den potentielle effekt af CT på den TRPV5 medierede Ca^{2+} reabsorption i den distal bøjede del af nefronet. Injektion af CT ændrede ikke den renale mængde af TRPV5. Vildtype mus (TRPV5^{+/+}) og mus der manglede *TRPV5* genet (TRPV5^{-/-}) havde den samme

Chapter 9

respons til CT. Baseret på de observationer lavet i vores studie, er det usandsynligt at den øgede Ca^{2+} reabsorption som man ser efter CT injektion er afhængig af TRPV5. Selvom CT ikke har nogen effekt på den TRPV5 medierede Ca^{2+} reabsorption, står det klart fra vores studier at CT kraftigt stimulerer den renale Ca^{2+} transport. Den stimulatoriske effekt af CT på Ca^{2+} transporten foregår sandsynligvis via primære ændringer i det tykke ascenderende ben og i DCT via en ukendt mekanisme. Vi kan derfor konkludere at CT øger den renale reabsorptive kapacitet for Ca^{2+} uafhængigt af TRPV5.

En gruppe af regulatoriske proteiner som udøver deres effekt fra den ekstracellulære side af cellen er for nyligt blevet vist at påvirke funktionen af elektrolyt transportere i den distal bøjede del. Klotho er et protein som agerer fra den ekstracellulære side af cellen, ved at fjerne oligosaccharider fra den komplekse N-glycan på TRPV5. Denne ekstracellulære modifikation gør at TRPV5 kanalen bliver længere på den apikale plasma membran. **Kapitel 6** beskriver identifikationen af vævs-transglutaminasen (tTG) som en ny molekylær hæmmer af TRPV5.

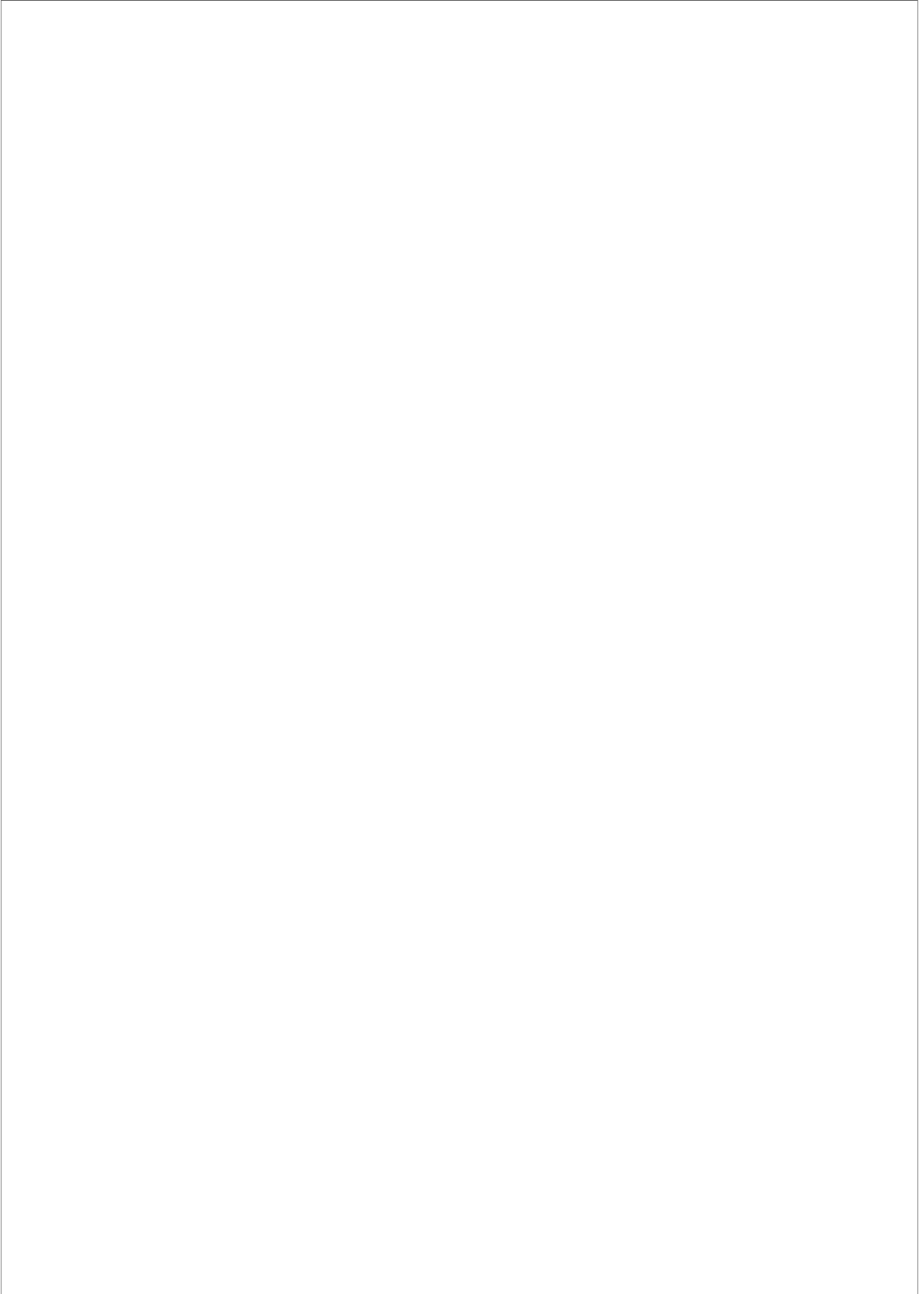
tTG er et multifunktionelt Ca^{2+} afhængigt enzym, der katalyserer den kovalente krydsbinding af proteiner. tTG er et intracellulært enzym, med det bliver også udskilt af cellerne, hvilket kan betyde at det i nyren kan agere fra den ekstracellulære side, altså i urinen. Det er tidligere blevet vist at tTG regulerer andre TRPV kanaler. I forhold til TRPV5 medieret Ca^{2+} transport så er det uvist om det Ca^{2+} aktiverede enzym har nogen effekt på Ca^{2+} transporten i den distal bøjede del. Vi kunne vise at tTG bliver udskilt i urinen, samt i primære CNT/CCD celler isoleret fra kaniner, hvor det bliver udskilt i det apikale medium. Derudover kunne tTG reducere aktiviteten af TRPV5 i HEK293 celler og inhibere den transcellulære Ca^{2+} transport i primære CNT/CCD celler. Denne proces sker sandsynligvis ved en kemisk krydsbinding af de individuelle TRPV5 monomere til hinanden, som resulterer i en nedsat pore størrelse af kanalen. Den hæmmede effekt af tTG afhænger af N-glycosyleringen af TRPV5, eftersom den N-glycosylerings deficiente mutant ikke kan modificeres af tTG.

Ca^{2+} transport i den distal bøjede del spiller en væsentlig rolle i reabsorptionen af den

Samenvatting/Sammendrag

totale mængde af Ca^{2+} i nyren. Dette står klart eftersom mus som mangler TRPV5 genet har en øget udskillelse af Ca^{2+} i urinen. Hypercalciuri kan føre til dannelsen af nyresten (nephrolithiasis). For at få et bedre indblik i de genetiske faktorer som er vigtig for dannelsen af hypercalciuri og dermed nyresten, screenede vi mus som var udsat for det mutagene stof *N*-ethyl-*N*-nitrosourea (ENU) for hypercalciuri. I **Kapitel 7** identificerede vi en muse stamme med autosomal dominant hypercalciuri, hvilket viste sig at være på grund af en S682P mutation i *TRPV5* genet. Mængden af TRPV5 i nyren hos mus der var heterozygote (*Trpv5*^{682P/+}) eller homozygote and (*Trpv5*^{682P/682P}) var nedsat. I *Trpv5*^{682P/+} musene, var ekspressionen af TRPV5 kun nedsat i DCT2, hvorimod mængden af TRPV5 var nedsat i både DCT2 og CNT i *Trpv5*^{682P/682P} musene. Ydermere var den renale expression af calbindin-D_{28K} nedsat i *Trpv5*^{682P/682P} musene. Mutationen af serine 682 til en proline resulterede i et reduceret basalt niveau af intracellulær Ca^{2+} i HEK293 celler der var transfectede med TRPV5 mutanten, hvilket indikerer en defekt i den TRPV5 afhængige Ca^{2+} permeabilitet af cellen.

Det overordnede formål med denne tese var at udrede de molekulære signalveje som regulerer elektrolyt transporten i den distal bøjede del. Denne tese lavede detaljerede undersøgelser af den molekulære regulering af NCC, TRPM6 og TRPV5. Det er nødvendigt at vedligeholde de systemiske koncentrationer af Na^+ , Cl^- , Ca^{2+} , and Mg^{2+} indenfor normale rammer, fordi ændringer af disse ioner påvirker mange fysiologiske processer. Den detaljerede karakterisation af de molekulære mekanismer som regulerer disse transport systemer kan hjælpe til en bredere forståelse af disse processer. En sådan viden kan derfor også hjælpe til behandlingen af sygdomme der fører til en ændret transport af elektrolytter i den distal bøjede del.



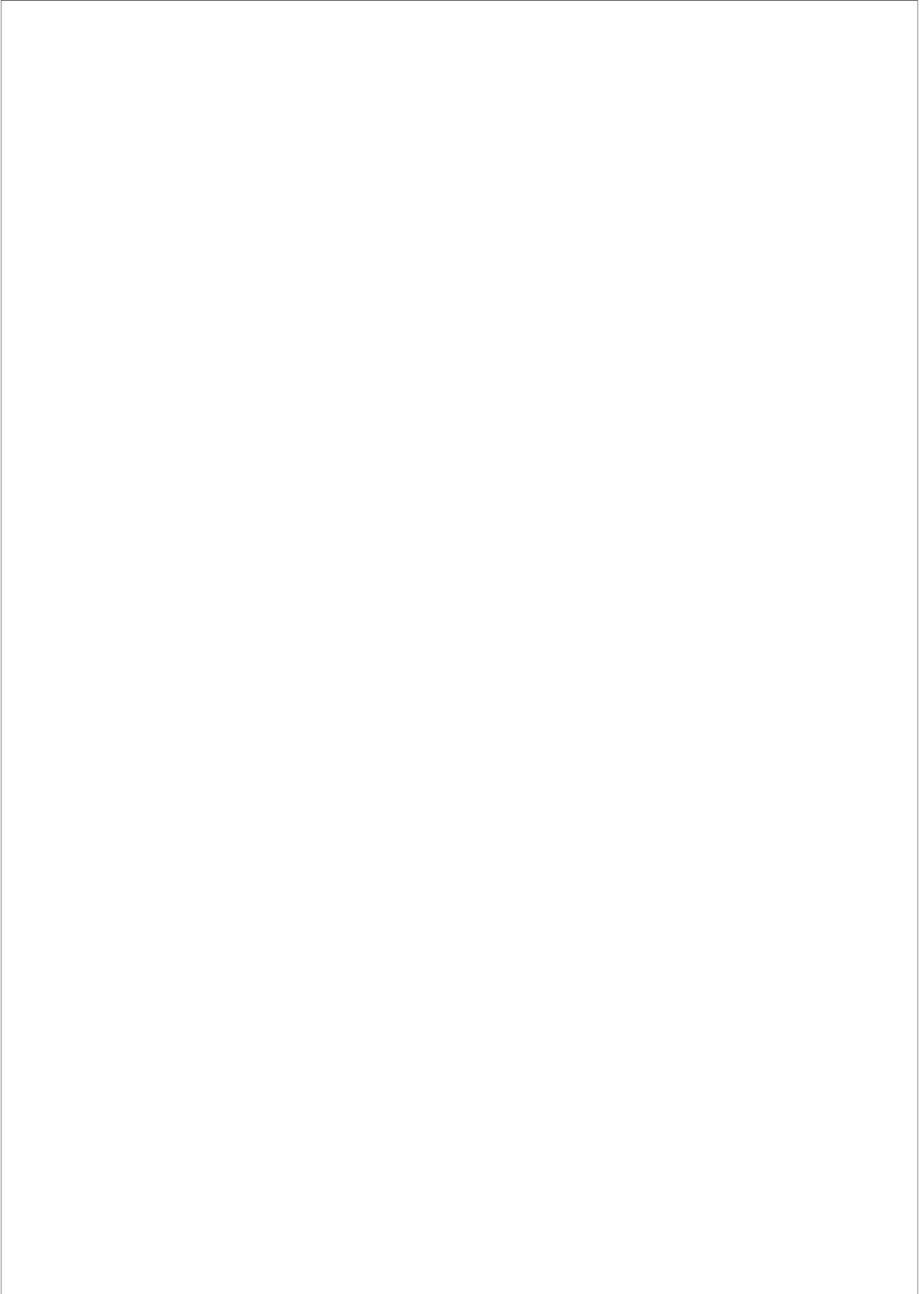
CHAPTER 10

Curriculum Vitae

List of abbreviations

List of publications

Acknowledgements



Curriculum Vitae

Henrik Dimke was born in Colombo, Sri Lanka on the 8th of November 1980. He was subsequently adopted by Lisbeth and Karsten Dimke of Lystrup, Denmark. He attended Risskov Amts-Gymnasium from 1997-2000. Henrik was enrolled at the University of Aarhus to study Biology in 2000, where he obtained a Bachelor of Science in Biology in 2003. Immediately thereafter he commenced his Master of Science in Molecular Biology at the same institution. His pre-thesis, a module required for the completion of the Master of Science degree in Molecular Biology was carried out at the Water & Salt Research Centre, Institute of Anatomy, University of Aarhus under the supervision of Prof. Dr. Søren Nielsen, and co-supervised by Associate Prof. Dr. Sebastian Frische, and Prof. Dr. Allan Flyvbjerg. In 2004 he started his master thesis in molecular biology, also at the Water & Salt Research Centre, Institute of Anatomy, under the direct supervision of Associate Prof. Dr. Sebastian Frische and co-supervised by the above-mentioned professors. In 2005 he completed his Master thesis in Renal Physiology and received the degree of Cand. Scient. (Master of Science) in Molecular Biology. In 2006 he worked as a Research Assistant at the Institute of Anatomy, until accepted as a PhD student by Prof. Dr. René Bindels and Prof. Dr. Joost Hoenderop in the Department of Physiology, Radboud University Nijmegen Medical Centre, the Netherlands. The project that was funded by the Dutch Kidney Foundation was co-supervised by Associate Prof. Dr. Jaap Deinum (Department of Internal Medicine), and Prof. Dr. Jacques Lenders (Department of Internal Medicine). The main focus of his thesis was the regulation of renal electrolyte transport and blood pressure.

Chapter 10

List of abbreviations

A

A, alanine
Ab, antibody
AngII, angiotensin II
ANOVA, analysis of variance
AQP, aquaporin
AR, androgen receptor
ATP, adenosine triphosphatase (AMPase, ADPase)
AU, arbitrary unit(s)

B

B6J, C57BL/6J mice strain
Brij97, Polyethylene Glycol Monooleyl Ether
BP, blood pressure
BSA, bovine serum albumin
BW, body weight

C

°C, degree Celsius
C3H, C3H/HeH mice strain
[Ca²⁺]_i, intracellular Ca²⁺
[Ca²⁺]_o, extracellular Ca²⁺
Ca²⁺/Cr, Ca²⁺/creatinine ratio
cAMP, cyclic adenosine monophosphate (cAMP)
CaSR, Ca²⁺-sensing receptor
CCD, cortical collecting duct
CD, collecting duct
Ci, curie
CNT, connecting tubule
COPAS, Complex Object Parametric Analyzer and Sorter
CP, coprecipitate
cpm, counts per minute
Cr, creatinine
cRNA, RNA derived from cDNA through standard RNA synthesis
Ct, threshold cycle
CT, calcitonin
CTX, kidney cortex

List of abbreviations

D

D, aspartate

Da, dalton(s)

DCT, distal convoluted tubule

DHT, dihydrotestosterone, (5 α ,17 β)-17-Hydroxy-androstan-3-one

DIC, differential interference contrast

DMA⁺, dimethylammonium

DMEM, dulbecco modified eagle medium

DMSO, dimethylsulfoxide

DNA, deoxyribonucleic acid

dsDNA, double-stranded DNA

E

E. coli, Escherichia coli

EDTA, ethylenediamine tetraacetic acid

EGF, epidermal growth factor

EGFR, epidermal growth factor receptor

eGFP, enhanced green fluorescent protein

EGTA, ethyleneglycol-bis-(b-aminoethylether)-N,N',N'-tetraacetic acid

ELISA, enzyme-linked immunosorbent assay

ENaC, epithelial Na⁺ channel

ENU, *N*-ethyl-*N*-nitrosourea

F

FCS, fetal calf serum

FE, fractional excretion

FRAP, fluorescent recovery after photobleaching

G

g, gram

G2, second generation offspring

GAPDH, glyceraldehyde-3-phosphate dehydrogenase

GFP, green fluorescent protein

GFR, glomerular filtration rate, estimated by creatinine clearance

GST, glutathione S-transferase

Chapter 10

H

hr, hour

HA, hemagglutinin

HCTZ, Hydrochlorothiazide

HEK293, human embryonic kidney 293 cells

HEPES, N-2-hydroxyethylpiperazine-N'-2-ethanesulfonic acid

HPRT, hypoxanthine-guanine phosphoribosyl transferase

HRP, horseradish peroxidase

HSH, hypomagnesemia with secondary hypocalciuria

I

IB, immunoblot

IC₅₀, 50% inhibitory concentration

iCD, initial collecting duct

Ig, immunoglobulin (IgE, IgG)

IGF, insulin-like growth factor

IOD, integrated optical density

IP, immunoprecipitate, immunoprecipitation

IRH, isolated renal hypomagnesemia

K

kb, kilobase

kDa, kilodalton(s)

K_m, Michaelis-Menten constant

L

l, liter(s)

LnCAP, androgen-responsive human prostate adenocarcinoma

M

M, molar

MA⁺, monomethylammonium

mAb, monoclonal Ab

maxi K, Ca²⁺-activated K⁺ channel

min, minute

MHS, Milan hypertensive rat strain

mRNA, messenger RNA

MW, molecular weight

List of abbreviations

N

n, number in group

N, amino

NCC, thiazide sensitive NaCl cotransporter (SLC12a3, TSC1)

NCX1, Na⁺/Ca²⁺ exchanger 1

NKCC2, kidney specific furosemide-sensitive Na⁺, K⁺, 2Cl⁻ cotransporter 2 (SLC13a1, BSC1)

NMDG, *N*-methyl-D-glutamine

NP-40, Nonidet P-40

NS, not significant

O

ODP, o-phenylenediamine

ORX, orchidectomy

ORX+T, orchidectomized mice supplemented with testosterone

osm, osmole

OSR1, oxidative stress response 1 kinase

P

p, probability of events

PAGE, polyacrylamide gel electrophoresis

PBS, phosphate-buffered saline

PCR, polymerase chain reaction

PEI, polyethylene-imine

pH, hydrogen ion concentration

PHII, pseudohypoaldosteronism type II

Phos/Cr, PO₄³⁻/creatinine ratio

PKA, protein kinase A

PKC, protein kinase C

PLP, periodate-lysine-paraformaldehyde

PMCA1b, plasma membrane Ca²⁺ ATPase 1b

PT, proximal tubule

PTH, parathyroid hormone

pTyr, tyrosine phosphorylation

PVDF, polyvinylidene fluoride

R

R, transepithelial resistance

RAAS, renin-angiotensin-aldosterone system

Chapter 10

REST, relative expression software tool

RNA, ribonucleic acid

ROI, region of interest

ROMK, renal outer medulla K⁺ channel

RT, reverse transcriptase

S

SDS, sodium dodecylsulfate

SEM, standard error of the mean

SGK, serum glucocorticoid kinase

siRNA, small, interference RNA

SNP, single nucleotide polymorphism

SPAK, serine-threonine proline-alanine rich kinase

T

t, time

TAL, thick ascending limb

TBS, triethanolamine-buffered saline

TetMA⁺, Tetramethylammonium

TriMA⁺, trimethylammonium

Tris, tris(hydroxymethyl)-aminomethan

TRPM6, transient receptor potential melastatin 6

TRPV5, transient receptor potential vallinoid 5

TRPV5^{-/-}, mice with a targeted deletion of the *TRPV5* gene

Trpv5^{682P/682P}, mice with a homozygotic S682P missense mutation in *TRPV5*

TPTX, thyroparathyroidectomy

tTG, tissue transglutaminase

V

v, volume

V, volt(s)

Vmax, maximum velocity

VUR, vesicoureteral reflux

W

W, weight

WNK, with no lysine (K)

List of publications

List of Publications

Boros S, **Dimke H**, Xi Q, van der Kemp AW, Verkaart S, Lee K, Bindels RJ, Hoenderop JG. Tissue transglutaminase inhibits TRPV5-dependent Ca^{2+} transport in a N-glycosylation-dependent manner. J. Am. Soc. Neph. *Submitted*.

Dimke H*, San-Cristobal P*, de Graaf M, Lenders JW, Deinum J, Hoenderop JG, Bindels RJ. γ -Adducin functions as a novel regulator of the thiazide-sensitive NaCl-cotransporter. J. Am. Soc. Neph. *Submitted*. *Authors contributed equally

O'Neill HA, Tae-Hwan K, Ring T, **Dimke H**, Lebeck J, Frøkiær J, Collins PB, Nielsen S, Frische S. Dietary NaCl restriction decreases urine volume in diabetic rats. Acta Physiol. Scand. *Submitted*.

San-Cristobal P, **Dimke H**, Hoenderop JG, Bindels RJ. Novel molecular pathways in renal Mg^{2+} transport: a guided tour along the nephron. Curr. Opin. Nephrol. Hypertens. *In press*, 2010.

Dimke H, vd Wijst J, Alexander TR, Meijer IMJ, Mulder GM, van Goor H, Tejpar S, Hoenderop JG, Bindels RJ. Effects of the Epidermal Growth Factor Receptor (EGFR) kinase inhibitor Erlotinib on renal and systemic Mg^{2+} handling. J. Am. Soc. Neph. *in press*, 2010.

Dimke H*, Hsu YJ*, Schoeber JP, Hsu SC, Lin SH, Chu P, Hoenderop JG, Bindels RJ. Testosterone increases urinary Ca^{2+} excretion and inhibits expression of renal Ca^{2+} transport proteins. Kidney Int. 77:601-608, 2010. *Authors contributed equally

Dimke H*, Hsu YJ*, Hoenderop JG, Bindels RJ. Calcitonin-stimulated renal Ca^{2+} reabsorption occurs independently of TRPV5. Nephrol Dial Transplant. 25:1428-1435, 2010. *Authors contributed equally

Chapter 10

Dimke H, Hoenderop JG, Bindels RJ. Hereditary tubular transport disorders: implications for renal handling of Ca^{2+} and Mg^{2+} . *Clin Sci (Lond)*. 118:1-18, 2010.

Dimke H, Flyvbjerg A, Frische S. Acute and chronic effects of growth hormone on renal regulation of electrolyte and water homeostasis. *Growth Horm IGF Res*. 17:353-368, 2007.

Nielsen S, Kwon T-H, **Dimke H**, Frøkiær J. Aquaporin water channels in mammalian kidney. In *The Kidney: Physiology and Pathophysiology*, 4th Edition, edited by Alpern RJ and Hebert SC, Elsevier 2007.

de Seigneux S, Nielsen J, Olesen ET, **Dimke H**, Kwon TH, Frøkiær J, Nielsen S. Long-term aldosterone treatment induces decreased apical but increased basolateral expression of AQP2 in CCD of rat kidney. *Am J Physiol Renal Physiol*. 293:F87-F99, 2007.

de Seigneux S, Malte H, **Dimke H**, Frøkiær J, Nielsen S, Frische S. Renal compensation to chronic hypoxic hypercapnia: downregulation of pendrin and adaptation of the proximal tubule. *Am J Physiol Renal Physiol*. 292:F1256-F1266, 2007.

Dimke H, Flyvbjerg A, Bourgeois S, Thomsen K, Frøkiær J, Houillier P, Nielsen S, Frische S. Acute growth hormone administration induces antidiuretic and antinatriuretic effects and increases phosphorylation of NKCC2. *Am J Physiol Renal Physiol*. 292:F723-F735, 2007.

Acknowledgements

Acknowledgements

The work presented in this thesis was carried out at the Department of Physiology, Radboud University Nijmegen Medical Centre, in the Netherlands from 2006-2010. Naturally, I would like to thank a large number of people for making the duration of my doctoral thesis an excellent learning experience and lots of fun.

Rene, first I would like to thank you for recruiting me to the Department of Physiology, I am very grateful for that. You have a solid knowledge of physiology, which has helped our scientific discussions. In addition, you run an exceptionally organized lab and have a very efficient work style. I have always admired that very few things seem to surprise or stress you, likely because of your very competent planning.

Big H, you have an extremely energetic approach to science and are always very enthusiastic about almost every result, which can be a good motivation. You have a very talented eye for making figure illustrations and presentations (an ability that I completely lack, obviously), and I would like to thank you for helping me out with the illustrations for the papers.

The combined guidance from you both has provided a good basis for the completion of this thesis and I would like to thank you for continuous support throughout this timeframe.

Mark, you helped me out a lot the last couple of years. You did a tremendous job on the γ -adducin paper, but also on a lot of other studies and ideas that we had. I think that quickly after we started to work together, it went very well. We (=you) did a lot of sequencing on the WNK Gordon patient project, which unfortunately did not result in any novel mutations. Your humor is sicker than mine, but still funny, so we always have a lot of laughs.

Pistolero, when you came to the lab we instantly started working together. Your considerable experience in oocyte work and your willingness to help quickly made the oocyte experiments run smoothly and we made some very cool studies (especially the γ -adducin). In

Chapter 10

combination, we motivate each other and work hard together. I am sure that if we had been allowed, our team could have generated much more data. In addition, we also had a lot of fun together and you always welcomed me in your house for dinners etc. I hope you and Caro will do very well here in the Netherlands, with the little Pistolito and your new house. Also a big thanks to Caro for letting Pistolero work with me in all those weekends.

Precooled W (a.k.a the Tree shredder), showing you the “L” after a good Halo game never gets tiring...Hanging out with you was always so much fun...it is rare that you meet someone with the same sick humor as one self. I am glad we managed to stay in touch throughout my stay here and I really hope we can stay in touch in the future as well. Also thanks for introducing me to Martijn and the rest of your family....and for always being there to help out with whatever problems I had.

Sinke, it was always fun to hang out with you, whether going to pinkpop, watching movies, or at your house parties. We had lots of discussions and you taught me a lot about the brain. It was also great to meet your friends, Tjeu and the others, with whom we had lots of fun (and beers). I am also pretty sure that we redefined how the international Chuck Norris day should be celebrated ☺. I wish you best of luck with your research, I am sure that it will turn out great in the end.

Professor Deen, I always appreciated our fruitful discussions, and hopefully we will have many more to come. It is nice to discuss with a person, who is almost as stubborn as myself, and who possesses a great knowledge of renal and cellular physiology. I would also like to thank you for always inviting me for dinners with investigators that you thought were for me beneficial to meet.

Theun, we did a lot of things together and had lots of fun. I guess I have to admit that you are still a little bit better at table-tennis than me, but I make it up in the table-football. It was always great to celebrate carnival with you and your friends as well as visiting your wonderful family who were always very kind and showed great hospitality, when I needed a place to sleep

Acknowledgements

during carnival. Also, thanks for always helping me out with uptakes etc. whenever I needed it. I wish you the best in the future, I am sure you will find a nice place to look at trafficking processes.

Todd, you were a very big help when you were here and you thought me a lot of cell biological microscopy work. Your knowledge of renal physiology always made discussions interesting, this is also why we continue to stay in contact bouncing ideas off each other. We had lots of fun together and I will never forget your bicycle experience (you should always be wary of street signs ☺). I hope in the future we can collaborate more and hopefully produce some nice papers together.

Grazie, (a.k.a. Grazia) it was great to work with you in the Netherlands and learn cell biology from you. I have always admired your intuition and ideas, which make you an excellent researcher. I hope you will do well in your laboratory with Giovanna and expand on your cytoskeleton work. We had lots of fun together and it was great seeing you at ASN (I don't know anyone who can drink Vodka like you ☺). It was also great to visit you in Bari, where you have a wonderful family and everything is great, especially the food.

Marloone, I really enjoyed all the nice things we did together and I value the great time we had. My life is not the same without you here and although I miss you a lot, I am sure that we will see each other again. I smile when I remember all the special moments we had, like just before we got dropped from the Skydive and when I hurt my foot at the Dolfinarium ☺. I hope you will do well in Rob's group and get all the nice papers. I would like to thank you for always helping me, with seeding cells or measuring Na^+ on the complicated flame spectrometer. Also thanks for writing the Dutch summary; I expect if there are any mistakes in there, people will approach you with the appropriate corrections ☺.

Jenny we shared a unit together for almost 4 years and I never got tired of you, which I must say is a real accomplishment (on your part), and it attest to your nice personality. We could always talk about everything in our unit, which was great. We also had lots of fun and you were continuously willing to help with whatever it might be. Special thanks for the collaboration of the

Chapter 10

Erlotinib paper and the HSH project, it was always really nice and easy to work with you.

Schroober, you were always there to help me out with my cars, which always seemed to break or something similar to that. We had a lot of fun together when you were still in the lab. It was also fun working together on the Androgen project, in conjunction with Ted. I would also like to thank you for helping me out in the lab, especially in the beginning, when I didn't know how to clone. I wish you the best of luck with your future research and hope everything is well with Sylvie.

Slubber (a.k.a grote bril), thanks for helping me out with all the fura experiments, especially on the S682P story, but also with all the other projects such as when we tried using BCECF or SBFI on the NKCC2 project. We had lots of fun in the lab, especially with your trackball mouse, but also at your place playing Kolonisten van Catan or enjoying a beer. Also, dinners with Martijn, whom I previously worked with in Denmark, were always great and should be continued in the future.

Gay Bab (a.k.a. the Babster), when I hear the "klik-klik" sound of shoes in the lab, I no longer expect to see a nice girl is walking into the lab, but instead you with your hat ☺. We had lots of fun together, where we always prioritized drinking beers, which I think was a good choice. In the lab we could always find something to laugh about and discuss something interesting about physiology.

Annemiete, you taught me how to immunoisolate rabbit CNT cells and helped setup the oocyte system, it was a massive effort so thank you for that. Also thanks for helping me out with the animal experiments when necessary. Irene, you do a terrific job at keeping the lab clean and organized.

Sandor, thanks for the collaboration on the tTG paper and for always helping me out with whatever I needed. Your solid knowledge of biochemistry always made for interesting discussions and new ideas. I wish you best of luck with your Klotho work and look forward to really understanding the underlying mechanism.

Acknowledgements

Arjen, we worked together the first year I was here and in practice you thought me all the basics of molecular biology. Unfortunately, the WNK project proved a bit more elusive than we first thought. In any case, thanks for all the help and I hope you are doing very well at your new department.

Anil, we had some good dinners, some nice drinks, and some interesting discussions together, it was always good to be able to sit on the back of your bike when necessary. Rob it was good having you around the lab. In addition, you are by far the best 'male' dancer I have ever met; when you "go pro" I will buy the DVD ☺. Gang (a.k.a. GBB) we had a great time together in the lab and playing football with your friends. Jorass, it was always nice climbing with you as well as discussing science. Peng thank you for your great hospitality, always bringing dumplings and other food to my house. Kirsten, thanks for helping me out with the all the SNP stuff and for your joyful personality. Yuedan, it was always nice enjoying a cigarette together with you on the 8th floor. Silvia (the Italian stallion), thanks for showing me that Italians can make decent pizza. Femke, we did a lot of work together with the COPAS machine, and I think we managed to optimize really well, thanks for your valuable help.

Thanks to all the other colleagues in the lab for making it such a nice place to be, especially Stephanie, Catalin, Stan, Anke, Gerke, Johan, Jan, Thijs, Eveline, Anne L, Titty, Leonie, Michelle, Jorass (biochem), Kyupil, Monique, Sjoeli, and Hanneke.

I would like to thank Jaap Deinum for always helping me out with whatever was needed for the kidney foundation project. We set up the SNP screen in low-renin hypertensives together and I think it will be a very interesting study in the end. Thanks should also be given to both you and Jacques Lenders for always attending the 8 weekly meetings with me and providing helpful suggestions and discussion. I would like to extend my appreciation, for the fruitful collaborative effort provided by Sabine Tejpar on the Erlotinib project. Nellie Loh and Rajesh Thakker at Oxford, thanks for a nice collaboration on the S682P mice project. Ted it was nice collaborating

Chapter 10

with you on the androgen and calcitonin papers.

Sebastian, en forsat stor tak til dig for din konstante støtte og opbakning igennem de sidste mange år. Jeg beundrer din evne til kritisk at vurdere selv de sværeste videnskabelige ideer. Det er altid rart at besøge dig og have spændende diskussioner omkring fysiologi såvel som alt det andet. Jeg håber at vores samarbejde kan fortsætte langt ud i fremtiden. I am grateful to Jurgen Schnermann for stimulating scientific discussions and continued willingness to help over the years.

I would also like to thank individuals at all the other departments who have assisted me with either experimental or other work during the duration of this thesis. Henk, thanks for always helping me out at the CDL with basically all my animal experiments, also a big thanks to your other colleagues at the CDL. Ron, thank you for helping me out with all the *Xenopus* frogs and making sure that they produced nice oocytes for our experiments. Thanks to Jan Janssen and Herman Swarts for help and maintenance of the radioactive lab. Jeroen Geurts, always cool meeting you at the lentilab and thanks for helping me optimize my lentiviral production. Huib, you were a big help with the microscope at times and I am impressed with the fact that you always could keep your mood constant, namely at 6. Ineke, it was a pleasure teaching renal histology with you. Tom, it was always great to discuss physiology with you and I admire your ability to determine what are the right experiments, which are necessary to make a paper. Also, thanks to my mentor Johan van der Vlag for willingness to help. Minja, thanks for lending your expertise on the Androgen paper and more importantly in the gym, both were much appreciated ☺.

A big thanks should also be given to all my dive buddies here in the Netherlands (Raymond, Martijn, the GUE team etc.), we had lots of fun together.

To all the people I forgot to acknowledge, sorry for forgetting you and thanks for whatever you may have helped me with.

Acknowledgements

Kære Mette, jeg nok aldrig fået gjort det klart for dig, hvor meget du betød for mig og mit liv. Du viste mig hvad kærlighed var. Det er med glæde at jeg husker de utrolig mange vidunderlige ting og stunder vi havde sammen (også sammen med din dejlige familie). Jeg var heller aldrig taget til Holland uden din uselviske støtte og hjælp, og ville derfor heller aldrig havde kunnet skrive min thesis her. Jeg vil altid elske dig og jeg håber at du snart bliver lykkelig igen.

Til sidste vil jeg give en stor tak til min familie. Mor og far, uden jeres uendelige støtte og hjælp har det ikke været muligt at færdiggøre universitetet og nu at få min PhD grad. Om det har været at få møbler ned i min studie lejlighed her i Holland eller hvad jeg nu ellers har behøvet hjælp med, så har i altid været der for mig. I har sjældent presset mig og har altid motiveret med jeres gode råd, støtte og hjælp. Der findes ikke bedre forældre end jer. Jeg takker samtidig for en dejlig opvækst i Lystrup. Kamilla, jeg håber at du får det rigtigt godt sammen med Kim og Trold i jeres lille hus i Horsens. Også en stor tak til resten af familien, især Ruth og Simon. Til mine venner hjemme i Danmark, især Winther, Iver, Bisgaard, Carlos, Paddy og Benne, det er altid godt at se jer og jeg er glad for at vi altid formår at holde kontakten.

